ДОКЛАДЫ
АКАДЕМИИ НАУК СССР

Volume 136, Numbers 1-6
January-February, 1961

PROCEEDINGS OF THE ACADEMY OF SCIENCES

OF THE USSR

(DOKLADY AKADEMII NAUK SSSR)

Physical Chemistry Section

IN ENGLISH TRANSLATION

M. I. T. Lincoln Laboratory
FEB 21 1962
Received-Library

c/b

CONSULTANTS BUREAU

Invaluable in the laboratory

Volumes 3 and 4

The third volume in this series contains laboratory methods for the preparation of 30 different compounds of furan derivatives, chosen because they can serve as intermediates in the synthesis of compounds of more complex structure. The sections on aldehydes and dicarboxylic acids are particularly interesting since they offer new perspectives in the synthesis of furan derivatives.

Volume 4, in addition to material on the synthesis of furan series derivatives, presents descriptions of preparation methods of derivatives of other heterocyclic systems. Checked synthesis procedures of many parent compounds of pyridine, chinoline, indole, and other series are included.

156 pages **$6.00**

CONTENTS include

5-(Benzylthiomethyl)-2-Furoic Acid
5-Benzyl-2-Furaldehyde
5-(Butylthiomethyl) Furfuryl Alcohol
5,5'-(Thiodimethylene)bis-2-Furamide
5,5'-Methylenedi-2-Furoic Acid
4,5-Dimethyl-2-Furaldehyde
2,5-Furandimethanol
2,2'-Methylenedifuran
N,N-Diethyl-2-Furamide
5-Carboxy-2-Furanacetic Acid
Methyl 5-Formyl-2-Furoate
4-(5-Methyl-2-Furyl)-3-Buten-2-One
4-(5-Methyl-2-Furyl)-2-Butanone
2-(5-Methylfurfurylamino)Pyridine
5-Nitrofurfuryl Alcohol
5-(Hydroxymethyl)-2-Furoic Acid

3-Aminopyridine
5-(Benzylsulfonylmethyl)-2-Furoic Acid
4-(5-Benzyl-2-Furyl)-3-Buten-2-One
Benzofuran (Coumarone)
N-Methyl-2-Benzofuranmethylamine
2,3-Dimethylindole-5-Carboxylic Acid
Tetrahydro-2,5-Furandimethanol
N,N-Diethyltetrahydrofurfurylamine
Indazole
Indole-3-Carboxaldehyde
3-(3-Piperidinopropyl)Indole
Indole-3-Acetic Acid (Heterouxin)
2,3-Dihydro-2-Methylbenzofuran
5-Methylisatin
2-Methylindole-3-Propionic Acid
2-Isoindolineethanol

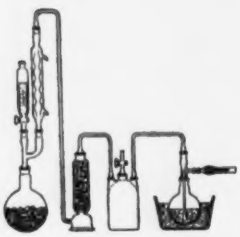

SYNTHESES OF HETEROCYCLIC COMPOUNDS

Edited by
A. L. MNDZHOIAN

TRANSLATED FROM RUSSIAN

Volumes 1 and 2

The lack of a practical guide to the laboratory preparation of heterocyclic compounds is being met by this series of collections of synthesis methods, originally published by the Armenian Academy of Sciences.

"... intended to fill the gap in the coverage of heterocyclic compounds ... The first two volumes are devoted entirely to the synthesis of furan derivatives. Each compound is described by its systematic name and structural formula; one method of preparation is given in detail; and other methods of preparation are referred to in the literature."

– SCIENCE REFERENCE NOTES,
Columbia University

155 pages **$6.00**

CONTENTS include

5-Benzyl-2-Furoic Acid
5-(5-Benzyl-2-Furyl)-s-Triazole-3-Thiol
5-Bromo-2-Furoic Acid
2-Furanmethanediol Diacetate
5-(Diethylaminomethyl) Furfuryl Alcohol
Methyl 5-Benzyl-2-Furoate
Methyl 5-(Bromomethyl)-2-Furoate
Methyl 5-(Diethylaminomethyl)-2-Furoate
Methyl 5-Methyl-2-Furoate
Methyl 5-(Propoxymethyl)-2-Furoate
Methyl 2-Furoate
Methyl 5-(Chloromethyl)-2-Furoate
2-Methylfuran (Sylvan)
5-Methyl-2-Furoic Acid
5-(Propoxymethyl)-2-Furoic Acid
Furan

5-(Aminomethyl)-2-Furoic Acid
5-Benzylfurfuryl Acetate
2-Furyl Methyl Ketone
2-Benzylfuran
5-Benzylfurfuryl Alcohol
5,5'-(Thiodimethylene) Di-2-Furoic Acid
2,3-Dimethylfuran
4,5-Dimethyl-2-Furoic-Acid
1,3-Difurfurylurea
Diethyl (Tetrahydrofurfuryl) Malonate
Diethyl Furfurylidenemalonate
5-Carboxy-2-Furanpropionic Acid
Methyl Tetrahydro-5-Methyl-2-Furoate
Methyl 4-(Chloromethyl)-5-Methyl-2-Furoate
Methyl 5-(Cyanomethyl)-2-Furoate
5-Methylfurfuryl Alcohol

c/b CONSULTANTS BUREAU
227 W. 17 ST., NEW YORK 11, N. Y.

Volume 136, Numbers 1-6
January-February, 1961

PROCEEDINGS OF THE ACADEMY OF SCIENCES

OF THE USSR

(DOKLADY AKADEMII NAUK SSSR)

Physical Chemistry Section

A publication of the Academy of Sciences of the USSR

IN ENGLISH TRANSLATION

Year and issue of first translation:
Vol. 112, Nos. 1-6 Jan.-Feb. 1957

Annual subscription *$160.00*
Single issue *35.00*

Copyright © 1961
CONSULTANTS BUREAU ENTERPRISES, INC.
227 West 17th Street, New York, N. Y.

A complete copy of any paper in this issue may be purchased from the publisher for \$5.00

Note: The sale of photostatic copies of any portion of this copyright translation is expressly prohibited by the copyright owners.

Printed in the United States of America

PROCEEDINGS OF THE ACADEMY OF SCIENCES OF THE USSR

Physical Chemistry Section

Volume 136, Numbers 1-6 January-February, 1961

CONTENTS

CONTENTS (continued)

CONTENTS (continued)

FREE RADICAL POLYMERIZATION AS AN EXAMPLE OF CHAIN TRANSFER OF ENERGY PROMOTED BY AN EXCITATION WAVE

É. I. Adirovich

P. N. Lebedev Physics Institute, Academy of Sciences of the USSR

(Presented by Academician N. N. Semenov, July 15, 1960)
Translated from Doklady Akademii Nauk SSSR,
Vol. 136, No. 1, pp. 117-120, January, 1961
Original article submitted July 13, 1960

1. After examining a large amount of data dealing with low-temperature polymerization, N. N. Semenov [1] proposed a theory, according to which, under geometrically favorable conditions, the addition of monomeric units to a growing polymer chain should not proceed through a series of consecutive jumps over the activation barrier, but through a concerted electronic interaction which would produce a rearrangement of bonds in an excited system. In this paper, an attempt is made to provide a quantum-mechanical basis for such behavior, and to expand the theory.

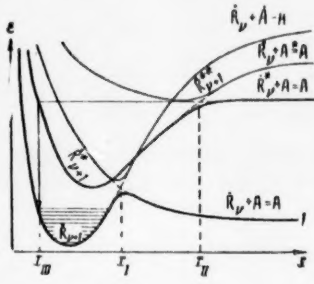

Fig. 1.

2. Let us examine a case where we have a polymeric free radical $\dot{R}_\nu$ and a monomer A = A, with a configuration favorable to addition (ν is the number of monomeric units in the polymer). If we disregard interactions involving σ-bonds and secondary bonds in both the polymer and the monomer, the reaction $\dot{R}_\nu + A = A \rightarrow \dot{R}_{\nu+1}$ can then be treated as a simple three-electron interaction of the type K + LM → KL + M, where K, L, and M are all monovalent atoms. The curves plotted in Fig. 1 show how the electronic energy ϵ of the entire system (polymeric free radical + monomer) changes along the reaction path. As an independent degree of freedom x we have selected the distance between the terminal carbon atom on the polymer and the nearest carbon atom of the olefinic monomer. As is well known, the electronic energy of a system computed by the adiabatic approximation represents the potential energy produced by the motion of the nuclei [2,3].

The numbers 1, 2, 3, and 4 shown on the right side of the graph represent the ground state and three low-lying excited states for a system in which the components are apart. The difference $\epsilon_2 - \epsilon_1$ gives the excitation energy of the unpaired electron on the terminal carbon atom of the free radical $\dot{R}_\nu$; $\epsilon_3 - \epsilon_1$ gives the excitation energy of the molecule A = A; $\epsilon_4 - \epsilon_1$ gives the energy for an adiabatic breaking of the π-bond. In assigning numbers 2 and 3 to the curves on the right-hand side of the graph (the case where the components are apart), we relied on the potential curves for diatomic molecules, where it is found that in general the excitation energy of a molecule is greater than the difference between the atomic levels which give rise to the particular ground and excited molecular states [4,5]. The position of Curve 4 relative to Curves 2 and 3 is unimportant, since the corresponding potential curves do not interact on intersection.

To determine theoretically the activation barrier ϵ_{act} for the reaction $\dot{R}_\nu + A = A \rightarrow \dot{R}_{\nu+1}$ (Curve 1), we have to know the shape of the potential energy surface [6]. Polyani's rule [7]: $\epsilon_{act} = 11.5 - 0.25q$ yields a value $\epsilon_{act} \approx$ 5-6 kcal/mole. Approximate quantum-mechanical calculations, as well as experimental studies, yield similar values [8]. According to [3,9], $\epsilon_{act} \approx$ 1-3 kcal/mole.

We will use the average value ϵ_{act} = 3 kcal/mole (0.13 ev/molecule). At 20°C, ϵ_{act} = 5 kT, while at −196°C, ϵ_{act} = 19kT. If the addition of every monomeric unit required thermal activation, the polymerization would be slow, particularly at low temperatures.

The polymerization could proceed without absorbing energy from the surrounding medium (thermostat) if an adequate fraction of the heat of reaction were used directly to provide activation energy for the subsequent addition of another monomeric unit (energy chain [10]). Let λ be the probability of concentrating all the energy liberated in the reaction along the selected degree of freedom. Then let ϵ_0 and ϵ_N be the energies localized on the reaction coordinate when the polymer consists of ν and ν + N units, respectively. Calculations show that

$$\varepsilon_N = \frac{\lambda}{1-\lambda} q + \lambda^N \left(\varepsilon_0 - \frac{\lambda}{1-\lambda} q\right). \quad (1)$$

From the condition that $\epsilon_N|_{N\to\infty} \geq \epsilon_{act}$, it follows that the polymerization will proceed uninterrupted if

$$\lambda \geqslant \lambda_0 = \frac{\varepsilon_{act}}{\varepsilon_{act} + q} \approx 0.13 \quad (2)$$

provided, of course, that the monomer is favorably oriented.

Due to the great number of degrees of freedom and strong bonding between the atoms and groups in a polymeric chain, and also as a result of heat losses, the actual value of λ will obviously be smaller than the critical value λ_0. When $\lambda < \lambda_0$, the polymer growth will rapidly come to an end. According to Eq. (1), the chain length will be:

$$N = \frac{\lg \dfrac{\lambda(\lambda_0 - \lambda)}{\dfrac{\varepsilon_0}{\varepsilon_{act}} \lambda_0 (1-\lambda) - \lambda(1-\lambda_0)}}{\lg \lambda}. \quad (3)$$

When λ_0 = 0.13, λ = 0.12, and $\epsilon_0 = 10\epsilon_{act}$, the polymeric chain will increase by only 3 molecules.

3. As one proceeds from a state in which the components are apart to the transition state, the repulsion and its unavoidable effects on the activation energy constitute an exchange interaction and are expressed by the integrals α in the London equation [6,8]:

$$E = E_0 + Q_{12} + Q_{23} + Q_{31} - \sqrt{(\alpha_{12} - \alpha_{23})^2 + (\alpha_{23} - \alpha_{31})^2 + (\alpha_{31} - \alpha_{12})^2}. \quad (4)$$

In contrast, as the components of the system approach each other, the coulomb integrals Q decline monotonically, assisting in the unactivated mutual attraction. It has already been shown [11-14] that the specific contribution of coulomb integrals to the total interaction energy is much greater when the reaction occurs between excited instead of unexcited atoms. We would consequently expect increased attraction during the initial stages of approach, or in other words, the activation energy for the addition of a monomer A = A to an excited polymeric free radical $\dot{R}_\nu^*$ should decrease appreciably, and possibly even drop to zero (see Curve 2; $\dot{R}_\nu^*$ is a radical with an excited unpaired electron on the terminal carbon atom).

In the reaction $\dot{R}_\nu^* + A = A \to \dot{R}_{\nu+1}^*$ the transfer of a free valence should be accompanied by the transfer of excitation energy to the new terminal C-atom on the newly attached polymer unit. The $\dot{R}_{\nu+1}^*$ state, in which the σ-bonds in the polymeric chain are also excited, is unstable with respect to a nonadiabatic transition to the configuration x_{II}. Thus, since each time that a radical $\dot{R}_{\nu+1}^*$ is formed by the addition of a monomeric molecule, the excitation energy becomes concentrated on the unpaired electron, we can have unactivated addition of a second, third, etc., molecule as long as the monomer remains favorably oriented. The transfer of excitation energy to the (ν + 2)th molecule stabilizes the (ν + 1)th σ-bond, etc. The arrow in Fig. 1 shows how the (ν + 1)th σ-bond in the polymer would become stabilized in an idealized case where

$$J_{\nu+1,\,\nu+2} \equiv \mathrm{Re}\int \Psi^+_{\nu+2} V_{\nu+1,\,\nu+2} \Psi_{\nu+1} d\Omega = \begin{cases} 0 & \text{when } x > x_{III}, \\ \infty & \text{when } x = x_{III}. \end{cases} \quad (5)$$

$\Psi_{\nu+1}$ and $\Psi_{\nu+2}$ are the electronic wave functions for the system when the $(\nu + 1)$th and the $(\nu + 2)$th molecules are excited, while $V_{\nu+1,\nu+2}$ is an interaction operator. The formula for the excitation energy transition period [15],

$$\tau \sim \frac{t}{J_{\nu+1,\,\nu+2}}, \tag{6}$$

indicates that under the conditions given in Eq. (5) the transfer of excitation energy from the $(\nu + 1)$th to the $(\nu + 2)$th molecule in the polymer would occur instantaneously in the x_{III} configuration, as if the exchange interaction between the $\dot{R}^*_{\nu+1}$ and the $\dot{R}^*_{\nu+2}$ states had arisen instantaneously.

In reality, the transfer of excitation energy to the $(\nu + 2)$th molecule in the polymer does not take place at a fixed atomic configuration, but during the formation of the $(\nu + 2)$th σ-bond, which occurs in exactly the same way as the formation of the $(\nu + 1)$th bond shown in Fig. 1. Hence, the $(\nu + 1)$th unit of the polymeric chain is not stabilized through a transition obeying the Franck-Condon principle, but by a gradual deformation of Curve 2 into Curve 1 in the course of a single or several atomic vibrations. Since the excitation energy of the unpaired electron in the polymeric free radical $\dot{R}^*_{\nu}$ remains independent of the chain length ν, as the polymeric chain increases in length, the transfer of excitation energy from one molecule to another will be accompanied by a transition of the stabilizing units into vibrationally excited states; the energy liberated is equal to the difference between the energy of a σ-bond in the polymer and that of the π-bond in the monomer (see Fig. 1).

Thus, it is the electronic excitation of the polymeric free radical which makes the unactivated growth of the chain possible. When the monomeric molecules are favorably oriented (for example, in a crystal), this type of polymerization represents an elementary process of electronic excitation propagation in which, as the excitation energy passes from one molecule to another, it "sews" the components into a single polymer. The duration of growth and the polymeric chain-length depend on the lifetime and the propagation velocity of the electronic excitation.

4. This type of free radical polymerization represents a novel manifestation of an excitation wave. As is well known, relatively long-life electronic excitations in a periodic structure do not remain localized on a particular atom or molecule but travel through the structure in the form of excitation waves [16,17]. An excitation wave travels with a velocity $v \sim a/\tau$, where $\underline{a}$ is the interval of structural periodicity, and τ is the time spent by an excitation wave at a given lattice node, which can be calculated from Eq. (6). If the atomic oscillation period τ_{at} exceeds the excitation energy transfer time τ the excitation wave will comprise only the electronic excitation energy. If $\tau_{at} < \tau$, the excitation wave can dislocate the atoms from their equilibrium position and will then represent a simultaneous displacement of the electronic excitation energy and the local elastic strain in the structure. The excitation wave occasionally becomes localized at points of structural defects.

Let us examine the case where a polymer $\dot{R}_{\nu}$ comes into close contact with a monomer which has a definite periodic structure. The electronic excitation of the polymer is localized on the terminal carbon atom (at one end of the polymeric chain) which carries the free valence. When contact is achieved with the monomer, the excitation wave can be further propagated by the concerted process of chain growth and excitation energy transfer. The arrival of an excitation wave at the end of the polymeric chain results in the attachment of the monomer, and the accompanying atomic rearrangement establishes favorable conditions for further propagation of the excitation wave. Hence, in olefinic systems, which can exist in two ordered modifications (monomeric and polymeric), it is possible to have a new form of excitation wave – an electronic excitation wave accompanied by an inelastic (residual) strain wave. When $a \sim 10^{-8}$ cm and $\tau \sim 10^{-13}$ sec the excitation wave (and consequently the polymerization front) travels with a velocity $v \sim 10^5$ cm/sec. During the lifetime of an excitation wave (about 10^{-8} to 10^{-9} sec) a chain consisting of from 10^4 to 10^5 molecules can be formed. Though heat is produced along the front (equal to the difference between the energies of σ- and π-bonds), it follows from the above-discussed excitation-wave mechanism that the chain growth is maintained by the transfer of electronic excitation energy, and not by the evolution and reabsorption of heat during the reaction.

The author wishes to thank Academician N. N. Semenov and Professor N. D. Sokolov for their valuable comments.

LITERATURE CITED

1. N. N. Semenov, Khim. i Tekh. Polimerov. 4, 7-8, 196 (1960).
2. L. D. Landau and E. M. Lifshits, Quantum Mechanics [in Russian] (1948) Ch. XI.
3. V. N. Kondrat'ev, The Kinetics of Gaseous Reactions [in Russian] (Izd. AN SSSR, 1958) Chs. III, IV, Sec. 14.
4. G. Herzberg, Spectra of Diatomic Molecules (New York, 1950).
5. R. F. Bacher and S. Goudsmitt, Atomic Energy States (New York, 1932).
6. S. Glasstone, K. Laidler, and H. Eyring, The Theory of Absolute Reaction Rates [Russian translation] (IL, 1948).
7. N. N. Semenov, Some Problems in Chemical Kinetics and Reactivity [in Russian] (Izd. AN SSSR, 1958) Ch. I, Secs. 4, 8.
8. Kh. S. Bagdasaryan, Theory of Free Radical Polymerization [in Russian] (Izd. AN SSSR, 1959), Ch. VII, Sec. 2; Ch. VIII, Secs. 2 and 5; Ch. X, Sec. 1.
9. E. W. R. Steacie, Atomic and Free Radical Reactions (New York, 1954) Vol. 2, Ch. VII.
10. N. N. Semenov, Chain Reactions [in Russian] (1934).
11. J. H. Bartlett, Phys. Rev. 37, 507 (1931).
12. N. Rosen and S. Ikehara, Phys. Rev. 43, 5 (1933).
13. J. L. Magee, J. Chem. Phys. 8, 677 (1940).
14. K. J. Laidler, The Chemical Kinetics of Excited States (Oxford, 1955).
15. W. Kauzman, Introduction to Quantum Chemistry [Russian translation] (IL, 1960) Ch. XIII.
16. J. Frenkel, Phys. Rev. 37, 17, 1276 (1931); Ya. I. Frenkel', Zhur. Éksp. i Teoret. Fiz. 6, 647 (1936).
17. G. Khaken, Uspekhi Fiz. Nauk 68, 565 (1959).

All abbreviations of periodicals in the above bibliography are letter-by-letter transliterations of the abbreviations as given in the original Russian journal. *Some or all of this periodical literature may well be available in English translation.* A complete list of the cover-to-cover English translations appears at the back of this issue.

AEROSOL FORMATION DURING THE RADIOLYSIS OF GASEOUS HYDROCARBONS

V. S. Bogdanov

N. D. Zelinskii Institute of Organic Chemistry, Academy of Sciences of the USSR

(Presented by Academician B. A. Kazanskii, July 7, 1960)
Translated from Doklady Akademii Nauk SSSR,
Vol. 136, No. 1, pp. 121-124, January, 1961
Original article submitted July 5, 1960

We have studied the formation and destruction of aerosols during the radiolysis of gaseous hydrocarbons, using optical and weight-concentration techniques. The methods themselves have already been described in [1], where the aerosols formed by the radiolysis of methane were investigated. The radiation consisted of fast electrons with an average energy of 112 kev. To make a comparison with other radiochemical studies [2-7] possible, experiments involving ethane, propane, n-butane, ethylene, propylene, and methane–oxygen mixtures were carried out in a brass reactor; experiments involving acetylene were carried out in an iron reactor, while those involving ethylene–oxygen mixtures were done in an aluminum reactor. Each reactor had a 2-liter capacity.

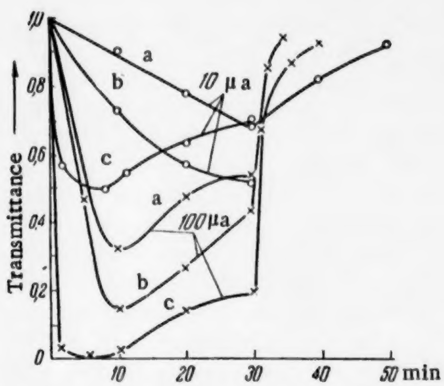

Fig. 1. Light transmittance as a function of time for the aerosols formed in the radiolysis of: a) propane; b) ethane; c) n-butane.

In Fig. 1 we have plotted curves which show how the extinction of light varies with time (with the amount of absorbed energy) in the case of aerosols formed during irradiation of ethane, propane, and n-butane at t = 20° and p = 1 atm; the exposure period was 30 min and the electron-beam intensity either 10 μamp or 100 μamp. The figure shows that the extinction of light is greatest in irradiated n-butane and least in propane; moreover, at 100 μamp, all the aerosol-formation curves exhibit a minimum which divides each curve into two distinct sections. At short time intervals (dosages), light extinction is a linear function of the energy absorbed; after that, although the aerosol formation continues, the coagulation and sedimentation processes result in reduced light extinction. When irradiation is stopped, the aerosols break up fairly rapidly. When the electron-beam intensity is decreased from 100 μamp to 10 μamp, the light extinction is reduced by one half.

In Fig. 2 we have similarly shown the variation of light extinction with time for the aerosols formed by irradiating a methane–oxygen mixture (4:1 ratio) and an ethylene–oxygen mixture (1:1) at p = 1 atm, I = 100 μamp, and t = −10° (Curves 1 and 2) or 20° (Curves 3 and 4); and for aerosols formed from propylene at p = 1 atm, t = 20°, and I = 10 μamp (Curve 5) or 100 μamp (Curve 6). The irradiation was continued for 30 min in all cases except Curve 6, where it was only 10 min. All the curves in Fig. 2 resemble those in Fig. 1 in having a maximum in light extinction after a certain amount of energy is absorbed.

Strongest dependence on temperature is observed in the cases of $CH_4 + O_2$ mixtures. On the other hand, temperature seems to have very little effect (within the investigated range) on the extinction of light in the case of the $C_2H_4 + O_2$ mixture. The difference is apparently due to the fact that the aerosols formed during irradiation

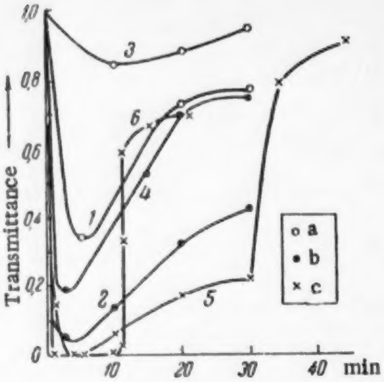

Fig. 2. Light transmittance as a function of time for the aerosols formed by the radiolysis of: a) methane–oxygen mixture; b) ethylene–oxygen mixture; c) propylene.

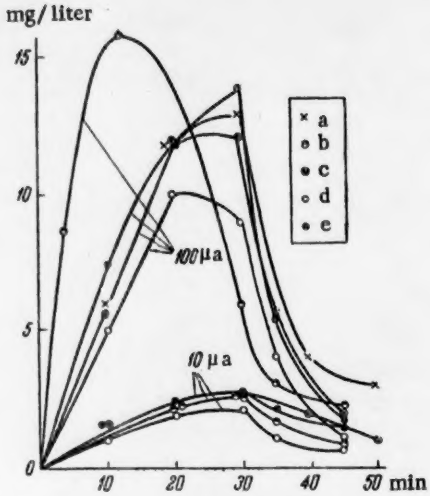

Fig. 3. Time dependence of the weight concentration of aerosols formed by the radiolysis of: a) methane–oxygen mixture; b) ethylene–oxygen; c) ethane; d) propane; e) butane.

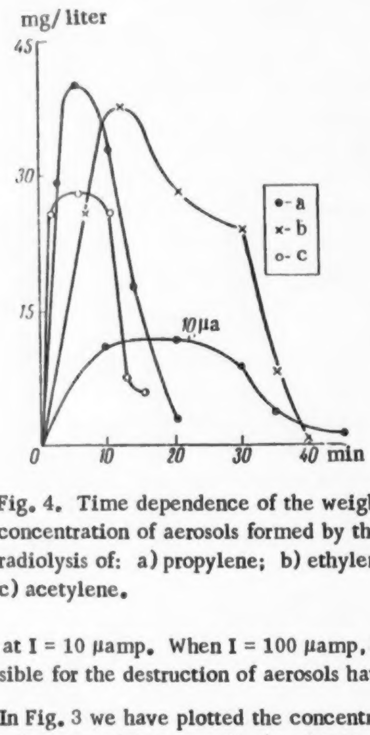

Fig. 4. Time dependence of the weight concentration of aerosols formed by the radiolysis of: a) propylene; b) ethylene; c) acetylene.

of $CH_4 + O_2$ mixtures consist of aqueous solutions of formic acid, formaldehyde, and peroxides, whereas the aerosols formed in $C_2H_4 + O_2$ mixtures consist primarily of high-boiling compounds [5]. The rapid increase in the concentration of the aerosol phase observed when the temperature of the $CH_4 + O_2$ mixture is lowered from 20 to −10°C seems to be responsible for a similarly sharp change in the qualitative composition of the oxidation products, which has been reported to occur in the same narrow temperature interval [6]. At the same time, the small temperature dependence of the aerosol phase concentration in mixtures of $C_2H_4 + O_2$ is entirely consistent with the fact that the composition of reaction products remains practically constant throughout this temperature range [5]. Consequently, variations in the composition and concentration of the aerosol phase can strongly influence the course of a radiochemical reaction. In the case of the aerosol formed during irradiation of propylene, an almost complete extinction of light occurs after only 4 min at I = 10 μamp. When I = 100 μamp, however, the curve has no minimum, indicating that the processes responsible for the destruction of aerosols have in this case reduced the extinction of light.

In Fig. 3 we have plotted the concentration (by weight) of aerosols formed in the radiolysis of ethane, propane, n-butane, and $CH_4 + O_2$ (4:1) and $C_2H_4 + O_2$ (1:1) mixtures as a function of time (energy absorbed); the electron beam intensity was either 10 μamp or 100 μamp at t = 20° and p = 1 atm. The radiation time was 30 min, as before. In the case of saturated hydrocarbons the maximum weight concentration, as well as light extinction, was exhibited by n-butane and the minimum by propane. The concentration maxima are displaced from the extinction maxima toward higher dosages, since the light extinction depends not only on the weight concentration of the aerosol, but also on the dimensions of the particles. The $C_2H_4 + O_2$ mixture attains a maximum weight concentration much more rapidly than does the $CH_4 + O_2$ mixture, and its aerosol concentration at the maximum is much higher too. When the electron beam intensity is boosted from 10 μamp to 100 μamp, the weight concentration increases by a factor of 5-8.

Compound	Energy absorbed, ev/min·10^{-21}	G	G_a				
			Exposure to radiation, min				
			3	5	10	20	30
CH_4	1.45	2.5			0.10	0.13	0.20
C_2H_6	2.63	4.1			0.85	0.90	0.60
C_3H_8	3.68	6.7			0.37	0.40	0.20
C_4H_{10}	3.68	11.0			0.42	0.30	0.27
C_2H_4	2.32	8.8		5.9	5.9	2.6	1.5
C_3H_6	3.49	20	7.8	6.5	2.8		
$CH_4 + O_2$	1.62	3.6			2.8	2.2	1.7
$C_2H_4 + O_2$	2.32	9.4	4.3	3.5	2.6	1.1	0.4
C_2H_2	2.04	56.6	18.7	11.8	6.1		

In Fig. 4 we have plotted the concentration by weight against time for the aerosols formed by the radiolysis of ethylene, propylene, and acetylene at 20°C, p = 1 atm, I = 100 μamp (for propylene also at I = 10 μamp). Acetylene and propylene at I = = 100 μamp were irradiated for 10 min, while ethylene and propylene at I = 10 μamp for 30 min. The highest concentration by weight (40 mg/liter) in the experiment involving propylene is observed after a 5-min exposure to radiation and absorption of $1.75 \cdot 10^{22}$ ev of energy. When the electron beam intensity is reduced to 10 μamp, the weight concentration of the aerosol formed in propylene declines by about one half. In the case of ethylene, about the same maximum concentration by weight is observed as in the case of propylene, but only after a greater amount of energy has been absorbed ($2.8 \cdot 10^{22}$ ev). In all these cases, after attaining its maximum value the weight concentration of the aerosol begins to decline as more energy is absorbed due to processes which destroy the aerosol. The aerosol formed during irradiation of acetylene consists of solid cuprene particles and attains a maximum concentration of 27 mg/liter.

Thus, with increasing radiation dosage we first observe the accumulation of the aerosol phase within the reaction zone; the rate and the amount formed depend on the reagents used, but after a certain amount of energy has been absorbed processes leading to the destruction of the aerosol tend to reduce the concentration. When the radiation is cut off, the newly formed systems persist for brief periods of time: from several minutes in the case of acetylene, to several tens of minutes, in the case of CH_4 + O_2 mixtures.

In the table we have compiled the yields of the aerosol phase G_a (the number of original hydrocarbon molecules which reacted to form the aerosol phase for each 100 ev of energy absorbed) for various radiation exposure lengths (dosages) at a pressure p = 1 atm, t = 20°C, and I = 100 μamp. For the sake of comparison, we have also tabulated the values of G, which give the corresponding number of the original hydrocarbon molecules converted into the isolated final liquid and solid products [2-7]. The data shown in the table indicate that a good percentage of the liquid products formed in the radiochemical reaction pass through an aerosol phase. The yields G_a may vary over a wide range of values, depending on the type of hydrocarbon used and the amount of energy absorbed. The highest yield is observed in the case of acetylene and the lowest in the case of methane, and as a rule the aerosol yield tends to decline when an excessive amount of energy is absorbed. Thus, when the irradiation period is increased tenfold, the yield in C_2H_4 + O_2 mixtures declines to one twelfth the value, while in the case of n-butane a threefold increase reduces the yield to two thirds the original value. The yields from unsaturated hydrocarbons and from mixtures of CH_4 and C_2H_4 with O_2 exceed the yields from saturated hydrocarbons by about one order of magnitude. Let us also note that the maximum yield G_a is not necessarily observed in cases where the concentration by weight is highest; for example, acetylene has G_a = 18.7 and a concentration of 27 mg/liter, while propylene has G_a = 7.8 and concentration 40 mg/liter.

LITERATURE CITED

1. V. S. Bogdanov, Zhur. Fiz. Khim. 34, No. 5, 1050 (1960).
2. B. M. Mikhailov, L. V. Tarasova, and V. S. Bogdanov, The Effects of Ionizing Radiation on Organic and Inorganic Compounds [in Russian] (Izd. AN SSSR, 1958) p. 218.
3. B. M. Mikhailov, M. E. Kuimova, and V. S. Bogdanov, The Effects of Ionizing Radiation on Organic and Inorganic Compounds [in Russian] (Izd. AN SSSR, 1958) p. 223.
4. B. M. Mikhailov, L. V. Tarasova, V. G. Kiselev, and V. S. Bogdanov, Transactions of the First All-Union Conference on Radiochemistry [in Russian] (Izd. AN SSSR, 1958).
5. B. M. Mikhailov and V. G. Kiselev, Izvest. Akad. Nauk SSSR, Otdel Khim. Nauk No. 9, 1619 (1960).
6. B. M. Mikhailov, M. E. Khimova, and V. S. Bogdanov, Transactions of the First All-Union Conference on Radiochemistry [in Russian] (Izd. AN SSSR, 1958).
7. L. M. Dorfman and F. J. Shipko, J. Am. Chem. Soc. 77, 4723 (1955).

THE EFFECTS OF WATER AND OXYGEN ON THE CATALYTIC POLYMERIZATION OF ETHYLENE ON CHROMIC OXIDE

Corr. Member AN SSSR G. K. Boreskov, V. A. Dzis'ko, and T. Ya. Tyulikova

L. Ya. Karpov Physicochemical Institute
Translated from Doklady Akademii Nauk SSSR, Vol. 136, No. 1, pp. 125-128, January, 1961
Original article submitted August 17, 1960

When ethylene undergoes deep polymerization catalyzed by chromic oxide, the yield of polymer per unit weight of catalyst varies over a wide range of values [1-3]. One would naturally assume that these variations result from differences in the concentration of impurities found in ethylene or the solvent. The present work represents an attempt to determine the effects of water and oxygen in ethylene on the yield of polymer.

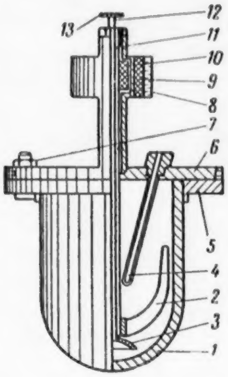

Fig. 1. The autoclave used for investigating catalytic polymerization. 1) Outer shell of autoclave; 2) stirrer; 3) a crucible for the tube; 4) thermocouple; 5) flange; 6) lid; 7) bolt and nut; 8) condenser; 9) stator; 10) rotor; 11) hollow shaft; 12) rod; 13) handle.

The catalyst was prepared by soaking an aluminum silicate carrier in a solution of chromic oxide. The carrier was made of granular aluminum silicate which had a dry weight of 0.43, an average pore radius of 40-60 A, and a specific surface of 300 m^2/g.* After soaking, the carrier was dried at 110°C and fired in a muffle furnace at 250°C. Activation was achieved by heating the catalyst for 4 hr at 400°C in vacuo (10^{-3} mm Hg). This was done by placing weighed samples of the catalyst into thin-wall glass tubes and sealing the tubes to the manifold of a vacuum apparatus. When the activation was terminated, the tubes were sealed, detached, and weighed. The final catalyst usually contained about 5% CrO_3.

The first set of experiments was carried out using ethylene of the highest purity possible. Ethylene was forced through a carbon filter at 50 atm, then through a column filled with a nickel–chromium catalyst to remove oxygen, and through two columns filled with activated alumina to remove water vapor. The ethylene eventually used for polymerization contained less than five parts per million of oxygen, and had a dew point below −65°C, which indicated that the water-vapor content was below three parts per million. Benzene (BR-1 brand), cyclohexane, heptane, and other hydrocarbons were used as solvents. To purify the solvents we stirred them over freshly fired aluminum oxide and bubbled through them nitrogen freed from oxygen and water. Solvents thus purified contained less than 5 parts per million of water.

*The authors wish to take this opportunity to thank the Chief Engineer at the Gor'kii station of the Scientific Research Institute of Petroleum Products, B. A. Lipkind, for providing us with samples of the carrier.

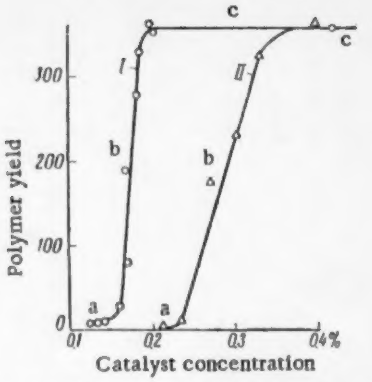

Fig. 2. The amount of polymer formed as a function of the catalyst concentration in solution. I) Water content of solution 5 ppm; II) water content 20 ppm.

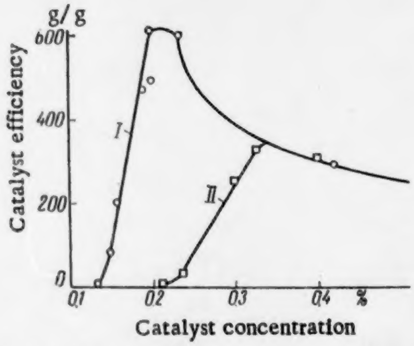

Fig. 3. Catalytic efficiency as a function of catalyst concentration. I) Water content in solution 5 ppm; II) water content 20 ppm.

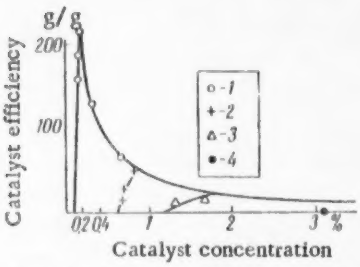

Fig. 4. 1) 0.0003%; 2) 0.001%; 3) 0.01%; 4) 0.1% O_2.

Catalytic polymerization was carried out in a one-liter autoclave made of stainless steel. Special precautions were taken to prevent any accidental introduction of impurities into the reaction mixture during the experiment. The autoclave (Fig. 1) was provided with a magnetic stirrer, a pocket for a thermocouple, and a special sealed-tube crusher.

Experiments were carried out in the following manner. The sealed tube with the catalyst inside was attached to the rod running through the hollow shaft. The autoclave was sealed with the lid, placed inside a dismountable electric furnace, and connected with the apparatus in which ethylene was purified. Using a simple force pump, we evacuated the autoclave and degassed it for 2 hr at 200°C; after that, the apparatus was cooled to 100° and flushed several times with the purified ethylene. Operating under dry nitrogen, we transferred 300 g of purified solvent into the evacuated autoclave, and then introduced dry ethylene until a pressure of 35 atm was attained. After the experimental conditions were established, we crushed the sealed tube containing the catalyst by applying pressure to the rod. Whenever, in the course of polymerization, the ethylene pressure in the autoclave dropped appreciably, it was restored back to the original 35 atm by introducing more ethylene from the purification apparatus, in which the pressure was maintained at 50 atm. The polyethylene recovered from the autoclave was dried to a constant weight and weighed. In figuring out the weight of the polymer, a correction was introduced for the glass tube and the catalyst.

The results from our polymerization experiments in which ethylene of highest purity was used are presented in Fig. 2,I. When the amount of polymer formed is plotted against the catalyst concentration in solution, one gets an S-shaped curve. The left-side section of the curve (section a) shows that unless a certain threshold concentration is exceeded no reaction takes place. Even a concentration slightly in excess of the threshold value results in a greatly increased polymer yield (section b). When the catalyst concentration attains a certain limiting value (which is determined by the length of the experiment), the polymer yield becomes independent of the catalyst concentration (section c).

This behavior is responsible for the appearance of a sharp maximum on the curve expressing the catalytic efficiency (in grams of polymer per gram of catalyst) as a function of the catalyst concentration in solution. Curve 1 in Fig. 3 shows that in experiments where the autoclave was degassed at 200°C and highest purity ethylene and solvent were used the threshold catalyst concentration was 0.15%. When the catalyst concentration is increased above its threshold value, the catalytic efficiency sharply increases, attaining a maximum of 600 g per 1 g of catalyst at a concentration of 0.2%. If the concentration is increased any further, the efficiency gradually

declines. When the concentration of impurities in the reaction mixture is raised, the curves of polymer yield against catalyst concentration in solution retain their shape, but the threshold concentrations become greater. As a result, the catalytic efficiency maximum is lowered. Curve 2 in Figs. 2 and 3 shows how the polymer yield varies with the concentration of catalyst in solution when a solvent containing 20 ppm of water is used. The graphs show that by raising the water concentration in the solvent from 50 to 20 ppm we raise the threshold catalyst concentration from 0.14 to 0.24%. This reduces the catalytic efficiency maximum from 610 to 360 g/g.

The presence of oxygen in ethylene also has a very pronounced effect on the yield of polyethylene. In Fig. 4 we have plotted the catalytic efficiency against the concentration of catalyst in solution for various concentrations of oxygen in ethylene. Experiments were run for 4 hr. It is apparent that with increasing concentration of oxygen in ethylene the threshold concentration of the catalyst rises substantially, and consequently, the catalytic efficiency maximum declines. When ethylene contains 0.1% oxygen, no polymerization takes place. Various explanations are possible to account for these effects of impurities on the threshold concentration of the catalyst. The most likely explanation is that the impurities block the catalytic surface, and only in cases where the amount of catalyst is such that the impurities introduced with the ethylene and the solvent fail to cover the entire activated surface can the polymerization proceed at any appreciable rate.

A preliminary study of the time dependence of the polymerization rate has revealed that at first the rate increases, attains a maximum, and then declines. The duration of the period during which the polymerization rate increases (which is associated with an increase in the number of new polymeric chains) depends on the purity of the ethylene and the solvent. This would lead one to assume that the impurities act in two ways: by an irreversible and slow blocking of the active centers on the catalytic surface; and by a reversible adsorption of impurities on these same centers, which slows down the primary process of chain generation.

When highly pure ethylene and solvent are used together with large amounts of catalyst, the total amount of polymer formed remains about the same – a 50% solution of polymer in the solvent. The total yield remains constant due to the fact that the rate of ethylene solution becomes very slow in the highly viscous solutions of the polymer.

The maximum yield of polymer makes it possible to estimate the number of chains generated by each atom of the active component in the catalyst. The polymers in our experiments had an average molecular weight of 100,000, and hence, if the yield is 600 g, each gram of the catalyst is responsible for the formation of $6.0 \cdot 10^{-3}$ moles of polymer. One gram of catalyst contained $5 \cdot 10^{-4}$ moles of chromium. Thus, if every chromium atom acted as a catalyst, it would be responsible for the formation of 12 chains.

In reality, however, only a very small fraction of chromium oxide is accessible to the ethylene, and hence the number of chains formed by each atom is greater. As a result, one must conclude that, in this reaction at least, chromium oxide does not simply initiate the polymerization but acts as a true catalyst by interacting repeatedly with the reagents.

LITERATURE CITED

1. M. A. Dalin, L. Ya. Vedeneeva, and R. I. Shenderova, Doklady Akad. Nauk SSSR 133, No. 1, 182 (1960).
2. Z. V. Arkhipova, A. S. Semenova, and E. Ya. Paramonkov, Zhur. Plastmass No. 1, 17 (1957).
3. Belg. Patent 570981, March 5, 1959; Chem. Abstr. 53, No. 17, 1659 (1959).

All abbreviations of periodicals in the above bibliography are letter-by-letter transliterations of the abbreviations as given in the original Russian journal. *Some or all of this periodical literature may well be available in English translation.* A complete list of the cover-to-cover English translations appears at the back of this issue.

THE INFRARED ABSORPTION SPECTRA OF THE ETHYLENIC SERIES OF ORGANOMETALLIC COMPOUNDS

CIS AND TRANS CONFIGURATIONS OF PROPENYLANTIMONY COMPOUNDS (Sb^{III} and Sb^{V})

A. E. Borisov, N. V. Novikova, and N. A. Chumaevskii

Institute of Heteroorganic Compounds, Academy of Sciences of the USSR
(Presented by Academician I. V. Obreimov, July 8, 1960)
Translated from Doklady Akademii Nauk SSSR ,
Vol. 136, No. 1, pp. 129-132, January, 1961
Original article submitted June 16, 1960

The present communication is devoted to the investigation of the infrared absorption spectra of the cis- and trans-isomers of the propenyl derivatives of trivalent and pentavalent antimony. The synthesis of these compounds has been described elsewhere [1]. As far as we know, there are no references in the chemical literature to any work devoted exclusively to the study of the infrared absorption spectra of the cis- and trans-isomers of organometallic compounds.

TABLE 1

Infrared Absorption Frequencies of the Propenyl Derivatives of Sb^{III} and Sb^{V}

$(CH_3CH{=}CH)_3 \cdot Sb$		$(CH_3CH{=}CH)_3 \cdot SbCl_2$		$(CH_3CH{=}CH)_3 \cdot SbBr_2$		$(CH_3CH{=}CH)_3 \cdot SbI_2$		$(CH_3CH{=}CH)_4 \cdot SbBr$		$(CH_3CH{=}CH)_5 Sb$	
cis, bp 70° at 4-5 mm	trans, bp 82° at 5 mm	cis, mp 74-75°	trans, bp 160-162/4	cis, mp 85-86°	trans, bp 166-167/4	cis, mp 122-123°	trans-	cis, mp 140-143°	trans, mp 45-48°	cis-, bp	trans-, bp
1600	1600	1606	1607	1604	1605	1600	1598	1600	1600	1600	1600
1438	1442	1446	1440	1443	1440	1425	1437	1445	1432	1440	1437
1378	1377	1385	1376	1382	1377	1378	1375	1380	1367	1380	1375
1320	1320	1308	1306	1305	1306	1297	1302	1305	1304	1321	1308
1193	1199	1201	1191	1199	1190	1196	1185	1195	1225	1200	1190
1115	1115	—	1109	—	1105	1100	1105	1109	1185	1115	1110
	1060	1047	1075	1045	1075		1065	1048	1062		1062
1039	1040		1042		1041	1040	1039		1043	1035	1040
970	971	940	957	939	951	{ 937	945	960	967	970	971
920	935	928		925		{ 925		924	945	920	938
710	720	665	724	—	722	—	718	700	726	—	722
660	655	625	667	663	655	660	660	660	663	660	662
	610	455	620	818	620	610	615	635	625		600
				452	—	452	—	452			

We are going to examine the results obtained from the infrared investigation of the above-mentioned compounds. Several workers [2,3] have reported on the possibility of distinguishing between the cis- and trans-isomers of organic compounds by means of infrared spectroscopy; disubstituted ethylene derivatives of the type $R_1-CH{=}$ $=CH-R_2$ have bonds at 690 cm^{-1} and 960-970 cm^{-1}, the former being characteristic for the cis- and the latter for the trans-configuration.

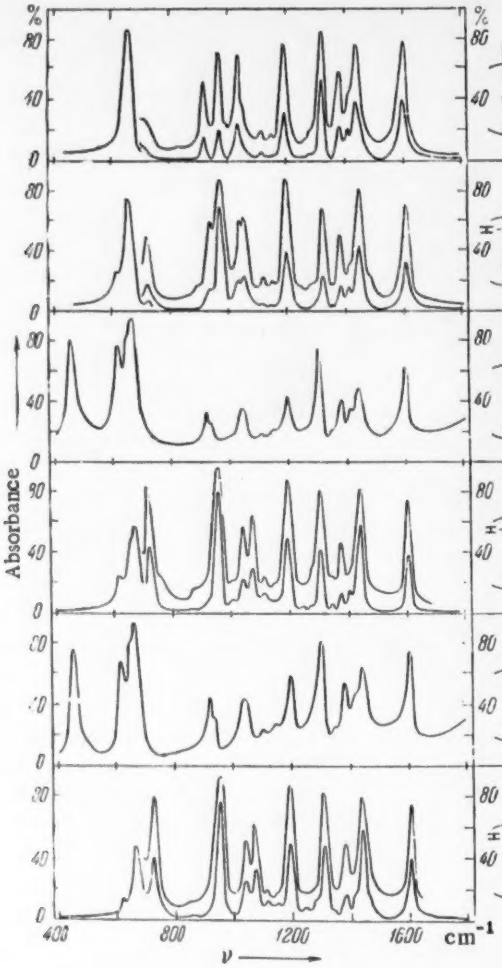

Fig. 1.

TABLE 2

Infrared Absorption Bands of Propenyl Bromide

Cis, bp 57.5-58°	Trans, bp 63.5°	Cis, bp 57.5-58°	Trans, bp 63.5°
1625	1650		{ 1100
	1610	1102	{ 1085
1587	1583	{ 1050	{ 1055
1448	1440	{ 1030	{ 1035
1392	1386	931	930
1305	1299		722
1212		674	675

According to the data reported in the two papers cited above, the isomers can be differentiated in most cases by the fact that the 970 cm^{-1} band found in the spectra of trans-isomers does not appear in the spectra of cis-isomers. We would like to point out, though, that certain calculations have been done [4], the results of which indicate that the absorption bands for the out-of-plane vibrations of the CH bonds adjacent to the double bond should appear at almost the same frequency in either isomer (the frequency range of 965-980 cm^{-1} is usually given for both the cis- and trans-configurations, for vibrations of the type

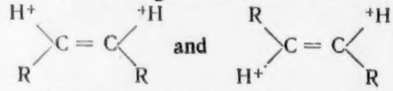

); the authors of the paper just cited utilized the experimental data reported in [5], where it is also shown that in the two isomeric forms of disubstituted butenes the out-of-plane vibrations of the corresponding CH bonds give rise to absorption bands at frequencies so similar as to be almost undistinguishable.

From what has just been said, it is quite obvious that above-mentioned criteria are inadequate by themselves for any conclusive assignment of geometrical configuration, and hence one has to be very careful in interpreting the infrared data connected with trans- and cis-isomerism.

We carried out our measurements on a double-beam model VIK M-3 infrared spectrometer using NaCl prisms (700-1800 cm^{-1} range), and on a single-beam IKS-12 spectrometer using KBr prisms (400-700 cm^{-1} range). Liquids were studied in cells of fixed dimensions (0.016 mm path length with KBr windows, and 0.050 mm with NaCl windows). Solids were compressed in KBr pellets.

The stereoisomers studied by us were assigned configurations through a careful comparison of the infrared absorption spectra [6] of each set of isomers, and on the basis of a rule previously established by us in cooperation with A. N. Nesmeyanov, that the configurations of cis- and trans-ethylene derivatives remain unchanged in electrophilic substitution reactions and in homolytic exchange [1,7,8]. All of the propenyl derivatives of antimony investigated by us (Sb^{III} and Sb^{V}) yielded distinctly different infrared absorption spectra for the cis- and trans-configurations (Figs. 1 and 2, Table 1).

All the trans-isomers (hydrogens trans across to the double bond) exhibited a characteristic strong absorption band in the 945-970 cm^{-1} region. Whereas the out-of-plane CH bond vibrations in tripropenyl and pentapropenyl stibine absorb at 971 cm^{-1}, the corresponding halo derivatives – dichloro, dibromo, and diiodotripropenyl stibine – exhibit a steady shift toward 945 cm^{-1} in that same order, while tetrapropenyl bromostibine absorbs at 967 cm^{-1}.

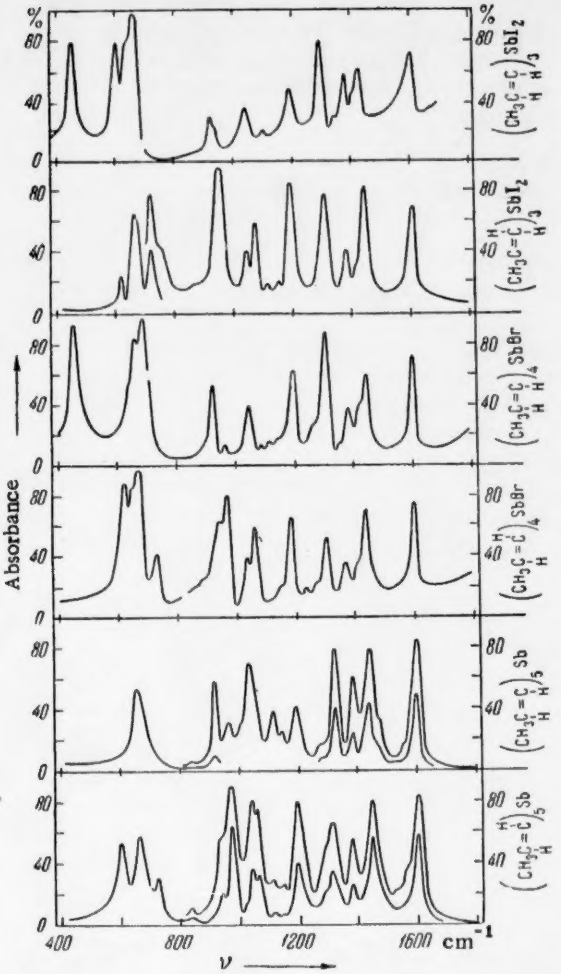

Fig. 2.

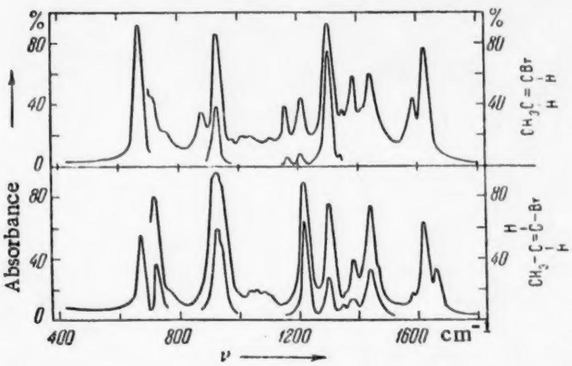

Fig. 3.

We also should mention another prominent feature in the infrared spectra of the trans-isomers by which this configuration may be recognized: absorption bands in the 718-726 cm^{-1} region (Table 1, Figs. 1 and 2); all of our trans-derivatives exhibited bands in this region, while none of the cis-derivatives did. Though the cis-isomers of our compounds exhibited absorption bands around 920-940 cm^{-1}, these were generally considerably weaker than the corresponding bands exhibited by the trans-isomers in the 945-970 cm^{-1} region. Only cis-tripropenyl stibine and cis-pentapropenyl stibine absorb at frequencies close to the absorption frequencies for the out-of-plane CH bond vibrations of the corresponding trans-isomers (970 cm^{-1}), but fortunately the bands of the trans-configuration are about three times as strong as those of the cis-isomers (we computed the areas under the bands). The same has previously been observed in the case of propenyl bromide (Table 2, Fig. 3): The 930 cm^{-1} absorption band of the trans-isomer is also about three times as intense as the corresponding band of the cis-isomer.

The infrared spectra of both the trans- and the cis-isomer exhibit absorption bands in the 655-660 cm^{-1} region, but these bands are about 2-2.5 times as intense in the spectra of the cis-isomers as are the corresponding bands in the spectra of trans-isomers (these values were obtained by comparing the spectra of isomeric tripropenyl stibines and the spectra of the cis- and trans-propenyl bromides). Of the low-frequency bands, we would like to mention the relatively strong bands at 452 cm^{-1}, which are found in the infrared spectra of cis-tripropenyl derivatives of dichloro, dibromo, and diiodostibine and cis-tetrapropenyl bromostibine; the corresponding trans-derivatives exhibit no bands at 452 cm^{-1}. These bands are also absent in the spectra of both the cis- and trans-isomers of tri- and pentapropenyl stibine.

As far as the in-plane vibrations* of the CH bonds adjacent to the double bond are concerned, they give rise to absorption bands (1200 to 1300 cm^{-1}) with frequencies apparently independent of molecular configuration; however, a certain inverse relationship exists between the intensities (measured at the band maximum) of the 1200 cm^{-1} and the 1300 cm^{-1} bands in the spectra of each set of isomers.

*Vibrations confined to the plane of the C=C bond.

Thus, if the trans-isomer has the 1300 cm^{-1} band more intense than the 1200 cm^{-1} band, the cis-isomer will have the intensities exactly reversed, i.e., the absorption band at 1300 cm^{-1} will be less intense than that at 1200 cm^{-1}. No differences attributable to isomerism are detected in the region of carbon—hydrogen deformation vibrations (1380-1450 cm^{-1}). The double bonds in each set of isomers absorb at about the same frequency and with about the same intensity, regardless of the configuration.

The authors wish to express their gratitude to Academician I. V. Obreimov for his interest in this work, and to R. A. Isaeva and E. D. Vlasov for their assistance in obtaining the infrared absorption spectra.

LITERATURE CITED

1. A. N. Nesmeyanov, A. E. Borisov, and N. V. Novikova, Izvest. Akad. Nauk SSSR, Otdel Khim. Nauk No. 7, 1216 (1959).
2. L. Bellamy, Infrared Spectra of Complex Organic Molecules [Russian translation] (IL, 1957) p. 53.
3. N. Sheppard, J. Inst. Petrol. 37, No. 327, 99 (1951).
4. N. Sheppard and A. B. B. M. Sutherland, Proc. Roy. Soc. A196, 195 (1949).
5. H. Gerschinowitz and E. B. Wilson, J. Chem. Phys. 6, 247 (1938).
6. A. N. Nesmeyanov, A. E. Borisov, and N. V. Novikova, Izvest. Akad. Nauk SSSR, Otdel Khim. Nauk No. 1, 147 (1960); Tetrahedron Letters No. 8, 23 (1960).
7. A. N. Nesmeyanov and A. E. Borisov, Doklady Akad. Nauk SSSR 60, 67 (1948).
8. A. N. Nesmeyanov, A. E. Borisov, and N. V. Novikova, Doklady Akad. Nauk SSSR 119, 504 (1958).

All abbreviations of periodicals in the above bibliography are letter-by-letter transliterations of the abbreviations as given in the original Russian journal. *Some or all of this periodical literature may well be available in English translation.* A complete list of the cover-to-cover English translations appears at the back of this issue.

INVESTIGATION OF THE FINE STRUCTURE IN THE K-EDGES OF THE X-RAY ABSORPTION SPECTRA OF MANGANESE IN MnTe AT THE ANTIFERROMAGNETIC TRANSITION TEMPERATURES

É. E. Vainshtein, B. I. Kotlyar, and R. M. Obrutskaya

Institute of Inorganic Chemistry, Siberian Branch, Academy of Sciences of the USSR
and the K. D. Ushinskii Odessa Pedagogical Institute
(Presented by Academician A. P. Vinogradov, July 4, 1960)
Translated from Doklady Akademii Nauk SSSR,
Vol. 136, No. 1, pp. 133-135, January, 1961
Original article submitted June 29, 1960

It has recently been proposed [1] that certain features of the fine structure in the x-ray absorption spectra of transition elements in ferrites may possibly be caused by the antiferromagnetic alignment of electron spins in the investigated compounds. The conclusion was based on the analysis of many absorption spectra of iron in various ferrites [1], not all of which have been thoroughly enough characterized with respect to their structure and magnetic properties, and consequently the preliminary results required further verification and improvement through a series of specifically designed experiments. It therefore seemed particularly important that we investigate the temperature dependence of the fine structure in the x-ray spectra of paramagnetic atoms in antiferromagnetic surroundings at magnetic transition temperatures. Of the relatively few antiferromagnetic compounds suitable for such a study, we selected MnTe. The compound has been previously examined very thoroughly by x-ray diffraction [2,3], and has a conveniently located Néel point ($T_N = 310°K$).

The experimental sample of manganese telluride was kindly donated to us by N. P. Grazhdankina, for which we would like to thank her. It was prepared by fusing finely dispersed and thoroughly mixed powdered manganese and tellurium in an evacuated and unsealed quartz tube at 800°C.* To eliminate gaseous impurities, the manganese was remelted several times in high vacuo.

The freshly prepared manganese telluride was annealed at low temperatures. An x-ray structural analysis indicated that the melt contained primarily a MnTe phase with only a trace of $MnTe_2$. Grazhdankina had previously investigated the physical properties of this melt in the 250-370°K temperature range [3], which spans the Néel point.

It has been found that when the electrical resistance and the magnetic susceptibility of MnTe are plotted against temperature both curves exhibit a sharp break at $T_N = 310°K$, while the curve representing the temperature dependence of the crystal lattice parameter $\underline{c}$ changes direction. However, a transition through the Néel point seems to leave the crystal lattice otherwise unchanged, since the second parameter remains a linear function of temperature. Hence, a transition from room temperature (antiferromagnetic state) to temperature above T_N seems to be only accompanied by an anomalous expansion of the crystal along the $\underline{c}$ axis, and since the c/a axial ratio thus increases, the unit cell dimensions of the compound do not remain the same.

*The original manganese contained: 0.07% S, 0.07% CO, and 0.03% P; tellurium contained: 10^{-4} % Cu, $2 \cdot 10^{-4}$ % Ag, $<10^{-4}$% Bi, and 10^{-4}% Sb and As.

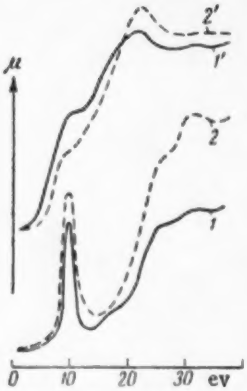

Fig. 1. K x-ray absorption spectra of manganese in: 1) $KMnO_4$; 2) pure metal; one set of measurements was obtained by us on the focusing spectrograph, while the other (broken lines) was obtained [4] on a double crystal spectrometer using an ionization gauge.

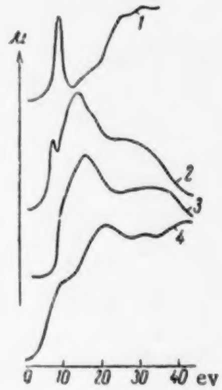

Fig. 2. A comparison between the fine structures in the absorption spectra of manganese in: 1) $KMnO_4$; 2) MnTe at 50°C; 3) MnTe at 8°C; 4) in pure metal (the two temperatures are above and below the Néel temperature, respectively).

Fig. 3. The fine structure in the absorption spectra of manganese in MnTe at various temperatures: 1) 50°C; 2) 44°C; 3) 38°C; 4) 21°C; 5) 8°C (T_N = = 310°K).

The K x-ray absorption spectra of manganese in the telluride were obtained on an x-ray spectrograph using the Johann focusing technique. As a reflecting crystal we used quartz cleaved along the (13$\bar{4}$0) plane and with d = 1.17 A. The crystal had a 500 mm radius of curvature. First-order reflections were recorded on photographic film. The $K\alpha_{1,2}$ lines of iron were used as reference. In this region, the instrument produced a dispersion of 2.6 X/mm. Since the solid contained a large amount of a relatively heavy element (tellurium), the optimum absorber thickness had to be chosen very carefully toensure good resolution of the structural details in the spectra. We found out that to get a well-resolved fine structure of the absorption edge it is best to use absorbers in which the specific content of Mn is 4 mg/cm². Any increase or decrease in the absorber thickness produces a loss of contrast at the edge.

The x-ray tube operated best at 30 kv and 40 milliamp. Exposure lasted 6 hr. In experiments where absorption spectra at various sample temperatures were desired, the absorber was deposited on an aluminum foil, which was then pressed tightly against a copper ring through which a liquid could be forced under pressure from an ultrathermostat. Provided the contact between the aluminum foil and the polished ring surface was good, the temperature throughout the absorber would remain constant during the entire exposure period. The temperature was recorded (with a precision of 0.2-0.3°C) by a means of a copper-constantan thermocouple tightly pressed against the sample.

The absorption spectra of Mn in MnTe were investigated at five different temperatures in the range from 280 to 325°K (T_N = 310°K). At each temperature we recorded 3-4 spectra; these were subjected to individual photometric measurements,and corresponding points averaged. To check the resolution of our spectroscopic apparatus, we used it also to record the x-ray absorption of Mn by itself and in $KMnO_4$; the resulting spectra were then compared with those obtained by Hanson and Beeman [4] on a double crystal spectrometer with ionization gauge recording. The spectra are compared in Fig. 1. In Figs. 2 and 3 we have presented our own experimental results. After analyzing these results, we arrived at the following conclusions:

1. A transition from the metallic state to manganese telluride is accompanied by a considerable decrease in the energy of the 4p state of the transition metal. The observed long-wave shift in the corresponding maximum on the absorption curve of manganese in MnTe is 5.4 ev

2. When MnTe is in the para state, a distinct long-wave "white" line appears in the absorption edge of manganese; the line is located very closely to the "region of initial absorption" found in the spectrum of pure metal, and practically coincides with the intensity maximum of the "white" absorption band observed in the spectrum of this same element in $KMnO_4$. It is now fairly well established [5,6] that in the latter case ($KMnO_4$) the appearance of this line in the spectra of manganese is somehow connected with the transition of photoelectrons into the region of hybridized 3d states of Mn in the compound.

3. As one approaches the Néel point with MnTe still in the para state, the "white" absorption line in the spectrum of manganese smoothly declines in intensity, which indicates that the probability of the corresponding electronic transitions gradually decreases. It is conceivable that this decline is somehow connected with the smooth (linear) change in the crystal lattice parameters of manganese telluride (previously detected in this temperature range [2,3]), and the corresponding decrease in the c/a ratio of the hexagonal lattice.

4. When the Néel temperature is passed, the long-wave "white" line in the absorption spectrum of the transition metal either disappears entirely or is greatly reduced in intensity. On the other hand, the position and the relative intensity of the first absorption maximum, which is connected with the transitions of the photoelectrons of the absorbing atom into the 4p states of the metal, remain about the same in the compound as in pure metal, and also remain unchanged after transition through the ferromagnetic Curie temperature [7,8].

And thus our new results are in good agreement with some of our earlier observations [1] and conclusions regarding the influence of antiferromagnetic alignment in compounds on the fine structure in the x-ray absorption spectra of the transition-metal components of such compounds as MnTe. With regard to the theoretically important questions: to what extent are tellurium atoms involved in interactions between the manganese atoms in antiferromagnetic MnTe, and whether one can apply to this case the criteria developed to account for the role of oxygen in antiferromagnetic crystals of transition-metal oxides, all we can say is that they cannot be answered at the present time strictly on the basis of the available experimental data but will require additional research.

LITERATURE CITED

1. É. E. Vainshtein, B. I. Kotlyar, and G. A. Shapiro, Doklady Akad. Nauk SSSR 125, 55 (1959).
2. S. Greenwald, Acta Crystallogr. 6, 396 (1953).
3. N. P. Grazhdankina and D. I. Gurfel', Zhur. Éksp. i Teoret. Fiz. 35, 907 (1958).
4. H. Hanson and W. W. Beeman, Phys. Rev. 76, 118 (1949).
5. R. L. Barinskii, É. E. Vainshtein, and K. I. Narbutt, Doklady Akad. Nauk SSSR 83, 199 (1952).
6. R. L. Barinskii and E. G. Nadzhakov, Izvest. Akad. Nauk SSSR, Ser. Fiz. 24, 407 (1960).
7. É. E. Vainshtein, X-ray Spectra of Atoms in Molecules and Fused Salts [in Russian] (Izd. AN SSSR, 1950).
8. A. V. Trapeznikov, Dissertation [in Russian] (Sverdlovsk, 1956).

All abbreviations of periodicals in the above bibliography are letter-by-letter transliterations of the abbreviations as given in the original Russian journal. *Some or all of this periodical literature may well be available in English translation.* A complete list of the cover-to-cover English translations appears at the back of this issue.

A MATHEMATICAL THEORY FOR THE STATIONARY COMBUSTION OF SOLIDS

V. N. Vilyunov

The Siberian Physicotechnical Institute at the V. V. Kuibyshev Tomsk State University

(Presented by Academician V. N. Kondrat'ev, July 2, 1960)
Tr- slated from Doklady Akademii Nauk SSSR,
Vol. 136, No. 1, pp. 136-139, January, 1961
Original article submitted June 23, 1960

One mathematical theory for the combustion of powders has already been proposed by Ya. B. Zel'dovich [1]. The theory was good for very high pressures, when the evolution of heat in the solid phase (s-phase) can be neglected in comparison with the heat generated in the gas phase (g-phase), and when the combustion is controlled by reactions in the g-phase. In the present paper we are going to extend the theory to cases involving combustion at low pressures.

We will assume a three-stage model for the combustion process (stages α, β, and γ). A coordinate system is chosen in which the flame is stationary. The process of stationary flame propagation by thermal diffusion in the ith stage can be described by the following system of equations:

$$\lambda_i T'' - c_i m T' + Q_i f_i(n, T) = 0, \tag{1}$$

$$\rho_i D_i n'' - mn' - f_i(n, T) = 0. \tag{2}$$

where T(y) is the temperature, n(y) is the ratio of two dimensionless concentrations of the reactant, λ_i and D_i are the thermal conductivity and diffusion coefficients respectively, c_i is the heat capacity, Q_i is the heat of reaction, $f_i(n,T)$ is the over-all rate of the chemical reaction, m is the rate of combustion (by weight) in the powder, and ρ_i is the density.

Stage α (s-phase). Let us assume that $D_\alpha = 0$, and that the over-all reaction rate is independent of pressure. Equations (1) and (2) yield the first integral:

$$\lambda_\alpha T_s' = c_\alpha m (T_s - T_0) - mQ_\alpha \quad \text{or} \quad \lambda_\alpha T_s' = c_\alpha m (T_s - T_{s1}) \tag{3}$$

where T_s (the temperature at the surface of the s-phase) is a parametric function of pressure p and initial temperature T_0; $Q_\alpha = c_\alpha (T_{s1} - T_0)$, where T_{s1} is the surface temperature during flameless combustion [2] (where the flow of heat from inside the g-phase is negligibly small).

The mass combustion rate can be determined by integrating the thermal conductivity equation (1) (with $i = \alpha$) and respecting the following boundary conditions:

$$\begin{aligned} y &= -\infty, \quad T = T_0 \quad (T'(-\infty) = 0); \\ y &= 0, \quad T = T_s, \lambda_\alpha T_s' = c_\alpha m (T_s - T_{s1}). \end{aligned} \tag{4}$$

To be more explicit, by using the approximate method of Ya. B. Zel'dovich and D. A. Frank-Kamenetskii [4], we can determine the mass combustion rate as a function of the physical constants of the s-phase,

$$m^2 = 2\delta k_\alpha \varkappa_\alpha \frac{RT_s^2}{E_\alpha (2T_s - T_{s1} - T_0)} e^{-E_\alpha/RT_s}, \tag{5}$$

where δ is the density of the powder, k_α is a frequency factor, and κ_α is the thermal conductivity of the s-phase.

Equation (5) is identical with the formula derived by A. G. Merzhanova and F. I. Dubovitskii [5]. The width of the combustion zone in the s-phase can be determined by solving the following approximate equations:

$$y_\alpha = \frac{\lambda_\alpha}{c_\alpha m} \ln \frac{0{,}05T_0}{T_s - T_0}. \tag{6}$$

We cannot get an expression for the linear combustion velocity as a function of pressure, since Eq. (5) includes the surface temperature T_s, a still unknown function of pressure; in order to get $m = m(p)$ and $T_s = T_s(p)$, we will connect the combustion rate with the physicochemical functions in the β-stage.

Stage β. Let us assume that the over-all reaction in this stage is exothermic and leads to incomplete combustion products (NO, CO). At low pressures this is the terminal stage in the combustion process. We will denote the maximum temperature achieved at this stage by T_{11}. At high pressures, the flame stage (stage γ) begins to exert an influence on the processes taking place in the β-stage, and a temperature $T_1 > T_{11}$ arises at the boundary separating stage β from stage γ. Let us assume that T_1 (just as T_s) is a parametric function of p and T_0. With the help of a commonly used assumption that $D_\beta = \lambda_\beta / c_\beta \rho_\beta$, we get a first integral from the system of equations (1) and (2) (with $i = \beta$),

$$n = \frac{a}{a_{s1}} = \frac{T_1 - T}{T_1 - T_s} \tag{7}$$

(this is the Ya. B. Zel'dovich integral).

By integrating Eq. (1) for $i = \beta$ and applying the following boundary conditions:

$$\begin{aligned} y &= 0, \quad T = T_s, \quad \lambda_\alpha T_s' = c_\alpha m\,(T_s - T_{s1}); \\ y &= y_1, \quad T = T_1, \lambda_\beta T_1' = c_\beta m\,(T_1 - T_{11}), \end{aligned} \tag{8}$$

we can get an expression for the mass rate.

Using the method given in [4], we finally get:

$$m^2 = \frac{2\lambda_\beta Z_\beta (\nu_\beta)! \left(\frac{RT_1^2}{E_\beta}\right)^{\nu_\beta + 1}}{c_o\,(2T_1 - T_{11} - T_{s1})\,(T_1 - T_s)^{\nu_\beta}} e^{-E_\beta/RT_1}, \quad Z_\beta = k_\beta \mu_\beta a_{s1}^{\nu_\beta - 1} \left(\frac{p}{RT_1}\right)^{\nu_\beta}. \tag{9}$$

Equation (9) expresses the mass combustion rate as a function of the physical constants in stage β. In integrating, we assumed the usual expression for the over-all chemical reaction rate

$$f_\beta(T) = k_\beta \frac{\mu_\beta}{a_{s1}} \left(\frac{a_s p}{RT}\right)^{\nu_\beta} \left(\frac{T_1 - T}{T_1 - T_s}\right)^{\nu_\beta} e^{-E_\beta/RT}, \tag{10}$$

where μ_β is the average molecular weight, ν_β is the over-all order of reaction, E_β is the effective activation energy, a_{s1} is the relative concentration of the reactant at the surface separating stage β from stage γ during flameless combustion, and a_s is the relative concentration when the g-phase exerts some influence on the processes taking place in the s-phase.

In deriving Eq. (9) we assumed that $a_s \equiv a_{s1}$.

The width of the combustion zone in the stage β can be determined from the equation

$$y_1 \simeq \frac{\lambda_\beta}{c_\beta m} \ln \frac{T_1 - T_{s1}}{T_s - T_{s1}}. \tag{11}$$

Stage γ (flame stage). In this stage, we have an exothermic reaction between the reaction products of the β-stage, mainly NO and CO. Assuming $D_\gamma = \lambda_\gamma / c_\gamma \rho_\gamma$, we get $n = \frac{T_{21} - T}{T_{21} - T_1}$. Integrating Eq. (1) (with $i = \gamma$), and maintaining the boundary conditions

$$\begin{aligned} y &= y_1, \quad T = T_1, \quad \lambda_\beta T_1' = c_\beta m\,(T_1 - T_{11}); \\ y &= +\infty, \ T = T_{21}\,(T'(+\infty) = 0), \end{aligned} \tag{12}$$

we get the equation

$$m^2 = \frac{2\lambda_\gamma Z_\gamma (\nu_\gamma)! \, (RT_{21}/E_\gamma)^{\nu_\gamma+1}}{c_\gamma (T_{21}-T_{11})(T_{21}-T_1)^{\nu_\gamma}} e^{-E_\gamma/RT_{21}}; \quad Z_\gamma = k_\gamma \mu_\gamma a_1^{\nu_\gamma - 1} \left(\frac{p}{RT_{21}}\right)^{\nu_\gamma}. \tag{13}$$

The width of the combustion zone in the flame stage is given by the equation

$$y_2 - y_1 = \frac{\lambda_\gamma}{c_\gamma m} \ln \frac{T_{21} - T_{11}}{T_1 - T_{11}}. \tag{14}$$

With increasing pressure, T_1 and m increase, and consequently the combustion zone becomes narrower. In the limiting case when $T_1 \to T_{21}$ the combustion will take place in only two stages. This limiting case will probably be found in cases where the combustion of powders takes place under very high pressure and the flame is very close to the surface of the s-phase.

T_0, °C	V, cm/sec	p, kg/cm²	k_p	k_T, $\frac{1}{°K}$	$y_1 \cdot 10^4$, cm	$y_n \cdot 10^4$, cm	T_s, °K
+25	0.2	3.0	0.56	0.0049	6.88	122	756
	0.4	10.0	0.58	0.0048	22.7	63.1	808
	1.0	44.0	0.67	0.0044	5.0	26.2	890
	1.4	71.2	0.74	0.0041	2.8	19.0	924
−55	0.2	6.2	0.58	0.0055	37.2	139	756
	0.4	19.5	0.63	0.0053	12.8	71.2	808
	1.0	71.0	0.87	0.0042	2.5	29.4	890

Equations (5), (9), and (13) essentially provide a solution of the problem inasmuch as they make it possible to evaluate the functions $m = m(p, T_0)$, $T_s = T_s(p, T_0)$, $T_1 = T_1(p, T_0)$. The calculations can be simplified considerably if we limit ourselves to the case of combustion at very low pressures, where the effects of the flame stage ($T_1 \equiv T_{11}$) can be neglected. For this particular case, the pressure coefficient k_p and the temperature coefficient k_T can be expressed in the form:

$$k_p = \left(\frac{\partial \ln m}{\partial \ln p}\right)_{T_0} \simeq \frac{\nu_\beta}{2}\left[1 - \frac{\nu_\beta}{T_{11} - T_s} \frac{RT_s^2}{E_\alpha}\right]^{-1}, \tag{15}$$

$$k_T = \left(\frac{\partial \ln m}{\partial T_0}\right)_p \simeq \frac{k_p}{\nu_\beta}\left[\frac{E_\beta}{RT_{11}^2} - \frac{\nu_\beta}{T_{11} - T_s} + \frac{\nu_\beta + 2}{T_{11}}\right]. \tag{16}$$

An examination of Eqs. (15) and (16) reveals that as T_s (or pressure) increases so does k_p; when $A < 1$, the temperature coefficient k_T increases with T_s, while if $A > 1$ it decreases with increasing T_s. The parameter A is equal to

$$A = \frac{E_\alpha}{E_\beta}\left(\frac{T_{11}}{T_s}\right)^2 \left(1 + \frac{\nu_\beta + 2}{E_\beta} RT_{11}\right)^{-1}. \tag{17}$$

Using the equations just derived, we carried out a series of calculations for the case of powdered nitroglycerin. The composition of this powder and experimental data pertaining to its combustion have been reported in [6]. The following data were used in our calculations: $T_{s1} = 700$°K, $E_\alpha = 32{,}000$ cal/mole, $\delta = 1.6$ g/cm³, $C_\alpha = C_\beta = 0.35$ cal/g · deg, $T_{11} = 1085$°K, $E_\beta = 21{,}000$ cal/mole, $\lambda_\alpha = \lambda_\beta = 4 \cdot 10^{-4}$ cal/cm · sec · deg, μ_β = = 27 g/mole, $k_\beta = 0.93 \cdot 10^{10}$ sec^{-1}, and $\nu_\beta = 1$.

To simplify our calculations, we replaced the exact equation (5) by the following approximate expression:

$$V = B_\alpha e^{-E_\alpha/2RT_s}, \text{where } B_\alpha = 0{,}875 \cdot 10^4 \text{ cm/sec}.$$

The results of our calculations are tabulated in the table.

LITERATURE CITED

1. Ya. B. Zel'dovich, Zhur. Éksp. i Teoret. Fiz. 12, 498 (1942).
2. P. F. Pokhil, Collection: Detonation Physics [in Russian] (1953) Vol. 2.
3. K. K. Andreev, Thermal Decomposition and Combustion of Explosives [in Russian] (Moscow, 1957).
4. Ya. B. Zel'dovich and D. A. Frank-Kamenetskii, Zhur. Fiz. Khim. 12, 100 (1938).
5. A. G. Merzhanov and F. I. Dubovitskii, Doklady Akad. Nauk SSSR 129, No. 1 (1959).
6. R. D. Geckler, Selected Combustion Problems (London, 1954) p. 289.

All abbreviations of periodicals in the above bibliography are letter-by-letter transliterations of the abbreviations as given in the original Russian journal. *Some or all of this periodical literature may well be available in English translation.* A complete list of the cover-to-cover English translations appears at the back of this issue.

THE NATURE OF ELECTRICAL CONDUCTANCE IN ALKALI-FREE BARIUM SILICATE GLASSES

K. K. Evstrop'ev and V. A. Khar'yuzov

(Presented by Academician A. N. Terenin, July 4, 1960)
Translated from Doklady Akademii Nauk SSSR,
Vol. 136, No. 1, pp. 140-142, January, 1961
Original article submitted June 24, 1960

The problem of electrical conductivity in alkali-free silicate and borate glasses is of considerable theoretical and practical importance, particularly in connection with electrical insulating technology. Whereas experimental evidence leaves no doubt as to the ionic nature of conductivity in alkali silicate and borate glasses, there is a great divergence of opinion concerning the nature of charge carriers in alkali-free glasses. As is well known, the most reliable technique for determining the nature of charge carriers in solid glasses has been devised by Tubandt [1-3]: It involves determining how well Faraday's law holds. If, however, the investigated glasses have a very low specific conductance (as is the case in alkali-free glasses of the type mentioned above), one cannot safely rely on the accuracy of the results obtained by this method.

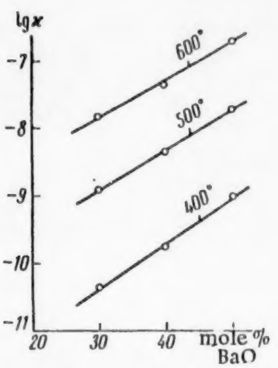

Specific electrical conductance isotherms for glasses of the $BaO-SiO_2$ system.

That quite a number of workers [4-7] have arrived at entirely conflicting conclusions, when they relied mainly on experiments in which electrical conductance was studied as a function of composition, is not at all surprising, since the method cannot distinguish between ionic and electronic conductance in alkali-free glasses.

In order to establish the nature of charge carriers in these glasses, we decided to use a method which had not been previously tried on such cases: The experimentally determined electrical conductance is simply compared with the conductance calculated from diffusion coefficients (which can be determined by means of radioactive isotopes) using Einstein's equation [8,9]. Einstein has derived a general equation connecting diffusion with electrical conductance: $D = \frac{n\kappa kT}{N(ze)^2}$, where D is the diffusion coefficient in cm^2/sec, κ is the specific conductance in $ohm^{-1} \cdot cm^{-1}$, $\underline{n}$ is the transference number of the diffusing ion, $\underline{k}$ is the Boltzmann constant, T is the absolute temperature in °K, N is the number of ions per 1 cm^3, $\underline{z}$ is the ionic valence, and $\underline{e}$ is the charge of the electron.

Blow and Fitzgerald [11], and also one of the authors [10], have shown that in alkali glasses the logarithms of the electrical conductivities computed from the experimentally determined diffusion coefficients of sodium ions do not differ by more than 0.3 units from the logs of directly measured conductances. Since there is no doubt about the ionic nature of conductance in alkali silicate glasses, then, if we should get good agreement between the directly measured conductances and those computed from diffusion coefficients, the problem of what the charge carriers in alkali-free glasses are would be solved conclusively. In cases where we have electron conductance, the specific conductance computed on the assumption of ionic mobility should differ by several orders of magnitude from that measured directly; this has indeed been found to be the case in calcium vanadate glasses (18 mole% CuO and 82% V_2O_5).

In accordance with what has just been discussed, our problem involved the following steps.

1. The electrical conductance of selected alkali-free glasses had to be measured over a wide range of temperatures.

2. The diffusion coefficients of ions (all potential charge carriers) had to be determined.

3. The experimentally determined electrical conductances were then compared with those computed from diffusion coefficients (using Einstein's equation) in order to deduce the correct conductance mechanism.

We selected for our work barium silicate glasses, since they remain as glasses over a wide range of temperatures. Glasses containing 30, 40, and 50 mole% BaO were prepared by fusing pure $BaCO_3$ with carefully picked sand in 6-liter quartz crucibles at 1550°C in a high-frequency furnace.* The specific conductance was measured in the usual way in the 350-650°C temperature range, by means of a model MOM-4 megohmmeter.

The experimental data are recorded in the figure. The figure shows that within the investigated temperature range, the specific conductance increases substantially with increasing BaO content. In one of the glasses (50 mole% BaO, 50% SiO_2) we also determined the diffusion coefficients of Na^+ and Ba^{++} at 655°C. The choice of glass and of such a high temperature was not intentional, but was forced upon us by the low diffusion coefficients of these ions. The diffusion coefficients were determined with the help of Na^{22} and Ba^{140} tracers by using the method in which successive thin layers of glass are ground away [12,13].

Let us compute what the electrical conductance of our glass would be if only Ba^{++} ions served as charge carriers. We will write Einstein's equation in a slightly different form:

$$\varkappa_{Ba} = \frac{4e^2 D_{Ba} \cdot N_{Ba}}{kT} = \frac{7,2 \cdot 10^{-15} D_{Ba} \cdot N_{Ba}}{T} =$$

$$= \frac{7,2 \cdot 10^{-15} \cdot 1,1 \cdot 10^{22} \cdot (2 \pm 1) \cdot 10^{-12}}{928} = (1,7 \pm 0,8) \cdot 10^{-7}\ \text{ohm}^{-1} \cdot \text{cm}^{-1},$$

where κ_{Ba} is the glass conductance if Ba^{++} ions are assumed to be the charge carriers, D_{Ba} is the experimentally determined diffusion coefficient of Ba^{++}, and N_{Ba} is the Ba^{++} concentration per 1 cm^3 of glass.

In precisely the same manner, we will compute what the electrical conductance of the glass would be if only the Na^+ ions still present in the glass as an impurity acted as charge carriers. A chemical analysis indicated that the Na_2O content did not exceed 0.02 weight %. Consequently,

$$\varkappa_{Na} = \frac{1,8 \cdot 10^{-15} D_{Na} \cdot N_{Na}}{T} = \frac{1,8 \cdot 10^{-15} \cdot 1,5 \cdot 10^{19} \cdot (2 \pm 1) \cdot 10^{-12}}{928} =$$

$$= (5,8 \pm 3) \cdot 10^{-11}\ \text{ohm}^{-1} \cdot \text{cm}^{-1}.$$

The experimentally determined diffusion coefficients of Na^+ and Ba^{++} at T = 655°C in a glass containing 50% (mole) BaO and 50% SiO_2, and the electrical conductances calculated for this glass from these data, are shown below, together with the experimental value of conductance:

D_{Ba}, cm^2/sec	D_{Na}, cm^2/sec	$-\lg \varkappa_{Ba}$	$-\lg \varkappa_{Na}$	$-\lg \varkappa_{exp}$
$(2 \pm 1) \cdot 10^{-12}$	$(2 \pm 1) \cdot 10^{-12}$	6,8±0,2	10,3±0,3	6,3±0,2

These results clearly show that the difference between the experimentally determined electrical conductance (κ_{exp}) and the one attributed to Ba^{++} ions (κ_{Ba}) lies entirely within the range of experimental errors, whereas that due to Na^+ ions (κ_{Na}) differs from κ_{exp} by almost 4 orders of magnitude.

Thus, after comparing the electrical conductances computed from experimentally determined diffusion coefficients with the conductance measured directly, we are obliged to conclude that it is barium ions which are responsible for the transfer of electricity in alkali-free barium silicate glasses.

It is obvious that these results can also be extended to other alkali-free silicate glasses containing oxides of divalent metal ions.

* The authors want to thank E. V. Podushko for his assistance in carrying out this high-temperature fusion.

And thus we have successfully established that, although the alkali ion impurities have mobilities comparable with those of barium ions in alkali-free barium silicate glasses, their contribution to the total conductance is rather small due to their low concentration. The principal carriers of electrical current in alkali-free barium silicate glasses are the barium ions.

LITERATURE CITED

1. G. Ostroumov, Zhur. Obshchei Khim. 19, 407 (1949).
2. K. S. Evstrop'ev and G. A. Pavlova, Trudy Leningrad. Tekhnolog. Instituta imeni Lensoveta No. 46, 49 (1958).
3. O. V. Mazurin, G. A. Pavlova, et al., Zhur. Tekh. Fiz. 27, 2702 (1957).
4. B. I. Markin and R. L. Myuller, Zhur. Fiz. Khim. 7, No. 4, 592 (1936).
5. O. V. Mazurin and E. Ya. Lev, Izvest. Vysshykh Ucheb. Zaved., Fizika No. 3 (1960).
6. S. W. Strauss, W. H. Harrison et al., J. Res. Nat. Bur. Stand. 56, No. 3, 135 (1956).
7. G. A. Pavlova, Izvest. Vysshykh Ucheb. Zaved., Khim. i Khim. Tekhnologiya No. 5 (1958).
8. N. Mott and R. Henry, Electronic Processes in Ionic Crystals [Russian translation] (IL, 1950).
9. A. B. Lidiard, Handbuch d. Physik 20, No. 20, 246 (1957).
10. K. K. Evstrop'ev, Transactions of the Second All-Union Conference on the Physics of Dielectrics [in Russian] (Moscow, 1960).
11. G. Bloe, Y. Haven, and J. Stevels, Transactions of the Fourth International Conference on Glass, Paris [Russian translation] [Inform. Byulleten'Gos. Opticheskogo Inst. No. 7 (30) (1958)].
12. P. L. Gruzin, Doklady Akad. Nauk SSSR 89, 290 (1952).
13. K. K. Evstrop'ev, Transactions of the Third All-Union Conference on the Physics of Dielectrics [in Russian] (Moscow, 1960).

All abbreviations of periodicals in the above bibliography are letter-by-letter transliterations of the abbreviations as given in the original Russian journal. *Some or all of this periodical literature may well be available in English translation.* A complete list of the cover-to-cover English translations appears at the back of this issue.

A TRACER INVESTIGATION OF THE RADIOLYTIC OXIDATION OF BENZENE IN AN AQUEOUS SOLUTION

L. I. Kartasheva, Z. S. Bulanovskaya, E. V. Barelko, Ya. M. Varshavskii, and M. A. Proskurnin

L. Ya. Karpov Physicochemical Institute
(Presented by Academician V. A. Kargin, July 16, 1960)
Translated from Doklady Akademii Nauk SSSR,
Vol. 136, No. 1, pp. 143-146, January, 1961
Original article submitted July 11, 1960

All the available experimental data [1-4] indicate that the absorption of radiation by water molecules constitutes the primary step in the radiolytic oxidation of benzene dissolved in water. Such an "indirect" action of radiation may either proceed by means of a direct attack on benzene by the activated species (free radicals and excited molecules), which result from the radiolysis of water and diffuse through the solution until they encounter a molecule of the solute, or it may involve a direct transfer of excitation energy to the benzene molecule by having the corresponding energy quanta migrate through water.

There are grounds for believing that in the benzene–water system both of these "indirect" action mechanisms are involved. The formation of certain reaction products, the fact that molecular oxygen apparently affects the reaction yield (at moderate temperatures), and the noticeable, though not pronounced, temperature dependence of the radiolysis yield [5], all would tend to favor the first mechanism. In support of the second mechanism, we may cite the formation of muconaldehyde in the presence of oxygen [6,7].

Several workers [2,8,9] who have investigated the radiolysis of aqueous solutions of aromatic compounds have also proposed another mechanism in which the hydrogen atoms and hydroxyl radicals formed by the radiolysis of water add to the benzene ring.

The water-insoluble compound which is formed alongside phenol when the benzene–water system is radiolyzed in vacuo has the general formula $C_{12}H_{|14|16|?}O_2$, and its infrared spectrum indicates the presence of aliphatic and aromatic double bonds and of hydroxyl groups [9]. Hence, the precipitate contains hydroxyhydrodiphenyls and possibly dihydroxydiphenyls. It follows, therefore, that phenyl radicals, which could be formed by stripping a hydrogen atom from the benzene ring in one of two ways:

$$C_6H_6 + OH^{\cdot} \rightarrow C_6H_5^{\cdot} + H_2O$$

or

$$C_6H_6 + H^{\cdot} \rightarrow C_6H_5^{\cdot} + H_2,$$

do not constitute the primary products in the radiolysis of benzene dissolved in water, as was wrongly assumed by Stein and Weiss [3]; instead, it is the radicals formed by the addition of OH • and H • radicals to benzene ($C_6H_7^{\cdot}$ and $C_6H_6OH^{\cdot}$) that recombine to yield the insoluble compound mentioned above.

In this work, we investigated the radiolysis of benzene in the presence of D_2O, hoping that this new approach might elucidate the mechanism of benzene oxidation and help confirm some of the above-discussed hypotheses. The following considerations led to the choice of experimental method. If the addition mechanism

holds for both the H • and OH • radicals, then both the HO − groups (the hydrogens on which exchange freely with water molecules) and the $=\overset{|}{C}-H$ groups (which do not exchange hydrogen in the absence of high-energy radiation [10]) should contain deuterium atoms. After benzene is radiolyzed in the presence of heavy water, the insoluble product is treated with a solvent which contains a hydroxyl group of normal isotopic composition; once the deuterium is "leached" out of the OD group in the precipitate and the amount still left behind is determined, one can establish how many CH bonds in the product are replaced by CD bonds, and determine by difference the number of deuterated OH groups. The ratio between the concentrations of deuterated OH and CH groups can serve as an indication of the relative probabilities of OH • and H • addition to a benzene ring if the addition should proceed through the mechanism proposed above. On the other hand, if phenyl radicals are produced during the reaction, some deuterobenzene should also be formed by the recombination of phenyl radicals with deuterium radicals. By determining the deuterium content of unreacted benzene, we can provide indirect evidence for or against the mechanism of Stein and Weiss.

Experimental

Mixtures of benzene and heavy water were exposed to a Co^{60} source with the γ-radiation intensity being 170 rad/sec; exposure lasted 250 hr; the original deuterium content of water was 26.7 at%. Prior to each experiment, both the water and benzene were carefully purified. The aqueous phase (which contained dissolved benzene) exposed to radiation had a volume of 95 ml, while the benzene layer over it had a volume of 15 ml. All experiments were carried out in sealed glass tubes. Before exposure, the solutions were thoroughly degassed by repeated freezing and melting in vacuo. The white-colored product which had formed together with phenol in the aqueous phase was separated from the bulk of solution by prolonged centrifugation as described before [2]. The isolated product (1.0-1.2 g) was dried in a vacuum desiccator and separated into three samples. In the first sample, the deuterium content was determined without any prior chemical treatment. The second sample was weighed, dissolved in ethyl alcohol, the solution evaporated to dryness, fresh alcohol added, and the entire process repeated (14 times, using 5 ml aliquots) until all the deuterium bonded to oxygen was "leached out" by isotopic exchange with alcohol. The "leaching" was assumed to be complete when further treatment with alcohol failed to change the deuterium content of the compound. After the last solution was evaporated to dryness, the residue was weighed and the concentration of deuterium remaining in it (bonded to carbon) was determined. The third sample was treated several times with an aqueous solution of sodium carbonate and washed with water. This treatment was designed to remove small amounts of phenol which might have been adsorbed on the solid (the bulk of phenol remains in solution). Moreover, this treatment would also "leach out" the deuterium attached to oxygen (OH group). The resulting powder was weighed and its deuterium content determined.

In addition to this, we also investigated the deuterium content of unreacted benzene. The benzene was pyrolyzed over hot copper oxide in the presence of excess oxygen; the resulting water was purified and its isotopic composition determined by the drop method [11]. We analyzed each sample three times and took the average value. Deuterium could be determined with an accuracy of 0.02 at%.

Experimental Results

Our experimental results are presented in the table. The data indicate that the insoluble product which is formed along withphenol by the radiolytic oxidation of benzene in the presence of heavy water contains not only deuterated OH groups, but also has some deuterium attached to the aromatic ring. After the deuterium attached to oxygen is completely "leached" out of the compound by repeated treatment (and subsequent evaporation) with ethyl alcohol, the deuterium content of the product declines to about one third of the initial value. Hence, the ratio of deuterated OH groups to deuterated = CH groups is about 2:1.

The fact that no deuterium was found in the benzene recovered from the irradiated mixture indicates that the radiation dosages used and the experimental conditions do not lead to any direct isotopic exchange between benzene and water. Therefore, the deuteration of aromatic double bonds in the benzene oxidation product could not have been produced by a simple isotopic exchange between benzene and water followed by a reaction of the deuterobenzene. The presence of deuterium in the aromatic ring of the product can be explained by assuming that a deuterium atom (created by the radiolysis of heavy water) adds to a benzene molecule,and the resulting deuteroradical C_6H_6D • then dimerizes. The hydroxyl groups are similarly formed when OD • radicals add to benzene,and the resulting radical C_6H_6OD • undergoes further reactions (same as C_6H_6D •), terminating in the formation of the insoluble compound or phenol.

Data from the Radiolysis of Benzene in the Presence of Heavy Water

Compound	Atomic% D	Weight, g	
		before treatment	after treatment
Solid radiolysis product, freshly isolated	11.2	1.1585	–
Solid product after treatment with alcohol*	3.8	0.3762	0.3766
Solid product after treatment with Na_2CO_3	3.8	0.3941	0.405
Benzene** after radiolysis	0.0	–	–

*After additional sixfold treatment, the deuterium concentration still remained 3.8 at%.

**Before pyrolysis, the benzene was dried and purified.

Since no deuterated benzene was found, no phenyl radicals could have been formed under our experimental conditions; otherwise, these radicals could not have avoided recombining with deuterium atoms (known to be present in solution) to form deuterobenzene.

Our experimental data provide unequivocal evidence in favor of a recently proposed [2] mechanism for the radiolytic oxydation of benzene in aqueous solution; according to this mechanism the hydrogen and hydroxyl radicals formed by the radiolysis of water add to benzene yielding the radicals $C_6H_7\cdot$ and $C_6H_6OH\cdot$, respectively, and these can then recombine in various ways to give the different oxidation products. In addition to this, the 2:1 ratio between the number of deuterated OH and $=\overset{|}{C}-H$ groups clearly indicates that the $C_6H_6OD\cdot$ radicals are formed about twice as fast as are the $C_6H_6D\cdot$ radicals; this could, of course, be attributed to the fact that hydrogen atoms combine much more readily to form hydrogen molecules than do hydroxyl radicals to form hydrogen peroxide.

LITERATURE CITED

1. M. A. Proskurnin and E. V. Barelko, Collected Works on Radiochemistry [in Russian] (Izd. AN SSSR, 1955) p. 99.
2. E. V. Barelko, L. I. Kartasheva, and M. A. Proskurnin, Doklady Akad. Nauk SSSR 116, 74 (1957).
3. I. Stein and J. Weiss, J. Chem. Soc., 3245 (1949).
4. P. Phuna and M. Burton, Radiation Res. 1, 199 (1957).
5. E. V. Barelko, L. I. Kartasheva, P. D. Novikov, and M. A. Proskurnin, Transactions of the First All-Union Conference on Radiochemistry [in Russian] (Izd. AN SSSR, 1958) p. 89.
6. M. A. Proskurnin and Ya. M. Kolotyrkin, Transactions of the Second Conference on the Peaceful Uses of Atomic Energy [in Russian] (1958) p. 211.
7. I. Loeff and G. Stein, Nature 19, 901 (1959).
8. N. P. Krushinskaya and M. A. Proskurnin, Zhur. Fiz. Khim. 33, 1954 (1959).
9. Masao Matsui, Sci. Papers. Inst. Phys. Chem. Res. 53, 82 (1959).
10. A. I. Brodskii, Isotopic Chemistry [in Russian] (Izd. AN SSSR, 1958) 2nd ed.
11. A. I. Shatenshtein and Ya. M. Varshavskii, Zhur. Anal. Khim. 11, 746 (1956).

All abbreviations of periodicals in the above bibliography are letter-by-letter transliterations of the abbreviations as given in the original Russian journal. *Some or all of this periodical literature may well be available in English translation.* A complete list of the cover-to-cover English translations appears at the back of this issue.

THE γ-RAY RADIOLYSIS OF n-HEPTANE ADSORBED ON OXIDE CATALYSTS

Yu. A. Kolbanovskii, L. S. Polak, and É. B. Shlikhter

Institute of Petrochemical Synthesis, Academy of Sciences of the USSR
(Presented by Academician A. V. Topchiev, July 5, 1960)
Translated from Doklady Akademii Nauk SSSR,
Vol. 136, No. 1, pp. 147-150, January, 1961
Original article submitted July 5, 1960

This work was a part of a general study of the radiolysis of n-alkanes in the adsorbed state; the choice of n-heptane was dictated by the fact that the homogeneous radiolysis of the compound has already been investigated quite exhaustively [1-3].

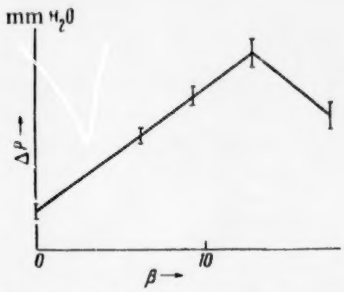

Fig. 1. The increase in gas pressure (relative to 1 g of heptane) as a function of the catalyst : heptane electron ratio (β); the plot is for catalyst II.

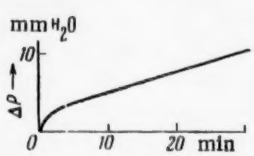

Fig. 2. Kinetic curve for the radiolysis of heptane on catalyst I.

TABLE 1

Description of the Catalysts Used in Our Work

Catalyst	Composition, weight %	Dry wt., g/cm³	Millimoles heptane in single layer, per 1 g catalyst
I	Al_2O_3 100	0.525	0.650
II	Al_2O_3 90 Cr_2O_3 8 K_2O 2	0.846	0.526
III	Al_2O_3 87 MoO_3 10 Alkali sulfates 3	0.836	0.881
IV	Al_2O_3 79 MoO_3 15.5 CoO 5.5	0.721	0.678

This type of a kinetic investigation was first undertaken by L. V. Pisarzhevskii in 1936 [4]. In 1959, Allen and co-workers studied the radiolysis of adsorbed n-heptane over a wide range of surface coverage $\theta < 1$. The found that with increasing θ the yield of $H_2 + CH_4$ increases by a factor of 2-4. They concluded that the absorbed radiation energy becomes redistributed between the solid and the adsorbed hydrocarbon. They assumed that the energy transfer is somehow connected with the migration of free electrons or holes [5].

We investigated the γ-ray radiolysis of n-heptane on the following catalysts: aluminum oxide (I), aluminochromium oxidedoped with potassium oxide (II), aluminomolybdenum oxide (III), and aluminocobaltomolybdenum oxide (IV). Most of the pertinent information about these catalysts is given in Table 1.

TABLE 2

Values of ΔP_{rel} and Z on Various Catalysts

Catalyst	$\epsilon \frac{k_1}{k_4} 10^2$	ΔP rel (W_s/W'_s)	Z
Homogeneous system		1.0	
I	3.5	12.7	0.41
II	3.24	2.0	0.032
III	3.36	1.7	0.026
IV	2.42	3.6	0.073

The preparation of samples has been described in [6], while the experimental procedure is given in [7]. We studied the radiolysis kinetics of n-heptane on catalyst (II) over the entire range of $\theta \leq 1$, and also for the case of multilayer adsorption. On all other catalysts, only the case where a monomolecular layer is adsorbed ($\theta = 1$) was investigated. We would like to point out that heptane was adsorbed at t ~10°, and the adsorption was fully reversible. Consequently, considering also that the heat of adsorption of heptane differs very little from its heat of condensation, there could not have been any chemisorption (in the usual sense of the word) in the experiments studied by us here.

In Fig. 1 we have plotted the increase in gas pressure ΔP (with reference to 1 g of heptane) as a function of the catalyst: heptane electron ratio for catalyst II. The measurements were quite reproducible, and the spread of ΔP values shown in Fig. 1 was not too large. The line shown in Fig. 1 breaks at a point corresponding to a monomolecular layer. It is obvious that the curve can be used for the determination of the specific surfaces of catalysts.

In Table 2 we have compiled the ΔP_{rel} values for monomolecular layers on various catalysts. The appropriate value of ΔP during homogeneous radiolysis was used as a reference point (unity).

Figure 2 shows the kinetic radiolysis curve (typical for the investigated set of catalysts) for heptane on catalyst I; this curve is a continuous plot of $\Delta P = f(t)$ obtained by means of an automatic recorder ÉPP-09. The initial curvature is quite apparent in this figure. In experiments where the catalysts were exposed to radiation prior to the adsorption, the yield of gaseous radiolysis products was considerably lower. Thus, for example, the value of ΔP_{rel} on catalyst I was reduced from 12.7 to 5.1, and on catalyst II from 2.0 to 0.27.*

We would now like to make several comments in connection with the data reported above.

The linear dependence between the radiolysis yield (ΔP) and the catalyst:heptane electron ratio (β) in the range of θ values from a monomolecular layer to a homogeneous system is consistent with the fact that the catalyst can only transfer its energy to a single adsorbed layer (the first layer), and hence the radiolysis rate in all successive layers should be the same as in a homogeneous system. The fact that in the range of $\theta < 1$ the yield increases with increasing surface coverage indicates that the amount of energy transferred from solid to a compound adsorbed on its surface is directly proportional to the fraction of surface covered.

The catalytic effect varied considerably from catalyst to catalyst. It is interesting to compare our current results with the data previously obtained by us from a p.m.r. study of these systems [6]. The most active catalyst turns out to be the one which yields the same p.m.r. spectrum when irradiated with or without the adsorbed hydrocarbon on its surface. And the catalytic activity in these experiments declined in the same order (I > IV > II > > III) as the difference between the p.m.r. spectra recorded under these two conditions increased (see Table 2). Electrical conductance measurements also showed that changes in the conductance were accompanied by parallel changes in the p.m.r. signal intensities.

The nonlinear initial section of the kinetic curve (Fig. 1) and the greatly reduced radiolysis rate on preirradiated surfaces may both be due to the formation of some acceptor centers (excitation or charge) in the solid. The already discussed p.m.r. study showed that the intrinsic signal from the catalyst becomes saturated at dosages well below 6 Mrad; Kitaigorodskii's data [8], which can be treated in about the same manner, indicate that the dosage at which the defects in a molecular crystal of p-dichlorobenzene become saturated cannot exceed 0.5 Mrad.

We would like to point out that the radiolysis rate on catalyst (I) after the sample had been exposed to radiation still remains greater than the homogeneous radiolysis rate, whereas in the case of catalyst (II) under

*The pressure increase data given here and above were obtained over a period of 1 hr, well beyond the nonlinear portion of the curve. Catalysts (I) and (II) were exposed to radiation for 0.5 hr and 1 hr, respectively, prior to the adsorption experiment.

similar circumstances the rate drops below the homogeneous radiolysis rate. In thermocatalytic reactions, catalyst (I) becomes more active after being exposed to radiation [9], while other catalysts (for example, ZnO) become less active [10,11]. It seems that impurities which can absorb some of the excitation energy play a very important role in determining how sensitive a catalyst will be to radiation. The elemental composition of our catalysts remained unchanged after the exposure to γ-rays. Therefore, it is reasonable to conclude that the extent of energy transfer from the catalyst to the adsorbed material depends on the amount of impurities. Since the increased yield of radiolysis products reflects only the amount of energy absorbed in excess of the amount absorbed directly (as if homogeneous) from outside, this energy can only come from the solid, which under our experimental conditions absorbs a very large fraction (99.9%) of the total radiation energy. One therefore has to assume that the electron-wave functions of the adsorbed molecules and of the adsorbent lattice overlap to some degree, and hence the forces binding these molecules to the surface depend, at least in part, on an exchange interaction.

We also found that the saturation dosage and the form of the initial portion of the kinetic curve depend considerably on the general preliminary treatment of the catalyst. A relationship between the radiation sensitivity and preliminary treatment of catalysts has also been observed [9]. Depending on their composition, the impurities may render a catalyst either more or less sensitive to radiation.

We will now compute the probability for the transfer of energy from the catalyst to the adsorbed compound by assuming the following rate mechanism. We will consider the following processes: 1) $X_{ads} \rightsquigarrow X^*$ (direct absorption of radiation by the adsorbate); 2) $X^* \to X$ (any deactivation process except a chemical reaction); 3) $X^* \to$ products (chemical reaction); 4) catalyst $\rightsquigarrow$ catalyst* (energy absorbed by the catalyst); 5) catalyst* $\to$ $\to$ catalyst (any form of energy dissipation except by transfer to the adsorbate); 6) catalyst* + $X_{ads} \to$ catalyst + + X_{ads}* (energy transfer to the adsorbate).

These processes take place at the following rates:

$$W_1 = k_1' I\theta; \quad W_2 = k_2 [X^*]; \quad W_3 = k_3 [X^*]; \quad W_4 = k_4' I;$$
$$W_5 = k_5 [D]; \quad W_6 = k_6 [D]\theta,$$

where [D] is the concentration of elementary excited sites in the solid

$$[D] = \frac{k_4' I}{k_5 + k_6\theta} \text{ and } W_6 = k_6\theta \frac{k_4' I}{k_5 + k_6\theta},$$

$$[X^*] = \frac{k_1' I\theta + k_6\theta \dfrac{k_4' I}{k_5 + k_6\theta}}{k_2 + k_3},$$

whence

$$W_3 = \frac{k_3 I\theta}{k_2 + k_3}\left(k_1' + \frac{k_4' k_6}{k_5 + k_6\theta}\right).$$

Neglecting any differences between bond energies of the adsorbed molecules located at the surface and those in inner layers (see below), we can write the following expression for the rate of homogeneous radiolysis:

$$W_3' = \frac{k_1' k_3 I}{k_2 + k_3}.$$

When $\theta = 1$ we get

$$W_3/W_3' = 1 + \frac{1}{\varepsilon \dfrac{k_1}{k_4}\left(\dfrac{k_5}{k_6} + 1\right)},$$

where ϵ is the ratio of the radiation energy absorbed by 1 cm^3 of heptane to that absorbed by the catalyst.

The W_3/W_3° ratios were determined experimentally. Using the known densities and the effective atomic numbers of heptane and the catalyst, we computed ϵ (for a given radiation intensity) by the method described in [12]. $k_1/k_4 \cong 1$, since in both cases we were interested solely in excitation energies in excess of the bond energies. Solution of the last equation yields the ratio k_5/k_6, from which the distribution probability of the effective energy $Z = \frac{k_5}{k_5 + k_6}$ can be computed. The calculated values of Z are listed in Table 2.

The calculated values of Z are only as accurate as are the experimentally determined values of W_3/W_3°, namely to within ± 5%.

We would like to point out that our Z values are somewhat too large due to the fact that molecules in inner layers have bond energies slightly different from those of molecules located on the surface. But the heats of adsorption of paraffins on these catalysts constitute only a small fraction of the bond energies,and we were unable to detect any correlation between the heats of adsorption and the radiolytic activity of our adsorbers. Hence,one may safely assume that the computed values of Z are entirely satisfactory.

We would like to thank V. V. Shchekin and A. L. Klyachko for carrying out the adsorption measurements, and Yu. L. Khait for helpful discussion.

LITERATURE CITED

1. H. A. Dewhurst, J. Phys. Chem. 61, 1466 (1958).
2. A. M. Brodskii, Yu. A. Kolbanovskii, et al., Doklady Akad. Nauk SSSR 122, 1035 (1958).
3. V. G. Berezhin, I. M. Kustanovich, et al., Doklady Akad. Nauk SSSR 131, 593 (1960).
4. L. V. Pisarzhevskii, Selected Works on Catalysts [in Russian] (Kiev, 1955) p. 133.
5. G. W. Sutherland and A. C. Allen, "Radiolysis in the adsorbed state," Conference on the Application of Large Radiation Sources in Industry, Warsaw, 1959.
6. Yu. A. Kolbanovskii, I. M. Kustanovich, et al., Doklady Akad. Nauk SSSR 129, 145 (1959).
7. A. M. Brodskii et al., Intern. J. Appl.Rad. No. 5, 57 (1959).
8. A. I. Kitaigorodskii and É. I. Fedin, Doklady Akad. Nauk SSSR 130, 1005 (1960).
9. E. H. Taylor and H. W. Kohn, J. Phys. Chem. 63, 500 (1959).
10. E. H. Taylor and H. W. Kohn, J. Am. Chem. Soc. 79, 252 (1957).
11. E. H. Taylor and J. A. Wethington, J. Am. Chem. Soc. 76, 971 (1954).
12. M. Day and H. Stein, Collection: Radiation Chemistry [Russian translation] (IL, 1953) p. 235.

All abbreviations of periodicals in the above bibliography are letter-by-letter transliterations of the abbreviations as given in the original Russian journal. *Some or all of this periodical literature may well be available in English translation.* A complete list of the cover-to-cover English translations appears at the back of this issue.

THE EFFECT OF ORGANIC SOLVENTS ON THE PROPERTIES OF CARBOXYLIC CATION-EXCHANGE RESINS

Lou Chih-Hsien, E. M. Savitskaya, and B. P. Bruns

All-Union Scientific Research Institute of Antibiotics

(Presented by Academician V. A. Kargin, June 27, 1960)
Translated from Doklady Akademii Nauk SSSR,
Vol. 136, No. 1, pp. 151-154, January, 1961
Original article submitted June 24, 1960

The ion-exchange properties of various resins undergo radical changes when one switches over from aqueous to mixed or pure organic solvents.

One of the principal causes for the changed kinetics and statics of ion-exchange processes resides in the fact that the resin itself has different properties in different solvents. Cation-exchange resins in their hydrogen form can be regarded as insoluble concentrated polybasic acids under a certain swelling pressure. Hence, various solvents and their mixtures should have a direct effect on the strength of these acids.

For our study we selected a cation-exchange resin which contained only carboxylic ionogenic groups. The solvent system consisted of water and methanol mixed in various proportions. The choice of system was motivated by certain practical considerations. Aqueous methanol solutions of various acids have already found widespread use in the elution of many complex organic ions from carboxylic resins, and in many cases the optimum conditions had to be determined by trial and error. The study of these systems is of a certain theoretical value too, since it might lead to a better understanding of the differences and similarities between high molecular weight acids and normal monocarboxylic acids in similar solvents.

The relationship between the strength of this ion-exchange resin and the composition of the surrounding medium was investigated by means of potentiometric titration.

Experimental Methods

The cation-exchange resin was prepared by the alkaline saponification of the copolymer of methylmethacrylate and divinylbenzene (DVB). The preliminary treatment of the resin and the method used for measuring the pH of water–methanol mixtures have already been described in full detail [1]. The pH readings in water–methanol mixtures were standardized with reference to the pH of HCl at infinite dilution in similar mixtures.

All the ionic adsorption data are given with reference to 1 g of dry resin in the hydrogen form. In water the resin (in its H-form) had a specific volume of 2.5 ml/g.

The experimental data were obtained by three different titration methods. The first method was devised by Kunin [2]; the second method involved a direct titration of the solution in the absence and in the presence of a weighted amount of resin. Both methods yielded identical results when used for the determination of resin capacity vs. the pH of the external solution; this was true for all the methanol concentrations. The titration curves for the cation-exchange resin in various solvents are shown in Fig. 1.

The H–Me exchange on carboxylic resins proceeds very slowly in pure water. We have previously shown that the exchange rate rapidly declines even more with increasing methanol concentration [3].

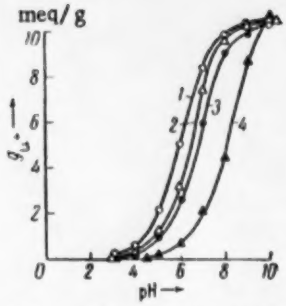

Fig. 1. Titration curves for the cation-exchange resin; C_{LiCl} = 0.5 N: 1) in H_2O; 2) in 40% CH_3OH; 3) in 60% CH_3OH; 4) in 95% CH_3OH.

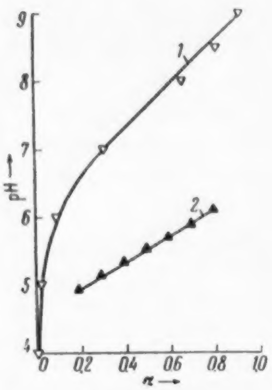

Fig. 2. pH of external solution as a function of the degree of neutralization α: C_{LiCl} = 0.1 N, 60% CH_3OH. 1) Cation-exchange resin; 2) CH_3COOH.

In order to demonstrate conclusively that the recorded pH readings represented true equilibrium values, the titration curves for each water–methanol mixture were recorded by starting from both the hydrogen and the salt form of the resin. In each given mixture the two curves were mirror images of each other.

In addition to the two methods mentioned above, we also developed a new rapid method of recording a set of potentiometric titration curves for a carboxylic cation-exchange resin in mixed and nonaqueous solvents. The method involved the determination of the equilibrium pH of the external solvent in systems consisting of cation-exchange resins at various degrees of neutralization submerged in aqueous organic solvents of known ionic strength. Resin samples with varying fractions of hydrogen ions substituted by metal ions were obtained by adding calculated amounts of aqueous alkali to weighed samples of the resin in the H-form. When the exchange was over (in about 1-2 days), the water over the resin was decanted, and the resin was then submerged in a fixed volume of mixed solvent in which a known concentration of an inert salt was dissolved. The pH was determined several times at daily intervals to make sure that the values were constant. From the measured pH values and the known degrees of resin neutralization we constructed a titration curve. To avoid any absorption of carbon dioxide from the air and consequent pH shift, it is advisable to carry out the experiments under nitrogen. When the first two methods were used, carbon dioxide was also rigorously excluded.

By transferring successively each one of the partially neutralized cation-exchange resin samples from a mixture of one composition into that of another, and measuring the equilibrium pH in each one, we can obtain within a brief period of time a complete picture of the changes which take place in the acid – cation-exchange resin system when the surrounding medium is changed. This method is particularly advantageous whenever the exchange process is very slow in a given medium. The results obtained by this method were in full accord with those obtained by Kunin's method.

Experimental Results

A typical curve showing the relationship between the degree of neutralization of the cation-exchange resin and the pH of the surrounding solution is shown in Fig. 2. If we compare this curve with the neutralization curve of a monocarboxylic acid titrated in the same solution, we can see right away that the neutralization curve of the cation-exchange resin has a greater slope than the corresponding curve of a soluble monocarboxylic acid. The reason that the curve of the three-dimensional weak electrolyte has a greater slope is that as we neutralize the cation-exchange resin the resulting negative field renders the detachment of protons from the remaining carboxylic groups more and more difficult. This electrostatic effect shifts the neutralization curve of the ion-exchange resin toward higher pH values (relative to the monomer curve). The more extensively neutralized the cation-exchange resin, the more pronounced is the electrostatic field effect.

The effect is reflected in the gradual weakening of the insoluble polyacid as more and more hydrogen ions on the resin become replaced by metal ions. This behavior is very similar to the stepwise decrease of the successive dissociation constants of a polybasic acid. N. A. Izmailov has reported a similar decline in the exchange constants of macromolecular silicic acids when hydrogen is replaced by metal ions [4,5]. In a series of papers [6-8], Katchalsky and co-workers studied the titration curves of soluble carboxylic polyacids and of strongly swelling gels, and developed a theory for the processes taking place in such systems. Unfortunately, their results cannot be extended directly to other cases and used to predict the behavior of real carboxylic cation-exchange resins, since the theory was derived only for gels which could be regarded as diluted polyelectrolytes. Nobody doubts that the factors considered in a theory developed for very strongly swelling gels (methacrylic acid chains

cross-polymerized with divinylbenzene) are also important in the titration of real carboxylic cation-exchange resins. Unfortunately, the titration of real ion-exchange resins is not well understood at the moment. So far, all the investigators in this field have made use of only the experimental data [9, 10]. To give a measure of the acid strength of a cation-exchange resin, it is now customary to use the average or apparent dissociation constant of the resin.

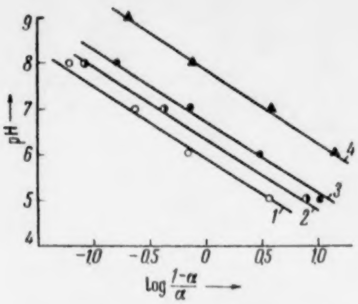

Fig. 3. The cation-exchange resin titration data represented by the Henderson equation; $C_{LiCl} = 0.5$ N: 1) in H_2O; 2) in 40% CH_3OH; 3) in 60% CH_3OH; 4) in 95% CH_3OH.

To get a better understanding of the effects of surrounding medium on the acid strength of carboxylic cation-exchange resins, we calculated the average or apparent dissociation constant of our resin by means of a modified Henderson equation,

$$\mathrm{pH} = \mathrm{p}\bar{K} - n \lg \frac{1-\alpha}{\alpha},$$

where pH represents the hydrogen ion concentration in the surrounding solution, $\mathrm{p}\bar{K}$ represents the average dissociation constant of the cation-exchange resin ($-\log \bar{K}$), α is the degree of neutralization of the ion-exchange resin, and $\underline{n}$ is a constant.

The $\mathrm{p}\bar{K}$ of the cation-exchange resin submerged in water–methanol mixtures was determined under conditions where the only variable was the methanol concentration. Figure 3 shows that the experimental results satisfy Henderson's equation at all the investigated methanol concentrations. Regardless of methanol concentration, $\underline{n}$ remained constant and equal to about 1.6. $\mathrm{p}\bar{K}$ increased with increasing methanol concentration.

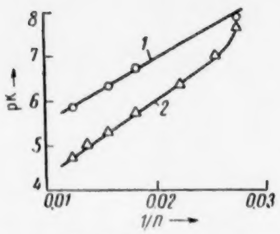

Fig. 4. $\mathrm{p}\bar{K}$ of the cation-exchange resin (1) and the pK of CH_3OOH (2) as a function of 1/D; $C_{LiCl} = 0.1$ N.

In solutions containing 0, 40, 60, and 95% methanol, the cation-exchange resin had a $\mathrm{p}\bar{K}$ of 5.90, 6.35, 6.75, and 7.85, respectively (the lithium chloride concentration in solution was maintained at 0.5 N).

These data show that with increasing alcohol concentration the acidity of the cation-exchange resin declines; the dissociation constants of monocarboxylic acids decline similarly in these solutions.

In Fig. 4 we have shown how the $\mathrm{p}\bar{K}$ of the cation-exchange resin, and the pK of acetic acid [11] depend on the dielectric constant of the medium (D). With decreasing dielectric constant, the interaction between the resin anion and the oppositely charged H^+ ion becomes stronger, and consequently the dissociation constant of the ion-exchange resin declines. The $\mathrm{p}\bar{K}$ of the resin is a linear function of 1/D of the solution, indicating that the dissociation process is fully consistent with Brönsted's theory [12]. This in turn indicates that within the investigated range of methanol concentrations the acidity of the solvent contained in the resin phase remains unchanged. It is quite possible that even in a solution containing 95% alcohol, water is still predominantly adsorbed on the resin.

When the ionic strength of the surrounding water–methanol solution is increased, the $\mathrm{p}\bar{K}$ of the cation-exchange resin decreases. Whereas in the absence of an inert electrolyte it is 8.70, it becomes 7.60 in a 0.1 N lithium chloride solution, and drops to 6.75 when the electrolyte concentration is raised to 0.5 N (the methanol concentration was 60% throughout). The decreased $\mathrm{p}\bar{K}$ can be attributed to the Donnan effect, wherein the increased concentration of the inert electrolyte screens the negative field in the resin.

LITERATURE CITED

1. Lou Chih-Hsien, E. M. Savitskaya, and B. P. Bruns, Vysokomolek. Soed. 2, 745 (1960).
2. R. Kunin and R. Myers, Ion Exchange Resins (New York, 1950).
3. Lou Chih-Hsien, E. M. Savitskaya, and B. P. Bruns, Vysokomolek. Soed. 2, 751 (1960).
4. N. A. Izmailov and A. M.Vasil'ev, Doklady Akad. Nauk SSSR 95, 579 (1954).
5. N. A. Izmailov, The Electrochemistry of Solutions [in Russian] (Kharkov, 1959) p. 693.
6. A. Katchalsky, Progress Biophys., Biophys. Chem. 4, 19 (1954).
7. A. Katchalsky and I. Michaeli, J. Polymer Sci. 15, 69 (1955).
8. I. Michaeli and A. Katchalsky, J. Polymer Sci. 23, 683 (1957).
9. H. P. Gregor, M. Y. Hamilton,et al., J. Phys. Chem. 59, 874 (1955).
10. S. Fisher and R. Kunin, J. Phys. Chem. 60, 1030 (1956).
11. T. Shedlovsky and R. L. Kay, J. Phys. Chem. 60, 151 (1956).
12. J. N. Brönsted, Z. Phys. A169, 52 (1934).

TWO TYPES OF ELEMENTARY REACTIONS IN THE CATALYTIC HYDROGENATION OF OLEFINS

R. E. Mardaleishvili, A. G. Popov, V. V. Nikisha, and F. S. Yakushin

M. V. Lomonosov Moscow State University

(Presented by Academician N. N. Semenov, July 14, 1960)
Translated from Doklady Akademii Nauk SSSR,
Vol. 136, No. 1, pp. 155-158, January, 1961
Original article submitted July 7, 1960

Several years ago, N. N. Semenov, V. V. Voevodskii, and F. F. Vol'kenshtein [1] had proposed that free valences may exist on solid surfaces and lead to the formation of so-called "surface radicals" when certain compounds are adsorbed on these surfaces. In their opinion, these surface radicals may be responsible for several heterogeneous catalytic reactions. Two types of radicals may be formed when olefins are adsorbed and hydrogenated on catalytic surfaces; for example, in the case of ethylene,

$$C_2H_4 + 2\dot{K} \rightleftarrows \underbrace{\underset{\substack{|\\ K}}{CH_2} - \dot{C}H_2}_{(a)} + \dot{K} \rightleftarrows \underset{\substack{|\\ K}}{CH_2} - \underset{\substack{|\\ K}}{CH_2}, \tag{1}$$

$$\underset{\substack{|\\ K}}{CH_2} - \dot{C}H_2 + \underbrace{\underset{\substack{\bullet\\ K}}{\dot{H}}}_{(b)} \rightleftarrows \underset{\substack{|\\ K}}{CH_2} - CH_3 \rightleftarrows \underbrace{\underset{\substack{\bullet\\ K}}{\dot{C}H_2} - CH_3}_{(b)} \tag{2}$$

we might have radicals (a) bound to the catalyst (K) by two-electron bonds, or radicals (b) bound by a one-electron bond. The latter ones combine with another hydrogen atom to yield the end product, in this case ethane,

$$\underset{\substack{\bullet\\ K}}{\dot{C}H_2} - CH_3 + \underset{\substack{\bullet\\ K}}{\dot{H}} \rightarrow C_2H_6 + 2\dot{K}. \tag{3}$$

The chemical processes (1)-(3) represented by these free radical reactions express the currently accepted mechanism for the catalytic hydrogenation of olefins [2]. It should be pointed out that if one assumes the actual existence of surface radicals then, under certain conditions of catalytic hydrogenation of olefins, one would expect the recombination reactions (2)-(3) to also be accompanied by disproportionation reactions such as

$$\underset{\substack{|\\ K}}{CH_2} - \dot{C}H_2 + \underset{\substack{|\\ K}}{CH_2} - \dot{C}H_2 \rightarrow \underset{\substack{|\\ K}}{CH_2} - CH_3 + \underset{\substack{|\\ K}}{CH} = CH_2, \tag{4}$$

$$\underset{\substack{\bullet\\ K}}{\dot{C}H_2} - CH_3 + \underset{\substack{\bullet\\ K}}{\dot{C}H_2} - CH_3 \rightarrow \underset{\substack{|\\ K}}{CH_2} - \dot{C}H_2 + C_2H_6 + \dot{K}, \tag{5}$$

$$\underset{\substack{\bullet\\ K}}{\dot{C}H_2} - CH_3 + \underset{\substack{|\\ K}}{CH_2} - \dot{C}H_2 \rightarrow \underset{\substack{|\\ K}}{CH} = CH_2 + C_2H_6 + \dot{K} \tag{6}$$

where the hydrogen transfer from one surface radical to another would proceed by a mechanism well known in homogeneous free radical reactions [3].

Expt. Nos.	H_2	C_2H_4	C_3H_6	w_2	w_3	w	w_{23}	w_{32}	$\frac{w_3}{w_2}$	$\frac{w_{32}}{w_{23}}$	$\frac{w_{23}}{w_2}$	$\frac{w_{32}}{w_3}$	$\frac{2w}{w_2+w_3}$
	mm Hg			mm Hg/ min									
40	25	25		0.45									
26	25		25		0.66				1.46	0.32	0.90	0.22	1.06
11 m	25	25	25			0.59	0.445	0.145					
4	50	25		0.95									
7	50		25		0.95				1.00	0.55	0.68	0.375	1.05
3 m	50	25	25			1.00	0.645	0.355					
19	100	25		1.87									
22	100		25		1.45				0.775	0.65	0.54	0.45	1.01
20 m	100	25	25			1.65	1.00	0.65					
34	150	25		2.85									
30	150		25		1.62				0.568	0.66	0.44	0.52	0.94
14 m	150	25	25			2.10	1.26	0.84					
18	200	25		3.75									
23	200		25		1.90				0.508				
	200	25	25										
15	250	25		3.90									
32	250		25		1.90				0.487	0.73	0.423	0.63	0.98
9 m	250	25	25			2.85	1.65	1.20					
43	350	25		2.80									
46	350		25		1.35				0.482	0.72	0.415	0.617	0.96
45 m	350	25	25			2.00	1.16	0.835					
37	500	25		1.06									
39	500		25		0.56				0.471	0.73	0.45	0.637	1.04
10 m	500	25	25			0.84	0.484	0.356					

Similar mechanisms for the disproportionation of the so-called "semihydrogenated complexes" [4] have been proposed by several workers [5] in order to account for the experimentally observed deuterium distribution among the products of catalytic deuteration. However, since in the opinion of other workers [2,3,6] the data could also be satisfactorily interpreted without invoking the disproportionation of "semihydrogenated complexes," the real nature of this process is still not clear.

Attempts to establish by ordinary methods what fraction of olefin hydrogenation proceeds by the recombination route (2)-(3) as opposed to the disproportionation route (4)-(6) are hampered by obvious difficulties, since both reactions yield the same final product. Moreover, the ratio between the rates for the two processes will obviously depend on the ratio between the concentrations of radicals and hydrogen atoms on the catalytic surface. And it is this particular relationship that we took advantage of in our present investigation; we decided to verify experimentally the postulated existence of surface radicals by checking whether disproportionations of the type (4)-(6) actually do take place. We investigated the hydrogenation of ethylene, propylene, and their mixtures at various hydrogen pressures and temperatures. If the postulated surface radicals do exist, and lead to the disproportionations mentioned above, then the hydrogenation of mixed olefins (for example, ethylene mixed with propylene) should produce certain reactions which do not normally occur when the olefins are hydrogenated individually. As an example of such a reaction, we can give the disproportionation of the two radicals formed from two different olefins:

$$\underset{}{CH_3} - \dot{C}H - \underset{\substack{|\\ K}}{CH_2} + \underset{}{\dot{C}H_2} - \underset{\substack{|\\ K}}{CH_2} \rightarrow CH_2 = CH - \underset{\substack{|\\ K}}{CH_2} + CH_3 - \underset{\substack{|\\ K}}{CH_2}\ ; \qquad (7)$$

one would expect that, since the radicals C3 and C2 have different reactivities, hydrogen should be transferred predominantly from one structure to the other and particularly, as in the case of homogeneous ethyl and propyl free radical reactions, from adsorbed propylene to adsorbed ethylene (reaction 7). Such preference would make the ratio of initial hydrogenation rates of propylene and ethylene w_{32}/w_{23} in the mixture smaller than the corresponding ratio w_3/w_2 for the two individually determined hydrogenations. The difference between the two ratios $(w_{32}/w_{23}) - (w_3/w_2)$ should disappear with increasing hydrogen pressure, since the recombination of surface radicals with hydrogen atoms would then become the predominant reaction. The ratio between the two recombination reactions should not depend on whether the two olefins are hydrogenated individually or in a mixture (as long as the two olefins are adsorbed with equal ease, the ratios will be equal in the presence of excess hydrogen).

The difference between the relative hydrogenation rates determined in a mixture of olefins and those determined individually will vary with temperature as it did with hydrogen pressure. The lower the temperature, the more should the two ratios w_{32}/w_{23} and w_3/w_2 differ, since the olefin concentration on the surface, and consequently the fraction of the reaction going by the disproportionation route, should be greater. As we raise the temperature to the temperature of maximum hydrogenation rate and above, the olefin concentration declines to

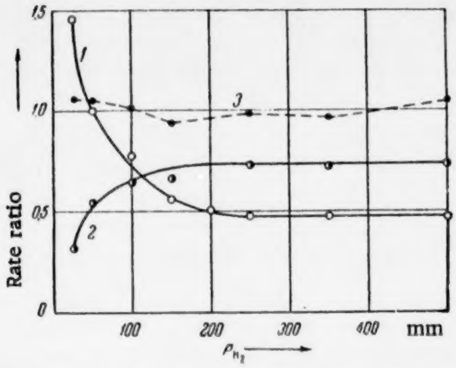

Fig. 1. The ratio of the formation rates of propane and ethane as a function of hydrogen pressure in the course of hydrogenation. The legend is the same for Fig. 2: 1) w_3/w_2, for C_3H_6 and C_2H_4, hydrogenated separately; 2) w_{32}/w_{23}, in an equimolar mixture; 3) $2w/(w_2 + w_3)$, a curve indicating the reproducibility of the experimental data.

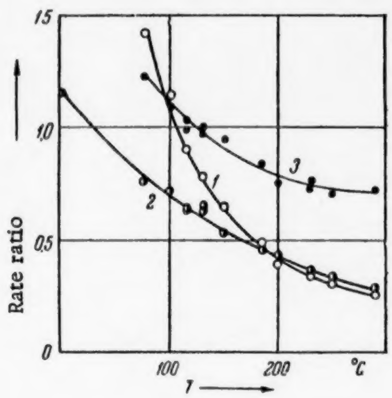

Fig. 2.

such an extent on account of desorption that the disproportionation reaction can be entirely neglected alongside the recombination with hydrogen atoms. Since with increasing temperature the two ratios w_{32}/w_{23} and w_3/w_2 will approach, while at the same time the difference between the adsorption of ethylene and propylene will also decrease, eventually the two ratios will assume exactly the same value.

Our experiments were carried out in a vacuum apparatus with the gaseous reactants circulating through a reactor in which a platinum wire catalyst (d = 0.1 mm, l = 150 mm) was located; the wire was heated by means of electric current. The course of the reaction was followed manometrically by recording pressure variations in the system, as well as mass-spectrophotometrically by examining small samples removed from the system at various stages of the reaction. The reaction was investigated at pressures up to 525 mm Hg, in the temperature range 0-280°C, and with the olefin:hydrogen ratios from 1:1 to 1:20; in all the cases, conditions of maximum catalytic activity were obtained by heating the platinum wire for 30 min at 300° first in oxygen, then in hydrogen, before each experiment. To prevent any poisoning of the catalytic surface by mercury vapor and vacuum grease, the gases were passed through two cold traps (maintained at −70°) located on each side of the reactor. The reactor was sealed off from the rest of the apparatus by means of metal stopcocks, and evacuated to a pressure of 10^{-6} mm Hg between experiments.

In the table we have compiled the initial rates of formation of ethane w_2 and propane w_3 when the olefins are hydrogenated individually, and also when ethylene–propylene mixtures are hydrogenated at various hydrogen pressures (w_{23} for ethane and w_{32} for propane). The ratio of the hydrogenation rate in an ethylene–propylene mixture (w) to the average hydrogenation rate of the two individual olefins is about unity, which is a good criterion of catalytic reproducibility.

An examination of the w_3/w_2 ratio at various hydrogen pressures (Fig. 1) reveals that at first it rapidly declines, and then levels off. This type of a variation in the w_3/w_2 ratio indicates that in the hydrogenation of ethylene the order of reaction with respect to hydrogen ($w_2 \sim p_{H_2}$) is higher than it is in the hydrogenation of propylene ($w_3 \sim \sqrt{p_{H_2}}$), which is entirely consistent with the literature data. However, when mixtures of these olefins are hydrogenated exactly the opposite behavior is observed with increasing hydrogen pressure – the w_{32}/w_{23} ratio increases to a certain fixed value, which of course is precisely what we had expected from our postulated model. If we plot the experimental data as w_{23}/w_2 and w_{32}/w_3 against p_{H_2}, both ratios should approach 0.5 under conditions where the adsorption of ethylene and propylene occurs with equal readiness, since we could then assume that each olefin is hydrogenated on one half the available catalytic surface, while the hydrogenation of each individual olefin involves the entire surface. As it turns out, the experimental values of w_{23}/w_2 and w_{32}/w_3 approach 0.43 and 0.63, respectively, with increasing hydrogen pressure; this indicates that propylene is apparently adsorbed more strongly than is ethylene.

In Fig. 2 we have plotted the experimentally determined w_3/w_2 and w_{32}/w_{23} ratios as a function of temperature. Curve 1, which represents the hydrogenation of propylene and ethylene (individually) on Pt, confirms

the data reported by Toyama [7] for similar hydrogenations on Ni. Curve 2 was obtained by plotting the ratio of the hydrogenation rate of propylene to that of ethylene as a function of temperature when the two reactants are mixed together. A simple comparison of Curves 1 and 2 shows right away that in the mixture examined by us ethylene has a higher relative (relative to propylene) hydrogenation rate than the value obtained by comparing the individually determined hydrogenation rates.

Thus, the initial relative formation rates of propane and ethane obtained by hydrogenating the reactants individually and in a mixture varied with temperature and hydrogen pressure exactly as we had predicted they would. Therefore, the results may be regarded as confirming the existence of two elementary reaction steps: the recombination and the disproportionation of the reactive intermediates formed during the hydrogenation of olefins. At the same time, the data can be cited in favor of the existence of the postulated surface radicals.

LITERATURE CITED

1. V. V. Voevodskii, F. F. Vol'kenshtein, and N. N. Semenov, Collection: Problems in Chemical Kinetics, Catalysis, and Reactivity [in Russian] (Izd. AN SSSR, 1955) p. 423; N. N. Semenov, Certain Problems in Chemical Kinetics and Reactivity [in Russian] (Izd. AN SSSR, 1959) p. 272.
2. D. D. Eley, Catalysis 3, 49 (1955); H. A. Taylor, Catalysis 5, 257 (1957); J. Horiuti, Catalysis 6, 250 (1958).
3. E. W. R. Steacie, Atomic and Free Radical Reactions (New York, 1954).
4. M. Polanyi and J. Horiuti, Trans. Faraday Soc. 30, 1164 (1934); M. Polanyi and R. K. Greenhalgh, Trans. Faraday Soc. 35, 520 (1939); E. K. Rideal and G. H. Twigg, Proc. Roy. Soc. (London) A171, 55 (1939); D. D. Eley, Advances in Catalysis 1, 157 (1948); D. D. Eley, Quart. Rev. Chem. Soc. 3, 209 (1949).
5. J. Turkevich, D. Schissler, and P. Irsa, J. Coll. and Phys. Chem. 55, 1078 (1951); G. G. Bond, Trans. Faraday Soc. 52, 1235 (1956).
6. T. Keii, J. Chem. Phys. 22, 144 (1954); G. I. Jenkins and E. K. Rideal, J. Chem. Soc. 1955, 2496.
7. O. Toyama, Rev. Phys. Chem. Japan 14, 86 (1940).

THE HEATS AND ENTROPIES OF ADSORPTION OF HEXANE AND BENZENE VAPORS ON AEROSILS HAVING A SURFACE CHEMICALLY MODIFIED BY TRIMETHYLSILYL GROUPS

I. Yu. Babkin, A. V. Kiselev, and A. Ya. Korolev

M. V. Lomonosov Moscow State University
(Presented by Academician M. M. Dubinin, July 2, 1960)
Translated from Doklady Akademii Nauk SSSR,
Vol. 136, No. 2, pp. 373-376, January, 1961
Original article submitted June 30, 1960

An investigation has been made of the adsorption of various vapors on the surface of aerosils which have been modified by reaction with trimethylchlorosilanes, and it has been shown that a very important characteristic of such modified adsorbents is the degree of the covering of the surface of the silica by the trimethylsilyl groups which have been chemically produced [1,2]. If the layer of these groups is insufficiently dense, adsorption proceeds in the first instance upon the nonmodified silica surface which lies between them. Thus, insufficiently complete modification leads to a great degree of inhomogeneity in the surface. In addition to this, there have been produced earlier [3] theoretical calculations of the energy of adsorption of molecules of n-hexane and benzene on the modified aerosil, related to the model of a complete layer of trimethylsilyl groups on the surface of the silica (tridymite). This calculation has shown that the removal of molecules of adsorbate from the silica surface by trimethylsilyl groups leads to a sudden reduction of the energy of adsorption. Even in the case of such large hydrocarbon molecules as those of n-hexane and benzene, the energy of adsorption of isolated molecules calculated theoretically has been shown to be less than the heat of condensation. It would therefore be expected that on an aerosil surface sufficiently completely modified by the trimethylsilyl groups the pure heats of adsorption of the vapors of these hydrocarbons would be negative.

Sample	Treatment in an autoclave		Specific surface after modification, m^2/g	Degree of covering of the surface by $Si(CH_3)_3$ groups, %
	temperature, °C	duration, hr		
1	–	–	170	0
2	–	–	170	~60
3	120	8	~165	~85
4	200	19.5	~142	~90
5	265	19.5	~ 71	~100

As can be seen from the publication [2], and the heats of adsorption measured by us on aerosils having a surface modified to approximately only 60 and 85 %[5], it is very important to obtain, if possible, a more complete layer of trimethylsilyl groups, which would practically exclude adsorption in the free silica spaces lying between these groups on the surface. With the object of obtaining an aerosil surface which, in the first place, had a greater geometrical uniformity and, in the second, possessed a maximum capacity for reacting with trimethylchlorosilanes, we first of all carried out a preliminary hydrothermal treatment of the aerosil, as a result of which its particles increased in size, while its surface became smoother and was found to be covered with

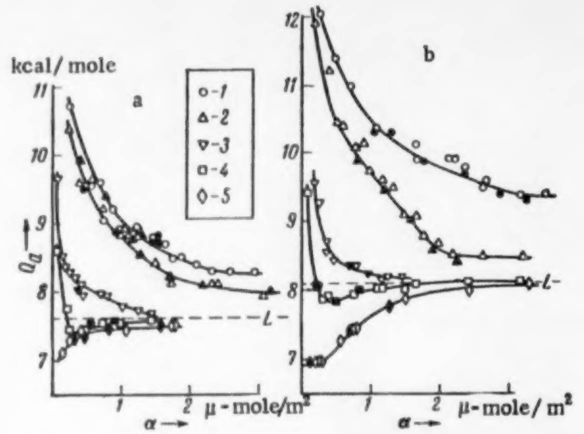

Fig. 1. Relationship between the differential heats of adsorption of the vapors of n-hexane (a) and benzene (b) and the degree of covering of the surface of the initial aerosil (1) and aerosils modified to the extent of 60%(2), 85% (3), 90% (4), and 100% (5). The black points here and on Fig. 2 denote desorption.

hydroxy groups to the maximum extent. This provided good conditions for the reaction with trimethylchlorosilane. The table gives the conditions for obtaining various samples of modified aerosils, and also the mean concentrations of trimethylsilyl groups on the surface, calculated from chemical analyses (after evacuation of the samples at 150°). It was assumed that the area occupied by these groups was equal to 42 Å^2 [2]. The measurements were carried out in a calorimeter [4].

It is seen from the table that the last specimen may really be considered as a satisfactory approximation to the theoretically calculated model [3].

Figure 1 shows the relationship obtained between the differential rate of adsorption Q_a and the magnitude of the adsorption α (μ -mole per m^2), while Fig. 2 gives the adsorption isotherm α as a function of the relative vapor pressure p/p_s. It can be seen from Fig. 1 that the heat of adsorption of these hydrocarbons when the surface is modified is diminished, while with increase in the degree of modification there is an abrupt change in the form of the relationship between Q_a and α, although when modification occurs to the extent of 60% and then of 85% the magnitude Q_a initially remains large and always exceeds the heat of condensation L; yet when modification approaches the value of 90%, the values of Q diminish for small values of α to magnitudes somewhat smaller than L, while for the most complete modification (approximately 100%) the heats of adsorption Q_a for n-hexane and benzene are equal to approximately 7 kcal/mole. That is, the pure heat of adsorption becomes definitely negative: for n-hexane, $Q_a - L = -0.5$; and for benzene, $Q_a - L = -1.0$ kcal/mole. In this work, however, we have not been able to observe the initial reduction in the heat of adsorption which is characteristic of adsorption on nonuniform places of the surface at high adsorption potential. With increase in the value of α, after the covering of the surface with molecules of n-hexane and benzene, the heat of adsorption increases by about 10%, and quickly attains the value of the heat of condensation.

As would be expected for such a great reduction in the heat of adsorption, a reduction also takes place in the magnitude of the adsorption α itself (Fig. 2). When $p/p_s = 0.1$, the adsorption of n-hexane, with increase in degree of modification to approximately 100%, is diminished by a factor of 12, while the adsorption of benzene is diminished by a factor of 35. The relatively stronger reduction of the adsorption and the heat of adsorption of benzene is due to the fact that according to the high content of hydroxide groups on the surface of the initial aerosil the benzene molecules are adsorbed both on account of electrokinetic (dispersion) effects and on account of electrostatic interaction of their quadrupoles with the dipoles of the hydroxyl groups of the silica surface [6]. It can be seen from Fig. 2 that for the most complete modification of the sample the adsorption isotherm of n-hexane is initially concave, while the adsorption isotherm of benzene is approximately linear.

Because of the very weak interaction of the adsorbate with the adsorbent, it follows that even to retain on the surface very small quantities of these adsorbates requires very large values of the ratio p/p_s. Under these conditions, the free surface of modified particles is covered only by an attenuated film of hydrocarbon molecules, while in the space between the particles of the aerosil, close to their points of contact, with sufficiently large values of p/p_s capillary condensation has already become possible. Corresponding to this also, the heats of intrinsic adsorption ought to be smaller than the measured values, since the measured magnitudes when $\alpha > 0.1$ μ-mole/m^2 (when p/p_s is greater than 0.2) include partially the heats of capillary condensation, close to the magnitude L. It is also probable that the approximately constant values of the measured heats of adsorption of benzene, seen from Curve 5 in Fig. 1 in the region of low values of α, are due to a certain amount of superimposition of the reduction of the heat associated with the residual nonuniformity, and the increase of heat associated

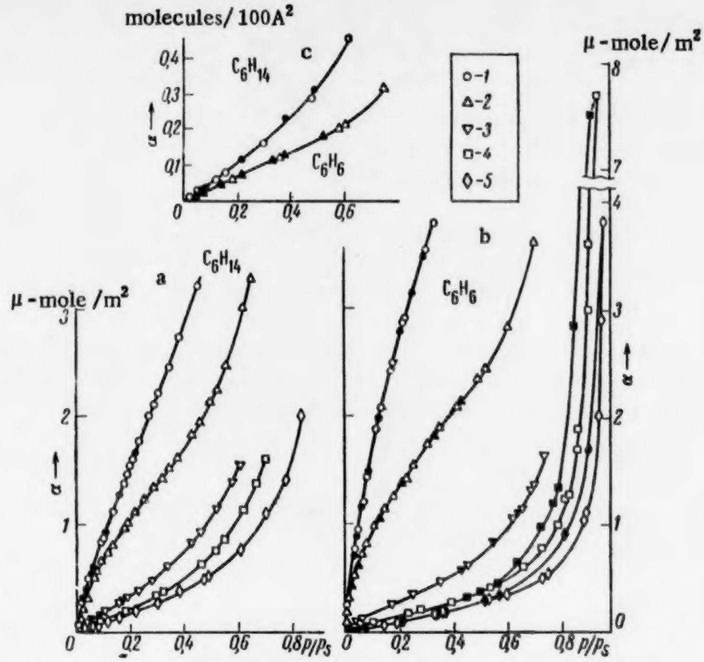

Fig. 2. Adsorption isotherms of the vapors of n-hexane (a) and benzene (b) on the initial aerosil (1) and aerosils modified to the extent of 60% (2), 85% (3), 90% (4), and 100% (5). c: Initial portion of the isotherm for the most completely modified specimen on a magnified scale.

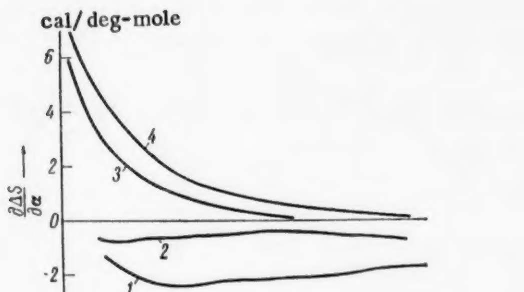

Fig. 3. Relationship between the differential entropy of adsorption of vapors of benzene (1, 4) and n-hexane (2,3), and the covering of the aerosil surface: the initial surface is denoted by (1) and (2), and the most completely modified surface by (3) and (4).

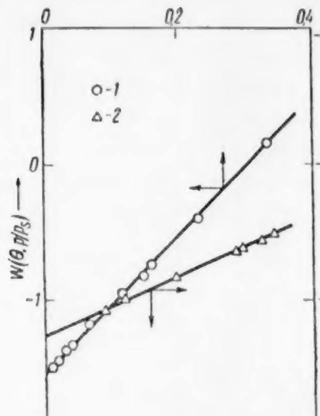

Fig. 4. Adsorption isotherms for the vapors of n-hexane (1) and benzene (2) on the most completely modified aerosil in the coordinates of Eq. (1).

with adsorbate-adsorbate attraction and with the increased contribution of capillary condensation. Thus, the true heat of intrinsic adsorption of these hydrocarbons on a completely uniform surface of the modifying layer (without capillary condensation) ought to be still lower: It might, for example, lie close to the very low values (4.3 and 4.0 kcal/mole for vapors of n-hexane and benzene) calculated theoretically in [3].

Figure 3 gives the curves showing the relationship between the differential entropy of adsorption of n-hexane and benzene on the initial and the most completely modified samples of aerosil, calculated from the adsorption isotherms and the heats of adsorption. Attention should be given to the transition of the entropy change upon modification, from the region of negative values to that of very large positive values (in relation to the entropy of the corresponding liquids). This gives evidence of the considerable mobility of the n-hexane and benzene molecules on the surface of the modified layer. Such large values of the entropy, very small values of the energy of adsorption, and great uniformity of the surface permit one to suppose that to a large extent the adsorption on the surface of n-hexane and benzene for samples with the most complete degree of modification is nonlocalized. In this connection, it is interesting to note that the adsorption isotherms of the vapors of these substances on the most completely modified samples, for the initial region in which the capillary condensation between the particles of the aerosil as yet introduces no appreciable distortion, are satisfactorily described by the Hill equation for nonlocalized molecular adsorption [7], taking approximate account of the adsorbate-adsorbate interaction.

Figure 4 gives the experimental points of the adsorption isotherm which are presented in the upper portion of Fig. 2, in coordinates of the linear form of this equation [8]:

$$W(\theta, p/p_s) = \frac{\theta}{1-\theta} + \ln\frac{\theta}{1-\theta} - \ln p/p_s = \ln K_1 + K_2\theta. \qquad (1)$$

Here θ is the degree of covering of the surface, K_1 is the equilibrium constant for the adsorbate-adsorbent interaction, and K_2 takes account of the adsorbate-adsorbate interaction. The quantity $\theta = \alpha/\alpha_m = \alpha\omega_m$, where α_m is the capacity of a complete monolayer, while $\omega_m = 1/\alpha_m$ is the area occupied in this layer by the molecule of the adsorbate. For n-hexane, $\omega_m = 51$ A^2, and for benzene $\omega_m = 40$ A^2 [9].

For the adsorption of n-hexane, $K_1 = 0.2$ and $K_2 = 5.0$, while for the benzene the values are $K_1 = 0.1$ and $K_2 = 4.3$. The low values of K_1 are associated with the weak adsorbate-adsorbent interaction. For benzene, K_2 is smaller than it is for n-hexane, in agreement with the lower absorbate-absorbate interaction.

Thus, the combination which has been used of geometrical modification of the particles of the aerosil (hydrothermal treatment) with subsequent modification of their surface (by reaction with trimethylchlorsilane) has led to a smoothing of the silica surface and the formation upon it of such a dense layer of attached trimethyl, silyl groups that the surface of this layer is extremely uniform, and the adsorption of hexane and benzene upon it proceeds in a nonlocalized fashion, while the energy of adsorption is so low that the pure heat of adsorption of these hydrocarbons is negative.

The authors wish to express their great gratitude to I. V. Drogleva and V. P. Marinkova for the preparation and analysis of the aerosil specimens.

LITERATURE CITED

1. Yu. I. Babkin, V. S. Vasil'eva, et al., Doklady Akad. Nauk SSSR 129, 131 (1959).
2. A. V. Kiselev, A. Ya. Korolev, et al., Koll. Zhur. 22, 671 (1960).
3. I. Yu. Babkin and A. V. Kiselev, Doklady Akad. Nauk SSSR 129, 357 (1959).
4. A. A. Isirikyan, A. V. Kiselev, and B. A. Frolov, Zhur. Fiz. Khim. 33, 389 (1959).
5. A. W. Kisselew and K. D. Schtscherbakowa, Gas-Chromatographie 1959, Material zum 2 Symposium über Gas-Chromatographie in Böhlen, Berlin, 1959, p. 198.
6. A. V. Kiselev and D. P. Poshkus, Doklady Akad. Nauk SSSR 120, 834 (1958).
7. T. H. Hill, J. Chem. Phys. 14, 441 (1946).
8. S. Ross and W. Winkler, J. Coll. Sci. 10, 319 (1955).
9. N. N. Avgul', G. I. Berezin, et al., Koll. Zhur. 20, 298 (1958).
10. A. V. Kiselev, Zhur. Fiz. Khim. 35, No. 2 (1961).

THE FORMATION OF SURFACE INTERMEDIATE FORMS IN HETEROGENEOUS CATALYSIS

V. É. Vasserberg, Academician A. A. Balandin, and I. R. Davydova

N. D. Zelinskii Institute of Organic Chemistry, Academy of Sciences of the USSR

Translated from Doklady Akademii Nauk SSSR,
Vol. 136, No. 2, pp. 371-380, January, 1961
Original article submitted August 30, 1960

Experimental material which has been accumulated during the investigation of heterogeneous catalytic reactions has for some time led many investigators to the belief that these processes take place through the intermediate formation of free radicals on the catalyst surface. This postulate, which was worked out by N. D. Zelinskii and his fellow workers, who were among the first in the field [1,2], has been further developed in the works of V. V. Voevodskii, F. F. Vol'kenshtein, and N. N. Semenov [3], Ya. T. Éidus [4], S. Z. Roginskii [5], M. I. Temkin [6], and other investigators (see, for example, [7]). In a theory of catalytic hydrogenation which was put forward by one of us [8], founded upon the multiplet theory, it has been shown, starting out from kinetic data, that the existence upon the surface of metals of weakly linked hydrogen atoms as intermediate forms in hydrogenation is probable.

Up to now, however, in spite of numerous attempts, direct experimental evidence of the existence of free radicals or structures resembling them, under the condition of heterogeneous catalysis, has not been obtained; the evidence in favor of their existence has been constructed on the basis of indirect data concerning kinetic processes, the composition of reaction products, and the like.

In the course of the study of the mechanism and the experimental stages of the dehydration reactions of the lower aliphatic alcohols in the adsorbed layer, for low degrees of covering of the surface on a series of catalysts (aluminum oxide prepared in various ways: alumina + zinc oxide, alumina + ferric oxide, tungsten trioxide, magnesium sulphate, and others), we have obtained numerous kinetic data [9,10], which may most easily be interpreted from the point of view that surface radicallike complexes are formed. In particular, we have shown that the rate of dehydration of any alcohol, such as isopropyl alcohol, in the adsorption layer on the surface of a catalyst with 2-4% surface covering (on the basis of a monolayer) may be changed within wide limits (usually undergoing reduction) if there are also present on the surface, in the proportion from 2 to 10-15% of a monolayer, other alcohols previously adsorbed (ethyl, methyl, and others), ethers (ethyl, diisopropyl), or other substances (such as acetone, acetoacetic ester, acetonitrile, dioxane, and others) [11,12]. It is found under such conditions that the different previously adsorbed substances, for a uniform density of adsorption on the surface, influenced to varying degrees the rate of decomposition of the initial alcohol. Other indirect confirmation of the formation of surface free radicallike forms may be found in the fact established by us that under the conditions of dehydration catalysis labelled atoms of radiocarbon C^{14} are transferred from dimethyl ether to unlabelled ethyl or isopropyl alcohol, and also to the products of their dehydration [13,14].

Since the dehydration reaction in an adsorbed layer takes place at comparatively lower temperatures (120 to 130° instead of 250-350° under ordinary conditions), while the length of life of the radicallike complexes on the surface ought to increase, we have carried out attempts to detect them directly for a series of compounds with unpaired electrons, among them free organic radicals, by means of the characteristic physical property of paramagnetism. The presence of paramagnetism may be detected, for example, by the acceleration of the para-ortho conversion of hydrogen in the presence of the given compound. Schwab [15] was the first to propose a

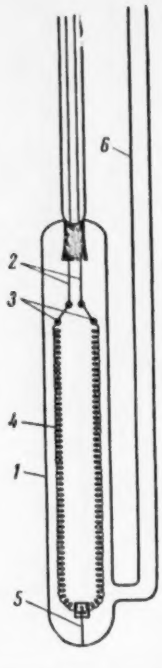

Fig. 1. Vessel for the measurement of thermal conductivity: 1) main body: glass tube (d = 12 mm, l = 100 mm); 2) molybdenum wire leads (d = 0.5 mm); 3) platinum wire (d = = 0.3 mm); 4) tungsten spiral made of wire (d = 20μ, resistance = about 300 ohm); 5) fixer for spiral–capillary piece with T-shaped glass thread fused to it, the thread being fused to the base of the vessel; 6) capillary lead from the tube.

similar method of detecting, and even of quantitatively estimating, the concentration of free organic radicals from their catalysis of their para-ortho conversion of hydrogen. In contrast with Schwab, however, we propose to investigate in this way not heavy hydrocarbon radicals (of the type of triphenylmethyl) in solutions, but the light lower radicallike structures which arise during the dehydration of isopropyl alcohol on the catalyst surface.

We had originally intended to use as catalyst one of the preparations of aluminum oxide which we had investigated in previous works [9,10]. However, it appeared that this catalyst itself was catalytically active in the ortho-para conversion of hydrogen not only at temperatures at which the dehydration reaction was carried out in a monolayer (120-150°), but also at room temperature. We then chose magnesium sulphate, which has been described as an active catalyst for the dehydration of secondary alcohols in publication [16] and has also been investigated by us under the conditions obtaining for the reaction in the adsorbed layer. It has been shown that on this catalyst the dehydration of alcohols in the adsorption layer proceeds with sufficient velocity at 150-180°, while the para-ortho conversion of hydrogen does not proceed appreciably even at temperatures as high as 300°. It has been observed, however, that under the conditions of the dehydration reaction for the alcohol with subsequent regeneration in a hydrogen atmosphere at 300° the catalyst is partially reduced with the formation of hydrogen sulphide and loses its activity. We are intending to investigate as a problem by itself the question of the possible influence of hydrogen sulphide or its intermediate reduction products. Because of this complication, we have carried out each experiment with a fresh sample of the catalyst, and have not carried out regeneration after the experiments. The catalyst was prepared according to the method described in [16]. The surface of the catalyst was determined by the BET method from the low-temperature adsorption isotherm of nitrogen, and amounted to 10-15 m^2/g.

The work was carried out in the following manner. We made use of a glass high-vacuum circulation plant which had been constructed and assembled by S. L. Kuperman and I. R. Davydova and had been used by us in work on the investigation of the ortho-para conversion of hydrogen on nickel [17]. Into this plant we introduced the catalyst sample and evacuated it carefully for a period of three hours at a temperature of 300° and a pressure of the order of 10^{-5} mm Hg. Before each experiment the absence of any conversion of parahydrogen on the given catalyst sample was confirmed. During the preliminary evacuation of the catalyst, and the cooling of it to the temperature of the experiment, there was circulated a 50% mixture of para- and orthohydrogen (obtained in the usual manner by desorption from activated charcoal, after exposure to the temperature of liquid nitrogen for several hours), and samples were periodically removed for checking in the vessel provided for the measurement of thermal conductivity.

In distinction from the method used in [14], the vessel used in the present case (Fig. 1) was a test tube of molybdenum glass in which had been introduced a spiral of tungsten wire of diameter 20μ, having a resistance at room temperature of 300 ohms.

After the absence of ortho-para conversion on the catalyst under the conditions of the experiment had been established, the catalyst was again evacuated under a vacuum of 10^{-5} mm Hg, and the vapor of isopropyl alcohol was introduced. This was done by using an electromagnet to break an ampoule of isopropyl alcohol which had previously been introduced into the setup. The ampoule was filled by alcohol in another setup, also under high-vacuum conditions, in order to exclude the introduction of oxygen, which also possesses paramagnetic

Effect of the Surface Catalytic Reaction on the Para-Ortho Conversion of Hydrogen

Expt. No.	Quantity of catalyst, g	Temp., °C	Quantity of initial alcohol, ml	Circulation time, min	Degree of conversion, %
1	0	180	0.2	Infinite	0
2	0	200	0.4	"	0
3	3.3	156	0.0	"	0
	3.3	156	0.05	15	13.3
	3.3	156	0.05	Infinite	13.3
4	10.7	185	0.0	"	0
	10.7	185	0.4	15	13.5
	10.7	185	0.4	Infinite	13.5
5	11.0	187	0.0	"	0
	11.0	187	0.2	15	5.3
	11.0	187	0.2	Infinite	5.3
6	11.0	183	0	"	0
	11.0	183	0.4	15	13.2
	11.0	183	0.4	Infinite	13.2

properties. When the alcohol had been evaporated from the broken ampoule and its vapor had been adsorbed upon the catalyst, i.e., after a period of 20-30 sec after the breaking of the ampoule, there was introduced into the system a 50% mixture of para- and orthohydrogen, and a sample was removed after 10-15 min for analysis with respect to its thermal conductivity. The length of time which was allowed to elapse before the removal of the sample was chosen on the basis of the fact that the half-decomposition period of isopropyl alcohol in the adsorption layer, determined in the setup [9] under the given conditions, amounted to 5-10 min.

After the conclusion of an experiment, the reaction products were removed from the setup containing the catalyst under a vacuum of the order of 10^{-5} mm Hg, and the setup was again filled with a 50% mixture of para- and orthohydrogen, and after 5-10 min circulation over the catalyst, the thermal conductivity of the gas was determined again and found to be practically indistinguishable from the initial value, which served as a confirmation of the reproducibility.

In certain experiments, so as to establish the absence of catalytic effect of extraneous substances on the ortho-para conversion reaction, the reaction products were added to the parahydrogen which was introduced after a reaction had been carried out, the products having previously been frozen out in a special trap; this mixture was then circulated over the catalyst. It was also shown by means of special experiments that the initial alcohol vapor had no effect (in the absence of the catalyst) on the ortho-para reaction.

A summary of the experimental data which have been obtained is given in the table.

It has been shown above that the 50% mixture of para- and orthohydrogen is practically unchanged under the conditions of the experiment in contact with the catalyst and with the vapors of the reaction products, and also with the alcohol vapor in the absence of the catalyst. From this, and from the information in the table, it is established that substantial conversion only takes place in contact with the catalyst on which there is taking place at the same time the catalytic dehydration of the alcohol. The extent of the ortho-para conversion of hydrogen amounts to 13.5% of the theoretically possible value, and the values obtained for the change of the resistance of the measuring wire lie well outside the limits of the possible experimental error. After the completion of the reaction, while maintaining all the remaining conditions, it is found that the ortho-para conversion of hydrogen again does not take place.

Thus, the results of our experiments may be interpreted as direct experimental confirmation of the reality of the development of such intermediate compounds during the conditions of heterogeneous catalysis. These

intermediate compounds are multiplet complexes which possess the characteristic paramagnetic properties of free radicals. This may also be regarded as confirmation of the utility of the assumption concerning the formation of surface free radicallike structures which has been used by us earlier for the explanation of a series of peculiarities of elementary kinetic reaction processes in the dehydration of alcohols and ethers in the adsorption layer.

Similar structures of a free radical type apparently arise also in other heterogeneous processes, but it would seem that the detection of these by means of the method which we have here used will only be possible as a result of a successful combination of catalyst and the nature of the reaction. The application of this method to other processes would meet with great difficulties since, for example, it would be expected that all catalysts for hydrogenation and dehydrogenation reactions would act on their own account as catalysts for the para-ortho conversion of hydrogen, while the investigation of catalytic oxidation reactions is impossible because of the poisoning influence of the oxygen, etc.

LITERATURE CITED

1. N. D. Zelinskii and N. I. Shuikin, Doklady Akad. Nauk SSSR 3, 225 (1934).
2. N. D. Zelinskii and Ya. T. Éidus, Izvest. Akad. Nauk SSSR, Otd. Khim. Nauk No. 2, 289 (1940).
3. V. V. Voevodskii, F. F. Vol'kenshtein, and N. N. Semenov, Collected Papers on Questions of Chemical Kinetics, Catalysis, and Reactivity [in Russian] (Izd. AN SSSR, 1955) p. 423.
4. Ya. T. Éidus and N. V. Ershov, Izvest. Akad. Nauk SSSR, Otd. Khim. Nauk No. 10, 1655 (1959).
5. S. Z. Roginskii, Collected Papers on Problems of Kinetics and Catalysis [in Russian] (Izd. AN SSSR, 1960) Vol. 10, p. 373.
6. M. I. Temkin, Collected Papers on Questions of Chemical Kinetics, Catalysis, and Reactivity [in Russian] (Izd. AN SSSR, 1955) p. 484.
7. C. Kemball, Bull. Soc. Chim. Belg. 67, 375 (1958).
8. A. A. Balandin, Zhur. Fiz. Khim. 31, No. 4, 745 (1957).
9. V. É. Vasserberg and A. A. Balandin, Collected Papers on Problems of Kinetics and Catalysis [in Russian] (Izd. AN SSSR, 1960) Vol. 10, p. 356.
10. V. É. Vasserberg, A. A. Balandin, et al., Papers Presented to the Eighth Mendeleev Convention, Collected Contributions [in Russian] (Izd. AN SSSR, 1958) Vol. 1, p. 174.
11. V. É. Vasserberg, A. A. Balandin, and T. V. Georgievskaya, Doklady Akad. Nauk SSSR 133, No. 2 (1960).
12. V. É. Vasserberg and T. V. Georgievskaya, Schedule of the Conference on Organic Catalysis [in Russian] (Izd. AN SSSR, 1959) p. 59.
13. V. É. Vasserberg, A. A. Balandin, and T. I. Levi, Kinetika i Kataliz 2, No. 1 (1961).
14. G. I. Levi and V. É. Vasserberg, Schedule of the Conference on Organic Catalysis [in Russian] (Izd. AN SSSR, 1959) p. 61.
15. G. M. Schwab and E. Agallidis, Z. Phys. Chem. B41, 59 (1938).
16. A. A. Balandin, M. B. Turova-Polyak, et al., Doklady Akad. Nauk SSSR 144, 773 (1957).
17. S. L. Kuperman and I. R. Davydova, Schedule of the Conference on Organic Catalysis [in Russian] (Izd. AN SSSR, 1959) p. 6.

All abbreviations of periodicals in the above bibliography are letter-by-letter transliterations of the abbreviations as given in the original Russian journal. *Some or all of this periodical literature may well be available in English translation.* A complete list of the cover-to-cover English translations appears at the back of this issue.

THE THEORY OF THE EROSION COMBUSTION OF POWDERS

V. I. Vilyunov

Siberian Physicotechnical Institute, V. V. Kuibyshev Tomsk State University

(Presented by Academician V. N. Kondrat'ev, July 2, 1960)
Translated from Doklady Akademii Nauk SSSR,
Vol. 136, No. 2, pp. 381-383, January, 1961
Original article submitted June 23, 1960

It is known [1-3] that a turbulent current of gas proceeding over a hot surface appreciably increases the rate of combustion of a powder. In this communication there is developed a theory of this process, based upon the theory of stationary combustion [4].

We consider a semiinfinite lamina of burning powder. It will be assumed that far from the front edge there is established an asymmetrical regime for the gas current. The system of equations which describes this case is:

$$\overline{\rho v} = m_t = \text{const}, \quad p = \text{const}; \tag{1}$$

$$\overline{\rho v}\frac{du}{dy} = \frac{d}{dy}\left[(\mu + \mu_t)\frac{d\bar{u}}{dy}\right]; \tag{2}$$

$$c\overline{\rho v}\frac{d\overline{T}}{dy} = \frac{d}{dy}\left[(\mu + \mu_t)\frac{d\overline{T}}{dy}\right] + Qf(\bar{a}, \overline{T}); \tag{3}$$

$$\overline{\rho v}\frac{d\bar{a}}{dy} = \frac{d}{dy}\left[(\mu + \mu_t)\frac{d\bar{a}}{dy}\right] - f(\bar{a}, \overline{T}); \tag{4}$$

where m_t is the mass rate of combustion in the turbulent stream; $\bar{\rho}$ is the density; $\bar{v}$ is the projection of velocity on the y axis; $\bar{u}$ is the projection of velocity on the x axis; μ_t is the coefficient of "turbulent" dynamic viscosity; $\overline{T}$ is the temperature; $\bar{a}$ is the relative concentration of the reacting substance; Q is the thermal effect; $f(\bar{a}, \overline{T})$ is the total velocity of the chemical reaction; c is the thermal capacity. The remaining terms are in agreement with those used in [4].

For the description of systems (2)-(4), we postulate that

$$c\mu = \lambda; \quad \nu = D; \quad c\mu_t = \lambda_t; \quad \nu_t = D_t, \tag{5}$$

where λ, D, and ν are the molecular coefficients of thermal conductivity, diffusion, and kinematic viscosity, respectively, while λ_t, D_t, and ν_t are the coefficients of "turbulent" thermal conductivity diffusion and kinematic viscosity. The postulates of Eq. (5) are those generally accepted. In addition to this, in Eq. (3) we neglect the frictional heat in comparison with the heat which arises as a result of the chemical reaction.

The system of equations (3) and (4) has as its first integral*

$$\frac{\bar{a}}{\bar{a}_{s1}} = \frac{\overline{T}_{11} - \overline{T}}{\overline{T}_{11} - \overline{T}_{su}}, \tag{6}$$

*In the subsequent discussion we shall only consider the α- and β-stages [4].

and consequently can be converted to the single equation:

$$\lambda \frac{d}{dy}\left[\left(1+\frac{\nu_t}{\nu}\right)\frac{d\overline{T}}{dy}\right]-cm_t\frac{d\overline{T}}{dy}+Q_\beta f_\beta(\overline{T})=0. \tag{7}$$

α-Stage. Postulating that the turbulent pulsations do not penetrate into the liquid-viscous layer of the k phase, we shall obtain the usual system of equations for the α-stage. Therefore,

$$m_t = B_{\alpha t}e^{-E_\alpha/2R\overline{T}_{su}}. \tag{8}$$

Here the surface temperature $\overline{T}_s$ of the k-phase is designated by the index u, which indicates that this temperature depends parametrically on the rate of the current core.

It is not difficult to conclude that the erosion relationship $\mathscr{E}$ is given by

$$\mathscr{E}=\frac{m_t}{m}=\exp\left[\frac{E_\alpha}{2R}\left(\frac{1}{\overline{T}_s}-\frac{1}{\overline{T}_{su}}\right)\right]. \tag{9}$$

β-Stage By integrating (3) we obtain

$$\sigma_s=(\mu+\mu_t)\frac{d\bar{u}}{dy}-m_t\bar{u}, \tag{10}$$

where σ_s is the tangential friction tension on the heating surface of the k-phase. Equation (10) may be replaced by the more simple equation

$$\frac{\sigma_s}{\rho_{11}}=(\nu_1+\nu_{t1})\frac{d\bar{u}}{dy};\quad \nu_1=\frac{\mu}{\rho_{11}};\quad \nu_{t1}=\frac{\mu_t}{\rho_{11}}, \tag{11}$$

in which no account is taken of the drop in temperature and the intake of gaseous mass from the heated surface of k-phase.

The assumptions which have been made are not crude, and possess a simple physical significance. Actually, from the theory of the boundary layer, it is known that the influx of gaseous mass from a powder lamina leads to a considerable reduction of the frictional resistance; on the other hand, the effect of cooling the wall around which the current of gas flows leads to an appreciable increase in the frictional resistance. Thus, if both factors operate at the same time, influx of mass and the loss of heat from the gas to the wall (as in the present case of the combustion of a powder lamina), then they will partially compensate one another.

Introducing the dynamic velocity $u_\tau = \sqrt{\sigma_s/\rho_{11}}$, and the dimensionless distance from the wall $y^* = u_\tau y/\nu_1$, we find:

$$\frac{d(\bar{u}/u_\tau)}{dy^*}=(1+\nu_{t1}/\nu_1)^{-1}. \tag{12}$$

Equation (12) permits us, for a known profile of velocities, to find the coefficient of turbulent viscosity ν_{t1}. In [5] it was shown that, for conditions in which $0 \le y^* \le 30$, the distribution of velocity is in accordance with the law

$$\frac{\bar{u}}{u_\tau}=\frac{1}{\sqrt{k_1}}\operatorname{th}\sqrt{k_1}y^*, \tag{13}$$

where k_1 is a constant coefficient; therefore,

$$\frac{\nu_{t1}}{\nu_1}=\operatorname{sh}^2\sqrt{k_1}y. \tag{14}$$

By the use of (14), it is easy to find the distribution of temperature in the β-stage heating zone:

$$\ln\frac{\overline{T}-\overline{T}_{s1}}{\overline{T}_{su}-\overline{T}_{s1}}=\frac{cm_t}{\lambda}\frac{\nu_1}{\sqrt{k_1}u_\tau}\operatorname{th}\sqrt{k_1}y_u^*. \tag{15}$$

In particular, for low values of $\sqrt{k_1}y_u^*$, $\overline{T}_{su} \to \overline{T}_s$, the usual temperature profile is obtained:

$$\ln\frac{\overline{T}-\overline{T}_{s1}}{\overline{T}_s-\overline{T}_{s1}} = \frac{cm}{\lambda}\frac{\nu_1}{\sqrt{k_1 u_\tau}}\sqrt{k_1}y_0^*. \tag{16}$$

For the zone of chemical reaction in the β-stage, a reasonable approximation of the equation is

$$\lambda\frac{d}{dy}\left[\left(1+\frac{\nu_{t1}}{\nu_1}\right)\frac{d\overline{T}}{dy}\right] = -Q_\beta t_\beta(\overline{T}). \tag{17}$$

If we adopt the framework of the postulates employed by Ya. B. Zel'dovich and D. A. Frank-Kamenetskii [6], it may be shown that

$$m_t^2 = \left(1+\frac{\nu_{t1}}{\nu_1}\right)\frac{2\lambda}{c(\overline{T}_{11}-\overline{T}_{s1})}\int\limits_{\overline{T}_{su}}^{\overline{T}_{11}} f_\beta(\overline{T})\,d\overline{T}, \tag{18}$$

where ν_{t1}/ν_1 is calculated for the point corresponding to the greatest temperature of the process of combustion in the β-stage.

Using (18), and the formula similar to it from the theory of stationary combustion [4], we obtain:

$$\frac{m_t}{m} = \sqrt{\left(\frac{\overline{T}_{11}-\overline{T}_s}{\overline{T}_{11}-\overline{T}_{su}}\right)^{\nu_\beta}\operatorname{ch}(\sqrt{k_1}y_{u1}^*)}, \tag{19}$$

where y_{u1}^* is calculated at the point $\overline{T}_{11}$. Eliminating y_{u1}^* in Eq. (19), we find

$$\left(\frac{m_t}{m}\right)^2 = \frac{\overline{T}_{11}-\overline{T}_s}{\overline{T}_{11}-\overline{T}_{su}} + \frac{\sqrt{k_1}}{2\sqrt{2}}\ln\left(\frac{\overline{T}_{11}-\overline{T}_{s1}}{\overline{T}_{su}-\overline{T}_{s1}}\right)\frac{\rho_{11}u_m}{m}\sqrt{\lambda_{res}}, \tag{20}$$

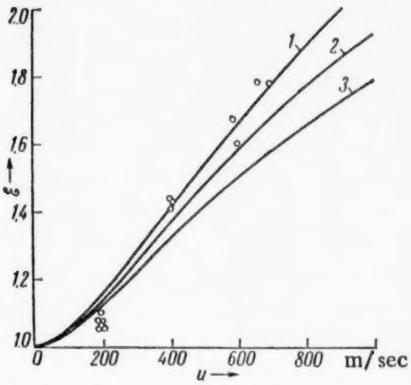

1) p = 19.6 atm; 2) p = 44.0 atm; 3) p = 71.2 atm.

where u_m is the mean velocity of current in the transverse section; λ_{res} is the coefficient of resistance, which may be obtained to a first approximation from the relationship [7]:

$$\lambda_{res} = 0{,}0032 + \frac{0{,}221}{Re^{0.237}}. \tag{21}$$

The equations (9) and (20) so obtained are sufficient to solve, in principal, the problem of the erosion burning of powders.

The figure gives the results of the calculation for the example of nitroglycerol powder when Re = 10^6 for various pressures, and the experimental points for this powder taken from [3]. It can be seen from the curves that the erosion relationship δ depends to a great extent on the rate of the gas current and on the pressure. If the erosion ratio is presented, not as a function of the rate of the gas current, but as the dimensionless complex $J = \frac{\rho_{11}u_m}{m}\sqrt{\lambda_{res}}$, then, probably, many experimental results for different brands of fuel may be introduced into a single universal curve.

LITERATURE CITED

1. L. Green, Jet Propulsion 24, 9 (1954).
2. L. Touchard, Mém. Artill. Franç. 26, 297 (1952).
3. R. N. Wimpress, Internal Ballistics of Solid Fuel Rockets (New York, 1950).
4. V. N. Vilyunov, Doklady Akad. Nauk SSSR 136, No. 1 (1961).
5. W. D. Rannie, J. Aeronaut. Sci. 23, No. 5, 485 (1956); V. D. Rénin, Sborn. Mekhanika No. 6 (40) (1956).
6. Ya. B. Zel'dovich and D. A. Frank-Kamenetskii, Zhur. Fiz. Khim. 12, 10 (1938).
7. L. G. Loitsyanskii, The Aerodynamics of the Boundary Layer [in Russian] (Moscow-Leningrad, 1941).

THE THEORY OF THE FLAME-SPREADING IN SYSTEMS WITH NONBRANCHING CHAIN REACTIONS

L. A. Lovachev

Institute of Chemical Physics, Academy of Sciences of the USSR
(Presented by Academician V. N. Kondrat'ev, July 20, 1960)
Translated from Doklady Akademii Nauk SSSR,
Vol. 136, No. 2, pp. 384-387, January, 1961
Original article submitted July 18, 1960

In previous publications [1-6], relationships have been found for the determination of the rate of flame-spreading for those cases in which the diffusion coefficients of the initial substances are compared with the coefficient of temperature conductivity; in this case, the concentrations of the initial substances are calculated as linear functions of the temperature. In the present article, a solution is offered to the problem, taking into account the equation for the diffusion of the initial substance.

The scheme of a model nonbranching chain reaction, in which A is the initial substance, P is an active center, and C is the product of reaction, is taken in accordance with [1,3,7] in the following form:

$$A \to 2P, \qquad \Phi_R = h_R R = h_R F_R (T')\, n_A; \tag{1}$$

$$P + A \to 2C + P, \qquad \Phi = hK (T')\, n_A\, n; \tag{2}$$

$$2P \to A, \qquad \Phi_W = h_W W (T')\, n^2. \tag{3}$$

The equations depicted on the right are those for the rates of evolution (or absorption) of heat. Here h_i* is the thermal effect of the reaction (cal/mole); R is the rate of chain initiation (mole/cm^3 · sec); K and W are rate constants for continuation and destruction of chains, respectively, (g^2/cm^3 · mole · sec); n_A is the concentration of A (mole/g of mixture); n is the concentration of P (mole/g of mixture); and T' is the temperature (°K).

The system of equations for flat laminar flames for the given reaction scheme can be presented in the form of the three equations:

$$\frac{d}{dx}\left(\lambda \frac{dT}{dx}\right) - Bc\frac{dT}{dx} + \Phi_R + \Phi + \Phi_W = 0, \tag{4}$$

$$\frac{d}{dx}\left(D_A \frac{dn_A}{dx}\right) - B\frac{dn_A}{dx} - Kn_A\, n - 0{,}5F_R n_A + 0{,}5\, Wn^2 = 0, \tag{5}$$

$$\frac{d}{dx}\left(D \frac{dn}{dx}\right) - B\frac{dn}{dx} + F_R n_A - Wn^2 = 0 \tag{6}$$

with the limiting conditions:

$$\left.\begin{matrix} T = 0, & n = n_0, & n_A = n_{A0}, \\ T = T_r, & n = n_r, & n_A = n_{Ar}, \end{matrix}\right\} \quad \frac{dT}{dx} = \frac{dn_A}{dx} = \frac{dn}{dx} = 0,$$

*As in original–Publisher.

where $B = u\rho$; $T = T' - T'_0$; $D_A = \rho D_{PA}$; $D = \rho D_P$; x is the coordinate (cm); u is the velocity of current (cm/sec); ρ is the density (g/cm³); λ is the thermal conductivity of mixture (cal/cm · sec · C°); c is the heat capacity (cal/g · C°); D_P and D_{PA} are the coefficients of diffusion corresponding to P and A, respectively (cm²/sec). The index 0 corresponds to the initial state of the fresh mixture ($T' = T'_0$), the index Γ to the state at the temperature of combustion ($T' = T'_\Gamma$), while the index m will be related to the state described by the maximum value of the temperature gradient $(dT/dx)_m = p_m (T' = T_m)$ [1,3].

If $\lambda = cD_A$, then, as we can see from (4) and (5), n_A will, in general, not be a function of temperature alone. This means that when chain reactions take place in a flame there cannot be a strict correspondence between the concentration of A and the temperature. It has been shown previously that in many cases [2] it is permissible to neglect the quadratic chain breaking for values of T close to T_m. (The estimation of the effect of W, however, must always be derived from the solution obtained in [2], taking account of quadratic chain breaking.) In addition, it must always be true that $0.5R_m \ll K_m n_{Am} n_m$, since the activation energy in R is appreciably larger than the activation energy of the continuation process (2). Therefore, it must be true that $|\Phi_{Rm}| \ll |\Phi_m|$, although $|h_R| > |h|$. Thus, we obtain from Eqs. (4)-(6) a system of equations similar to those used in [1,3,7]:

$$\frac{d}{dx}\left(\lambda \frac{dT}{dx}\right) - Bc\frac{dT}{dx} + \Phi = 0, \tag{7}$$

$$\frac{d}{dx}\left(D_A \frac{dn_A}{dx}\right) - B\frac{dn_A}{dx} - Kn_A n = 0, \tag{8}$$

$$\frac{d}{dx}\left(D \frac{dn}{dx}\right) - B\frac{dn}{dx} + F_R n_A = 0. \tag{9}$$

On the basis of the method previously worked out for the approximate solution of the diffusion equations [1-3], the concentrations of A and P at a temperature $T = T_m$ may be described in the following form:

$$n_{Am} = t_A\omega_A - K_m N_A n_{Am} n_m, \tag{10}$$

$$n_m = t\omega + F_{Rm} N n_{Am}, \tag{11}$$

where $t = n_0 + lT_m$; $t_A = n_{A0} + l_A T_m$, $l = (n_\Gamma - n_0)/T_\Gamma$, $l_A = (n_{A\Gamma} - n_{A0})/T_\Gamma$, $\omega = 1 - 2q/\varkappa$, $\omega_A = 1 + 2q_A/\varkappa_A$, $\varkappa = c_0 D_0/\lambda_0$, $\varkappa_A = c_0 D_{A0}/\lambda_0$, $D_0 = D_m q$, $D_{A0} = D_{Am} q_A$, $q = \frac{\mu_0}{\mu_m}\left(\frac{T'_0}{T'_m}\right)^{a-1}$ when $D_P \sim (T')^a$, $q_A = \frac{\mu_0}{\mu_m}\left(\frac{T'_0}{T'_m}\right)^{a_A - 1}$ when $D_{PA} \sim (T')^{a_A}$, $N = r/2D_m p_m^2$, $N_A = r/2D_{Am} p_m^2$, $r = T_m(T_\Gamma - T_m)$, $T_m = 0{,}5\,T_\Gamma$.

Solving (10) and (11), we obtain the relationship

$$n_{Am} = \frac{(1 + t\omega K_m N_A)}{2F_{Rm} K_m N N_A}\left[\sqrt{1 + \frac{4t_A\omega_A F_{Rm} K_m N N_A}{(1 + t\omega K_m N_A)^2}} - 1\right], \tag{12}$$

and after inserting the value of this in Eq. (11), we determine n_m.

It may be shown, on the basis of the previous results [2,8], that the relationship $t\omega K_m N_A \cong 2q_A/\xi\varkappa_A$, where ξ is a coefficient taking into account the effect of the rate of chain initiation [8]. When $\lambda = cD_A$ and $t_A h = c_m T_m$, the equality will be exact. Since this equality is necessary only for rough estimation, then it may also be used when $\lambda \neq cD_A$. If we postulate that the fraction beneath the square-root sign in Eq. (12) is less than unity, and make use of the equation so obtained, we find that

$$\frac{4t_A\omega_A D_{Am}\,(2q_A)^2}{(t\omega)^2 D_m\,(\varkappa_A + 2q_A)^2}\,\frac{F_{Rm}}{K_m} < 1. \tag{13}$$

If the inequality (13) is satisfied, then the term beneath the square root in Eq. (12) may be resolved into a series, and we may obtain for n_{Am} the simple relationship

$$n_{Am} = \frac{t_A\omega_A}{(1 + t\omega K_m N_A)}. \tag{14}$$

Inserting Eq. (14) in (11), we find

$$n_m = t\omega\left[1 + \frac{t_A\omega_A F_{Rm} N}{t\omega\,(1+t\omega K_m N_A)}\right]. \tag{15}$$

The fraction contained within the square brackets in Eq. (15) is of the same order as the fraction beneath the square root in Eq. (12), but in Eq. (15) the fraction is added to unity, and therefore the requirement that it should be small must be more rigid. If the fraction is equal to unity, then if we postulate that $F_{Rm} \sim 0$, the error in n_{Am} according to Eq. (14) amounts to 18%, while the error in n_m according to Eq. (15) amounts under the same conditions to 50%.

Inserting Eqs. (14) and (15) in (7), and taking $F_{Rm} = 0$, we find, when $T = T_m$, after rearrangement:

$$p_m^2 = \frac{1}{c_m\eta} t\omega K_m\left[ht_A + \frac{2q_A}{\varkappa_A}(ht_A - c_m T_m)\right]. \tag{16}$$

Inserting Eqs. (14) and (15) in (7) when $T = T_m$, but when $F_{Rm} \neq 0$, we obtain

$$\begin{aligned} c_m\eta\, p_m^4 &- t\omega\,(ht_A\omega_A - 2c_m\eta\delta_A)p_m^2 - hK_m(t_A\omega_A)^2\,\delta F_{Rm} - \\ &- K_m^2\,(t\omega)^2\delta_A\,(ht_A\omega_A - c_m\eta\delta_A) = 0, \end{aligned} \tag{17}$$

where $\eta = 4\lambda_0/c\sigma T_m$, $\delta_A = r/2D_{Am}$, $\delta = r/2D_m$.

The rate of propagation of the flame is determined by the relationship [1,3]:

$$u_0 = \frac{1}{\rho_0}\eta p_m, \tag{18}$$

where p_m is found from Eqs. (16) and (17). If it is necessary to use Eq. (12) instead of (14), then Eqs. (12) and (11) should be inserted in (7) when $T = T_m$. From the equation obtained, it is possible to determine p_m for (18).

Inserting (16) in (18), we obtain the final relationship for determining the rate of propagation of the flame:

$$u_0 = \varphi\,\frac{1}{\rho_0}\sqrt{\frac{n_r Q_m' \rho_m D_{\rho m}}{2c_m T_r}}, \tag{19}$$

where $\varphi = 2\sqrt{\frac{2q}{\varkappa}\left(1 - \frac{2q}{\varkappa}\right)}$; $Q_m' = Q_m\left[1 + \frac{2q_A}{\varkappa_A}\left(1 - \frac{c_m T_m}{ht_A}\right)\right]$; $Q_m = hK_m t_A$; when $n_{Ar} = 0$, $t_A =$ $= n_{A0}/2$. This relationship, when $c_m T_m = ht_A$, should be in agreement with those equations which were obtained in [1-3] for the conditions in which $n_{Am} = t_A$.

The distribution of concentrations in relationships to the temperature according to Eqs. (14) and (15) should be determined, according to [1,3] by

$$n_A(T) = \frac{(n_{A0} + l_A T) - \frac{\eta l_A}{2D_{Am}}(T_r - T)T}{1 + \frac{K_m}{2D_{Am}p_m^2}\left[(n_0 + lT) - \frac{\eta l}{2D_m}(T_r - T)T\right](T_r - T)T}, \tag{20}$$

$$n(T) = (n_0 + lT) - \frac{\eta l}{2D_m}(T_r - T)T + F_{Rm}\frac{(T_r - T)T}{2D_m p_m^2}n_A(T), \tag{21}$$

where p_m is found from Eqs. (16) or (17).

If the effect of R on u_0 is negligibly small, then $\xi = 1$, and when $c_m T_m = ht_A$, $t\omega K_m N_A = 2q_A/\varkappa_A$. In this case, since $\omega_A = 1 + 2q_A/\kappa_A$, we obtain from Eq. (14) that $n_{Am} = t_A$. This means that, irrespective of the magnitude of the diffusion coefficient of the initial substance A, its concentration at T_m is that concentration which is obtained when $\lambda = cD_A$. Change in the magnitude D_A ought only to arise when there is a certain deformation of the relationship $n_A(T)$ in comparison with the case for which $\lambda = cD_A$, and should therefore reveal a very small influence on the magnitude of the rate of propagation of the flames. To illustrate this set of

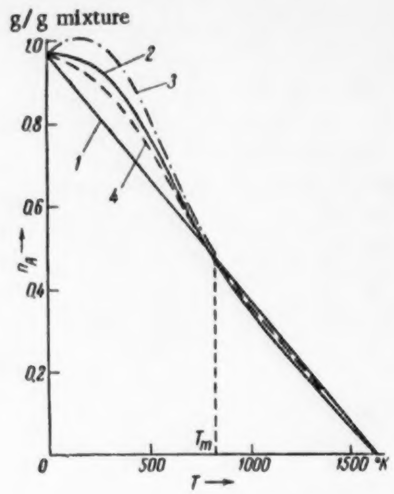

Relationship between the concentration n_A of the initial substance A (in g/g mixture) and the temperature in the flame for the decomposition of hydrazine: 1) exact solution when $\lambda = c(D_A)_1$; 2) approximate solution from Eq. (20) when $\lambda = c(D_A)_2 = c(D_A)_1$; 3) from Eq. (20) when $(D_A)_3 = (D_A)_1/1.5$; 4) from Eq. (20) when $(D_A)_4 = 1.5(D_A)_1$.

conditions we have performed numerical calculations for the example of the flame in the decomposition of hydrazine, which was investigated in [1,3,7]. All the initial data for the flame, when the combustion temperature $T_\Gamma = 1950°K$, have been taken from [7] and were also employed in [3].

The figure gives the relationship of the concentration of the initial substance A to the temperature. The initial concentration $n_{A0} = 0.972$ g/g mixture, while the concentration at the combustion temperature $n_{A\Gamma} = 0$. Curve 1 corresponds to the case in which $\lambda = cD_A$, and is an exact solution. Curve 2 corresponds also to $\lambda = cD_A$, but it has been calculated from the approximate solution (20), obtained as a result of the solution of the system of equations (7)-(9). Comparison of the relationships 1 and 2 shows that the approximate solution (20) gives $n_A(T)$ in practical agreement with the exact relationship. This signifies that for systems with nonbranching chains the solution of the problem of flame propagation may be obtained approximately on the assumption that the concentration of the initial substances is a linear function of the temperature, without thereby introducing any appreciable errors into the final results. Such an assumption, which was used in previous works [1-6,8], appreciably simplifies the solution of the problem in question.

Comparison of relationships 3 and 4 with relationship 2 in the figure permits us to draw the conclusion that the magnitude of the diffusion coefficient of the initial substance under ordinary conditions shows no appreciable influence on the magnitude of the rate of flame propagation in systems with nonbranching reaction chains. When $T = T_m$, the relationship $n_A(T)$ for all values of D_A reduces to a single point. Strictly speaking, however, this correspondence, as can be seen from relationships (16) and (14), should take place only when $c_m T_m = ht_A$, i.e., under conditions for which the dissociation of the combustion products does not lead to any perceptible reduction of the combustion temperature. For appreciable dissociation, even when $\lambda = cD_A$, there cannot strictly exist a correlation between the temperature and the concentration of the initial substance.

LITERATURE CITED

1. L. A. Lovachev, Doklady Akad. Nauk SSSR 120, No. 6, 1287 (1958).
2. L. A. Lovachev, Doklady Akad. Nauk SSSR 123, No. 3, 501 (1958).
3. L. A. Lovachev, Izvest. Akad. Nauk SSSR, Otd. Khim. Nauk. No. 10, 1740 (1959).
4. L. A. Lovachev, Doklady Akad. Nauk SSSR 124, No. 6, 1271 (1959).
5. L. A. Lovachev, Doklady Akad. Nauk SSSR 125, No. 1, 129 (1959).
6. L. A. Lovachev, Izvest. Akad. Nauk SSSR, Otd. Khim. Nauk. No. 6, 1022 (1960).
7. D. B. Spalding, Phil. Trans. Roy. Soc. London A249, No. 957, 1 (1956).
8. L. A. Lovachev, Izvest. Akad. Nauk SSSR, Otd. Khim. Nauk No. 3, 442 (1960).

All abbreviations of periodicals in the above bibliography are letter-by-letter transliterations of the abbreviations as given in the original Russian journal. *Some or all of this periodical literature may well be available in English translation.* A complete list of the cover-to-cover English translations appears at the back of this issue.

THE DIFFUSION COEFFICIENTS OF IONS IN FUSED SLAGS

V. I. Musikhin and O. A. Esin

Institute of Metallurgy of the Ural Branch of the Academy of Sciences of the USSR
(Presented by Academician A. N. Frumkin, July 20, 1960)
Translated from Doklady Akademii Nauk SSSR,
Vol. 136, No. 2, pp. 388-390, January, 1961
Original article submitted July 9, 1960

The cathodic deposition of various elements from molten slags is accompanied by concentration polarization [1]. This makes it possible to use oscillography at a given current strength [2-5] for the determination of the diffusion coefficients (D) of ions in liquid slags. For values of the current density (i) greater than the limiting value, the concentration (C_0) of the substance undergoing reduction at the cathode is rapidly reduced, and after a definite time (t_0) is equal to zero, thus causing a jump in the electrode potential. From the experimentally determined value of t_0 for chosen values of C_0 and i, the value of D may be calculated from the formula [2]:

$$D = \frac{4i^2 t_0}{\pi C_0^2 n^2 F^2}, \tag{1}$$

in which n is the number of electrons in the elementary discharge act, and F is the Faraday constant.

The slags investigated, the electrolytic vessel, and the electrodes were the same in this investigation as in the previous work [6]. Variation of electrode potential against time was registered by means of a series oscillograph for several speeds of movement of the photographic film. An amplified signal was imposed upon the oscillograph. The amplifier was based upon tubes 6N9 and 6G7, according to a bridge plan, and permitted the preliminary compensation of potential loss caused by the ohmic resistance of the cell, as well as registration of the electrode polarization. For the determination of the surface dimensions of the working cathode (liquid copper), an x-ray investigation of it was carried out, in contact with the slag being studied, for various temperatures (1350-1550°C) and various current densities (0.13-0.40 amp/cm²). It was found that the meniscus had the form of a hemisphere, the radius of which was close to that of the tube (3.25 mm). The working area of the cathode changed comparatively slightly with variation in conditions, from 0.60 to 0.66 cm², and the average value was 0.63 cm².

For the purpose of calculating the value of C_0 (g • ion/cm³) on the basis of the atomic % (2%) of additive, the density of the molten materials which served as the polarographic base liquid was measured. The values found by this method were discovered to be in satisfactory agreement with those contained in the literature [7].

Diffusion Coefficients (cm² • sec⁻¹) of the Ions of Iron and Calcium, Found by Various Experimental Methods

Temp., °C	D_{Fe}	D_{Fe} [8]	D_{Ca} [8]	D_{Ca} [9,10]
1360	$2.2\cdot10^{-6}$	—	—	$3.5\cdot10^{-7}$ (1350°)
1400	$2.7\cdot10^{-6}$	$1.1 - 1.9\cdot10^{-6}$	$0.7 - 1.3\cdot10^{-6}$	$1.0\cdot10^{-6}$ (1430°)
1460	$4.2\cdot10^{-6}$	—	—	$9.6\cdot10^{-6}$ (1450°)
1500	$5.1\cdot10^{-6}$	$2.1\cdot10^{-6}$	$1.8\cdot10^{-6}$	$2 - 12\cdot10^{-6}$
1510	$6.6\cdot10^{-6}$	$5.0\cdot10^{-6}$	$4.0\cdot10^{-6}$	$3.4\cdot10^{-6}$ (1540°)

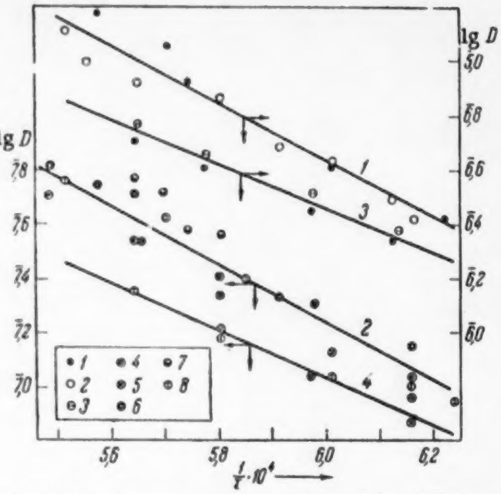

Relationship between the logarithm of the diffusion coefficients (lg D) for various ions in liquid melts, and 1/T, for the diffusion of: 1) iron; 2) cobalt; 3) nickel; 4) silicon; 5) vanadium; 6) titanium; 7) zirconium; 8) niobium.

The results of measuring the diffusion coefficient of ions of iron, cobalt, silicon, niobium, vanadium, titanium, and zirconium in an aluminum slag (45% CaO, 47% Al_2O_3, 6% MgO, and 2% B_2O_3), as well as of ions of nickel, iron, vanadium, and niobium in silicate melt (40% CaO, 40% SiO_2, and 20% Al_2O_3) are given in the figure, using the coordinates lg D and 1/T. It is a matter for regret that the literature contains no data for comparison, with the exception of the values for D_{Fe} in a silicate slag, obtained by the method of radioactive indicators [8]. It can be seen from the table that both the methods give comparable values of D_{Fe}.

The figure shows that in both melts the ions are divided sharply into two groups. The diffusion coefficients of modifiers of the first group (iron, cobalt, and nickel) at 1450° are approximately 20 times greater than for the lattice-forming elements of the second group (silicon, niobium, vanadium, titanium, and zirconium). It is known that calcium also belongs to the first group. In agreement with this, the magnitude of D_{Ca} found by other methods [8-10] is close to that for iron (D_{Fe}).

As can be seen from the figure, the relationship of the diffusion coefficient to the temperature is depicted by the equation:

$$D = D^0 e^{-E/RT}. \qquad (2)$$

Using this equation, all values of D for each group of ions are included, for the given melt, approximately on a single straight line. This, it seems, is connected with the fact that the ions of the first group occupy octahedral holes, formed by the oxygen anions; while the ions of the second group occupy tetrahedral positions. Since in the melt in question, the mean distance between corresponding holes and the energy barrier separating the latter is of the same order, it would be expected that the diffusion coefficients of ions of each of these groups would lie close to each other. There are thus in all four straight lines for the relationship lg D, 1/T, arranged in two parallel pairs for the corresponding melts. The mean activation energy (E), for the two groups of ions with a silicate melt lies within the limits 37-38 kcal/g · ion, while for the other aluminate melt the values are from 47-48 kcal/g · ion. The considerable growth of the magnitude of E is probably due to the greater strength of the bonds between the particles in the aluminate melt, which is confirmed by the increased values of the surface tension of these melts in comparison with those of the silicates [7,11].

Despite this, the diffusion coefficients in the aluminate melt (I) are greater than those in the silicate melt (II) ($D_I > D_{II}$), which is particularly strongly expressed in the values of D^0 for the first and the second groups of ions: $D_{I,1} = 4.85$, $D_{I,2} = 0.49$, $D_{II,1} = 0.23$, and $D_{II,2} = 0.014$.

According to the theory of absolute rates of reaction [12]:

$$D^0 = e\lambda^2 \frac{kT}{h} e^{\Delta S^*/R}, \qquad (3)$$

where λ is the distance between neighboring equilibrium positions for the diffusing particles, k and h are the Boltzmann and Planck constants, respectively, and ΔS^* is the activation entropy.

If we postulate that Eq. (3) is applicable to both groups of ions, the derivative

$$\lambda_{i,j} e^{\Delta S^*_{ij}/2R} = \Pi_{ij}$$

amounts to $\Pi_{I,1}$ = 22.2 A, $\Pi_{I,2}$ = 7.0 A, $\Pi_{II,1}$ = 4.8 A, and $\Pi_{II,2}$ = 1.2 A. Although the distance λ in the aluminate melt is greater than that in the silicate melt, it is questionable whether this exceeds 3-4 A [13,14]. Hence, the high values of the derivatives for the aluminosilicate melt are probably due to the greater activation entropy ($\Delta S^{*}_{I} > \Delta S^{*}_{II}$).

However, the difference in the values of ΔS^{*} for the first and second groups of ions ($\Delta S_{i,1} > \Delta S^{*}_{i,2}$) cannot be explained by the observed inequality of the derivatives corresponding to them ($\Pi_{i,1} > \Pi_{i,2}$). The problem is that the ions of the first group, moving from one octahedral hole to another, are found in a region of tetrahedral holes, where the number of neighbors is fewer. This has the effect of reducing the thermodynamic probability of the transitional state. On the other hand, ions of the second group, when leaving a stable state in a tetrahedral hole, are found temporarily in an octahedral coordination with a greater number of neighbors, which increases the number of possible states corresponding to the existence of the transitional condition. It would, in this connection, be expected that an inverse relationship would arise for the activation entropy, i.e., $\Delta S^{*}_{i,1} > \Delta S_{i,2}$.

It seems that the only slightly lattice-forming cations move together with the large oxygen anion [6]. In such a case the diffusion is determined by the transfer of the relatively small cations of the modifiers [12], while the large complexes of the lattice-forming ion with the oxygen anion only occupy the vacated sites. It is natural that the size of such movement is small (0.6-0.7 A) in comparison with the movement (2.7-3.5 A) of the ion of the modifier from one position of equilibrium to another. This is also due to the smaller value of D^0_2 in comparison with D^0_1.

LITERATURE CITED

1. O. A. Esin, Proceedings of the Fourth Conference on Electrochemistry [in Russian] (Izd. AN SSSR, 1959) p. 311.
2. A. N. Frumkin, V. S. Bagotskii, Z. A. Iofa, and B. N. Kabanov, The Kinetics of Electrode Processes [in Russian] (Moscow, 1952) p. 91.
3. H. Sand, Phil. Mag. 1, 45 (1901).
4. M. Stackelberg, M. Pilgram, and V. Toome, Z. Elektrochem. 57, 342 (1953).
5. G. A. Emel'yanenko and E. Ya. Baibarova, Ukr. Khim. Zhur. 25, No. 5, 591 (1959).
6. V. I. Musikhin and O. A. Esin, Izvest. Vyssh. Uch.Zav., The Metallurgy of Ferrous Metals [in Russian] No. 12, 3 (1959).
7. E. V. Ermolaeva, Ogneupory No. 5, 221 (1955).
8. E. S. Vorontsov and O. A. Esin, Proceedings of the All-Union Conference on the Application of Radioactive and Stable Isotopes in the Public Economy and in Science, Metallurgy, and Metallography [in Russian] (Izd. AN SSSR, 1958) p. 29.
9. H. Towers, M. Paris, and J. Chipman, J. Metals 5, No. 11, 1455 (1953).
10. H. Towers and J. Chipman, J. Metals 9, No. 6, 769 (1957).
11. S. I. Popel' and O. A. Esin, Zhur. Neorg. Khim. 2, No. 3, 632 (1957).
12. S. Glasstone, K. Laidler, and G. Eyring, The Theory of the Absolute Velocities of Reactions [Russian translation] (IL, 1948) pp. 497, 501.
13. J. O'M. Bockris, J. A. Kitchener, et al., Trans. Faraday Soc. 48, No. 1, 75 (1952).
14. O. Gassel', Crystal Chemistry [in Russian] (Leningrad, 1936) p. 30.

THE EFFECT OF GAMMA IRRADIATION ON AQUEOUS SOLUTIONS OF THIOPHENE

S. A. Safarov, A. I. Chernova, and M. A. Proskurnin

Karpov Physicochemical Institute and the Institute of Chemistry,
Academy of Sciences of the AzSSR
(Presented by Academician S. S. Medvedev, July 7, 1960)
Translated from Doklady Akademii Nauk SSSR,
Vol. 136, No. 2, pp. 391-393, January, 1961
Original article submitted July 4, 1960

Great interest is felt at the present time in reactions in which organic substances interact with the products of the radiolysis of water. Up to now, the number of systems which have been investigated is very limited. In particular, there has been no investigation of the possibility of radiolytic oxidation in the presence of water of such heterocyclic compounds as, for example, those of the thiophene series. Such processes are of great interest, since the hydroxy derivatives of thiophene have not been obtained by a number of the usual oxidation processes. The possibility of synthesizing them directly, therefore, by a radiochemical method could have considerable practical importance.

The authors of the present communication have studied the effect of irradiation on solutions of thiophene in water saturated with oxygen, with the object of elucidating the direction of the oxidation process and the possibility of forming hydroxythiophene – thienol. In the course of the work, the influence of a variety of factors on the process has been studied: the concentration of the dissolved products, the pH of the medium, and some others.

The irradiation was carried out using as source the equivalent of 50 g radium. The power of the dose was varied from 0.5 to $1.1 \cdot 10^{15}$ ev/ml • sec. The irradiation was carried out in glass ampoules. In work which involved elevated oxygen pressure, steel ampoules were used, provided with glass linings. The mixture of thiophene and water was prepared by mixing 0.1 ml of thiophene with 100 ml of water saturated with oxygen. The concentration of thiophene in this mixture corresponded to $1.265 \cdot 10^{-2}$ mole/liter. The solutions containing thiophene in lower concentrations were prepared by means of dilution.

The identification of the products obtained was carried out by means of colorimetric and spectrophotometric methods. The colorimetric method was based on the combination of the thienol, the formation of which was believed to have occurred in the course of the reactions with p-nitroaniline, or with sulfanilic acid. Both these methods showed the presence of compounds in the irradiated solutions which give a coloration with these substances, characteristic of the phenolic compounds (λ_{max} = 520 mμ) [1]. The spectrophotometric method used in this work was based upon a recording of the absorption spectra in the ultraviolet region. The spectrometer used for this purpose was of the SF-4 type.

Figure 1 gives the absorption spectra of the initial (1) and irradiated (2) aqueous solutions of thiophene. It is seen that a product is found in the irradiated solution which is capable of absorbing ultraviolet light with a greater wavelength than is thiophene. It should be noted in this connection that the position of the absorption maximum depends on the pH of the solution undergoing irradiation, and is shifted from the value 256 mμ in acid solutions to that of 268 mμ in alkaline solutions. The same occurs in the relationship between the absorption of α-hydroxythiophene in water and the wavelength of the light (Fig. 1,3) obtained on the basis of the

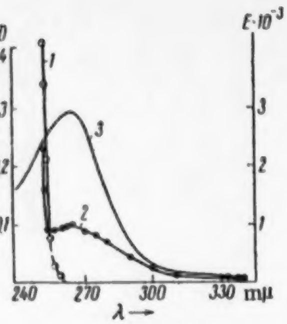

Fig. 1. Absorption spectra of aqueous solutions of thiophene: 1) before irradiation; 2) after irradiation; 3) relationship of extinction coefficient of α-hydroxythiophene and wavelength.

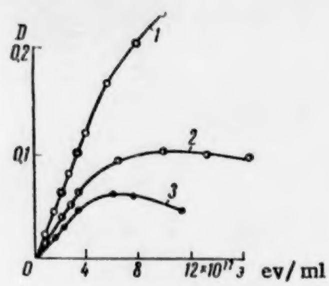

Fig. 2. The increase in the optical density of a solution of thiophene in 0.8 N sulfuric acid when λ = 260 mμ in relation to radiation dose: 1) dark circles: $1.2 \cdot 10^{-2}$ M thiophene; open circles: the same under an oxygen pressure of 25 atm; 2) $1.26 \cdot 10^{-4}$ M thiophene; 3) $0.52 \cdot 10^{-5}$ M solution of thiophene in 0.8 N sulfuric acid.

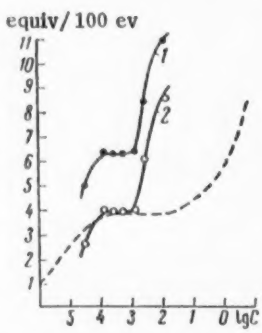

Fig. 3. Relationship between yield of thienol and thiophene concentration in an irradiated solution in 0.8 N sulfuric acid: 1) E (mole/cm) = $2.83 \cdot 10^3$; 2) combination of 1 with the theoretical (broken lines).

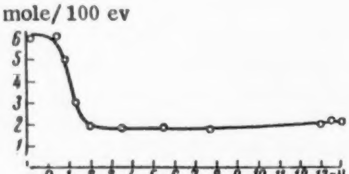

Fig. 4. Relationship between the yield in the oxidation of thiophene and the pH of the irradiated solution.

published data [2]. It is clear that the only reasonable procedure is to compare the right-hand parts of the spectra (Curves 2 and 3) since for wavelengths lower than 258 mμ the absorption in the irradiated solution is due to the residual thiophene.

Comparison and qualitative reactions give ground to suppose that one of the principal products of the oxidation of thiophene is thienol. The production of a more diffuse peak in the course of irradiation may be explained by the existence of thienol in two tautomeric forms.

Figure 2 shows the relationship between the optical density of the solutions undergoing irradiation for 260 mμ and the radiation dose, for solutions with various initial thiophene concentrations. Increase in the dose causes increase in the optical density of the solution, but the radiation-chemical yield of the thienol formed diminishes rather rapidly. Experiments carried out with increased oxygen pressure (up to 25 atm) showed that the reduction of the yield is not connected with the exhaustion of the dissolved oxygen (compare Fig. 2,1), but is apparently connected with the conversion of the product which has been formed, by reactions which proceed with an appreciable velocity in oxygenated solutions. When experiments are carried out in a neutral medium, the yield begins to diminish only at appreciably higher doses. In this case, the pressure of the oxygen considerably increases the rectilinear portion.

It has been shown that the initial size of the yield of thienol formed depends on the initial concentration of the thiophene in the solution (compare, for example, Curves 2 and 3 in Fig. 2 and Curve 1 in Fig. 3).

For the calculation of the radiation-chemical yields* in the oxidation of thiophene there was employed the molar extinction of α-hydroxythiophene. As can be seen from Fig. 3, Curve 1, constructed as a result of such an estimation, has the typical form for the concentration dependency of the yield obtained by the transformation of a dissolved substance [3]. With the introduction of the corresponding correction, the curves are easily superimposed. For this purpose, all the values of the thienol yields obtained by the first procedure need only to be diminished by a factor of 1.55. This confirmation of the results obtained gives ground to suppose that the yield of thienol formed is determined with sufficient accuracy with only a small increase above the true value. In considering Curves 2 and 3 in Fig. 2, it is easy to calculate that the percent conversion of the thiophene into hydroxythiophene is considerable: it amounts to 50% by the first method of calculation, and 30% by the second.

In connection with the mechanism of the oxidation of thiophene in its aqueous solution, it must be supposed that the thienol, like the product of the oxidation of benzene [4,5], is formed through the interaction of the thiophene with the hydroxyl radicals according to the over-all reaction:

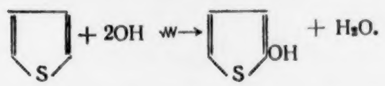

The relationship obtained by us between the magnitudes of the yield from the oxidation of thiophene and the pH of the medium (see Fig. 4) corresponds to the same relationship for benzene [6], which confirms the similarity of the oxidation mechanisms in the two cases. Evidence in favor of this mechanism is also provided by the nature of the influence of competing acceptors for the hydroxyl radicals. It has been shown, for example, that the introduction of glycerol into the thiophene solution in a concentration of 0.5 N leads to a complete inhibition of the formation of thienol.

The concentrations obtained with the help of the calculation procedure described above for the thienol formed amount in favorable circumstances to 8 equiv/100 ev. These evidently correspond to the high degree of participation of radiolyzed molecules of water in the oxidation process according to a nonchain mechanism.

LITERATURE CITED

1. F. Shell and C. Shell, Analyst 2 (1937).
2. C. D. Hurd and K. L. Krenz, J. Am. Chem. Soc. 72, No. 12, 5543 (1950).
3. M. A. Proskurnin, B. D. Orekhov, and A. I. Chernova, Contribution to the Tashkent Conference on the Peaceful Uses of Atomic Energy.
4. M. A. Proskurnin and E. V. Barelko, Collected Works on Radiation Chemistry [in Russian] (Moscow, 1955).
5. E. V. Barelko, L. I. Kartasheva et al., Transactions of the First All-Union Conference on Radiation Chemistry [in Russian] (Izd. AN SSSR, 1958) p. 89.
6. G. Stein and J. Weiss, J. Chem. Soc. 1949, 3245.

* The yield has been calculated from the initial portion of the curve relating accumulation of thiophene to dosage (from 1 to 10,000 roentgen).

THE SURFACE TENSION AT THE BOUNDARY BETWEEN TWO GASEOUS PHASES AT HIGH PRESSURES

D. S. Tsiklis and Yu. N. Vasil'ev*

Scientific Investigation and Planning Institute of the Nitrogen Industry
and the Products of Organic Synthesis

(Presented by Academician P. A. Rebinder, July 18, 1960)
Translated from Doklady Akademii Nauk SSSR,
Vol. 136, No. 2, pp. 394-397, January, 1961
Original article submitted July 13, 1960

There is at present no agreement as to the possible existence of a gas–gas equilibrium [1,2]. The current work has been undertaken with the object of studying further the interesting phenomenon involved, by measurement of the surface tension at the boundary between two gas phases.

The helium–ethylene system has been chosen as the material for investigation [3]. The measurement of the surface tension has been performed by the method of capillary rise [4,5]. The principle of this method consists in measuring the height difference Δh of the column of the phase in capillaries of radius R_1 and R_2. If the wetting angle Θ of the capillary wall by a dense phase is equal to zero, and R_1 and R_2 are small, then

$$\sigma_2 = \frac{\Delta h}{1/R_1 - 1/R_2}\,\frac{1}{2}\,g\,(\rho' - \rho''), \tag{1}$$

where ρ' and ρ'' are the densities of the gas, and **g** is the acceleration due to gravity.

We have measured the density of gas in the helium–ethylene system by a method described earlier [6]. Helium and ethylene were introduced into the high-pressure apparatus; conditions were created for which the mixture underwent stratification; the phases were agitated by means of electromagnetic agitator, and the upper phase was selected for analysis at constant pressure. For the purpose of determining the composition of the phase on the basis of its molecular weight, a portion of this phase was passed into a calibrated vessel, such a quantity of mercury being introduced at the same time into the apparatus, by means of a calibrated press, that the pressure remained constant. Knowing the quantity of mercury introduced, and the amount of the separated phase, the density of the latter was determined. Subsequently, the whole of the upper phase was removed from the apparatus and the procedure was repeated in an analogous way with the lower phase.

The data obtained on the composition and densities of the phases in the system under investigation are shown in Table 1. The composition of the phases at 16° are somewhat different from those obtained in a previous work [3], but the more recent data, obtained under conditions of intense agitation of the phases, are to be preferred.

The capillary rise was determined in an apparatus (Fig. 1) consisting of a high-pressure column 1 contained in a thermostat. Into the column opposite the window 2 were inserted capillaries 3, supported in the frame 4; behind the capillaries was located a matte glass background 7. When the framework connected to the armature of the electromagnetic mixer 5 was moved, mixing of the phases took place both within the vessel and in the interior of the capillaries themselves.

* A. N. Kofman took part in the experimental part of this work.

TABLE 1

Density and Composition of the Phases in the Helium–Ethylene System. ρ'' and ρ' Are the Densities of the Light and the Heavy Phases, Respectively; N_2'' and N_2' Are the Mole Percents of Ethylene in the Light and the Heavy Phases

p, kg/cm²	N_2''	ρ'', g/cm³	N_2'	ρ', g/cm³	p, kg/cm²	N_2''	ρ'', g/cm³	N_2'	ρ', g/cm³
At 13°					At 16°				
220	57.8		80.5		300	50.4	0.211	76.0	0.323
280	37.5	0.142	79.3	0.327	420	29.5	0.166	73.0	0.349
360	35.4	0.153	76.6	0.350	500	27.5	0.168	73.0	0.391
400	33.6		71.8		600	18.0		70.0	
420	30.4	0.158			680	20.0	0.186	69.0	0.394
550	23.5	0.164	69.7	0.410	At 18°				
660	20.0	0.173	71.8	0.406					
					400	40.4	0.212	65.5	0.299
					490	28.8	0.180	68.0	0.363
					620	23.1	0.174	66.0	0.385
					720	20.8	0.184	65.9	0.388

TABLE 2

The Capillary Constant a^2 in the Helium–Ethylene System

p, kg/cm²	$a^2 \cdot 10^5$, cm²	p, kg/cm²	$a^2 \cdot 10^5$, cm²
At 13°		At 16°	
227	48.0	415	54.0
300	49.0	450	104.0
310	105	480	104
355	129	520	207
380	150	550	256
400	196	590	315
415	205	650	410
480	284	680	446
520	344	At 18°	
535	354		
600	470	490	51.6
635	550	505	66.0
665	592	575	140
		610	207
		655	267
		720	362

TABLE 3

Surface Tension in the Helium–Ethylene System (Interpolated Data)

p, kg/cm²	σ, erg/cm²	p, kg/cm²	σ, erg/cm²
At 13°		At 16°	
280	0.055	420	0.050
300	0.070	450	0.105
350	0.125	480	0.255
400	0.190	500	0.195
450	0.275	550	0.280
500	0.360	600	0.355
550	0.460	650	0.420
600	0.561	680	0.440
650	0.654		
		At 18°	
		490	0.045
		500	0.055
		550	0.110
		600	0.190
		650	0.270
		720	0.355

Ethylene and helium were introduced into the plant in the necessary quantities to obtain a mixture of a predetermined composition, and the mercury press in the vessel 6 was compressed, thus compressing the mixture to the necessary pressures. The quantity of the mixture was chosen in such a way that the level of the phase boundary occurred opposite the inspection window, while the ends of the capillaries were immersed in the dense phase.

The height of the rise of the dense phase in the capillaries of various diameter (from 0.2 to 0.6 mm) was measured by means of a cathetometer of type KM-6, with an accuracy of 0.005 mm. The framework contained three capillaries of various diameters, so that we were able to determine in the course of a single experiment three different levels.

The materials used for the investigation were: helium of a purity of 99.6% and ethylene purified by a method involving the formation of a complex with cuprous chloride [7]. The results of the measurement (capillary constant $a^2 = \dfrac{\Delta h}{1/R_1 - 1/R_2}$) are presented in Table 2.

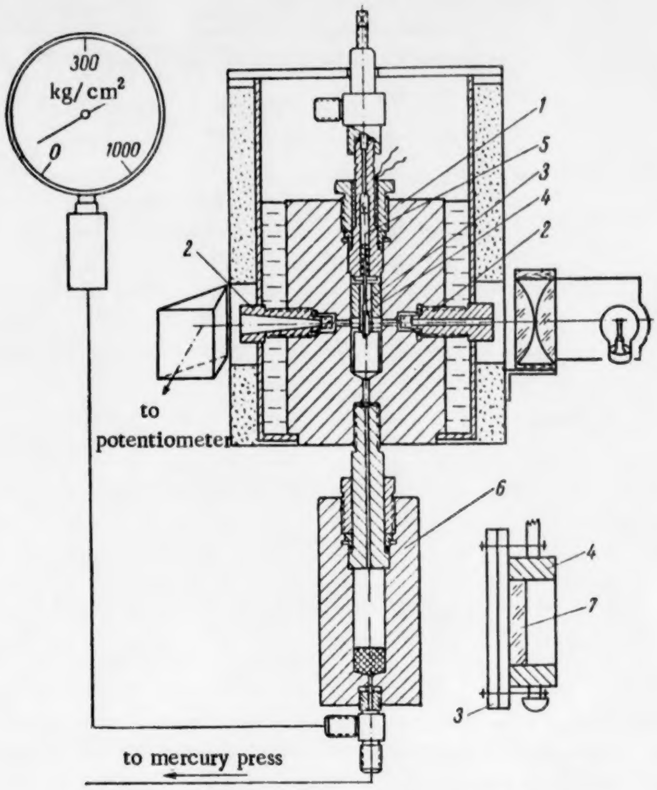

Fig. 1. Setup for measurement of capillary rise.

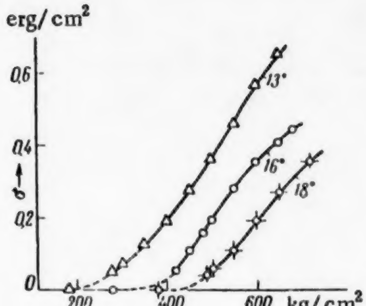

Fig. 2. Surface tension in the helium–ethylene system.

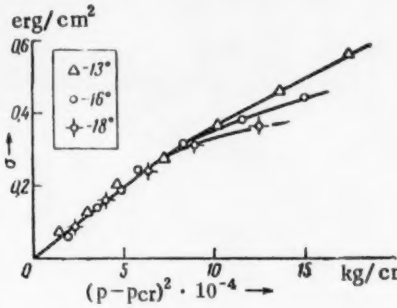

Fig. 3. Relationship between σ and $(p-p_{cr})^2$.

For the determination of the wetting angle, we photographed the capillaries immersed in the dense phase for different pressures and temperatures, and showed by considering the enlarged images of the capillaries that the angle was equal to zero. The data on the surface tensions, calculated on the basis of Eq. (1), are presented in Table 3 and in Fig. 2.

Estimation of the errors in the measurement of the magnitudes entering into Eq. (1) has shown that the total maximum relative error of measurement of surface tension, taking into account the precision with which the pressure and temperature could be measured, was about 5%.

We may surmise that the curves expressed in coordinates $\sigma - p$ approximate to the axis of abscissas with a horizontal tangent, and that the surface tension becomes equal to zero at the critical point (Fig. 2).

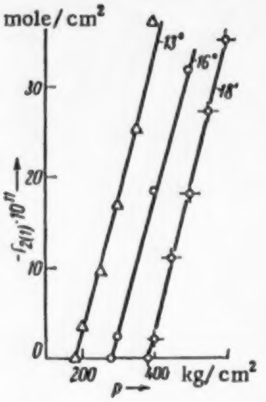

Fig. 4. Change in adsorption with pressure in the helium–ethylene system.

According to Gibbs [8], adsorption at the separation boundary of neighboring phases may be expressed by the equation

$$\Gamma_{2(1)} = -(\partial\sigma/\partial\mu_2)_{12,\,T}; \tag{2}$$

where μ_2 is the chemical potential of component 2; $\Gamma_{2(1)}$ is the excess moles of the second component related to unit area of the surface layer, in comparison with the number of moles which would have been present in the surface if the concentration of the component in the volume phase remained unchanged right up to the geometrical separation surface. The place of this surface is so chosen that the excess of the other component (in the present case, the first component) can be made equal to zero $[\Gamma_{1(2)} = 0]$. Since

$$(d\mu_2)_{12,T} = (\partial\mu_2/\partial N_2)_{T,\,p}\, dN_2 + (\partial\mu_2/\partial p)_{T,N_2}\, dp, \tag{3}$$

$$(\partial\mu_2/\partial p)_{T,\,N_2} = \bar{v}_2, \tag{4}$$

where $\bar{v}_2$ is the partial molar volume of the component, then

$$\frac{\partial\sigma/\partial p}{(\partial\mu_2/\partial N_2)_{p,\,T}\,(\partial N_2/\partial p)_{12,T} + \bar{v}_2} = -\Gamma_{2(1)}. \tag{5}$$

For the critical phase of the binary solution $(d\mu_2/dN_2)_{p,T} = 0$; therefore, at the critical point,

$$-\Gamma_{2(1)} = \frac{1}{\bar{v}_2}\frac{d\sigma}{dp}. \tag{6}$$

But, at the critical point, all the properties of both phases are identical, and therefore $\Gamma_{2(1)} = 0$, and consequently $d\sigma/dp = 0$. Therefore, the analytical curve expressing the relationship between σ and p must be a parabola of the second degree.

On this basis, we may write that

$$\sigma = \alpha\,(p - p_{cr})^2, \tag{7}$$

where α is a constant. If we plot on a curve the values of σ obtained by us against the difference $(p - p_{cr})^2$, we obtain the straight line shown in Fig. 3, on which the points for all three temperatures over a large interval of pressure are found to lie.

For neighboring phases,

$$(\partial\mu_2)_{12,\,T} = \frac{v'N_1' - v''N_1''}{N_1'' - N_1'}\, dp, \tag{8}$$

where v' and v'' are the molar volumes of the dense and light phases, respectively; N_1' and N_1'' are the molar fractions of the first component (in the present case of helium) in the dense and light phases, respectively.

By combining Eqs. (4) and (8) it may be shown that, at the critical point,

$$-\Gamma_{2(1)} = \frac{N_1'' - N_1'}{v'N_1'' - v''N_1'}\left(\frac{\partial\sigma}{\partial p}\right)_{12,T}. \tag{9}$$

Further, since it follows from Eq. (7) that $\left(\frac{\partial\sigma}{\partial p}\right)_{12\,T} = 2\alpha\,(p - p_{cr})$, then, finally:

$$-\Gamma_{2(1)} = \frac{2\alpha\,(p - p_{cr})\,(N_1'' - N_1')}{v'N_1'' - v''N_1'}. \tag{10}$$

If we determine the coefficient α from the slope of the straight line in Fig. 3, we may calculate $-\Gamma_{2(1)}$

for the three temperatures, and plot these data against the pressure. As can be seen from Fig. 4, the points lie well upon straight lines over a wide interval of pressure.

The results of this work show that the surface tension of the boundary between two gaseous phases increases considerably with increase in pressure. The reason for the increase in σ may be the change in the composition of the phases and of the surface layer (adsorption), as well as the large change in the densities of the phases with pressure.

The authors wish to express their deep gratitude to I. R. Krichevskii for his constant interest, advice, and help in the work.

LITERATURE CITED

1. I. R. Krichevskii, Phase Equilibria in Solutions at High Pressures [in Russian] (1952).
2. D. S. Tsiklis, Proceedings of the Conference on the Thermodynamics and Structure of Solutions [in Russian] (1959) p. 191.
3. D. S. Tsiklis, Doklady Akad. Nauk SSSR 91, 1361 (1953).
4. L. D. Volyak, Doklady Akad. Nauk SSSR 74, 307 (1950).
5. D. S. Tsiklis, The Technique of Physicochemical Investigations at High Pressures [in Russian] (1958).
6. I. R. Krichevskii and D. S. Tsiklis, Doklady Akad. Nauk SSSR 78, 1169 (1951).
7. E. R. Gilliland, J. E. Geebold, et al., J. Am. Chem. Soc. 61, 1960 (1939).
8. G. V. Gibbs, Thermodynamic Works [Russian translation] (Moscow, 1950).

THE THEORY OF IMPACT INDUCTION OF EXPLOSION

G. T. Afanas'ev, V. K. Bobolev, and L. G. Bolkhovitinov

Institute of Chemical Physics, Academy of Sciences of the USSR
(Presented by Academician V. N. Kondrat'ev, August 30, 1960)
Translated from Doklady Akademii Nauk SSSR,
Vol. 136, No. 3, pp. 642-643, January, 1961
Original article submitted August 28, 1960

Modern theory considers the induction of an explosive reaction to be a purely thermal effect, and shows that spontaneous thermal ignition will occur when the temperature of a definite volume of explosive is raised to that critical point at which it is impossible to fully dissipate the heat evolved in chemical reaction. Experiments on the impact sensitivity of solid explosives involve an elevation of temperature through adiabatic compression, and an evolution of thermal energy through plastic deformation and chemical reaction. The thermal effect of reaction can be neglected at subcritical temperatures which do not exceed those values calculated by Rideal and Robertson [1] and confirmed experimentally by [2], since impact is of brief duration and reaction rate is strongly dependent on temperature. Estimates show that the heating of an explosive through adibatic compression is slight in comparison with the critical temperature [3].

Thus, plastic deformation is the principal factor in the formation of high-temperature centers. The intensity of thermal evolution is dependent on the plastic properties of the material in question and on the conditions of loading. The load required for passage of a specimen into a state of plastic deformation is fixed by a scale factor. V. R. Regel' and G. V. Berezhkova have studied the relation between load and specimen dimensions in various types of plastic, showing the load to increase with diminishing α, from about 1.5 on (α is the ratio of specimen height to diameter) [4]. Impact machine experiments with explosives usually make use of charges whose depth is less than 1 mm at a diameter of 10 mm. The depth of layer compressed between the impacting surfaces is usually less than 0.1 mm, so that $\alpha = 0.01$. It is clear that the scale effect must be significant for work on the impact machine. L. M. Kachanov [5] has considered the compression of a thin homogeneous disk ($\alpha \ll 1$) between the rough ends of absolutely rigid cylinders. The load under which a specimen will pass into the plastic state can be found from the theory of elastoplastic deformation. This value is related to α through:

$$P = \frac{\sigma_s}{3\sqrt{3\alpha}}, \tag{1}$$

where σ_s is the flow limit.

Thus, the thinner the specimen, the greater the effect of the fixed flow boundaries, and the more difficult it is to induce plastic deformation. Thermal evolution does not occur if the impact pressure remains less than the pressure given by (1), which is to say that each value of the impact energy is associated with a critical value of α below which explosive decomposition cannot occur.

On the other hand, autocatalytic chemical reaction results when the condition of the Frank-Kamenetskii criterion is fulfilled, i.e., when [6]:

$$\frac{d^2 QEze^{-E/RT}}{4\varkappa RT^2} = \delta.$$

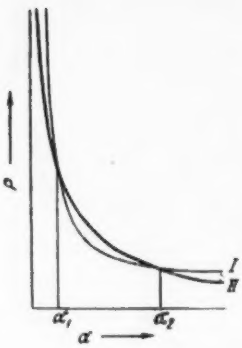

Here Q is the heat of reaction per unit volume, E is the activation energy, z is the frequency factor, κ is the coefficient of thermal conductivity, and $\delta = 3.32$ for a spherical center. The critical temperature T, corresponding to any dimension d, can be calculated from the known values of these quantities. One of the present authors has shown [7] that heating must be accompanied by a uniform compression in order to form a center when the calculated T proves to be greater than the melting point T_{mp} of the given substance. The magnitude of this compression is given by $P = (T - T_{mp})/\chi$, where χ represents the elevation of melting point per atmosphere, a quantity equal to 0.02 deg/atmos for most secondary explosives. Setting the dimensions of the hot center equal to the height of the compressed specimen gives:

$$\frac{(\alpha D)^2 \cdot QEze^{-E/R\,(T_{mp}+\chi P)}}{4\kappa R\,(T_{mp}+\chi P)^2} = \delta, \tag{2}$$

where D is the specimen diameter. Pressures higher than those found through (2) will be required for local superheating of dimensions less than assumed here.

One thus obtains the necessary conditions for the formation of a hot center through plastic deformation. Equation (1) gives the condition for specimen flow ($\alpha \ll 1$). This condition reduces to the requirement that $P = \sigma_s$ when the value of α is such that the scale effect is without significance. Equation (2) gives the critical stress as a function of the dimensions of the test specimen. It is impossible to induce explosion if the pressure developed in impact proves to be less than one of the values obtained from these two conditions.

It is of interest to consider two sharply divergent cases, $T_{fl} < T_{mp}$ and $T_{fl} > T_{mp}$, in the light of conditions (1) and (2). A number of initiating explosives flash up to the appearance of a liquid phase. Equation (2) falls out of account for these materials, and the condition for flow becomes the necessary requirement for explosion. $T_{fl} > T_{mp}$ for most secondary explosives, and the flow limit is not high. For these materials, the condition of critical stresses is the principal requirement to be fulfilled in explosion, just as would be anticipated.

The aggregate of quantities entering conditions (1) and (2) will determine the pressure required for the formation of a center in each experiment. The significance of these conditions can alter, since α varies during impact deformation. The case in the figure, in which Curve I gives the pressure required by (1), and Curve II that required by (2), will be considered as an illustration. Limitation will be made to the ideal plastic body. The alteration of pressure in deformation then follows Curve I, and condition (2) is fulfilled only for $\alpha \leq \alpha_1$ and $\alpha \geq \alpha_2$. It is only under these latter conditions that an effective hot center can arise.

LITERATURE CITED

1. E. K. Rideal and J. B. Robertson, Proc. Roy. Soc. A195, 135 (1949).
2. F. P. Bowden and A. D. Ioffe, Induction and Development of Explosions in Solid and Liquid Substances [Russian translation] (IL, 1955).
3. Yu. B. Khariton, Collection on the Theory of Explosives [in Russian] (Moscow, 1940).
4. V. R. Regel' and G. V. Berezhkova, Collection: Certain Problems in the Stability of the Solid Body [in Russian] (Moscow-Leningrad, 1959).
5. L. M. Kachanov, Doklady Akad. Nauk SSSR 96, No. 2 (1954).
6. D. A. Frank-Kamenetskii, Diffusion and Thermal Transfer in Chemical Kinetics [in Russian] (AN SSSR Press, 1947).
7. L. G. Bolkhovitinov, Doklady Akad. Nauk SSSR 125, No. 3 (1959).

All abbreviations of periodicals in the above bibliography are letter-by-letter transliterations of the abbreviations as given in the original Russian journal. *Some or all of this periodical literature may well be available in English translation.* A complete list of the cover-to-cover English translations appears at the back of this issue.

THE STRUCTURE OF MOLTEN NIOBATE SURFACE LAYERS

A. I. Manakov, O. A. Esin, and B. M. Lepinskikh

Institute of Metallurgy, Ural Branch, Academy of Sciences of the USSR
(Presented by Academician A. N. Frumkin, August 20, 1960)
Translated from Doklady Akademii Nauk SSSR,
Vol. 136, No. 3, pp. 644-646, January, 1961
Original article submitted August 9, 1960

The studies of A. N. Frumkin et al. [1,2] and the work of others [3], have shown that a capillary active substance will form an electrical double layer at an air–water interface. The charge distribution in this double layer is determined by the orientation of polar molecules and by the preferential adsorption of ions of some particular charge.

There is reason to suppose that the energy relations favor a surface of oxygen anions in solid [4] and liquid [5] oxides, just as in aqueous solutions [6,7]. This does not exclude the possibility, however, that large singly charged alkali metal cations might partially replace oxygen ions from a melt surface [8] and reverse the charge distribution in the double layer.

We have checked this point experimentally by studying the variation with concentration of the 1500°C surface tension (σ) and potential (ϵ_s) at the air interface of $Cs_2O-Nb_2O_5$, $K_2O-Nb_2O_5$, and $CaO-Nb_2O_5$ systems.

These experiments were carried out in a graphite resistance furnace which was equipped with a quartz tube to protect the cell from a reducing atmosphere. The starting materials were pure cesium and potassium carbonates, calcium oxide, and niobium pentoxide containing 1.5% TiO_2, SiO_2, Fe_2O_3, and Ta_2O_5, and 0.55% K and Na.

The surface tension was determined by the method of maximum bubble pressure [9], using oxygen as the working gas. A corundum tube, 4 mm in internal diameter, was raised with the wetting melt to a position 1.5 mm above the melt surface, and the pressure measurements there carried out. The technique was tested on water and on molten $PbCl_2$ and KCl.

The surface potential (ϵ_s) was studied by the method of Guyot and Frumkin [10], using the following cell:

$$\mathrm{Pt}\underset{1}{|}\mathrm{Nb_2O_5}\underset{2}{|}\mathrm{O_2}\underset{3}{|}\mathrm{Pt}\underset{4}{|}\mathrm{O_2}\underset{5}{|}\mathrm{Nb_2O_5}+\mathrm{MeO}\underset{6}{|}\mathrm{Pt}.$$

The platinum electrodes at the extremities of this cell were in contact with Nb_2O_5 and Nb_2O_5 + MeO melts in separate ZrO_2 crucibles. The middle electrode was sheathed in an alundum tube, just as the others, and was continually bathed in oxygen.

The sum of the junction potentials 6 (ϵ) and 5 (ϵ_s) with respect to a gas electrode (ϵ_g) was measured on a PPTV-1 potentiometer, and proved to be positive in each case, i.e.,

$$\Delta\varepsilon = \varepsilon + \varepsilon_s - \varepsilon_g > 0.$$

A radioactive substance was not used here because there was considerable ionization of the furnace atmosphere at 1500° [10]. The constancy of the potential was checked against a standard electrode immersed in the Nb_2O_5. The quantity

$$\Delta\varepsilon_0 = \varepsilon_0 + \varepsilon_s^0 - \varepsilon_r$$

(junctions 1, 2, 3) proved to be practically constant in most cases. A time of about 40 min was often required for attaining a constant reading.

The difference in the electrochemical potentials at junctions 1 and 6, $\Delta\epsilon_1 = \epsilon_0 - \epsilon$, was measured by juxtaposing the crucibles, and using a thin Nb_2O_5 layer to form a liquid bridge between them. The electromotive force of such a cell was presumed equal to $\Delta\epsilon_1$, the diffusion potential being neglected [11].

The difference in the surface potentials was calculated by using the quantities $\Delta\epsilon^0$, $\Delta\epsilon$, and $\Delta\epsilon_1$:

$$\Delta\varepsilon_s = \varepsilon_s^0 - \varepsilon_s = \Delta\varepsilon_0 - \Delta\varepsilon - \Delta\varepsilon_1.$$

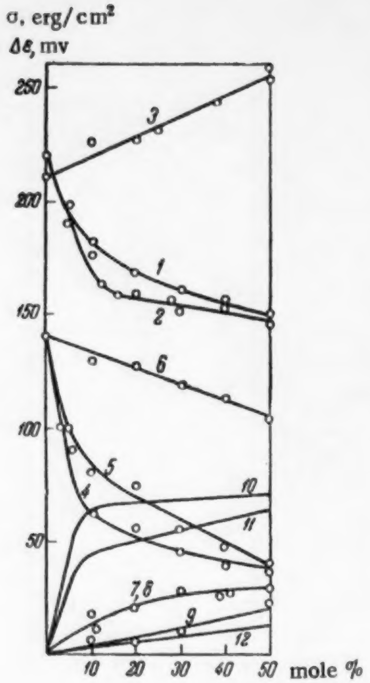

Isotherms for surface tension and alteration in surface potential: 1), 2), 3) $\sigma = f(N)$ for Nb_2O_5 with Cs_2O, K_2O, and CaO, respectively; 4), 5), 6) $\Delta\epsilon = f(N)$; 7), 8), 9) $\Delta\epsilon_1 = -f(N)$; 10), 11), 12) $\Delta\epsilon_s = f(N)$ for these same systems.

The figure shows that the values of σ and $\Delta\epsilon$ diminish sharply as K_2O and Cs_2O are added up to 10 mole percent, and then fall off gradually as the Me_2O concentration is increased.* On the other hand, addition of CaO raises the surface tension and leaves the value of $\Delta\epsilon$ almost unaltered. Curves of this type show that the Cs^+ and K^+ cations have capillary activity, whereas the Ca^{2+} ion does not.

The increase in the value of $\Delta\epsilon_s$ indicates that the potential of the melt surface (ϵ_s) becomes less positive as the Me_2O concentration rises. At 10 mole percent, this diminution amounts to approximately 65 mv for Cs_2O, to 45 mv for K_2O, and to only 2 mv for CaO.

Platinum is known [12] to be covered with oxygen ions in an oxygen atmosphere and to be, itself, positively charged, i.e., $\epsilon_g > 0$. Since $\Delta\epsilon_1$ and $\Delta\epsilon_s$ are positive in the present case, it can be assumed that the outer envelope of the melt surface layer is also principally formed from oxygen anions. The adsorbed Cs^+ and K^+ cations must replace the oxygen from the double layer rather than the niobium anions, since the charge of this layer diminishes with decreasing ϵ_s. In other words, the Cs^+ and K^+ cations are distributed in the external envelope at the interface between the melt and the gas. The fraction of the adsorbed cations located on this interface was determined from the surface concentration (N_s) as evaluated by two different methods. One of these methods utilized the Gibbs equation for ideal solutions:

$$\Gamma = -\frac{N(1-N)}{RT}\frac{\partial\sigma}{\partial N}.$$

Values thus obtained for the adsorption Γ, at 10 mole percent of added oxide, are presented in the table. This same table gives surface concentrations of the oxides (N_s) as calculated from the value of Γ, and the geometrically possible number of molecules per 1 cm² (n): $\Gamma = n(N_s - N)$. The other method determines the value of $N_s^{\cdot}$ from the alteration in the surface charge (Δq) by supposing the double layer to approximate a plane condenser. From the known value of $\Delta\epsilon_s$, and the assumption that C = 15 mf/cm² [13], we obtained:

$$\Delta q = \Delta\varepsilon_s C,$$

from which it follows that

$$N_s^{\cdot} = \frac{\Delta q}{2nN_0e}.$$

Here, N_0 is the Avogadro number, e is the electronic charge, and the factor 2 takes account of the number of ions in the Me_2O molecule.

* The Me_2O concentration was actually higher, since the niobium pentoxide originally contained 2.3 mole percent $K_2O + Na_2O$.

A Comparison of Values of N_S Calculated from $\Delta\sigma$ and from $\Delta\epsilon_s$

Oxide	N	$\Gamma \cdot 10^{10}$, mole/cm^2 (from σ)	N_S, (from σ)	N_S^*, (from ϵ_s)	N_S^*/N_S
Cs_2O	0.1	2.45	0.436	0.0228	0.052
K_2O	0.1	3.18	0.415	0.0112	0.027
CaO	0.1	−0.52	0.072	0.0003	0.004

The data of the table show that N_S^* is considerably less than N_S, a fact which can scarcely be due to errors in measurement or to the approximate nature of the calculations. The observed discrepancy between the values of N_S^* and N_S indicates that it is principally the niobium cations which are found distributed more deeply below the surface than the oxygen anions that are displaced by those Me^+ ions which fall into the double layer. Only a small fraction of these Me^+ ions displace the O^{2-} anions from the surface. In other words, the adsorbed Me_2O in the surface is orientated principally by the oxygen anions, and only to an insignificant extent by the Me^+ cations. A similar situation has been observed in aqueous solutions [2], where the potential ϵ_s is less than that calculated for full dipole orientation.

It is interesting to note that the ability to displace O^{2-} anions diminishes in going from Cs^+ to K^+, and practically disappears in Ca^{2+} (see table). In other words, this ability diminishes with an increase in the electrostatic potential.

The difficulty associated with the displacement of the oxygen ions from the melt surface is the result of the high polarizability of these ions [5]. The one-sided deformation of the electron cloud of the O^{2-} ion by the niobium cations lying further from the surface leads to a marked diminution in effective charge (from 2e to 1e, for example). The energy of binding of such ions with the surface proves to be comparable with, or even somewhat lower than, the energy of binding of the singly charged cesium and potassium cations.

LITERATURE CITED

1. A. N. Frumkin, Z. Phys. Chem. 109, 34 (1924); 111, 190 (1924); 116, 485 (1925); 123, 321 (1926).
2. S. Iofa, A. Frumkin, and P. Tschugunoff, Acta Physicochim. URSS 1, No. 6, 883 (1935).
3. R. Parsons, Certain Problems in Modern Electrochemistry [Russian translation] (IL, 1958) p. 147.
4. D. T. Livey and P. Murray, J. Am. Ceram. Soc. 39, 363 (1956).
5. O. A. Esin, Usp. Khim. 26, 1374 (1957).
6. A. N. Fumkin, Ergebenisse exakt. Naturwissensch. 7, 258 (1928).
7. W. Weyl, J. Coll. Sci. 6, 389 (1951).
8. S. I. Popel', Izvest. Vyssh. Uch. Zav., Chem. Metallurgiya No. 4, 61 (1958).
9. S. I. Popel' and O. A. Esin, Zhur. Fiz. Khim. 30, 1193 (1957); Zhur. Neorg. Khim. 2, 632 (1957).
10. Guyot, Ann. Phys. Paris 10, 508 (1924).
11. I. G. Murgulescu and D. I. Marchidan, Rev. Chim. (Romîn) 3, No. 1, 69 (1958).
12. Zh.G. De-Bur,* Electron Emission and Adsorption Effects [Russian translation] (Moscow-Leningrad, 1936).
13. Yu. P. Nikitin and O. A. Esin, Doklady Akad. Nauk SSSR 111, 133 (1956).

All abbreviations of periodicals in the above bibliography are letter-by-letter transliterations of the abbreviations as given in the original Russian journal. *Some or all of this periodical literature may well be available in English translation.* A complete list of the cover-to-cover English translations appears at the back of this issue.

* Name not verified.

THE RELATION BETWEEN THE OXIDATION INDUCTION PERIOD AND THE ANTIOXIDANT CONCENTRATION

M. B. Neiman, V. B. Miller, Yu. A. Shlyapnikov, and E. S. Torsueva

Institute of Chemical Physics, Academy of Sciences of the USSR
(Presented by Academician V. N. Kondrat'ev, August 29, 1960)
Translated from Doklady Akademii Nauk SSSR,
Vol. 136, No. 3, pp. 647-650, January, 1961
Original article submitted August 29, 1960

Numerous papers on the mechanism of the action of antioxidants have appeared in the forty-five years that have elapsed since the discovery of the first of these substances by Muro and Dyufress * (the fundamental work on oxidation inhibitors has been systematized and generalized in the review [1]).

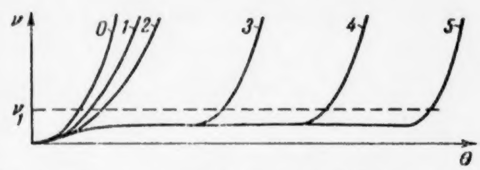

Fig. 1. The time rate of increase of the concentration of active centers during oxidation in the presence of various amounts of added antioxidant: 0) without addition; 1) with addition of an amount of κ_0; 2) $2\kappa_0$; 3) $3\kappa_0$; 4) $4\kappa_0$; 5) $5\kappa_0$.

Fig. 2. The increase of the induction period as a function of the initial concentration of the antioxidant.

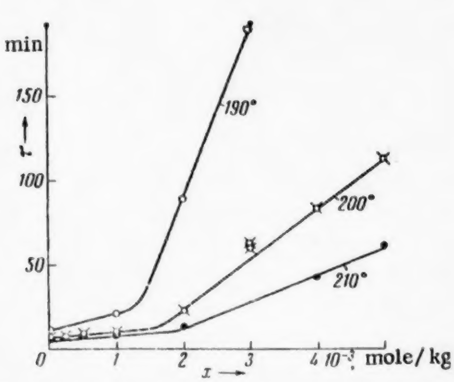

Fig. 3. The relation between the induction period for the destruction of polypropylene by thermal oxidation and the amount of added antioxidant. p_{O_2} = 300 mm in each experiment.

Nevertheless, adequate study has not yet been made of the relation between the induction period in oxidation and the antioxidant concentration. In work on polymerization [2] it has been assumed that a relation of the type

$$\tau = x/w_i \qquad (1)$$

exists between the rate of initiation w_i, the induction period τ, and the inhibitor concentration $\underline{x}$.

Equation (1) predicts a linear increase in the induction period with the inhibitor concentration. This equation is also frequently applied for determining the rate of initiation of liquid phase hydrocarbon oxidation.

* Names not verified.

In a recent paper [3] it has been shown that the induction period for the oxidation of rubber rises linearly with the concentration of antioxidant, but only up to certain rather low antioxidant concentration. This relation breaks down with further increase in the antioxidant concentration, since the inhibitor is then itself markedly oxidized and begins to function as an initiator.

The effect of very low concentrations of antioxidant on the induction period for oxidations has not yet been studied.

Oxidation in the gaseous, liquid, and solid phases is known to proceed according to the theory of degenerative branching which has been developed by N. N. Semenov [4]. The concentration of active centers n increases with time according to the equation

$$\frac{dn}{dt} = w_i + \varphi n, \quad (2)$$

where φ is the factor of autoacceleration.

If an antioxidant which will break the chain is added to the reacting substance to a concentration x, the reaction will then be described by the following system of equations:

$$\frac{dn}{dt} = w_i + \varphi n - kxn, \quad (3)$$

$$-\frac{dx}{dt} = kxn. \quad (4)$$

The k term of these equations represents the rate constant for reaction of the inhibitor with the active centers. It is here supposed that chain rupture leads to the formation of a stable radical which is practically without effect on the course of oxidation.

We will now introduce the dimensionless variables: concentration of active centers $\nu = n/w_i\tau_0$; concentration of antioxidant $\kappa = x/w_i\tau_0$; and time $\theta = t/\tau_0$. Equations (3) and (4) then take the form:

$$\frac{d\nu}{d\theta} = 1 + a\nu - b\kappa\nu, \quad (5)$$

$$-\frac{d\kappa}{d\theta} = b\kappa\nu. \quad (6)$$

Here $a = \varphi\tau_0$ and $b = kw_i\tau_0^2$.

When $\kappa_0 < a/b$, the dimensionless concentration of active centers and the rate of oxidation increase exponentially with time, as indicated by the curves 0-2 of Fig. 1. When $\kappa_0 > a/b$, the reaction rate quickly takes on a low, approximately stationary value, and the concentration of active centers is then given by:

$$\nu \cong 1/(b\kappa_0 - a). \quad (7)$$

The induction period comes to an end only after consumption of the antioxidant has reduced the value of the product $b\kappa_0$ approximately to a, and the reaction rate then begins to increase, as shown by Curves 3-5 of Fig. 1.

It is customary to consider the end of the induction period to be the time at which a measurable amount of the reaction products corresponding to the value ν_1 has accumulated in the system. This value of ν_1 is indicated in Fig. 1 by a broken line, the length of induction period for a given amount of added antioxidant κ_0 being determined by the abscissa of the point of intersection of this line with the curve $\nu = f(\theta)$.

It is understood that the length of the induction period alters comparatively slowly at low values of κ_0, and much more rapidly at high values, as is shown by Fig. 2. Here, the segment AB corresponds to values such that $\kappa_0 < a/b$, and the segment BC to values such that $\kappa_0 > a/b$. There is actually a gradual transition from segment AB to segment BC, as shown by the dotted curve in the figure.

We have tested these conclusions by carrying out a series of determinations of the length of induction period in the destruction of polypropylene by thermal oxidation, using derivatives of phenol and aromatic amines at various concentrations as antioxidants.

Each of the investigated cases confirmed the considerations adduced above, insofar as the value of the derivative $d\tau/dx$ was low at low concentrations x, and increased rapidly at higher concentrations.

The results of our experiments on the determination of the length of the induction period for the oxidation of molten polypropylene in the presence of various amounts of added antioxidant A,

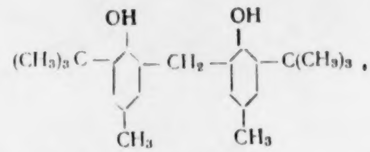

are presented in Fig. 3 by way of illustration.

These experiments were carried out statically at an oxygen pressure of 300 mm. The experimental technique has been described in [5]. The induction period τ increased very slowly as the concentration of the antioxidant was altered from zero to 10^{-3} mole/kg. The slope of the curve $\tau = f(x)$ rose sharply with further increase in the inhibitor concentration, the break point moving into the region of higher concentrations with increasing temperature.

In the region of low concentrations of the antioxidant, the value of the slope $d\tau/dx$ was 10^6, $3 \cdot 10^5$, and $2 \cdot 10^5$ sec • kg/mole at 190, 200, and 210°, respectively. Limiting values of these slopes can be obtained from Eq. (3) by an elementary procedure. Integration of this equation, considering x_0 to be small and constant, gives

$$n \cong \frac{w_i}{\varphi - kx_0} e^{(\varphi - kx_0)t}. \tag{8}$$

It has been shown by one of us [6] that it can be assumed that τn = const at the end of the induction period; this leads to the approximation relation

$$(\varphi - kx_0)\tau = \text{const}. \tag{9}$$

When $x_0 = 0$, $\tau = \tau_0$, we have:

$$\tau = \frac{\tau_0}{1 - \frac{k}{\varphi}x_0} \simeq \tau_0\left(1 + \frac{k}{\varphi}x_0\right) = \tau_0 + \frac{k\tau_0}{\varphi}x_0. \tag{10}$$

Thus the limiting slope of the curves of Fig. 3 is expressed by $k\tau_0/\varphi$ at low values of x_0. At our experimental temperatures of 190, 200, and 210°, τ_0 has the value 720, 600, and 480 sec, respectively, while φ has the value 0.015, 0.027, and 0.037 sec^{-1}. The values of the limiting slope developed above can be used to obtain values of k at the indicated temperatures, namely 21, 14, and 15 kg/mole • sec. These results point to very low values for the activation energy and the steric factor in the reaction between the antioxidant and the active centers.

We will now consider the slopes of the $\tau = f(x)$ curves of Fig. 3 at higher values of x. At 190, 200, and 210° these slopes were equal to $6 \cdot 10^6$, $2 \cdot 10^6$, and 10^6 sec • kg/mole, respectively. It follows from Eq. (1) that the limiting value of the slope under these conditions is equal to $1/w_i$. From this it is clear that w_i alters from $1.6 \cdot 10^{-7}$ to $10 \cdot 10^{-7}$ mole/kg • sec over our interval of working temperatures. This corresponds to an activation energy of approximately 40,000 kcal/mole.

The generally accepted reaction for the initiation of hydrocarbon oxidation,

$$RH + O_2 = R + HOO^{\cdot},$$

is characterized by activation energies of 40,000-50,000 kcal/mole [7].

The effectiveness of various inhibitors can be compared in terms of the rate constants k, determined as indicated above. In this way, we have shown that N,N'-phenylcyclohexyl-n-phenylenediamine is approximately twice as effective an antioxidant for polypropylene as inhibitor A at low concentrations.

LITERATURE CITED

1. E. T. Denisov and N. M. Émanuél', Usp. Khim. 27, 365 (1958).
2. S. Foord, J. Chem. Soc. 1940, 48.
3. L. G. Angert and A. S. Kuz'minskii, International Symposium on Macromolecular Chemistry [in Russian] (AN SSSR Press, 1960) Vol. 3, p. 423.
4. N. N. Semenov, Chain Reactions [in Russian] (Leningrad, 1934).
5. Yu. A. Shlyapnikov, V. B. Miller, M. B. Neiman, E. S. Torsueva, and B. A. Gromov, Vysokomolekul. Soed. 2, No. 9 (1960).
6. M. B. Neiman and L. N. Egorov, Zhur. Fiz. Khim. 3, 61 (1932).
7. V. N. Kondrat'ev, The Kinetics of Gaseous Chemical Reactions [in Russian] (AN SSSR Press, 1958) p. 489.

All abbreviations of periodicals in the above bibliography are letter-by-letter transliterations of the abbreviations as given in the original Russian journal. *Some or all of this periodical literature may well be available in English translation.* A complete list of the cover-to-cover English translations appears at the back of this issue.

THE ROLE OF CHEMICAL AND CRYSTALLIZATION PROCESSES IN REVERSIBLE TOPOCHEMICAL REACTIONS

M. M. Pavlyuchenko, Academician Acad. Sci. Belorus.SSR, and E. A. Prodan

V. I. Lenin Belorussian State University

Translated from Doklady Akademii Nauk SSSR, Vol. 136, No. 3, pp. 651-653, January, 1961
Original article submitted September 17, 1960

The participation of solid bodies in a heterogeneous chemical reaction entails the existence not only of chemical processes but also of those crystallization processes which are involved in the lattice breakdown of the parent substances and the formation (in most cases) of new lattices of product materials. The formation and growth of nuclei of a new phase will occur in this last case. The laws governing this process when it occurs in the presence of a solid phase of a parent substance from which the new solid phase is to be formed by chemical reaction are unknown. There has also been no study of the effect of chemical and crystallization processes in fixing the observed reaction rate, nor of the interrelation of these processes and their effect on one another and on the over-all reaction.

Work on the decomposition of carbonates [1-7], crystal hydrates [8-10], etc. has shown that the character of the kinetic curves for reversible reactions is dependent on the degree of departure of the system from equilibrium during the course of the reaction. The rate of a vacuum decomposition reaction is at a maximum initially, and falls toward zero with the passage of time. The rate vs. time curve passes through a maximum in the neighborhood of the equilibrium point as a result of the difficulty of forming nuclei of the new phase. Thus, the rate of formation of a new phase can prove to be the decisive factor for the over-all solid-phase reaction near equilibrium. The work required for the formation of stable nuclei from a gaseous phase or a solution is known to be fixed by the equation

$$A = \frac{16\pi\sigma^3 M^2}{3R^2T^2\rho^2\left(\ln\frac{P}{P_0}\right)^2}. \tag{1}$$

This work becomes infinite for unit supersaturation, so that stable nuclei of the new phase cannot then be formed.

Considerable scientific interest attaches to an elucidation of the role of supersaturation and crystallization processes in reactions. We will treat certain of these processes for reversible reactions.

Consider the reaction

$$AB_s \underset{K_2}{\overset{K_1}{\rightleftarrows}} A_s + B_g - Q.$$

The reaction rate is given by

$$V = K_2 S\,[f(P_{0g}) - f(P_g)], \tag{2}$$

where P_{0g} is the equilibrium pressure, P_g is the working pressure, and $f(P_{0g})$ and $f(P_g)$ are the corresponding quantities of adsorbed gas.

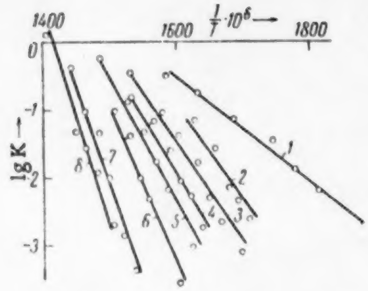

Fig. 1. The relation between the temperature and the logarithm of the rate constant for the decomposition of cadmium carbonate under the following carbon dioxide pressures (mm Hg): 1) 0; 2) 1.5; 3) 10; 4) 100; 5) 200; 6) 400; 7) 600; 8) 755.

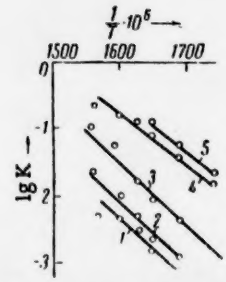

Fig. 2. The relation between the temperature and the logarithm of the rate constants for the decomposition of cadmium carbonate at the following supersaturations $P^0_{CO_2}/P_{CO_2}$. 1) 5; 2) 10; 3) 100; 4) 1000; 5) 10,000.

In a first approximation it can be assumed that

$$f(P_{0g}) = aP^n_{0g};\quad f(P_g) = aP^n_g;\quad n \leqslant 1. \tag{3}$$

Over a comparatively narrow temperature interval it can be supposed that

$$P_{0g} = Ce^{-Q/RT}. \tag{4}$$

The reaction rate is then

$$V = KS,\quad K = K_2 a\,[C^n e^{-nQ/RT} - P^n_g]. \tag{2a}$$

Introducing $K^0e^{-q_1/RT}$ in place of K, and $K^0_2e^{-q_2/RT}$ in place of K_2, supposing that $a = a_0e^{\lambda/RT}$, and that n is independent of temperature, we obtain the equation

$$q_1 = q_2 + nQ - \lambda \tag{5}$$

at $P^n_g = 0$.

The case n = 1 gives the equation $q_1 = q_2 + Q - \lambda$; for other cases, we have

$$q_1 < q_2 + Q - \lambda\,. \tag{6}$$

We will consider two situations.

Case 1. Reaction proceeds at various temperatures and fixed degree of supersaturation or unsaturation. Here,

$$K = K_2 a\left[\left(\frac{P_{0g}}{P_g}\right)^n - 1\right]P^n_g. \tag{7}$$

If the supersaturation is the same for all temperatures, it follows that

$$\left(\frac{P_{0g}}{P_g}\right)^n = \text{const}. \tag{8}$$

The substitution of (8), together with the expressions for K, K_2, and P^n_{0g} into Eq. (7) gives

$$K^0e^{-q_1/RT} = K^0_2e^{-q_2/RT}\,a\,[\text{const} - 1]\frac{C^n e^{-nQ/RT}}{\text{const}}, \tag{9}$$

from which it follows that

$$q_1 = q_2 + nQ - \lambda.$$

Thus, the energy of activation obtained from the reaction rates at fixed supersaturation and various temperatures is a constant quantity, invariant under change in the degree of supersaturation, and equal to the activation energy for vacuum decomposition [Eq. (5)].

Case 2. Reaction is carried out at various temperatures and fixed gas pressure. In this case,

$$\frac{q_1}{RT^2} = \frac{q_2}{RT^2} + \frac{d}{dT}\ln\left(C^n e^{-nQ/RT} - P_g^n\right) - \frac{\lambda}{RT^2} =$$

$$= \frac{q_2}{RT^2} + \frac{nQ}{RT^2}\,\frac{C^n e^{-nQ/RT}}{\left(C^n e^{-nQ/RT} - P_g^n\right)} - \frac{\lambda}{RT^2}. \qquad (10)$$

Equation (10) reduces to (5) when $P_g^n = 0$, i.e., when decomposition occurs in vacuum.

When $P_g^n > 0$ we have $q_1 > q_2 + nQ - \lambda$, and when $P_g^n = P_g^0$,

$$q_1 = \infty. \qquad (11)$$

Thus, the activation energy can vary from $q_2 + nQ - \lambda$ (5) to infinity, depending on the initial gas pressure.

We have checked these conclusions by studying in detail the kinetics of the decomposition of cadmium carbonate in vacuum at constant CO_2 pressure under variation of temperature and degree of supersaturation. The pressure and supersaturation were held constant in the course of each experiment.

The results of our measurements are presented in Figs. 1 and 2. Each curve of Fig. 1 was obtained by varying the temperature at a constant pressure, while each curve of Fig. 2 corresponds to a temperature variation at constant supersaturation.

Values of the activation energy calculated from Figs. 1 and 2 are given in the table. The data of this table are in complete agreement with the ideas presented above. At the same time, the rate constant and the activation energy prove to be independent of the crystallization process at supersaturations of 5-10,000, the work of formation of the nucleus varying with the supersaturation, while the calculated activation energy is independent of it.

P_{CO_2}, mm	0	1.5	10	100	200	400	600	755
q, kcal/mole	36	65	68	77	85	107	140	160
$\overset{\circ}{P}_{CO_2}/P_{CO_2}$	5		10	100		1000	10000	
q, kcal/mole	39		43	43		36	36	

Since the crystallization processes are without effect on the rate constant and the activation energy in reversible reactions over the indicated interval of supersaturations, there is all the more reason that they would not influence irreversible topochemical reactions.

LITERATURE CITED

1. K. G. Khomyakov, S. F. Yavorskaya, and V. A. Arbuzov, Uch. Zap. Mosk. Univ. Khim. No. 6, 77 (1936).
2. O. A. Esin and P. V. Gel'd, The Physical Chemistry of Pyrometallurgical Processes [in Russian] (Sverdlosk-Moscow, 1950) Chap. 1.
3. J. Zawadzki, Festlar. Tillägnad. J. Arvid Hedvall 1948, 611.
4. J. Zawadzki and S. Bretsznajder, Trans. Faraday Soc. 34, 951 (1938).
5. J. Zawadzki and S. Bretsznajder, Z. Phys. Chem. 22, 60, 79 (1933).
6. J. Zawadzki and S. Bretsznajder, Compt. rend. 194, 1160 (1932).
7. S. Bretsznajder, Roczn. Chem. 12, 799 (1932).
8. W. E. Garner, Trans. Faraday Soc. 34, 940 (1938).
9. M. Volmer and G. Seidel, Z. Phys. Chem. A179, 153 (1937).
10. B. Topley and M. L. Smith, J. Chem. Soc. 1935, 321.

THE EFFECT OF CATHODICALLY REDUCED HYDROGEN ON THE PROPERTIES OF METALS

O. S. Popova and A. T. Sanzharovskii

Institute of Physical Chemistry, Academy of Sciences of the USSR
(Presented by Academician P. A. Rebinder, July 26, 1960)
Translated from Doklady Akademii Nauk SSSR,
Vol. 136, No. 3, pp. 654-656, January, 1961
Original article submitted July 14, 1960

We have investigated the mechanism of the action of hydrogen in altering the mechanical properties of metals by studying the effect of cathodic polarization on certain characteristics of rolled iron, rolled nickel, and of dull and bright electrolytic nickel. Cathodic polarization was carried out in 10% H_2SO_4 containing 0.1 g/liter of Na_2S, working at a current density of 100 ma/cm² and a temperature of 20-25°C.

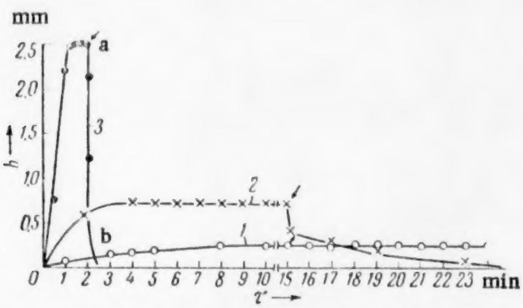

Fig. 1. Curves showing plate bending during cathodic polarization: 1) iron; 2) rolled nickel; 3) electrolytic nickel (the arrow indicates the instant of opening the circuit).

The following methods were used in this study: 1) diffusion of hydrogen through a diaphragm; 2) bending of single and double plates during one-sided polarization [1] [h = $f(\tau)$ curves obtained by this procedure are presented in Fig. 1]; 3) determination of hydrogen by vacuum extraction; 4) x-ray analysis; and 5) determination of mechanical strength before and after polarization.

Diffusion studies showed that hydrogen penetrated rolled nickel to a depth of 30μ or less, and gave rise to internal stresses of the order of 10 kg per mm². Hydrogenation of the nickel led to brittleness,* and to a reduction in the mechanical strength. The absence of plastic deformation was indicated by the fact that the internal stress disappeared completely after turning off the polarizing current (Fig. 1, 2), although the metal still remained brittle.

Brittleness disappeared after the metal had been held in air for 60-70 hours. All of the occluded hydrogen passed out of the metal during this time.

X-ray studies showed that grain disintegration occurred during hydrogenation (Fig. 2). The mechanical strength of nickel increased by 5-6% as the result of hydrogenation.

Studies on the diffusion of hydrogen through deposits of dull and shiny electrolytic nickel showed a deeper and more rapid penetration than in the case of rolled nickel. In turn, the hydrogen penetrated shiny nickel more rapidly than dull. The internal stresses due to the occlusion of hydrogen in nickel were also of the order of 10 kg/mm². Cracking of the deposit occurred during hydrogenation (Fig. 3a). There was an intense evolution of

*The change in the degree of brittleness of nickel can pass unnoticed in working with thick plates, since embrittlement occurs only to the depth of penetration of the hydrogen, and this depth is quite minute.

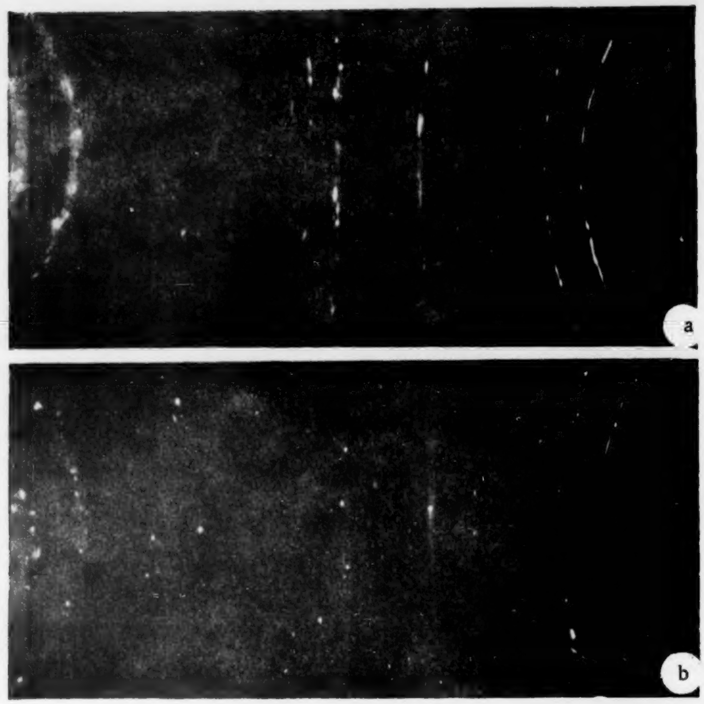

Fig. 2. X-ray diagram of nickel: a) prior to hydrogenation; b) after hydrogenation.

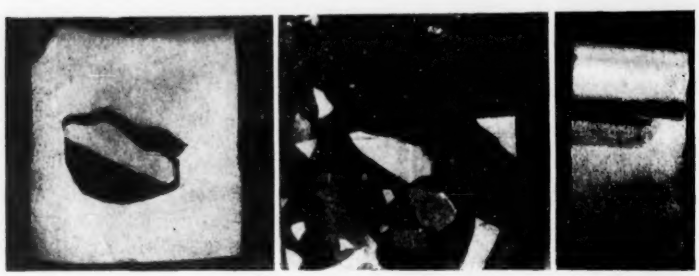

a b c

Fig. 3. Electrolytic nickel: a) during polarization; b) immediately after removal of polarization; c) after holding in air.

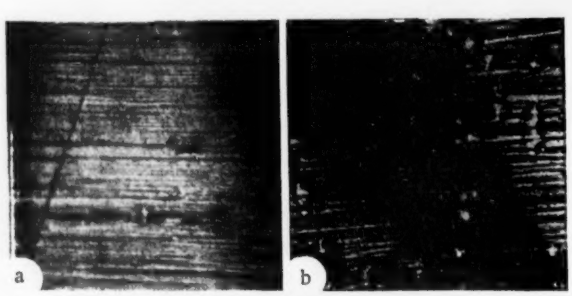

Fig. 4. Iron: a) prior to hydrogenation; b) after hydrogenation. 225 ×.

hydrogen from the metal when the polarizing current was turned off, and the internal stress disappeared (Fig. 1, 3, segment ab), but the deposit remained brittle.* Holding the deposit in air for 60-70 hours brought about the escape of all of the occluded hydrogen from the metal and a disappearance of brittleness (Fig. 3c).

After loss of brittleness, the mechanical strength of the electrolytic nickel proved to be 15-20% greater than it had been initially. X-ray studies showed a widening of the lines in the pattern obtained from the deposit after hydrogenation.

Diffusion studies showed that hydrogen rapidly penetrates iron to a considerable depth. The diffusion of hydrogen into iron is accompanied by the formation of stresses of the order of 15 kg/mm^2 [2], with enhanced embrittlement and local breakdown (Fig. 4). A considerable quantity of hydrogen is thereby occluded in the iron. Experiments showed that the hydrogen will pass out of hydrogenated iron spontaneously when the latter is held in the air for 6-7 days. Measurements indicated that the mechanical strength is lowered by 15-20% as a result of hydrogenation, the change being irreversible. Bending studies (number of bends required for rupture) showed that freshly hydrogenated iron foil will withstand 60-70% fewer bends than iron which had not been hydrogenated. Holding the metal in air brought about complete escape of the hydrogen, but the bend strength remained 50% lower than it had been initially, so that the reduction here is only partially reversible and conforms with the data on the reduction of mechanical strength. X-ray studies showed that there was no alteration of the crystal-lattice parameter of the iron.

Thus, these studies have disclosed the formation of internal stresses with a simultaneous reduction of the mechanical strength as the result of diffusion of hydrogen into a metal. The mechanism of this process can be represented in the following manner. The hydrogen which diffuses into the interior of a metal accumulates in the structural defect cavities, and there builds up a pressure of the order of 10 kg/mm^2, while another part of this hydrogen adsorbs on the surface of these defects and thereby reduces the surface energy. This last leads to the adsorptional reduction of the mechanical strength of the metal.

The metal will begin to disintegrate if adsorption reduces its mechanical strength to the value of the resulting internal stresses. This effect is observed in the polarization of electrolytic nickel. The metal will break down without plastic deformation if the value of the internal stresses remains less than the flow limit.** The quantitative relation between the processes involved in metallic breakdown under high pressure and in breakdown as the result of adsorptional diminution of mechanical strength will alter markedly in passing from metal to metal (iron, nickel). Moreover, supplementary processes occurring in one metal may not be observed in others. Thus, diffusion of hydrogen into iron results in grain disintegration, whereas no similar effect is observed in iron.

Analysis of the experimental results on the diffusion of hydrogen into nickel led to the conclusion that the principal factor in lowering the mechanical strength is the adsorptional reduction of strength, the internal stresses resulting from the occluded hydrogen playing a secondary role.***

Experiments showed that the internal stresses which are produced in nickel disappear completely and comparatively rapidly on turning off the polarization current, although the metal remains quite brittle and has a mechanical strength of approximately zero. This indicates that there is no connection between the internal stresses on the one hand, and the reduction of strength and the appearance of brittleness on the other. The hydrogen passes out of the nickel spontaneously and completely when the metal is held in the air for three days, and the brittleness disappears. The strength of the metal, on the other hand, not only returns to its original value, but exceeds this value by 15-20%. It might be supposed that the disappearance of brittleness and the escape of the hydrogen were two independent processes which occur simultaneously in nickel. If this were the case, brittleness would persist when the hydrogen was removed rapidly. Experiments showed that the rapid removal of hydrogen from a deposit over 10-15 minutes, working in vacuum without heating, would result in the same loss of brittleness as a long holding in the air.

---

*The mechanical strength of electrolytic nickel is practically equal to zero, and the metal can be ground to a powder (Fig. 3b).

**Thus, nickel breaks down without plastic deformation, whereas bending and breakdown of iron are accompanied by such deformation (Fig. 1, 2 and 1, respectively).

***The mechanical strength of shiny nickel is 88 kg/mm^2 prior to hydrogenation. Pulverization occurs at $\sigma_b = 10$ kg/mm^2.

All that has been said points to the existence of a unique relation between the residual brittleness and the adsorbed hydrogen which spontaneously but slowly escapes from the metal. The observed increase in the mechanical strength of nickel resulting from hydrogenation and the escape of the occluded hydrogen are obviously consequences of an adsorptional disintegration of the metal grains. It is quite unlikely that the effect here is much the same as that described in [3].

Analysis of the experimental data led to the conclusion that the mechanical strength of iron is reduced in hydrogenation as a result of the pressure which is produced in the metal. Thus, the irreversible deformation on bending, the irreversible reduction of mechanical strength on pulverization and bending, and the presence of local disintegration are all results of hydrogen pressure rather than the adsorptional effects. This conclusion is in agreement with the data of [4].

Thus, hydrogen diffusing through a metal will alter the metal's properties by generating stresses and by the adsorption which it experiences. The adsorptional reduction of mechanical strength can be of considerable proportions in some cases, amounting to 90% or more of the initial value for a nickel deposit.

The data which have been presented are in conformity with the concept of the adsorptional diminution of mechanical strength through the action of surface active substances (gaseous, in the present case), which has been advanced by P. A. Rebinder and his co-workers [5].

LITERATURE CITED

1. A. T. Sanzharovskii, Zhur. Fiz. Khim. 34, No. 9 (1960).
2. M. Smyalovskii and Z. Shlyarskaya-Smyalovskaya, Byull. Pol. Akad. Nauk, Otd. III, 1, No. 7 (1953).
3. E. D. Shchukin, N. V. Pertsov, and Yu. V. Goryunov, Kristallografiya No. 6, 887 (1959).
4. G. V. Karpenko and R. I. Kripyakevich, Doklady Akad. Nauk SSSR 120, No. 4 (1958).
5. V. I. Likhtman, P. A. Rebinder, and G. V. Karpenko, The Effect of Surface-Active Media on the Deformation of Metals [in Russian] (Izd. AN SSSR, 1954).

All abbreviations of periodicals in the above bibliography are letter-by-letter transliterations of the abbreviations as given in the original Russian journal. *Some or all of this periodical literature may well be available in English translation.* A complete list of the cover-to-cover English translations appears at the back of this issue.

THE THERMAL DECOMPOSITION OF CERTAIN ORGANIC COMPOUNDS IN THE PRESENCE OF DEUTERIUM

L. Radich, I. P. Kravchuk, and R. E. Mardaleishvili

M. V. Lomonosov Moscow State University
(Presented by Academician N. N. Semenov, July 14, 1960)
Translated from Doklady Akademii Nauk SSSR,
Vol. 136, No. 3, pp. 657-659, January, 1961
Original article submitted July 7, 1960

Study of the photolysis of organic compounds under various conditions has made it possible to develop a method for determining the ratio of the rate constants and the difference of the activation energies of competing elementary radical reactions [1].

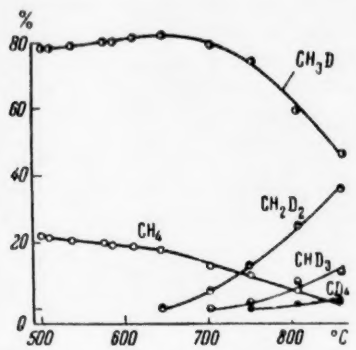

Fig. 1. The temperature dependence of the proportions of various deuteromethanes formed in the pyrolysis of acetone.

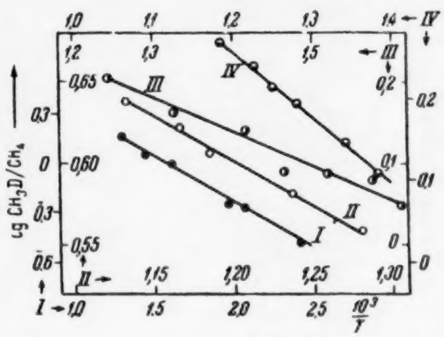

Fig. 2. The temperature dependence of the CH_3D/CH_4 ratio in experiments on the pyrolysis of: I) di-tertiary butyl peroxide; II) acetone; III) dimethyl mercury; IV) acetaldehyde.

A knowledge of the rate constant and the activation energy of one elementary step makes it possible to determine corresponding values for other elementary reactions as well. The reaction of radicals with molecular deuterium is one of the elementary processes which is most frequently used for this purpose.

Here, comparison is made of the rates of two processes, such as:

$$\dot{R} + R_1H \rightarrow RH + \dot{R}; \tag{1}$$

$$R + D_2 \rightarrow RD + \dot{D}. \tag{2}$$

From a knowledge of values of the RH and RD ratio in the products obtained at various temperatures, and the activation energy for reaction (2), E_2 (equal to 11.7 ± 0.1 kcal for methyl radicals [2]), it is possible to find the activation energy for the elementary reaction (1).

It should be noted, however, that this method was developed for exclusive use with photochemical reactions, and that considerable experimental difficulties attend its application to other types of reactions, in general, and to thermal processes, in particular. These difficulties arise principally from the possibility of secondary reactions which give the same products as are obtained from reactions (1) and (2).

We have investigated the application of deuterium for determining the rate constants of the elementary processes involved in the pyrolysis of certain organic compounds which we had under study. We also hoped to obtain experimental confirmation of the conclusions of Voevodskii, Lavrovskaya, and Mardaleishvili [3] concerning the possibility of isotopic exchange between free radicals and molecular deuterium.

It is the opinion of these authors that the exchange reaction

$$R-CH_2+D_2 \rightleftarrows R-\overset{H}{\underset{H\cdots D}{C}}\cdots D \rightleftarrows R-\dot{C}HD+HD \qquad (3)$$

proceeds at high velocity, and results in complete displacement of the hydrogen atoms attached to the valence-unsaturated carbon when the deuterium is present in excess.

TABLE 1

Pyrolysis of Acetone, 508°C

Expt. No.	τ, sec	CH_3D/CH_4	Expt. No.	p, mm Hg	CH_3D/CH_4
Unpacked reactor					
$P = 0.8$ mm Hg			$\tau = 1.60$ sec		
266	0.34	3.61	271	6.0	3.60
267	0.45	3.58	272	5.0	3.61
268	0.77	3.63	273	4.0	3.59
269	1.48	3.59	274	2.0	3.61
270	1.72	3.60	275	1.0	3.60
Packed reactor					
$P = 1.0$ mm Hg			$\tau = 1.46$ sec		
279	0.24	2.98	296	6.0	3.60
280	0.35	2,97	297	5.0	3.61
281	0.65	2.99	298	4.0	3.54
282	1.17	2.98	299	2.0	3.30
823	1.70	2.99	300	1.0	2.98
			301	0.5	2.44

TABLE 2

Substance	ΔE	E_1	Literature E_1
$CH_3-CO-CH_3$	2.5±0.2	9,2±0,3	9.6±0.4 (6) 9.7±0.1 (7) 9.5±1.0 (8)
CH_3CHO	3.8±0.4	7.9±0.5	7.5±0.4 (9)
$(CH_3)_3CO_2$	2.2±0.2	9.5±0.3	11.7±0.3 (4)
$Hg(CH_3)_2$	1.9±0.4	9.8±0.5	10.8±0.5 (10)

The present work has studied the displacement of hydrogen atoms from molecules of a reacting substance by the methyl radicals which are formed in the pyrolysis of acetaldehyde, acetone, dimethyl mercury, and di-tertiary butyl peroxide in the presence of D_2. These experiments were carried out in a jet in a high-vacuum apparatus, working over the temperature interval from 130-850°C (the temperature was measured with an accuracy of ± 1°) with various times of contact (0.1-4 sec) and total pressures (0.6-5 mm Hg). The investigated compounds were subjected to thermal decomposition in a quartz vessel ($V = 130\ cm^3$) with a 10- to 15-fold excess of deuterium, the percentage reaction ranging from 0.001 to 10%.

The reactor was filled with quartz tubes in one series of experiments to alter the S/V ratio by a factor of 15.

Principal attention was directed to a study of the composition of the methane which was the basic product obtained by subjecting each of the investigated substances to pyrolysis under various conditions. Measurements of the relative amounts of the different deuteromethanes were carried out on a MS-4 mass spectrometer.

Figure 1 shows the temperature dependence of the proportions of the various deuteromethanes which were formed in the pyrolysis of acetone. A similar distribution was found for the deuteromethanes which were formed from the other investigated substances. The percentage reaction varied with the time of contact, ranging from 0.01 to 5% for temperatures up to 500-600°. Here the methane consisted exclusively of CH_3D and CH_4 molecules. The ratio between the numbers of these molecules was independent of the total pressure and the time of contact, at fixed temperature, a fact which could serve as indication of the absence of secondary processes under these conditions. The percentage reaction increased at temperatures in excess of approximately 600°, rising to 10-30%, and the product contained polysubstituted methanes ranging all the way to CD_4. This last was the result of secondary reactions that

arise, principally because of an increase in the concentration of the deuterium atoms in the reaction zone. In the experiments on the thermal decomposition of acetone at 500° it was observed that the reactor filled with quartz tubes gave the same value of the CH_3D/CH_4 ratio at pressures above 4-5 mm Hg as the unpacked reactor. The first case differed from the second, however, in that a diminution of the total pressure on the mixture led to a reduction in the CH_3D/CH_4 ratio (Table 1).

The CH_3D/CH_4 ratio was independent of the time of contact in both the packed and unpacked reactors.

These facts indicate that the reactor surface and the packing affect the reaction rate through heterogeneous processes and point to an increase in the proportion of CH_4 in the product which appears only at low pressures ($P < 4$ mm Hg).

The experimental data obtained without packing at $P > 1$ mm Hg are presented below. On the basis of these results, it can be affirmed that secondary processes make no essential contribution to the reaction under these conditions, and the reaction is not appreciably affected by the reactor walls.

Figure 2 presents the experimental data which were obtained from the study of the temperature dependence of the CH_3D/CH_4 ratio in pyrolysis of the investigated compounds. Differences in the activation energies for processes (1) and (2) and absolute values of the activation energy for the displacement of hydrogen atoms from the various compounds by methyl radicals have been obtained on the basis of these data and are presented in Table 2; they are in good agreement with the results reported in the literature. The considerable deviation of the E_1 value for the displacement of the hydrogen atom from di-tertiary butyl peroxide clearly results from the fact that the energy of activation given in the paper of Pritchard, Pritchard, and Trotman-Dickenson [4] is too high, activation energies of this magnitude being found only for the displacement of the hydrogen atom from methane by the methyl radical (E_1 = 12.8 kcal [1]).

The experimental data can serve as indication that, up to temperatures of 500-550°, secondary reactions will not cause difficulties in measurements of the rate constants of elementary radical reactions by comparison of the rates of reactions (1) and (2).

A comparison of the energies of activation for displacement of the hydrogen atoms from the various organic compounds by methyl radicals in photochemical and in thermochemical decomposition shows that the "hot" radicals which have been discussed in the literature [5] are not formed in the photolysis of these substances.

At the same time, it can be concluded that the mechanism proposed by Voevodskii and his co-workers for exchange between radicals and molecular deuterium is not valid for the conditions of thermal reaction, since polysubstitution final products result from secondary substitution processes only at temperatures above 600°.

LITERATURE CITED

1. E. W. R. Steacie, Atomic and Free Radical Reactions (New York, 1954).
2. T. G. Majuary and E. W. R. Steacie, Disc. Faraday Soc. 14, 45 (1953).
3. V. V. Voevodskii, G. K. Lavrovskaya, and R. E. Mardaleishvili, Doklady Akad. Nauk SSSR 81, 215 (1951).
4. G. O. Pritchard, H. O. Pritchard, and A. F. Trotman-Dickenson, J. Chem. Soc. 1954, No. 5, 1425.
5. V. N. Kondrat'ev, The Kinetics of Gaseous Chemical Reactions [in Russian] (AN SSSR Press, 1958).
6. K. N. Saunders and H. A. Taylor, J. Chem. Phys. 9, 616 (1941).
7. A. F. Trotman-Dickenson and E. W. R. Steacie, J. Phys. Chem. 55, 908 (1951).
8. M. T. Jacquiss, J. S. Roberts, and M. Szwarc, J. Am. Chem. Soc. 74, 6005 (1952).
9. R. K. Brintor and D. H. Volnan, J. Chem. Phys. 20, 1053 (1953).
10. R. Gomer and W. A. Noyes, J. Am. Chem. Soc. 71, 3390 (1949).

THE ELECTRON DENSITY DISTRIBUTION IN INDIUM ARSENIDE

N. N. Sirota, Academician, Acad. Sci. Belorus.SSR, and

N. M. Olekhnovich

Division of Solid State Physics and Semiconductors, Academy of Sciences of the Belorus.SSR

Translated from Doklady Akademii Nauk SSSR,
Vol. 136, No. 3, pp. 660-662, January, 1961
Original article submitted September 16, 1960

Special interest attaches to the arsenides which are found among the semiconducting compounds of sphalerite structure that are formed from the elements of groups three and five, $A^{III}B^{V}$. This is due not only to the properties which they show as semiconductors, but also to the fact that they combine high current mobility with a relatively wide forbidden zone. Thus, a study of electron density distributions could be quite significant for an understanding of the nature and energy of the interatomic bonding in such compounds, and for an elucidation of the factors which are responsible for their peculiar physical properties.

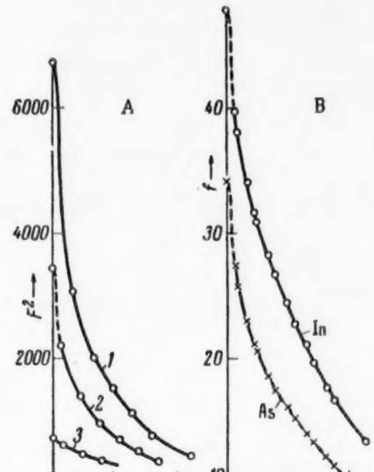

Fig. 1. A) The square of the structure amplitude F^2 of indium arsenide plotted as a function of Σh_i^2. B) The atomic scattering factor f plotted as a function of Σh_i^2 for the indium and arsenic ions of indium arsenide: 1) F_1^2; 2) F_2^2; 3) F_3^2.

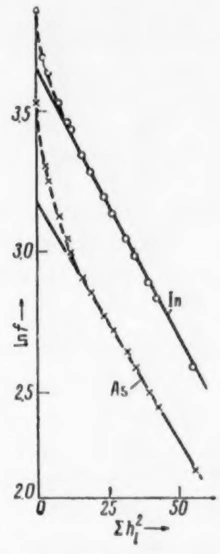

Fig. 2. The atomic scattering factor plotted as a function of Σh_i^2 for indium and arsenic ions.

Study was made on polycrystalline indium arsenide which was ground in an agate mortar and then washed with toluene. The diameters of the powder particles fell in the 6-8μ interval. The polycrystalline indium arsenide was prepared from the pure elements by direct synthesis in evacuated and sealed quartz ampoules, following the procedure which has been described earlier in [1].

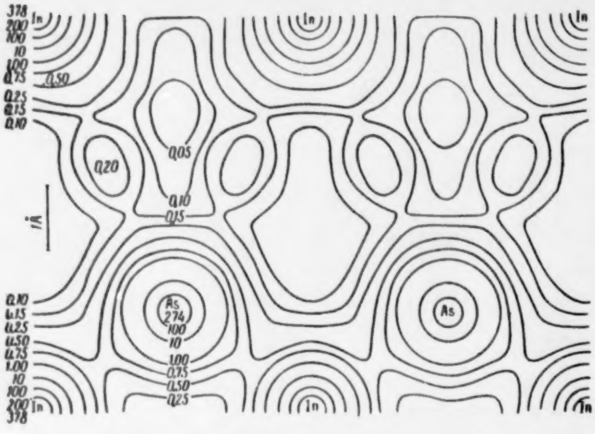

Fig. 3. Diagram showing the electron density distribution in the (110) plane of the elementary cell of indium arsenide.

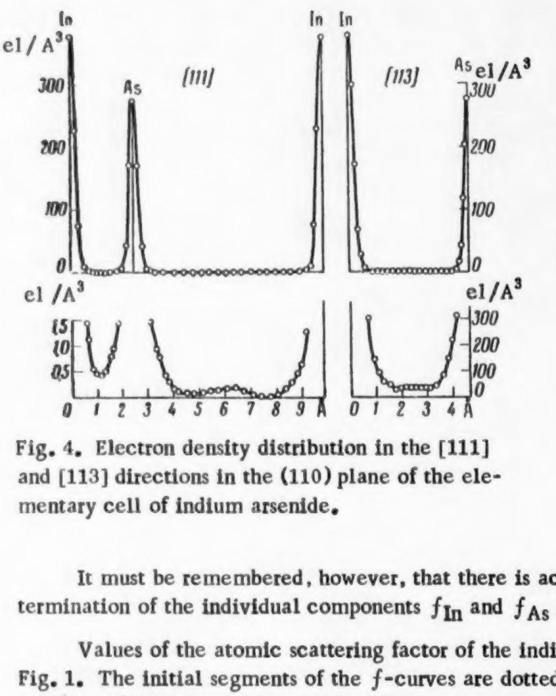

Fig. 4. Electron density distribution in the [111] and [113] directions in the (110) plane of the elementary cell of indium arsenide.

X-ray diagrams were obtained at room temperature in a URS-50-I system, using CuKα radiation, and following a technique similar to that described in [2]. These experimental data were used for calculating the square of the structure amplitude F^2, at various Σh_i^2 values for lines with even *hkl* indices, the index sum being divisible by four (1); lines with even *hkl*, the index sum being indivisible by four (3); and lines with odd indices (2) (Fig. 1A). Figure 1A gives values of the square of the structure amplitude referred to the individual molecule, i.e., to one pair of InAs atoms.

Since $F_1^2=(f_{\text{In}}+f_{\text{As}})^2$, $F_2^2=f_{\text{In}}^2+f_{\text{As}}^2$ and $F_3^2=(f_{\text{In}}-f_{\text{As}})^2$, it follows that $F_3^2=2F_2^2-F_1^2$.

If only F_1^2 and F_2^2 are taken into account, one obtains

$$f_{\text{In}}=\frac{F_1}{2}+\frac{1}{2}\sqrt{2F_2^2-F_1^2}, \qquad \text{(a)}$$

$$f_{\text{As}}=\frac{F_1}{2}-\frac{1}{2}\sqrt{2F_2^2-F_1^2}. \qquad \text{(b)}$$

It must be remembered, however, that there is actually only one line for each value of Σh_i^2. Thus, a determination of the individual components f_{In} and f_{As} always involves interpolation between neighboring points.

Values of the atomic scattering factor of the indium ion f_{In} and the arsenic ion f_{As} in InAs are given in Fig. 1. The initial segments of the f-curves are dotted, since it is only F_1^2, the square of the sum of the order numbers of the components, which is known with accuracy at $\Sigma h_i^2 = 0$, while F_2^2 and F_3^2 depend on the degree of ionization of the In and As atoms and are not known exactly.

It is possible to obtain null values of f_{In} and f_{As}, since the F_3^2 curve can be extrapolated to zero with considerable assurance. It is to be noted that the dotted segments of the f_{In} and f_{As} curves do not affect the calculation of the electron density in the InAs lattice. This is true because the values of f_{In} and f_{As} at $\Sigma h_i^2 = 0$ enter into the zeroth member of the three-dimension Fourier series as the sum of the order numbers of In and As in the Mendeleev periodic system.

The logarithms of the atomic scattering factors of the indium and arsenic ions fall nicely on straight lines when $\Sigma h_i^2 > 12$ (Fig. 2).

Calculation of the electron density distribution in the elementary cell of InAs was made on the basis of the

values of f_{In} and f_{As}, following the method described earlier [3], and summing the three-dimensional Fourier series. Here, the side of the elementary cell was divided into 60 equal parts.

A diagram of the electron density distribution in the (110) plane of the elementary cell of InAs is given in Fig. 3. Figure 4 shows the electron density distribution between the indium and arsenic ions in the [111] and the [113] directions in the (110) plane.

These experimental results can be used for drawing certain conclusions concerning the electron density distribution in the elementary cell of indium arsenide, the values of the ionic radii, and the degree of ionization of indium and arsenic.

Considerable interest attaches to the variation of the electron density in various directions. A "bridge" is observed in the electron density in the [111] direction over the interval $\frac{1}{2}\,\frac{1}{2}\,\frac{1}{2} - \frac{3}{4}\,\frac{3}{4}\,\frac{3}{4}$, the density reaching a value of 0.20 el/A^3 in the neighborhood of the point $\frac{5}{8}\,\frac{5}{8}\,\frac{5}{8}$, and falling to 0.03 el/A^3 near $\frac{3}{4}\,\frac{3}{4}\,\frac{3}{4}$. The electron density diagram (Fig. 3) shows that this "bridge" extends between the indium and arsenic ions in the [113] direction in the (110) plane. It is to be noted that such "bridges" are not observed in germanium.

There is a pronounced "bridge" of enhanced electron density in the [111] direction between the points of coordinates 000 and $\frac{1}{4}\,\frac{1}{4}\,\frac{1}{4}$, its form being similar to that observed in germanium [2], silicon [4,5], and diamond [3]. The lowest electron density in this interval is 0.45 el/A^3.

It is also to be noted that the electron density at the midpoint between neighboring metallic In ions is of the order of 0.15 el/A^3 in the [110] direction, and 0.07 el/A^3 in the [001] direction. Midway between the arsenic ions, the electron density is of the order of 0.10-0.15 el/A^3 in the [110] direction, and <0.03 el/A^3 in the [001] direction.

These results are of considerable interest for the elucidation of the interatomic interaction in indium arsenide.

LITERATURE CITED

1. N. N. Sirota and Yu. M. Pashintsev, Inzh.-Fiz. Zhur. No. 12, 38 (1958).
2. N. N. Sirota and A. U. Sheleg, Doklady Akad. Nauk SSSR 135, No. 5 (1960).
3. N. N. Sirota, N. M. Olekhnovich, and A. U. Sheleg, Doklady Akad. Nauk SSSR 132, No. 1, 160 (1960).
4. N. N. Sirota, N. M. Olekhnovich, and A. U. Sheleg, Doklady Akad. Nauk Belorus.SSR 4, No. 4, 144 (1960).
5. S. Göttlicher, R. Kuphal, G. Nagorsen, and E. Wölfel, Z. Phys. Chem. 21, 133 (1959).

All abbreviations of periodicals in the above bibliography are letter-by-letter transliterations of the abbreviations as given in the original Russian journal. *Some or all of this periodical literature may well be available in English translation.* A complete list of the cover-to-cover English translations appears at the back of this issue.

THE TUNNEL EFFECT IN CHEMICAL REACTIONS

St. G. Khristov

Chemicotechnological Institute, Sofia, Bulgaria

(Presented by Academician A. N. Frumkin, November 3, 1960)
Translated from Doklady Akademii Nauk SSSR,
Vol. 136, No. 3, pp. 663-666, January, 1961
Original article submitted April 29, 1960

The theory of the tunnel effect in the passage of atoms across a potential barrier [1-6] has recently attracted renewed interest among numerous investigators [7-13], and possibilities of detecting such an effect experimentally have been pointed out. Importance attaches to the development of an equation relating the barrier parameters, the particle mass, and the temperature at which the tunnel effect begins to be appreciable. An equation of this type was first derived for a rectangular barrier in [7].* V. I. Gol'danskii [11] has recently proposed a similar criterion for a smooth barrier with a parabolic peak.** This criterion does not, however, permit a precise determination of that critical temperature T_c above which the tunnel effect is negligible. With it no more can be done than to find a certain temperature $T_c^{'} < T_c$ below which the reaction rate is fixed by the tunnel effect alone. This region of very low temperatures ($T < T_c^{'}$) is one which has not yet been investigated. At the same time, special interest attaches to the region of moderate temperatures ($T_c^{'} < T < T_c$), since the tunnel effect is not very large here but can still be significant and therefore open to experimental detection. The Gol'danskii criterion is unsuitable for delineating the $T < T_c$ region from the $T > T_c$ region, since it was derived from an approximation for the maximum of the integrated function in the expression

$$P = \int_0^\infty W(U)\, w(U,\ T)\, dU \tag{1}$$

giving the total probability of transmission P in terms of W(U), the barrier penetrability, and w(U,T), the distribution function for the energy U. The function $f(U) = W(U)w(U,T)$ does not, however, always have a maximum, and the presence of such maximum is not always a significant factor in fixing the contribution of the tunnel effect to the total rate of reaction.***

---

*This relation can be written as

$$32\pi^2 m\delta^2 (RT)^2 / h^2 E_0 \approx 1 \quad \text{or} \quad T_c = h\sqrt{E_0} / 8\pi R l \sqrt{2m}\ ; \tag{a}$$

$l = \delta/2$ is the half-width of the barrier, E_0 is the barrier height, m is the particle mass, and T_c is the temperature below which the reaction rate is almost completely determined by the tunnel effect.

**The Gol'danskii relation has the form

$$T_c^{'} = h\sqrt{E_0}/2\pi^2 R d\sqrt{2m}, \tag{b}$$

where d is the effective half-width of the barrier ($d = l$ for the parabolic barrier, while $d = l/\pi$ for the Eckart barrier, l being the half-width of the barrier base).

***The F(U) functions for rectangular and parabolic barriers do not show maxima in the region where $U < E_0$ (there is, on the contrary, a minimum in the first case [6,7]) if the penetrability of the barrier is defined by the Wentzel-Brillouin approximation: $W(U) = D\exp[(-4\pi/h)\int\sqrt{2m(V(x)-U)}\,dx]$, with constant D, and the energy

Thus, it is of interest to find a more exact relation which would permit the delineation of the region of moderate temperatures in which the tunnel effect is of considerable magnitude from the region of higher temperatures in which this effect can be considered as having minor significance for the observed reaction rate. Such a relation can be derived for any smooth unidimensional barrier by determining the P'/P" ratio through the same method as was employed earlier for the rectangular barrier [7]. Here

$$P' = \int_Q^E W(U)\, w(U,\ T)\, dU, \quad P'' = \int_E^\infty W(U)\, w(U,\ T)\, dU \tag{2}$$

are the total probabilities for transmission through and over the barrier, respectively (E is the barrier height, and Q is the heat of reaction).

A preliminary expression for P'/P" can be obtained in the case of the parabolic barrier by making use of the Wentzel-Brillouin approximation for P' and the classical expression for P" [4,6,11,13]. Thus, it is found that [13]*

$$P'/P'' = P'/P^{cl} = \gamma\,(1 - e^{-(\delta-\gamma)\omega})/(\delta-\gamma), \tag{3}$$

$$\gamma = E_0/RT, \quad \delta = 2\pi^2 d\sqrt{2mE_0}/h, \quad \omega = (E-Q)/E_0 \tag{4}$$

(E_0 is the height of the corresponding symmetric barrier for which Q = 0, i.e., $\omega = 1$). Usually $\gamma \gg 1$, $\delta \gg 1$, and $\gamma\omega = (E-Q)/RT \gg 1$.

When $\gamma > \delta$ and $(\gamma-\delta)\omega \gtrsim 2$, we have $P'/P'' = (\gamma \exp(\gamma-\delta)\omega)/(\gamma-\delta) \gtrsim 3\gamma \gg 1$; when, on the other hand, $\delta > \gamma$ and $(\delta-\gamma)\omega \gtrsim 2$, then $P'/P'' = \gamma/(\delta-\gamma)$ will be considerably greater than unity if the difference $\delta - \gamma$ is not too large. Series decomposition in (3) will give $P'/P'' = \gamma\omega \simeq \delta\omega \gg 1$ when $\gamma \to \delta$. Equations (4) show the condition $\gamma \simeq \delta$ to lead to the Gol'danskii criterion (b), and this criterion thus corresponds to a considerable preponderance of tunnel transmissions over transmissions above the barrier. Here the contribution from the tunnel effect will make up 90-98% of the total reaction rate, and will correspond to an alteration of $\delta\omega$ over the interval from 10 to 50.

It can be supposed that the tunnel effect will certainly begin to be a decisive factor in fixing the reaction rate when P'/P" ≈1 [7].** This condition corresponds to the relation $\gamma \approx \delta/2$ which, according to (3), will give $P'/P'' = 1 - e^{-\gamma\omega} \simeq 1$, since $\gamma\omega \gg 1$. Equation (4) can be combined with the equality $\delta = 2\gamma$ to obtain an expression

$$T_c = h\sqrt{E_0}/\pi^2 Rd\sqrt{2m} \tag{5}$$

---

distribution function is given by an expression of the form $w(U,T) = \varphi(T)\exp(-U/RT)$. A maximum in the $U < E_0$ region will arise from use of an exact expression for W(U) (one in which $D \to 0$ when $U \to 0$ [6,7,9]), or from application of the more general expression $w(U,T) = \varphi(T)U^n \exp(-U/RT)$ [11], and will somewhat diminish the proportion of tunnel transmissions ($U < E_0$) in comparison with classical transmissions ($U > E_0$), but the presence of such maximum is not an essential condition for the existence of an appreciable contribution from the tunnel effect. Only in the case of the Eckart barrier is there a sharply defined maximum [3,7,8] under all conditions, and the presence of this maximum is certainly closely related to the contribution of the tunnel effect to the rate of transmission of particles through the barrier. The position of this maximum U_m is determined very inaccurately by the Wentzel-Brillouin approximation [11], however, when $U_m \to E_0$ (see following footnote).

*For greater generality, we consider the case of an unsymmetrical barrier [13] resulting from the superposition of a linear potential on a parabolic barrier (the P'/P" ratio is independent of the direction of transmission).

**Distinction should be made between the contribution of the tunnel effect to the actual rate, and the tunnel correction to the "classical" reaction rate. The fraction of tunnel transitions can be a quantity of considerable magnitude (about 30%) even in cases where there is no essential difference between the actual rate and the classical rate [8,9].

for T_c, the temperature below which tunnel transitions will make up more than 50% of all particle transitions across the barrier. This temperature is twice as large as the temperature $T_c^{\bullet}$ given by the Gol'danskii relation. When $P'/P^{\bullet} = 1$ (i.e., $T = T_c$), the corrective multiplicative factor for the classical reaction rate will be $\kappa = P/P^{cl} = P/P^{\bullet} = (P' + P^{\bullet})/P^{\bullet} = 2$.

Equation (5) remains valid even in a rigorous derivation based on a combination of approximations due to V. B. Wigner [9,13], in which

$$\varkappa = P / P^{cl} = 1 + \pi^2\gamma^2 / 6\delta^2 + \gamma\,[e^{-(\delta-\gamma)/10} - e^{-(\delta-\gamma)\omega}] / (\delta-\gamma). \tag{6}$$

When $\delta = 2\gamma$, one obtains $\varkappa = 1 + \pi^2/24 + e^{-\gamma/10} - e^{-\gamma\omega} \geqslant 1.41$ (if $\gamma\omega > 5$). A good approximation for κ is obtained from the relation which results from making use of a more exact expression for the barrier transparency $W(U)$ in (1) [7,10,13], namely [13]:

$$\varkappa = P / P^{el} = (\pi\gamma / \delta)/\sin(\pi\gamma / \delta) - \gamma e^{-(\delta-\gamma)\omega} / (\delta - \gamma). \tag{7}$$

From this it follows that $\delta = 2\gamma$ when $\varkappa = \pi/2 - e^{-\gamma\omega} = 1.57$ (if $\gamma\omega > 5$). The value of $P^{\bullet}/P^{cl}$ in the expression $\kappa = P'/P^{cl} + P^{\bullet}/P^{cl}$ varies between 0.5 and 1 [5], so that P'/P^{cl} must vary between 0.6 and 1, and $P'/P^{\bullet}$ between 0.6 and 2. It can be shown that $P'/P^{\bullet} = 1$ is exact when $\delta = 2\gamma$. Actually, the exact expressions for P' and $P^{\bullet}$ can be written as [13]: $\dfrac{P'}{P^{cl}} = \gamma\displaystyle\int_0^{\infty} \frac{e^{\gamma y}\,dy}{1+e^{\delta y}}$, $\dfrac{P''}{P^{cl}} = \gamma\displaystyle\int_{-\infty}^{0} \frac{e^{\gamma y}\,dy}{1+e^{\delta y}}$, where $y = (E - U)/E_0$. Setting $\delta = 2\gamma$ gives:

$$\frac{P'}{P^{cl}} = \frac{1}{2}\gamma \int_0^{\infty} \frac{dy}{\operatorname{ch}\gamma y} = \operatorname{arctg} e^{\gamma\omega} - \frac{\pi}{4}, \quad \frac{P''}{P^{cl}} = \frac{1}{2}\gamma \int_{-\infty}^{0} \frac{dy}{\operatorname{ch}\gamma y} = \frac{\pi}{4}. \tag{8}$$

Values obtained from these two expressions are practically identical when $\gamma\omega > 5$ (when $\operatorname{arctg} e^{\gamma\omega} \simeq \pi/2$), so that $P'/P^{\bullet} = 1$ for all chemical reactions. Thus, relation (5) is strictly valid for the parabolic barrier.

The Eckart Barrier

δ	γ	δ/γ	P'/P''	P/P^{el}	T_c, °K	$T_c^{\bullet}$, °K	T_c Eq. (5), °K
17.3	9.65	1.79	1.1	1.6	750	418	836
52.6	31.1	1.69	1.1	1.4	373	219	440
71.5	42.5	1.68	0.96	1.3	273	162	322

It can be supposed that this same expression would be applicable in a first approximation to any barrier whose peak is approximately parabolic, d then representing the half-width of the base of the parabola. It could be anticipated, however, that the error in the determination of T_c from Eq. (5) would be all the greater if the width of base l of the barrier in question was markedly different from d. An exact calculation of this error can be made in the case of the Eckart barrier, where $l = \pi d$ [11]. Such a barrier can be considered as parabolic for all particles whose energy is greater than $U = 0.9E$ [11], but a considerable proportion of the particles will traverse the barrier at a much lower level (down to $U = 0.5E$ [7,8]) when $T = T_c$, i.e., when $P'/P^{\bullet} = 1$, so that the δ/γ ratio for this barrier must be considerably different from 2.

This fact is brought out by the table, which contains the results of calculations for three pairs of values of δ and γ under which the condition $P'/P^{\bullet} \simeq 1$ is satisfied. Values of P, P', and $P^{\bullet}$ at $Q = 0$ were calculated from Eqs. (1) and (2) by graphic integration [3,7,8,12]. In these three cases, the maximum of the integrated function in (1), U_m, falls at the peak of the barrier, so that $U_m = E_0$.* The quantity δ/γ remains almost constant at 1.7 to 1.8 for very pronounced variations in δ (~20 to ~70) and γ (~10 to ~40). From this it follows that a more exact expression for T_c in the case of the Eckart barrier would be one corresponding to the condition $\delta \simeq 1.75\gamma$ ($\delta = 2\gamma$ for the parabolic barrier), so that

$$T_c = {}^7/_8\, h\sqrt{E_0} / \pi R l \sqrt{2m}. \tag{9}$$

* According to Gol'danskii [11], $U_m \approx E_0(\delta/\gamma)^2$. The U_m values which this expression gives for the cases covered by the table are 3-5 times greater than E_0. From this it follows that $T_c^{\bullet}$ is much lower than T_c.

This result shows that the values of T_c in the table are greater than the T_c' values obtained from the Gol'danskii relation (b) by a factor of approximately 1.75, and are less than the values obtained from Eq. (5) for the parabolic barrier by a factor of 1.15.

It is clear that Eq. (5) can be used in approximating T_c for any barrier which has a parabolic peak. A comparison of (5) and (9) with one another and with (a) for the rectangular barrier will show, however, that T_c is strongly dependent not only on the dimensions, but also on the form of the barrier. These relations can be used for fixing the geometric properties of barriers in a study of the temperature dependence of reaction rates [7,8,11].

The above discussion of Eqs. (5) and (9) gives grounds for supposing that these relations would be approximately valid for any smooth barrier, even if the barrier peak cannot be well represented by a parabola. The work with the parabolic barrier has shown that the relation $\kappa = P/P^{cl} \simeq 1.5$ is valid when $T = T_c$, the difference $\kappa - 1 \simeq \simeq 0.5$ being essentially fixed by the value assumed by the $\pi^2\gamma^2/6\delta^2$ term in Eq. (6) when $\delta = 2\delta$ (i.e., $T = T_c$), namely 0.41. This same term appears when the first member of (7) is decomposed in a series [10, 13]. It is, however, nothing other than the Wigner correction [2] q_W to the reaction rate.* For the Eckart barrier at $T = T_c$ (see table), $\kappa - 1 \simeq 0.4$, so that $q_W = 0.53$ (when $\delta = 1.75\gamma$). From this it follows that a crude derivation of (5) and (9) can be obtained with the aid of a general expression for q_W: $q_W = h^2A/96\pi^2m(RT)^2 \simeq 0.5$ $[A = -\partial^2V(x_m)/\partial x^2 > > 0]$, i.e., from the generalized expression

$$T_c = h\sqrt{A}/2\pi\sqrt{2m}. \tag{10}$$

This last shows T_c to be determined essentially by the curvature of the potential barrier at the maximum. It can be assumed that this relation would be applicable to any barrier of finite curvature, which is to say, to practically all real barriers.

It follows from what has been said that the quantum correction to the classical reaction rate at the temperature fixed by Eqs. (5), (9), and (10) is already in excess of the first approximation ch^2. The Wigner correction vanishes at temperatures (see second footnote on page 102) which are approximately 100° above T_c. (Higher powers of the Planck constant become significant in the series decomposition of the quantum correction when $T < < T_c$ [10,13].) Tunnel effects can be detected experimentally in this region of moderate temperatures by studying the influence of isotopic effects on the observed activation energy and frequency factor in the commonly employed expression for the reaction rate [8-10]. The temperature $T_c' \simeq T_c/2$, obtained from the Gol'danskii relation (b), can serve to mark out the low-temperature region where an abnormal tunnel effect must give rise to extremely low values of the effective activation energy and the frequency factor [4,8,11]. This is an interesting region for study.

LITERATURE CITED

1. D. Bourgin, Proc. Nat. Acad. Sci., Washington 15, 357 (1929); R. Langer, Phys. Rev. 34, 92 (1929); S. Roginsky and L. Rosenkewitsch, Z. Phys. Chem. 10, 47 (1930).
2. E. Wigner, Z. phys. Chem. 19, 203 (1932).
3. R. P. Bell, Proc. Roy. Soc. A139, 466 (1933).
4. R. P. Bell, Proc. Roy. Soc. A148, 241 (1935).
5. R. P. Bell, Proc. Roy. Soc. A158, 128 (1937).
6. St. G. Khristov, Ann. Univ. Sofia, Fac. Phys.-Math. 42, 69 (1945-1946); 63 (1946-1947).
7. St. G. Christov, Z. Elektrochem. 62, 567 (1958).
8. St. G. Khristov, Doklady Akad. Nauk SSSR 125, 143 (1959); Z. phys. Chem. (1960) (in press).
9. St. G. Christov, Z. phys. Chem. 212, 40 (1959).
10. R. P. Bell, Trans. Faraday Soc. 55, 1 (1959); Reports, Abstracts of Reports, and Communications of Foreign Scientists, Eighth Mendeleev Conference [in Russian] (Moscow, 1959) p. 43.
11. V. I. Gol'danskii, Doklady Akad. Nauk SSSR 124, 1261 (1959); 127, 1037 (1959).
12. B. E. Conway, Canad. J. Chem. 37, 178 (1959).
13. St. G. Christov, Z. Elektrochem. (in press).

* See [8b] with reference to the deviation of the Wigner correction factor from the values obtained from Eq. (1) by using the classical Boltzmann expression for w(U,T).

THE KINETICS OF HYDRIDE TRANSFER REDUCTION OF TRIPHENYLCARBINOL BY ISOPROPYL ALCOHOL IN AQUEOUS SULFURIC ACID SOLUTION

S. G. Éntelis, G. V. Épple, and N. M. Chirkov

Institute of Chemical Physics, Academy of Sciences of the USSR

(Presented by Academician V. N. Kondrat'ev, May 30, 1960)
Translated from Doklady Akademii Nauk SSSR,
Vol. 136, No. 3, pp. 667-670, January, 1961
Original article submitted May 24, 1960

The study of the kinetics and mechanisms of reactions involving hydride ion (H^-) transfer has been undertaken only recently [1-4], although the existence of such reactions was postulated long ago. Meerwein-Pandorf reactions of reduction of aryl carbinols by aliphatic alcohols in acid media are special instances of such processes.

The present work has involved a detailed study of the kinetics of reduction of triphenylcarbinol (TPhC) to triphenylmethane by isopropyl alcohol in aqueous sulfuric acid solution, working over a wide range of concentrations (H_2SO_4, from 45 to 75%; TPhC, from $4 \cdot 10^{-7}$ to $4 \cdot 10^{-6}$ mole/liter; and iso-C_3H_7OH, from 0.2 to 1.5 mole per liter) and temperatures (from 35 to 60°).

A preliminary study of this reaction has been made by Bartlett and Collum [2], who have concluded that it involves a transfer of the H^- ion of the isopropyl alcohol molecule to the triphenylmethylcarbinol ion according to

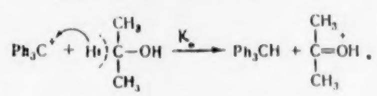

(1)

The TPhC arylmethyl cation is formed through protonization of TPhC, as shown by the equation

$$Ph_3COH + H^+ \underset{}{\overset{K_{ArCOH}}{\rightleftarrows}} Ph_3C^+ + H_2O, \tag{2}$$

and it therefore follows that the total TPhC concentration $[Ph_3COH]_0$ of the reacting mixture is the sum of the concentration of the ion $[Ph_3C^+]$ and the concentration of the un-ionized carbinol $[Ph_3COH]$:

$$[Ph_3COH]_0 = [Ph_3C^+] + [Ph_3COH]. \tag{3}$$

Scheme (1) can be combined with Eqs. (2) and (3), and the reaction for the protonization of iso-C_3H_7OH

$$\text{iso-}C_3H_7OH + H^+ \overset{K_{ROH}}{\rightleftarrows} \text{iso-}C_3H_7OH_2^+ \tag{4}$$

to prove that the rate of decrease of $[Ph_3C^+]$ in the presence of an excess of alcohol will be expressed by

$$-d[Ph_3C^+]/dt = k_{ef}[Ph_3C^+], \tag{5}$$

the experimentally observed effective rate constant being given by

$$k_{ef} = k_0 \frac{K_{ArCOH}c_0}{1 + K_{ArCOH}c_0} \frac{1}{1 + K_{ROH}h_0} C_{al}. \tag{6}$$

TABLE 1

$k_{ef} \cdot 10^2$, min^{-1}	C_{al}, mole/liter	$k_{ef} \cdot 10^2$, min^{-1}	C_{al}, mole/liter	$k_{ef} \cdot 10^2$, min^{-1}	C_{al}, mole/liter	$k_{ef} \cdot 10^2$, min^{-1}	C_{al}, mole/liter	$k_{ef} \cdot 10^2$, min^{-1}	C_{al}, mole/liter	$k_{ef} \cdot 10^2$, min^{-1}	C_{al}, mole/liter	$k_{ef} \cdot 10^2$, min^{-1}	C_{al}, mole/liter
44,52%	H_2SO_4	48,26%	H_2SO_4	50,46%	H_2SO_4	51,46%	H_2SO_4	53,42%	H_2SO_4	54,95%	H_2SO_4	58,60%	H_2SO_4
0,40	0.39	1,56	0,16	1,51	0,13	1,10	0,10	0,97	0,10	1,48	0,16	0,94	0,19
0,45	0,43	3,28	0,32	1,74	0.16	2,25	0,2	1,62	0,14	4,91	0,30	2,36	0,45
1,24	1,06	3,78	0,43	2.53	0,21	2,48	0,21	1,49	0,14	3,52	0,38	4,86	0,80
46,54%	H_2SO_4	4,80	0,59	2,89	0,22	2,92	0,25	2,07	0,19	5,46	0,48	60,70%	H_2SO_4
2,10	0,29	4,95	0,69	4,92	0,33	2,92	0,26	2,60	0,26	55,70%	H_2SO_4	0,56	0,26
2,59	0,43	5,50	0,71	5,16	0,43	3,26	0,28	4,37	0,40	1,68	0,21	1,99	0,50
2,92	0,44	49,33%	H_2SO_4	5,26	0,44	5,59	0,44	4,74	0,45	3,62	0,50	2,46	0,59
47,474%	H_2SO_4	3,70	0,31	5,70	0,46	7,41	0,59	5,03	0,45	4,33	0,67	64,80%	H_2SO_4
2,12	0,29	4,01	0,36	6,04	0,48	9,56	0,75	5,01	0,47	8,70	0,81	0,21	0,50
3,74	0,48	4,44	0,46	6,19	0,48	10,3	0,76	5,06	0,48	9,62	0,90	67,0%	H_2SO_4
		5,86	0,68	6,21	0,51	20,9	1,38	5,77	0,50			0	0,5
				7,17	0,53	52,405%	H_2SO_4	7,60	0,72			70,0%	H_2SO_4
				8,11	0,60	4,61	0,34	6,75	0,83			0	0,5
				8,15	0,65	4,70	0,40					75%	H_2SO_4
				9,80	0,72	5,60	0,44					0	0,5
				4,04	0,97	6,91	0,58						
				15,00	1,99								

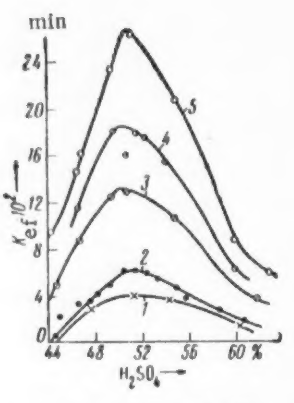

Fig. 1. Dependence of effective rate constant on sulfuric acid concentration at C_{al} = 0.5 mole per liter: 1) 35°; 2) 40°; 3) 50°; 4) 54°; 5) 60°.

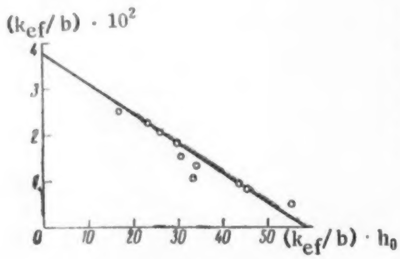

Fig. 2. Graphical determination of the true rate constant and pK_B for isopropyl alcohol at 40° and C_{al} = 0.1 mole/liter.

In Eq. (6), k_0 is the true rate constant for the limiting step (1); K_{ArCOH} is the equilibrium constant for reaction (2); K_{ROH} is the equilibrium constant for reaction (4); C_{al} is the total concentration of iso-C_3H_7OH in solution; and h_0 and c_0 are the negative antilogarithms of the acidity functions of Hammett and Deno, respectively [5,6]. Values of the effective rate constants are found from the slopes of semilogarithmic plots of kinetic data on the diminution of the optical density of the solution at 432 mμ. Equation (5) shows the diminution of the optical density to follow a first-order reaction law, since it parallels the decrease in the concentration of the triphenylmethylcarbinol ion, which has an absorption band with a maximum at 432 mμ.

Reaction was followed on an SF-2M double-ray spectrophotometer which was equipped with a device for registering kinetics. Reaction was carried out in sealed bulbs which were set into a thermostatted bulb holder. The temperature of each bulb was held constant to within ± 0.5°.

For illustration, experimentally determined values of k_{ef} obtained at 40° with various values of C_{al} and sulfuric acid concentration are given in Table 1. Figure 1 shows the dependence of k_{ef} on the initial H_2SO_4 concentration at C_{al} = 0.5 mole/liter. It is clear that reaction is limited to the narrow concentration region which is bounded by the bell-shaped curves. The maximum on these curves is independent of the temperature, and lies near 50.5% H_2SO_4. This curve form results from the fact that the limiting step (1) involves the ion, whose concentration increases with the concentration of the acid, and the un-ionized iso-C_3H_7OH, whose concentration diminishes with rising acid concentration.

The temperature dependence of k_{ef} was determined from the data contained in Fig. 1. The effective energy of activation E_{ef} at C_{al} = = 0.5 diminishes from 28 to 16 kcal/mole when the H_2SO_4 concentration rises from 45 to 60%. Equation (6) shows the variation of E_{ef} with the acid concentration to be due to the fact that k_{ef} is a complex quantity which contains not only the rate constant for the limiting step but also the ionization constants for iso-C_3H_7OH and TPhC, and the quantities c_0 and h_0 [5,7]. Values of the true rate constant k_0 and the constant for protonization of iso-C_3H_7OH, K_{ROH}, can be obtained from Eq. (6). It

TABLE 2

Temperature Dependence of k_0 and K_{ROH}

	35°C	40°C	50°C	54°C	60°C
$k_0 \cdot 10^2$, liter per mole · sec	4.02	6.25	18.20	29.40	53.90
$K_{ROH} \cdot 10^3$, liter/mole	0.574	0.65	1.008	1.41	1.78
pK_B*	−3.24	−3.19	−3.00	−2.85	−2.75

* $K_B = 1/K_{ROH}$ is the basicity constant of the alcohol. $pK_B = -\lg K_B$.

is advantageous to use a graphical method for this purpose. The multiplying factor can be written as $K_{ArCOH}c_0/(1 + K_{ArCOH}c_0) = b$, and Eq. (6) then is expressed in the form

$$\frac{k_{ef}}{bC_{al}} = k_0 - K_{ROH}\frac{k_{ef}}{bC_{al}}. \qquad (7)$$

A plot showing k_{ef}/bC_{al} as a function of $(k_{ef}/bC_{al})h_0$ is a straight line whose intercept on the axis of ordinates is equal to k_0. The value of K_{ROH} is found from the slope of this line. Figure 2 gives an example of such relationship for the case in which C_{al} = 0.1 mole/liter at 40°. This relation was developed on the basis of k_{ef} values obtained by interpolation of the kinetic curves for an alcohol concentration C_{al} of 0.10 mole/liter, considering this concentration to be so low as to produce no diminution in the acidity functions H_0 and C_0 [7]. The resulting values of k_0 and K_{ROH} are presented in Table 2.

These data were used in calculating the true activation energy and the frequency factor for the reaction. Figure 3 presents the graph which was employed in the determination of the activation energy. The activation energy E_{true} was found to have a value of 21,000 ± 500 cal/mole, and to differ from E_{ef} in being independent of the acid concentration. The frequency factor A in the expression $k_0 = Ae^{-E_{true}/RT}$ is equal to $2.81 \cdot 10^{12}$ liter per mole · sec. This value is almost identical with the number of two-body collisions $Z_0 = 1.59 \cdot 10^{12}$, determined from the gas-phase equation:

$$Z_0 = \frac{N_0}{1000}(r_1 + r_2)^2\left[8\pi kT\left(\frac{1}{m_1} + \frac{1}{m_2}\right)\right]^{1/2},$$

in which $r_{1\,iso\text{-}C_3H_7OH}$ = 3.12 A, and the radius of the arylmethyl cation r_2 is set equal to r_{TPhC} = 4.43 A, these radii being calculated from mean molar volumes.

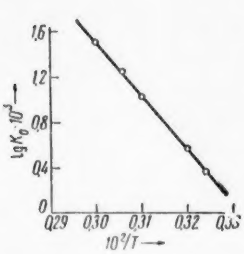

Fig. 3. The temperature dependence of the true constant for hydride transfer.

The existence of such a quantitative relation between the quantities A and Z_0 for reaction of two monatomic molecules would seem to contradict the theory of absolute reaction rates [8]. Paradoxical as it may seem, the formation of a linear activated complex in hydride transfer reactions (and in a number of other reactions in solution [9]) can be treated in terms of the arylmethyl cation and alcohol active centers alone

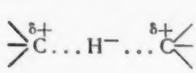

without considering the internal degrees of freedom of the polyatomic molecules, or their interaction with the solvent.

The data of Table 2 were used to evaluate the heat and entropy of protonization of isopropyl alcohol, the results being ΔH = 9800 ± 700 cal/mole, and ΔS = +16.8 ± 0.15 cal/mole · deg; from this it follows that the free-energy change in the reaction, ΔF, is 4800 cal/mole at 298°K.

It is interesting that corresponding values for methyl alcohol evaluated from the data of [10] prove to be ΔH = 4600 cal/mole, ΔS = 12.5, and ΔF = 880 cal/mole at 298°K. The entropy change (positive) of these two reactions is approximately the same, although the ΔF values would indicate that methyl alcohol is the more basic compound. It is clear that the entropy increase is to be explained by the fact that protonization converts the small H_3O^+ ion into the larger iso-C_3H_7OH ion, and at the same time decreases the regularity of packing of the solvent molecules in the solvation cloud of the ion.

The negative entropy of ionization of the arylcarbinols can result from the fact that the product arylmethyl cation has a single empty orbit. Thus, this ion can undergo not only an electrostatic solvation, but also a solvation

from coordination bonding of the solvent molecules, or the anions, which are present in solution [11]. The appearance of the arylmethyl cation results in a still higher degree of ordering of the particles in solution and thus leads to a diminution of the entropy of the system.

Calculations lead to:

$$k_0 = 2.81 \cdot 10^{12} e^{-21000/RT}, \quad K_{ROH} = 4.68 \cdot 10^{3} e^{-9800/RT}, \quad K_{ArCOH} = 1.05 \cdot 10^{-4} e^{-3280/RT}. \tag{8}$$

These results can be used in developing the following expressions for the effective rate constant:

$$k_{ef} = 2.81 \cdot 10^{12} e^{-21000/RT} \left[\frac{1.05 \cdot 10^{-4} e^{-3280/RT} c_0}{1 + 1.05 \cdot 10^{-4} e^{-3280/RT} c_0} \right] \cdot \left[\frac{1}{1 + 4.68 \cdot 10^{3} e^{-9800/RT} h_0} \right]. \tag{9}$$

A quantitative explanation of the alteration of E_{ef} with the sulfuric acid concentration can be set up on the basis of Eq. (9). In the limiting case, in which the acid concentration is low and $K_{ArCOH} c_0 \ll 1$ and $K_{ROH} h_0 \ll 1$, the expression for k_{ef} takes the form

$$k_{ef} = 2.81 \cdot 10^{12} e^{-21000/RT} \cdot 1.05 \cdot 10^{-4} e^{-3280/RT} c_0,$$

and E_{ef} = 21,000 + 3280 = 24,280 cal/mole. If, on the other hand, the acid concentration is sufficiently high and $K_{ArCOH} c_0 \gg 1$ and $K_{ROH} h_0 \gg 1$, the expression for k_{ef} takes the form

$$k_{ef} = 2.81 \cdot 10^{12} e^{-21000/RT} \cdot 2.13 \cdot 10^{-4} e^{9800/RT} \frac{1}{h_0},$$

i.e., E_{ef} = 21,000 − 9800 = 11,200 cal/mole.

LITERATURE CITED

1. R. Stewart, Canad. J. Chem. 35, 766 (1957).
2. P. D. Bartlett and I.D.M. Collum, J.Am. Chem. Soc. 78, 1441 (1956).
3. J. Roček and J. Krupička, Collection 23, 2068 (1958).
4. J. Krupička and J. Kadlec, Collection 24, 1783 (1959).
5. A. I. Gel'bshtein, G. G. Shcheglova, and M. I. Temkin, Zhur. Neorg. Khim. 1, 506 (1956).
6. N. C. Deno, J. J. Jaruzelski, and A. Schriesheim, J. Am. Chem. Soc. 77, 3044 (1955).
7. S. G. Éntelis, G. V. Épple, and N. M. Chirkov, Doklady Akad. Nauk SSSR 130, 826 (1960).
8. S. Glasstone, K. Laidler, and H. Eyring, The Theory of Absolute Reaction Rates [Russian translation] (IL, 1948).
9. E. A. Moelwin-Hughes, The Kinetics of Reactions in Solution (Oxford, 1947) p. 76.
10. H. A. Smith, J. Am. Chem. Soc. 61, 254 (1939).
11. S. G. Éntelis, K. S. Kazanskii, and N. M. Chirkov, Doklady Akad. Nauk SSSR 132, 1152 (1960).

All abbreviations of periodicals in the above bibliography are letter-by-letter transliterations of the abbreviations as given in the original Russian journal. *Some or all of this periodical literature may well be available in English translation.* A complete list of the cover-to-cover English translations appears at the back of this issue.

GEOMETRICAL AND CHEMICAL MODIFICATION OF SILICA GEL FOR GAS CHROMATOGRAPHY

V. S. Vasil'eva, I. V. Drogaleva, A. V. Kiselev,
A. Ya. Korolev, and K. D. Shcherbakova

Institute of Physical Chemistry, Academy of Sciences of the USSR
and M. V. Lomonosov Moscow State University
(Presented by Academician D. I. Shcherbakov, December 28, 1960)
Translated from Doklady Akademii Nauk SSSR,
Vol. 136, No. 4, pp. 852-855, February, 1961
Original article submitted July 25, 1960

In [1-5] we showed that by combining the geometrical modification of silica by hydrothermal treatment with the chemical modification of its surface by reaction with trimethylchlorosilane it is possible greatly to reduce adsorption energy and takeup for the vapors of various substances, particularly hydrocarbons, and to make the surface considerably more uniform. We also observed that such modification may be of value both for improved coverage of packings with media [1,2], and to extend the advantages of gas-liquid chromatography (gas-liquid) to gas adsorption chromatography (gas-solid) [2,6]. The shortcomings of the gas-adsorption method are due to excessively large and variable energies of adsorption on nonuniform solid surfaces, which generally causes long retention times and marked peak asymmetry. Liquid films applied to a solid which merely acts as packing for the column possess a uniform surface. However, they decompose at high temperatures, and over an operating period of long duration they are entrained by the stream of carrier gas. Thus, the gas-liquid type of chromatographic separation cannot provide a high degree of stability at high temperatures (i.e., when dealing with fairly large molecules). In addition, diffusion into the liquid film retards mass transfer. The liquid film also does not prevent possible reactions with the carrier. In the present study, therefore, an attempt was made at the geometrical and chemical modification of an adsorbent suitable for gas chromatography – wide-pore silica gel – with the aim of forming on its surface a sufficiently stable and uniform film chemically linked with it, specifically, a film of a heteroorganic silicon compound.

Silica gel, type ShSK, was chosen as the starting material. Industrial grade silica gel was washed free of impurities consisting of ions of iron and other metals with dilute hydrochloric acid (1:1) (until no reaction was obtained with ammonium thiocyanate), and then with distilled water to remove chlorine ions (until no reaction was obtained with silver nitrate). Sample SI (initial silica gel), with an extremely nonuniform surface, was obtained in this manner. A portion of this silica gel was subjected to further treatment with the purpose of obtaining geometrical and chemical modification.

Geometrical modification of the silica gel was carried out by treatment with water in an autoclave at 275° for 19.5 hours. Sample SG was obtained in this manner. The third sample was prepared by chemical modification of the surface of sample SG by treating it with liquid trimethylchlorosilane (sample SGM). The sample was analyzed for carbon content. At 1.22% carbon content, when related to the surface of the hydrated silica gel, on the average about 2.7 trimethylsilyl groups occur on every 100 $Å^2$ of the surface of the sample, which corresponds to a heteroorganic silicon film of nearly maximum density. The geometrical and chemical properties of the samples are presented in the table.

Prior to the adsorption experiments, the samples were heated for a long period in an adsorption vacuum apparatus on the pans of a quartz balance at 150° down to a pressure of $1 \cdot 10^{-5}$ mm mercury [7].

Properties of Silica Gel Samples Used

Sample	Method of modification	Pore volume v_s, cm^3/g	Specific surface S, m^2/g	Mean diameter silica globules D, A	Mean diameter pore orifices d, A	Carbon content, %
SI	Untreated	0.89	310	100	90	–
SG	Treated in autoclave with water vapor at 275° for 19.5 hours	0.78	80	400	340	–
SGM	SG treated with liquid trimethylchlorosilane at 20-57°, then subjected to vacuum	0.60	(80)	(400)	(380)	1.21 1.23
					Mean	1.22

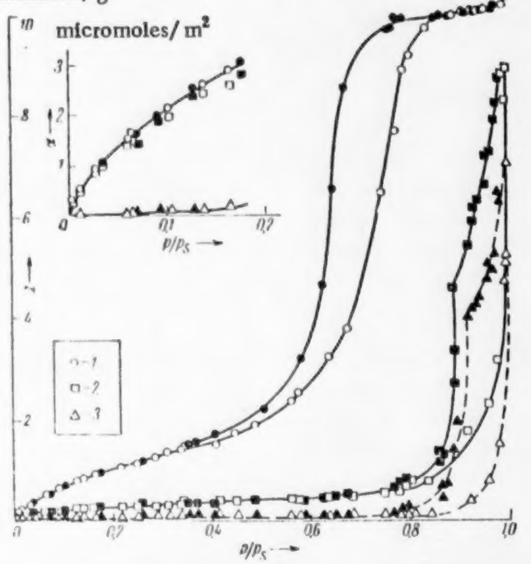

Fig. 1. Adsorption isotherms for benzene vapor on silica gel samples: 1) original silica gel SI; 2) SG hydrated in autoclave; 3) SGM modified after hydration. Black points: desorption.

Isotherms were obtained for the adsorption and desorption of benzene vapor in a range of relative pressures p/p_s from 0 to 1. From Fig. 1 it can be seen that, in consequence of the hydrothermal treatment of the original silica gel, the isotherm has been markedly displaced downward and to the right. The point at which hysteresis due to capillary condensation begins has shifted from p/p_s = = 0.2 for sample SI, and to $p/p_s = 0.75$ for sample SG. This all points to a marked change in geometrical structure.

The marked reduction in surface area resulted from a considerable increase in the size of the globules forming the silica gel skeleton [8]. The mean diameter of the silica gel globules after hydrothermal treatment increased by almost 4 times (see table). The number of small pores decreased.

Thus, as a result of hydrothermal treatment of the silica gel, the particles forming its skeleton were enlarged and made smoother, while the surface was completely hydrated. This made it possible to obtain a silica gel having its surface fairly densely covered with a layer of trimethylsilyl groups (by further treatment of sample SG with trimethylchlorosilane). This chemical modification of the silica gel surface, as in the case of aerosil [2,5], led to a marked drop in the benzene takeup up to the onset of capillary condensation. In the upper left part of Fig. 1 the initial portions of the benzene adsorption isotherms related to unit surface area are given for all three silica gel samples. The adsorption of benzene per unit surface area for sample SGM was considerably reduced in comparison with the two samples with a hydrated surface. Thus, at $p/p_s = 0.1$, the absolute adsorption α of benzene on samples SI and SG was approximately equal to 2 micromoles/m^2, while on sample SGM α was approximately equal to 0.1 micromole/m^2, i.e., chemical modification caused a reduction in benzene adsorption by 20 times. Benzene adsorption on the chemically modified sample remained extremely insignificant right up to $p/p_s \approx 0.8$. Capillary condensation, however, which begins in the neighborhood of the points of contact of the globules in the silica gel skeleton at high p/p_s plays the main part at high values of p/p_s, similar to the weak adsorption and appreciable capillary condensation of water in the pores of active carbon containing no surface oxides [9].

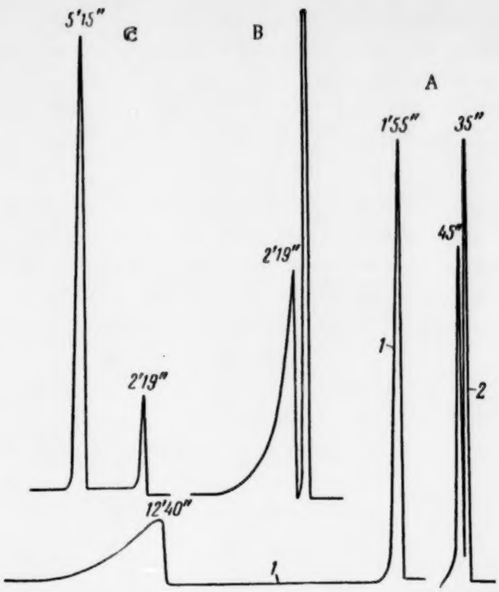

Fig. 2. Chromatograms of a mixture of benzene and n-hexane vapors: A) at 82° on silica gels: 1) SG; 2) SGM; B) at 35° on SGM; C) at 74° on Celite impregnated with E-301 silicone.

From these data, it was permissible to suppose that silica gel modified in this or a similar manner might be used for the chromatographic separation of, for example, hydrocarbon mixtures by the gas-adsorption method, even if the composition of the mixture included components which are strongly adsorbed on the original silica gel. Measurements of the heats of adsorption of n-hexane and benzene [5] on the surface of aerosil which had been drastically modified by trimethylchlorosilane showed that these substances are adsorbed extremely weakly, and at the same time the shapes of the adsorption isotherms at small values of p/p_s approximate to the linear.

Some exploratory experiments were carried out to assess the possibility of using silica gel sample SGM* in gas chromatography. The experiments were carried out on a Griffin and George chromatograph with a 4-mm diameter column 1 m long. Two silica gel samples, processed by the same method as samples SG and SGM (0.25-0.5 mm fraction) were used as packing for the column.

In the case of the hydrated silica gel of type SG, benzene did not come out of the column within even half an hour at a normal temperature. Benzene and hexane peaks were obtained at 82°, but the benzene retention time was still long: 12 min 40 sec (it totalled 1 min 50 sec for hexane). At the same time, the benzene peak was appreciably spread out (Fig. 2, A1). The modified type SGM silica gel was tried out in the same conditions. The retention times of both hexane and benzene were considerably shortened. In addition, the benzene peak was unlike the peak for sample SG: The "tail" of the peak almost disappeared (Fig. 2, A2).

The same experiment was carried out at lower temperatures. At 35°, benzene did not give a definite peak at all on hydrated type SG silica gel, while the retention time for benzene with the modified silica gel was equal to only 2 min 20 sec. In accordance with this, a mixture of hexane and benzene was separated satisfactorily at 35° with the modified silica gel. The chromatogram obtained is presented in Fig. 2B.

The gas-adsorption chromatograms obtained were compared with the chromatogram of a benzene—hexane mixture produced by the gas-liquid method, where Celite impregnated with silicone E-301 was used as column packing. Thus, the nature of the liquid layer in the latter case was somewhat similar to that of the chemically modified film on the silica gel surface. The chromatogram of a benzene-hexane mixture, obtained in this case at 74° (the other conditions being the same as in the case of silica gel), is presented in Fig. 2C. No separation occurred at 35°.

As may be seen from a comparison of Figs. 2B and 2C, a benzene—hexane mixture can be separated by means of the gas-adsorption method more quickly in the case of the modified silica gel than by means of the more usually employed gas-liquid method and, at the same time, at a lower temperature: The retention times of benzene and hexane at 35° on the modified silica gel are almost half as long as their retention times at 74° on Celite impregnated with silicone. The shape of the benzene peak in the case of gas-adsorption separation with type SGM silica gel is still less symmetrical than with the use of the gas-liquid method. This may clearly be explained by insufficient uniformity of the pores and surface of the modified layer. An even more radical geometrical and chemical modification of the silica gel skeleton and surface** should therefore be aimed at. Although

*Jointly with R. S. Petrova, with the collaboration of N.Ya. Smirnov, V. I. Kalmanovskii, N. Balakhnina, and Ya. I. Yashin. The authors express their indebtedness to them.

**At $p/p_s = 0.1$, as a result of the modification of aerosil [5], benzene-vapor adsorption was reduced by 35 times, while, in going from SG to SGM, it was reduced by only 20 times.

this aim was not accomplished in the present work, the experiments which have been carried out on the separation of benzene and hexane with a modified silica gel give good reason to suppose that chemical modification of silica gel, and also other adsorbents, or the walls of capillary columns, accompanied by the formation of thermally stable films of compounds which remain attached to the surface, may replace impregnation with liquids in chromatography, thus eliminating difficulties associated with the liquids and the shortcomings of the gas-liquid type of chromatography, while retaining its advantages.

Thus, combining geometrical modification of the adsorbent skeleton with chemical modification of its surface, particularly by reaction with trimethylchlorosilane, leads to the production of a silica gel with very large pores, the surface of which is fairly uniform. Modified adsorbents, particularly those which have chemically attached functional groups on top of the heteroorganic silicon layer, may probably be of value for the purposes of gas chromatography, enabling the advantages of the gas-adsorption and gas-liquid types of chromatography to be combined.

LITERATURE CITED

1. A. V. Kiselev, N. V. Kovaleva, A. Ya. Korolev, and K. D. Shcherbakova, Doklady Akad. Nauk SSSR 124, 617 (1959).
2. I. Yu. Babkin, V. S. Vasil'eva, I. V. Drogaleva, A. V. Kiselev, A. Ya. Korolev, and K. D. Shcherbakova, Doklady Akad. Nauk SSSR 129, 131 (1959).
3. I. Yu. Babkin and A. V. Kiselev, Doklady Akad. Nauk SSSR 129, 357 (1959).
4. A. V. Kiselev, A. Ya. Korolev, R. S. Petrova, and K. D. Shcherbakova, Koll. Zhur. 22, No. 6 (1960).
5. I. Yu. Babkin, A. V. Kiselev, and A. Ya. Korolev, Doklady Akad. Nauk SSSR 136, No. 2 (1961).
6. A. V. Kiselev and K. D. Shcherbakova, Material zum 2 Symp. über Gas-Chromatogr. in Böhlen, October 1959 (Berlin, 1959).
7. A. V. Kiselev and T. A. Pogosyan, Koll. Zhur. 22, No. 3 (1960).
8. A. V. Kiselev, E. A. Leont'ev, et al., Zhur. Fiz. Khim. 30, 2149 (1956).
9. A. V. Kiselev and N. V. Kovaleva, Zhur. Fiz. Khim. 30, 2775 (1956).

All abbreviations of periodicals in the above bibliography are letter-by-letter transliterations of the abbreviations as given in the original Russian journal. *Some or all of this periodical literature may well be available in English translation.* A complete list of the cover-to-cover English translations appears at the back of this issue.

MASS SPECTRA AND PRIMARY PROCESSES IN THE RADIATION CHEMISTRY OF PARAFFINS

M. V. Gur'ev

L. Ya. Karpov Institute of Physical Chemistry
(Presented by Academician S. S. Medvedev, August 23, 1960)
Translated from Doklady Akademii Nauk SSSR,
Vol. 136, No. 4, pp. 856-859, February, 1961
Original article submitted August 22, 1960

Until recent years the statistical theory, in which it is postulated that dissociation of a molecular ion occurs in the majority of cases after a long period (up to about 10^{-6} sec) following ionization and excitation, has remained the sole attempt at a quantitative explanation of the mass spectra of complex molecules. According to this theory, complete redistribution and further migration of excitation energy over the whole molecule occurs during the interval of time stated, and dissociation is caused by a chance concentration of energy at one of the bonds [1,2].

It has been shown previously that any theory (including the one mentioned) which postulates that the excitation energy transmitted by an electron is distributed over the whole molecule cannot be applied, at least to large molecules, and another hypothesis for the dissociation of large molecules on collision with an electron was advanced, which made it possible to explain qualitatively many of the laws to which mass spectra conform [3,4]. In the present study, we will show that, by making the most elementary assumptions, the proposed theory makes it possible to calculate quantitatively the mass spectra of practically all the n-paraffins, without having to use any arbitrary quantities. It will be noted that an arbitrary excitation energy distribution function, which is adjusted for each substance until the calculated mass spectrum matches the experimental one, is introduced into the calculation of mass spectra by the statistical theory. Quite apart from the initial premises and the many simplifying assumptions, this fact deprives the theory of any practical value.

The basic postulate of the "local" theory of mass spectra is that dissociation occurs on electron impact in the collision zone without any significant redistribution of energy over the whole molecule, i.e., ion fragments are formed due to the breaking away from the molecule of the collision region,together with the electron.

Depending on the nature of the collision, both the size of the region and the probability of its breaking away (for the same electron energy) will vary. In this way, the fact of the existence of mass spectra, i.e., differences in the probability of formation of different fragments, is itself interpreted. From this point of view, the mass spectrum of an infinitely large n-paraffin molecule, which is in fact taken as a basis of calculation, is the most simple. Group mass spectra only are considered, i.e., the total probability of the formation of ions with a given number of carbon atoms, irrespective of the number of hydrogen atoms. The mass spectrum of an infinitely large molecule may be considered known by experiment, as it is sufficient in practice to take the mass spectrum of an n-paraffin 2-3 times heavier than the one whose mass spectrum it is required to calculate.

In the calculation, the following assumptions are employed:

1. The formation of an ion fragment results from the breaking away of the charged portion of the molecule in the region of the electron impact.

2. Ruptures of C—C bonds occur at equal distances from the "point" of impact.

TABLE 1

No. of C atoms in ion	Calculated probability, %	Observed probability, %
Ethane		
1	2,2	3
2	100	100
Propane		
1	4,5	4,5
2	75	100
3	100	50
n-Butane		
1	3,2	4,2
2	64	75
3	100	100
4	50	13
n-Pentane		
1	2,6	2,5
2	53	31
3	100	100
4	63	9
5	29	4,5
n-Hexane		
1	2,7	4,0
2	46	40
3	100	100
4	71	70
5	32	3,1
6	21	7

No. of C atoms in ion	Calculated probability, %	Observed probability, %
n-Heptane		
1	2,1	2,7
2	42	48
3	100	100
4	77	45
5	38	32
6	17	1,1
7	16	7
n-Octane		
1	1,9	2
2	38	42
3	100	100
4	80	39
5	42	22
6	21	22
7	7	0,1
8	13	4,2
n-Nonane		
1	1,8	2
2	36	42
3	100	100
4	84	59
5	45	20
6	25	18
7	8,8	4,6
8	4,6	0,13
9	11	3,9

x	$f(x)$
1	0,9
2	17
3	95
4	100
5	64
6	47
7	18
8	10.5
9	6.8
10	5.3
11	4.1
12	3.5
13	3.1
14	2.7
15	2.4
16	2.0
17	1.8

3. The probability of formation of a fragment is determined by its size (number of carbon atoms), but at every point of impact the full range of probabilities available in the mass spectrum of an infinitely large molecule is open, irrespective of whether for the given size of the finite molecule and point of impact the corresponding fragment can actually be formed or not. This means that, if the rupture of one of the bonds would have to occur outside the limits of the molecule, only one bond ruptures, and a fragment smaller than the one which should have been formed is, generally speaking, formed. If the rupture of both bonds should have occurred outside the limits of the molecule, then a molecular ion, as a special case of ion fragment, is formed.

4. The number of carbon atoms $\underline{n}$ in the molecule is sufficiently large for the molecule to be considered continuous. The dependence of the probability of formation of a fragment for a finite molecule $\varphi_n(x)$, and also for an infinitely large molecule $f(x)$, we consider to be a continuous function of the fragment length $\underline{x}$.

5. We assume that molecules of different sizes differ only in total length and that their ends do not differ from the middle portions.

All these assumptions, of course, very much simplify the real picture. Assumption 1, which we have previously substantiated [3,4], is the basic postulate of the "local" theory of mass spectra and is the most important of all. Assumptions 2 and 3 are only substantiated by the agreement of the results of calculation with experimental data.

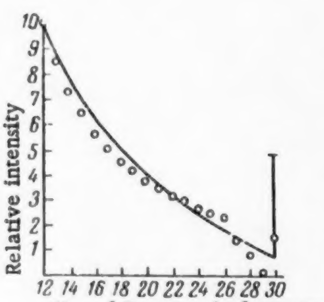

Fig. 1.

Other assumptions were also considered, particularly concerning asymmetrical (with respect to the point of impact) formation of fragments, but they all showed a quantitative divergence from experiment. The assumptions of continuity and the absence of dissimilarities at the ends of the molecule are simplifications and are not essential.

To carry out the calculation electron impacts having an equal probability at any point in the molecule are considered, and the probabilities of the formation of each fragment are averaged over the whole molecule. The probability $\varphi(x, l)$ of formation at one impact of a fragment of a given length is a function of the fragment length $\underline{x}$ and the distance of the point of impact from the end of the molecule l. It is sufficient to consider one half of the molecule (when $0 \leq l \leq n/2$).

It follows from the assumptions that $\varphi(x, l) = f(x)$ when $x < 2l$ or $l > x/2$, i.e., when both bonds can actually rupture. If, however, $l < x/2$, an ion is formed from the end of the molecule, only one bond ruptures, and a fragment $x = l + y/2$ is formed with a probability $f(y)$, whence $y = 2x - 2l$. Hence,

$$\begin{aligned} \varphi(x, l) &= f(x), & l &> \frac{x}{2}; \\ \varphi(x, l) &= f(2x - 2l), & l &< \frac{x}{2}. \end{aligned} \tag{1}$$

The mass spectrum is the mean probability taken over the whole molecule

$$\varphi_n(x) = \frac{2}{n}\int_0^{n/2} \varphi(x, l)\, dl.$$

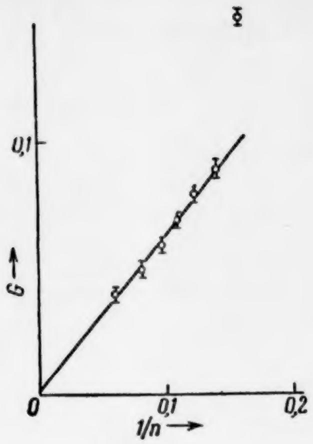

Fig. 2.

Substituting the values of $\varphi(x,l)$ from (1), we have, on rearrangement,

$$\varphi_n(x) = \left(1 - \frac{x}{n}\right) f(x) + \frac{1}{n}\int_{x}^{2x} f(t)\,dt. \qquad (2)$$

For molecular ions by a similar procedure, we obtain

$$\varphi_n(n) = \frac{1}{2n}\int_{n}^{2n}\int_{t}^{\infty} f(z)\,dz\,dt. \qquad (3)$$

The results of calculations by Eqs. (2) and (3) and experimental data are presented in Table 1; part of the mass spectrum of n-$C_{30}H_{62}$ [5][with slight corrections for the ends of the molecule in accordance with Eq. (2)], which was employed as the mass spectrum of an infinitely large molecule, is also given. The maximum probability is taken, as usual, as 100%. For lightfragments ($x < n/2$), the divergence is within the limits of experimental error. The systematic divergence in the case of ions approaching the molecular ion is greater, although the form of the mass spectrum in this region was indicated correctly, particularly in the case of the heavier molecules.*

For heavy molecules ($x > 13$), the mass spectrum is calculated on the basis of Eq. (3) and the experimentally observed exponential relationship between the probability of the formation of molecular ions and the number of carbon atoms in n-paraffins [6]. The solution of the simple function obtained is substituted in Eq. (2). The result for the calculation for n-$C_{30}H_{62}$ is given in the form of a curve in Fig. 1. Experimental data are indicated by points. It can be seen from Fig. 1 that the main relationships of the mass spectrum are fairly well explained by the theory. Divergences in the region of the molecular ion are evidently due to the special nature of the process occurring at the ends of the molecule.

TABLE 2

No. of C atoms in product	Calc.,%	Observed [7], %
1	15	9
2	23	40
3	32	25
4	22	22
5	8	4

This method was also applied to the calculation of the yield of neutral fragments on electron impact. In this case, it is assumed that the portions of the molecule remaining after separation of the ion fragment are uncharged. An identical treatment to that given above leads to the expression for the distribution of neutral fragments r(x):

$$r(x) = \frac{1}{n}\int_{0}^{2n-2x} f(t)\,dt. \qquad (4)$$

The distribution of the primary dissociation products from gas-phase radiolysis may be calculated from Eqs. (1) and (2). Of course, in the actual conditions of radiolysis, this distribution may be altered out of all recognition due to secondary processes and a different molecular state in the condensed phase. However, the yields of products resulting from the rupture of C−C bonds in the radiolysis of n-hexane are extremely similar, both in the liquid and gas phases [7]. This may mean that in the very simple case of paraffins the role of distorting factors is not very important, and therefore a direct comparison of the calculated distributions of primary products with the final products is not devoid of meaning. The results of calculation and the experimental data for n-hexane are given in Table 2 (the total yield is taken as 100%).

For the yield of methane from the radiolysis of various fairly heavy n-paraffins ($x = 1$, $n > 5$) from Eqs. (2) and (4), is obtained $G = a/n + b$, where G is the yield (molecules/100 ev); a and b are constants ($b \ll a$). It can be seen from Fig. 2 that the experimental data [8] are, in fact, well fitted by a hyperbola.

* The mass spectra of labelled heavy n-paraffins, kindly communicated to us by J. H. Beynon (through J. Phys. Chem.), can be calculated more accurately by the method under discussion than by that used previously [3,4].

It is possible to estimate the relative yield of olefins from radiolysis by the theory. For hexane this works out to be about 1.5 times less than the yield of paraffins having the same number of carbon atoms, which agrees with experiment [8,9].

It should be noted that the rupture of C−C bonds in the radiolysis of paraffins is, practically speaking, not liable to "shielding" [7,9]. This is in good agreement with the fact that, according to the "local" theory, dissociation takes place within a period of the order of 10^{-13} sec [3]. The effect of benzene on the yields of heavy products and hydrogen may indicate a different mechanism for the corresponding primary processes, differing from the mechanism of mass spectra. It should be emphasized that the fact that a correlation exists between mass spectra and radiolysis products (see, for example, [7,9]) can in the general case only be explained by the "local theory."

The author expresses his gratitude to Professor N. N. Tunitskii for his help in this work and in assessing the results.

LITERATURE CITED

1. H. M. Rosenstock, A. L. Wahrhaftig et al., Proc. Nat. Acad. Sci. 38, 667 (1952).
2. A. Kropf, E. M. Eyring et al., J. Chem. Phys. 32, 149 (1960).
3. M. V. Gur'ev, Thesis [in Russian] (L. Ya. Karpov Inst. of Phys. Chem., Moscow, 1959).
4. M. V. Gur'ev, M. V. Tikhomirov, and N. N. Tunitskii, Doklady Akad. Nauk SSSR 123, 120 (1958).
5. Catalog of Mass-Spectral Data, American Petroleum Institute, Research Project, 44.
6. M. V. Gur'ev, Zhur. Fiz. Khim. 34, 475 (1960).
7. J. Futrell, J. Am. Chem. Soc. 81, 5922 (1959).
8. H. A. Dewhurst, J. Phys. Chem. 61, 1466 (1957).
9. H. A. Dewhurst, J. Am. Chem. Soc. 80, 5607 (1958).

All abbreviations of periodicals in the above bibliography are letter-by-letter transliterations of the abbreviations as given in the original Russian journal. *Some or all of this periodical literature may well be available in English translation.* A complete list of the cover-to-cover English translations appears at the back of this issue.

THE CATALYTIC PROPERTIES OF COBALT-MANGANESE SPINELS

V. P. Linde, L. Ya. Margolis, and Corr. Member AN SSSR S. Z. Roginskii

Institute of Physical Chemistry, Academy of Sciences of the USSR
Translated from Doklady Akademii Nauk SSSR,
Vol. 136, No. 4, pp. 860-863, February, 1961
Original article submitted October 19, 1960

Compounds with a spinel structure are fairly widely used in industrial catalytic operations as catalysts for oxidation, hydrogenation, and the conversion of carbon monoxide [1]. The structure and the electrical and magnetic properties of the complex spinels employed under the name "ferrites" in technology have been thoroughly investigated. At the same time, a limited number of studies devoted to the elucidation of the specificity of the catalytic action of spinels and the establishment of a connection between the catalytic activity of these compounds and the physical characteristics of the solid has been published in the literature [2-5].

In the present work, the effect of structure on the catalytic properties of the normal ($CoMn_2O_4$) and the reversed ($MnCo_2O_4$) cobalt–manganese spinels has been studied. Catalytic activity was assessed with respect to the complete oxidation of propylene.

The preparation of the normal and reversed spinels has been described previously [6]. Catalytic activity was determined by the rate of oxidation of propylene with oxygen present in the stoichiometric ratio $C_3H_6:O_2 = 2:9$. The reaction products were carbon dioxide and water. The values for the specific surface of the catalysts, determined by the Brunauer–Emmett–Teller method from the equilibrium isotherms for low-temperature sorption of krypton, were equal to 0.70 m^2/g ($CoMn_2O_4$) and 0.25 m^2/g ($MnCo_2O_4$). The reaction was carried out in static conditions with a constant initial pressure of the mixture (0.450 mm mercury) in the temperature range 200 to 350°C. The catalyst samples were pretreated in a vacuum of 10^{-6} mm mercury at 550° for 4 hours. Water formed was continuously frozen out in the course of the reaction. Repetition of the experiments for one weight of catalyst indicated good reproducibility of the results.

If the oxidation of propylene is carried out with continuous absorption of the CO_2 formed during the reaction and freezing out of the water, the kinetics of the reaction conform to a monomolecular law: Using the coordinates $\lg P - \tau$ strict linearity is observed, whereas a square law does not fit (Fig. 1). The specific velocity constant K^{I}_{sp}, calculated from the equation for a first-order reaction, remains constant (Fig. 2).

In Figs. 3 and 4 kinetic curves are presented for the oxidation of a mixture ($2C_3H_6 + 9O_2$) at various temperatures, where the reaction is carried out without the removal of carbon dioxide from the reaction space. The over-all velocity constant for the oxidation process in these conditions was described approximately by the equation for a second-order reaction from which were calculated values of the velocity constant referred to unit area (1 m^2) of catalyst (K^{II}_{sp}). Experiments on the oxidation of the mixture at various initial pressures indicated that K^{II}_{sp}, calculated from the equation for a second-order reaction, is dependent on the initial pressure (Fig. 2). One of the writers showed previously [7] that an increase in observed reaction order in comparison with the true one may be caused by self-retardation of the process by the blocking of active sites on the catalyst by reaction products. In the present case, molecules of CO_2, which probably form complexes of the CO_3^- type [14] on the catalyst surface, may exhibit an effect of this kind.

The specific nature of the reaction conditions (possibility of reduction of the catalyst surface by propylene at high concentrations of the latter in the mixture, reduced accuracy of measurement at high oxygen concentration),

TABLE 1

$P^0_{C_3H_6} : P^0_{O_2}$	$P^0_{O_2}$ = const = 0,320		$P^0_{C_3H_6}$ = const = 0,048	
	$P^0_{C_3H_6}$	K^1_{sp}	$P^0_{O_2}$	K^1_{sp}
1 : 9	0.036	0.105	0.433	0.105
1 : 4.5	0.072	0.105	0.217	0.090
1 : 2	0.160	0.105	0.096	0.030

Note: Pressures are given in mm Hg.

TABLE 2

Temp. of reaction or oxygen chemisorption, °C	$CoMn_2O_4$		$MnCo_2O_4$		$\frac{K^1_{sp}\text{ nor.}}{K^1_{sp}\text{ rev.}}$	$\frac{\theta_{O_2}\text{ nor.}}{\theta_{O_2}\text{ rev.}}$	Activation energy of reaction, kcal / mole	
	K^1_{sp}	θ_{O_2}, $\frac{cm^3}{m^2}$	K^1_{sp}	θ_{O_2}, $\frac{cm^3}{m^2}$			$CoMn_2O_4$	$MnCo_2O_4$
200	0.019	0.026	0.0124	0.017*	1.52	1.53		
250	0.150	0.052	0.075	0.026	2.00	2.00	19.4	17.0
300	0.690	0.083	0.300	0.039	2.30	2.13		
350	2.74	0.138	0.975	0.054	2.70	2.56		

*Extrapolated value.

did not permit wide variation of the composition of the initial mixture. In Table 1, results are given for experiments on the oxidation of propylene on $MnCo_2O_4$ at 250°.

It may be seen from Table 1 that changing the concentration of propylene by 4.5 times does not affect the velocity constant, while increasing the oxygen content from 0.096 to 0.433 mm Hg leads to an increase in the velocity constant, i.e., the reaction rate is independent of propylene concentration and is determined by oxygen concentration according to the equation

$$W = K^1_{sp}\,[P_{O_2}]^1\,[P_{C_3H_6}]^0.$$

It has been shown earlier [6] that oxygen is irreversibly chemisorbed on both spinels, and that the kinetics of this chemisorption conform to the laws:

$$\theta = A\tau^{1/n} \quad \text{for} \quad MnCo_2O_4; \quad \theta = a + b \lg \tau \quad \text{for} \quad CoMn_2O_4,$$

where θ is surface coverage and τ is time. From additional measurements of the chemisorption of oxygen on both spinels in the temperature range 200-350°, the activation energies for chemisorption were found to be 18 kcal per mole for $CoMn_2O_4$ and 14 kcal/mole for $MnCo_2O_4$ (at a surface coverage θ = 0.03 cm^3/m^2).

Propylene is sorbed on these catalysts, as on a large number of other oxides, reversibly, in quasi-equilibrium,* with small values of surface coverage and activation energy. Previous sorption of oxygen on the spinels (at temperatures below 200°) does not affect the rate of propylene sorption and the final surface coverage. Separate experiments indicated the absence of CO_2 chemisorption by either the normal or the reversed spinel in the temperature range 100-350°. It has been shown by the work of other authors [2,8] that the oxidation of hydrocarbons over spinel catalysts may continue in the bulk of the gas phase. In order to elucidate the question of the possibility of a heterogeneous-homogeneous mechanism for the oxidation of propylene over $CoMn_2O_4$ and $MnCo_2O_4$, we used the Koval'skii– Bogoyavlenskaya method of separate calorimetry [9]. The diameter of the reaction vessel was 50 mm; a nichrome-constantan differential thermocouple made from 0.05-mm diameter wires was employed to measure the temperature difference. The sensitivity of measurement of the temperature difference Δt was 0.05°.

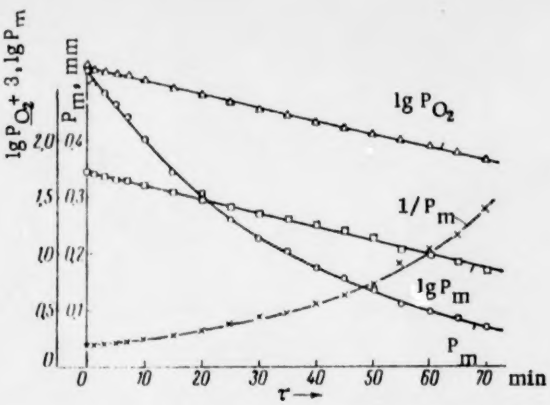

Fig. 1. Kinetic isotherm for the oxidation of a mixture $2C_3H_6 + 9O_2$ on $MnCo_2O_4$ at t = 250°, with continuous absorption of CO_2 during the course of the reaction. $P^0_{mixture}$ = 0.522 mm.

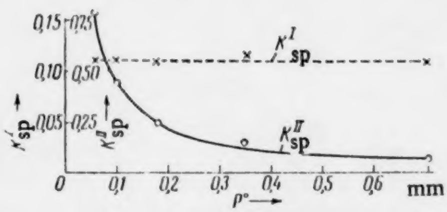

Fig. 2. Relationship between the velocity constants K^I_{sp} and K^{II}_{sp} for the oxidation of the mixture $2C_3H_6 + 9O_2$ and initial mixture pressure.

The following reactions were employed for the calibration of the apparatus: purely heterogeneous oxidation with oxygen of a fine copper powder treated with propylene at 450° for 4 hours; oxidation of propylene over platinized asbestos, being a reaction with a homogeneous component [10]; and the homogeneous oxidation of acetaldehyde at 200° [11]. It was established that the oxidation of a stoichiometric mixture of propylene and oxygen at 300° and initial pressures of 0.5 and 40.0 mm Hg takes place over both spinels by a purely heterogeneous mechanism. Oxidation of propylene takes place only on the catalyst surface, and the absence of a detectable amount of products of incomplete oxidation is evidently due to the presence of fixed chains on the surface of the catalyst [12].

In Table 2 are given values of the specific velocity constants (K^I_{sp}) for the oxidation of a mixture of $2C_3H_6 + 9O_2$, and the specific surface coverage with respect to oxygen taken from the oxygen chemisorption isotherms for a single time (30 min) at temperatures corresponding to the reaction temperatures.

It may be seen from the data of Table 2 that there exists a linear relationship between the velocity constant for the oxidation of propylene over the spinels and the rate of oxygen chemisorption.

It was pointed out above that the chemisorption of oxygen on the normal and reversed spinels was described by different kinetic laws which are characteristic of a nonuniform surface having a different type of distribution of active sites with respect to the activation energies (exponential for $MnCo_2O_4$ and linear for $CoMn_2O_4$). At the same time, the different nonuniformity statistics for the surfaces of the normal and reversed spinels do not make themselves evident in the kinetics of propylene oxidation over these catalysts.

The oxidation reaction probably occurs, in both cases, at a limited number of active sites, which may be regarded as uniform. The existence of an identical kinetic law, the similarity of the activation energies for the oxidation reaction, and the proportionality between the reaction velocity constants and oxygen chemisorption rate may be cited as confirmation of this.

The kinetic law is the same for both the normal and the reversed spinel, but their catalytic activity is different. Consequently, lattice structure has no effect on the nature of the rate-controlling stage or on the activation energy, but it changes the factor by which the exponential term is multiplied, and which is probably linked with the number of active sites.

From an examination of the structural formulas of the normal – $Co^{2+}[Mn^{3+}Mn^{3+}]O_4^{2-}$ – and reversed – $Co^{3+}[Mn^{2+}Co^{3+}]O_4^{2-}$ – spinels, it may be seen that manganese cations present at the surface can, to a greater extent than cobalt cations, become electron donors for chemisorbed oxygen atoms. Because of the considerable degree of dispersion of the catalyst powders, proportionality between the quantity of manganese cations in the bulk and at the surface of the particles may probably be assumed without introducing much error.

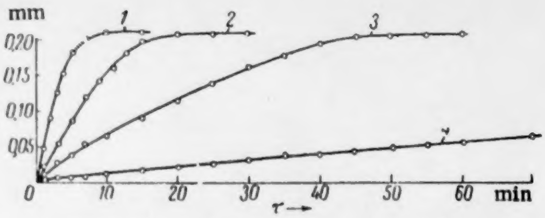

Fig. 3. Kinetic isotherms for the oxidation of a mixture $2C_3H_6$ + + $9O_2$ over $CoMn_2O_4$: 1) t = 350°, S = 0.14 m^2; 2) t = 300°, S = = 0.25 m^2; 3) t = 250°, S = 0.50 m^2; 4) t = 200°, S = 0.50 m^2.

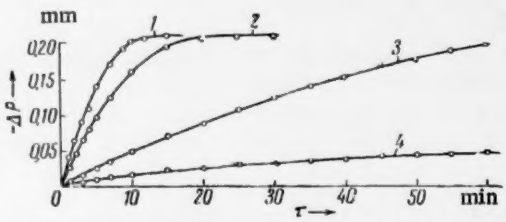

Fig. 4. Kinetic isotherms for the oxidation of the mixture $2C_3H_6$ + + $9O_2$ over $MnCo_2O_4$. S = 0.5 m^2. 1) t = 350°; 2) t = 300°; 3) t = = 250°; 4) t = 200°.

The higher chemisorption capacity and catalytic activity of the normal spinel is possibly due to a higher concentration in it of manganese cations, which have the principal effect on the formation of active sites at the surface.

As the rate of oxidation of propylene is proportional to the rate of chemisorption of oxygen, one might hope to alter the catalytic properties of the normal and reversed spinel by introducing modifying additives which control oxygen chemisorption into the spinel lattice.

LITERATURE CITED

1. B. N. Dolgov, Catalysis in Organic Chemistry [in Russian] (1959) pp.177, 342, 711.
2. L. Ya. Margolis, Thesis [in Russian] (Inst. of Phys. Chem., AN SSSR, 1947).
3. Z. G. Szabo and F. Salimosi, Z. Elektrochem. B63, No. 9/10, 1177 (1959).
4. G. M. Schwab and E. Roth, Structure and Properties of Solid Surfaces (1953) p. 465.
5. W. Wolski, Roczn. Chem. 34, 305, 309 (1960).
6. V. P. Linde, Doklady Akad. Nauk SSSR 127, No. 6, 1249 (1959).
7. S. Z. Roginskii, Zhur. Fiz. Khim. 13, No. 12, 1787 (1939).
8. P. Yu. Butyagin and S. Yu. Elovich, Doklady Akad. Nauk SSSR 54, 607 (1946).
9. M. L. Bogoyavlenskaya and A. A. Koval'skii, Zhur. Fiz. Khim. 20, 1325 (1946).
10. P. Yu. Butyagin, Thesis [in Russian] (Inst. of Phys. Chem., AN SSSR, 1949).
11. N. M. Émanuél, Kinetics of Chain Oxidation Reactions [in Russian] (AN SSSR Press, 1950) p. 185.
12. S. Z. Roginskii, Problems in Kinetics and Catalysis [in Russian] (1960) Vol. 10, p. 373.
13. É. Kh. Enikeev, L. Ya. Margolis, and S. Z. Roginskii, Doklady Akad. Nauk SSSR 124, No. 3, 606 (1959).
14. W. E. Garner, T. J. Gray, and F. S. Stone, Proc. Roy. Soc. A197, 249 (1949).

All abbreviations of periodicals in the above bibliography are letter-by-letter transliterations of the abbreviations as given in the original Russian journal. *Some or all of this periodical literature may well be available in English translation.* A complete list of the cover-to-cover English translations appears at the back of this issue.

THE BEHAVIOR OF WATER OF CRYSTALLIZATION IN THE SEIGNETTE DIELECTRIC $K_4Fe(CN)_6 \cdot 3H_2O$

A. G. Lundin, G. M. Mikhailov, and S. P. Gabuda

Physics Institute, Siberian Division, Academy of Sciences of the USSR
and the Siberian Technological Institute, Krasnoyarsk
(Presented by Academician V. N. Kondrat'ev, July 21, 1960)
Translated from Doklady Akademii Nauk SSSR,
Vol. 136, No. 4, pp. 864-867, February, 1961
Original article submitted July 18, 1960

The Seignettoelectric* properties of potassium ferrocyanide (PFC) below −22° were discovered by Waku et al. [1]. Monoclinic crystals of PFC contain four molecules of $K_4Fe(CN)_6 \cdot 3H_2O$ per unit cell having dimensions a = = 9.32 A, b = 16.84 A, c = 9.32 A [2]. In the study of PFC by the proton magnetic resonance method, a significant change in the second moment of the proton absorption line was noted in passing through the Curie point.

The second moment of the absorption line

$$S = \int_{-\infty}^{+\infty} f(H)(H - H_0)^2 \, dH \qquad (1)$$

[where $f(H)$ is the normalized function describing the line and $(H - H_0)$ is the difference between the instantaneous magnetic field intensity and its resonance value] characterizes the interaction of protons in the substance, and a change in its value indicates a change in position or in mobility of the protons [4].

In connection with the temperature correlation of change in the second moment of the absorption line with the appearance of spontaneous polarization which had been found in PFC, we carried out a more detailed study of the behavior of molecules of water of crystallization in PFC by the proton magnetic resonance method.

The apparatus employed is described in [5]. In order to increase the ratio of signal to noise in the study of polycrystalline samples, PFC powder was pressed at a pressure of up to 150 kg/cm² into a cylinder of 13-mm diameter and 20 mm long. PFC monocrystals with dimensions 12 × 6 × 20 mm and 12 × 8 × 20 mm were also studied.** The study of temperature effects was carried out in the temperature range 77-400°K in a special Dewar flask, similar to the one described in [6].

The absorption spectrum traces were obtained with a time constant of 3.5 sec in a magnetic field of H_0 = = 3000 oersteds, at a rate of change of intensity of 0.0194 and 0.0097 oersted /sec. The amplitude of modulation in the traces did not exceed 0.8 oersted.

The temperature dependence of the second moment for polycrystalline PFC is given in Fig. 1, and in Fig. 2 the forms of the derived absorption spectra at different temperatures.

The expression for the second moment may be written in the form

$$S = S_0 + S_1, \qquad (2)$$

---

* Ferroelectric.

** The monocrystals were cut out in the form of parallelepipeds having edges denoted x, y, z. Axis b of the unit cell was chosen as axis y, axes x and z coincided with the [101] and [10$\bar{1}$] directions, respectively.

where S_0 is an internal component due to interaction between the proton pairs with the water molecules, and S_1 is an intermolecular component due to the interaction of the protons of a "pair" with other nuclei which possess a magnetic moment. The second-moment components, written for the case of a polycrystal containing water molecules, have the form [7]:

$$S_0 = 358.1 \cdot 10^{-48} r^{-6},$$

$$S_1 = 358.1 \cdot 10^{-48} \sum_j r_j^{-6} + \frac{4}{15} \sum_k I_k (I_k + 1) g_k^2 \beta^2 r_k^{-6}, \tag{3}$$

where $\underline{r}$ is the interproton distance in a water molecule (in cm); r_j is the distance to the protons of other water molecules; r_k is the distance to other nuclei having spin I_k, and hydromagnetic ratio g_k; β is the nuclear magneton.

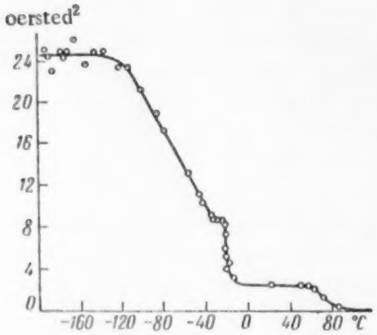

Fig. 1. Temperature dependence of the second moment of the proton magnetic resonance line for polycrystalline $K_4Fe(CN)_6 \cdot 3H_2O$.

In order to split the experimental value of the second moment, as determined at liquid-oxygen temperatures, into S_0 and S_1, measurements were carried out with a monocrystal. The proton magnetic resonance spectrum of a PFC monocrystal at a temperature of $-183°$, with a maximum spacing ΔH_{max} of 21.6 oersteds between the components (peaks) for one of the doublets is shown in Fig. 3.

The magnitude of the intermolecular component can be determined, starting with the width of a resolved peak, since the broadening of the peak is basically due to intermolecular interaction. This gives $S_1 = 0.6 \pm 0.06$ oersted², and from (2), at $S = 24.6 \pm 1.2$ oersted², we get $S_0 = 24.0 \pm 1.2$ oersted².

It is also possible to determine the value of S_0 [4], starting from the spacing ΔH_{max} between peaks (Fig. 3), using the formula $\Delta H_{max} = 3\mu r^{-3}$ (μ is the magnetic moment of a proton); whence $r = 1.575 \pm 0.015$ A, and from (3) $S_0 = 23.5 \pm 1.2$ oersted², which gives good agreement with the value obtained above.

It should be noted that the distance between the protons in water molecules is about 1.58 A, and correspondingly a second moment of 23.5 oersted² is typical for the rigid water molecules in crystalline hydrates.

The drop in the second moment, beginning at a temperature of about $-150°$, may in general be due to two reasons: increase of the distance between protons, or the appearance of rotational or translational degrees of freedom in the water molecules [4]. The occurrence of retarded rotation (reorientation) appears at first sight to be improbable for a large polar molecular of asymmetrical shape at such low temperatures. It should, however, be noted that the reorientation of water molecules in certain crystalline hydrates at comparable temperatures was recently reported in [9]. Apart from this fact, if it is postulated that the reduction in second moment is due to the protons moving away along the hydrogen bonds O–H . . . N, then, first, the existence of a strong temperature dependence is not in accordance with the usual behavior of hydrogen bonds, and, second, the calculated values of the moments to be expected, made on the basis of the structural data given in [2], render this hypothesis implausible.

Thus, it should be held that the drop in second moment above $-150°$ is due to a reorientation of the water molecules in PFC. From a theoretical consideration, it follows that for proton–proton (p–p) vectors which are isotropically distributed within a polycrystal and which are orientated about a fixed axis, the second moment should be four times less than for fixed (p–p) vectors. This ratio is not observed in our case at a temperature of $-35°$, at which decrease in the moment ceases.

Some additional experiments were carried out with a monocrystal in order to explain this fact. The directions of the (p–p) vectors of all 12 water molecules occurring in a unit cell were found by rotating the crystal about three mutually perpendicular axes at a temperature of $-183°$. It was found that 4 (p–p) vectors, of which one pair is perpendicular to the other, and which are disposed at an angle of 45° to the edges of the cell [actually

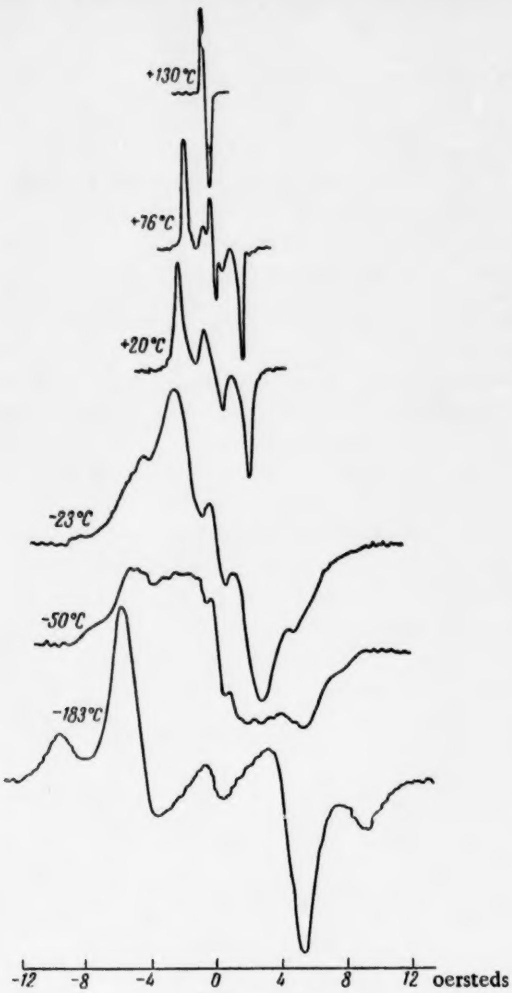

Fig. 2. Derived proton resonance spectrums for a PFC polycrystal.

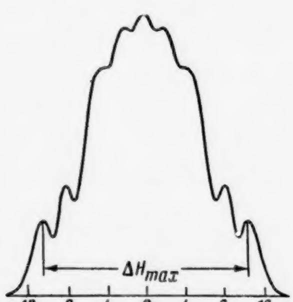

Fig. 3. Absorption lines of a PFC monocrystal at a temperature of −183°. The magnetic field enters at an angle of ~45° to the [111] direction. ΔH_{max} = 21.6 oersteds.

the planes in which the (p−p) vectors are located are inclined at an angle of about 10° to the corresponding faces], lie in each of the three mutually perpendicular planes coinciding with the crystal faces.

In the positions corresponding to the maximum spacing between doublets, the temperature dependence of the intensity of these doublets was measured for all three planes. The (p−p)-vector doublets lying in the X and Z planes disappear at a temperature of about −35°. These evidently correspond to the two water molecules whose oxygen atoms were localized in [2], where it was shown that these molecules have identical environments. The disappearance of the peaks for these protons at −35° implies that at that temperature all the corresponding molecules participate in the reorientation.

For the "third" water molecule composing the $K_4Fe(CN)_6 \cdot 3H_2O$ molecule, the position of which was not established in [2], and to which the (p−p) vectors lying in the Y plane probably correspond, the doublet disappears at only −20°. Therefore, the potential barrier for the reorientation of this molecule differs from those for the first two molecules, as a result of which the moment at −35° is not reduced by four times.

The appreciable change in the second moment of the absorption line for PFC in the region of the Curie point demands some attention. This indicates the maximum lowering of the potential barriers for the reorientation of water molecules at the Curie point, which is probably connected with change in crystal symmetry; consequently, the axes of reorientation have no fixed position in space, which is implied, in particular, by a low value of the second moment above the transition point.

Beyond this, the magnitude of the second moment and the shape of the absorption line change little up to a temperature of the order of +60°, where a small central peak appears, evidently due to self-diffusion of water molecules, which leads to further reduction of the second moment.

By 130°, the curve loses its "wings" (see Fig. 2), and only a narrow peak remains.

It should be noted that in all the spectra from −138° even up to temperatures of the order of +100° a central peak is observed whose intensity changes little with temperature; the occurrence of this peak is unusual in the spectra of crystalline hydrates. It may be supposed that it is caused by the presence of a small number of hydrogen bonds of the O . . . H−N type. The presence of such bonds causes the occurrence of protons which are separated from one another, which explains the existence of the central peak.

The authors acknowledge their indebtedness to K. S. Aleksandrov for supplying the PFC monocrystals and for discussing the results of the work.

LITERATURE CITED

1. S. Waku, H. Hirabayashi et al., J. Phys. Soc. Japan 14, 973 (1959).
2. V. A. Pospelov and G. S. Zhdanov, Zhur. Fiz. Khim. 21, 404, 521, 879 (1947).
3. A. G. Lundin, K. S. Aleksandrov, G. M. Mikhailov, and S. P. Gabuda, Transactions of the Third All-Union Symposium on Seignettoelectric Effects [in Russian] (Moscow, January 1960).
4. A. Andrew, Nuclear Magnetic Resonance [Russian translation] (IL, 1957).
5. A. G. Lundin and G. M. Mikhailov, Pribory i tekh. ėksp. No. 2, 90 (1960).
6. H. S. Gutowsky, L. H. Meyer, and R. E. McClure, Rev. Sci. Instr. 24, 644 (1953).
7. J. H. Van Vleck, Phys. Rev. 74, 1168 (1948).
8. J. H. Wertz, Chem. Rev. 55, 829 (1955).
9. S. Yano. J. Phys. Soc. Japan 14, 942 (1959).
10. H. S. Gutowsky and G. E. Pake, J. Chem. Phys. 18, 162 (1950).

THE DIFFUSION OF HYDROGEN IN MOLTEN SLAGS

I. A. Novokhatskii, O. A. Esin, and S. K. Chuchmarev

The S. M. Kirov Ural Polytechnic Institute, Sverdlovsk
(Presented by Academician A. N. Frumkin, July 20, 1960)
Translated from Doklady Akademii Nauk SSSR,
Vol. 136, No. 4, pp. 868-870, February, 1961
Original article submitted July 9, 1960

Values of the mass transfer coefficient D_M which are available in the literature [1] for hydrogen in slags are very large (10^{-3} to 10^{-2} $cm^2 \cdot sec^{-1}$). They have been obtained in the conditions of the Martin furnace, and they primarily indicate not molecular diffusion D_H, but convection, which inevitably occurs in a large volume of liquid at high temperatures. To achieve maximum suppression of convection currents and an approximation to DH we experimentally produced the case of unsteady-state diffusion by removing the gas from a membrane with one impervious boundary [2].

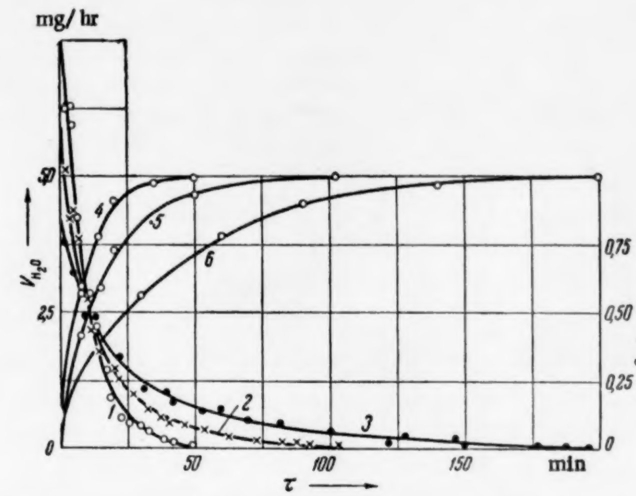

Fig. 1. Kinetic curves for the removal of water from slag No. 2 (27.3% CaO; 56.4% SiO_2; 16.3% Al_2O_3) at 1410° for films of different thicknesses. Curves 1, 2, and 3 for V_{H_2O} at δ = 1.3 mm, 1.8 mm, and 2.6 mm, respectively; similarly, Curves 4, 5, and 6 for Q/Q_0.

A thin ($\delta \simeq 1.5$ mm) layer of viscous (η = 3-100 poises) liquid (1410-1600°C) slag containing 16.5-53.0% CaO, 8.2-41.0% Al_2O_3, and 6.0-58.3% SiO_2 was placed in a corundum boat located in an Al_2O_3 tube. Water separating from the slag was carried out to a hygrometer by purging with carefully dried nitrogen. When the dew (or ice) point was reached, the mirror, initially dark, turned bright. Knowing the purge rate and the dew point, the rate of water removal from the slag V_{H_2O} was determined.

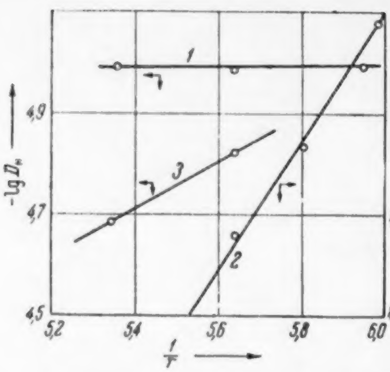

Fig. 2. Temperature dependence of diffusion coefficient (1, 3) and viscosity (2). 1), 2) For slag No. 2; 3) for slag No. 7 (53% CaO, 6% SiO_2, and 41% Al_2O_3).

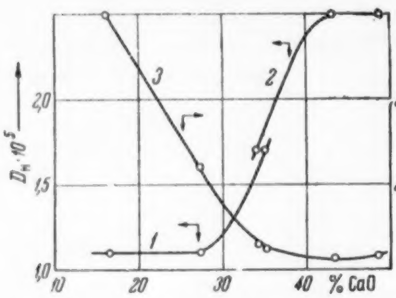

Fig. 3. Relationship between diffusion coefficient (1,2) and viscosity (3) and slag composition at 1600°: 1) for 57% SiO_2; 2) for 28% Al_2O_3.

In Fig. 1, Curves 1, 2, and 3 for the relationship between V_{H_2O} and time τ for three slag thicknesses are presented as an illustration. The instantaneous Q_τ and initial Q_0 quantities of water dissolved in the slag were determined by graphical integration. The ratio of these (Curves 4, 5, and 6) were employed to estimate the parameter θ, which, in the conditions of our experiment, can be calculated with an accuracy of 1% from the formula:

$$Q_\tau / Q_0 \simeq 1 - 8/\pi^2 (e^{-\theta}). \qquad (1)$$

Knowing θ, the value of the diffusion coefficient can be determined:

$$D_H = \frac{4\delta^2\theta}{\pi^2\tau}. \qquad (2)$$

The values of D_H, obtained for three slag thicknesses (1.3, 1.8, and 2.6 mm), were extremely close [(1.0, 1.1, and 0.9) $\cdot 10^{-5}$ cm²/sec]. This confirms that in this case diffusion is the rate-controlling step in the removal of water from slag. If the slowest stage was passage through the slag-gas boundary, for any given value of Q_τ / Q_0 the concentration of water in the slag would be the same, and V_{H_2O} would be independent of film thickness. As can be seen from Fig. 1, this is not so.

In order to make certain that mixing by convection was eliminated in our experiments, we applied a relationship obtained by Lin Tsa-Tsao [3]. In an investigation of the onset of convection in a thin incompressible liquid film heated from below, he found the lower limit for instability to be equal to:

$$\mathrm{Re} = \frac{g\alpha(-\beta)\delta^4}{x\nu} = 1708. \qquad (3)$$

In our case, the temperature gradient $(-\beta) \leq 50° / \delta$, the coefficient of thermal expansion $\alpha = 1.1 \cdot 10^{-5}$ deg^{-1} [3], $\delta < 0.3$ cm, the kinematic viscosity $\nu = \frac{32 \text{ (poises)}}{2.7\ (\text{g} \cdot \text{cm}^{-3})} \simeq 1.2$ cm² sec [5], and the thermal diffusivity $x = \frac{\gamma}{c\gamma} 1.53 \cdot 10^{-2}$ cm²/sec [6]. Hence, Re = 0.8, i.e., convection cannot have a detectible effect in the conditions of our experiment. Thus, the observed values of D_H are predominantly a measure of the molecular diffusion of hydrogen through the slag materials.

In the results obtained, the following special features merit attention. First of all, the diffusion coefficient for hydrogen is at least a factor of ten greater than those obtained [7-9] for other ions (Ca, Fe, P, S, Si). It is unlikely that OH^- anions, in which form water is dissolved in slags [1,10], could migrate with such a large velocity. For the viscosities of the melts we were dealing with at 1600°, lying in the range 3.2-75 poises [5,11], the value of D for the OH^- ion, calculated from the Stokes-Einstein equation, is considerably less and amounts to 10^{-7} to 10^{-8} cm²/sec.

In connection with the foregoing statements it may be postulated, as one of us has done [1], that hydrogen migrates in slags (like aqueous solutions [12-15]) in the form of protons, which pass from one oxygen ion to the next:

$$OH^- + O^{2-} \rightarrow O^{2-} + OH^-. \qquad (4)$$

The next peculiarity is the slight temperature dependence of D_H in slags rich in SiO_2. Thus, in slag No. 2,

when the temperature is raised from 1410 to 1600°, the value of D_H remains practically constant (see Curve 1 in Fig. 2), while the viscosity drops sharply (Curve 2). Zero activation energy indicates that the diffusing particle moves without an energy barrier. This is hardly possible for the OH^- anion, but is extremely probable for the proton. In fact, as shown by M. Huggins [15], when hydrogen moves from a hydroxyl to oxygen there is no energy barrier until the distance between the centers of neighboring oxygen atoms exceeds 2.65 A. The latter value is very close to the distance (d = 2.64 A) between oxygen ions in SiO_2 [16].

The third peculiarity lies in the fact that the coefficient D_H increases (Curves 1 and 2 in Fig. 3) with rise in the concentration of CaO in the slag, but at the same time the activation energy also increases (Curve 3 in Fig. 3). According to the theory of absolute rates [12]:

$$D = 2.72 \frac{kT}{h} \lambda^2 \exp(\Delta S^* / R) \exp(-E/RT), \tag{5}$$

where k and h are the Boltzmann and Planck constants, ΔS^* is the entropy of activation, which is usually small, λ is the distance between neighboring equilibrium positions of the migrating particle. It follows from Eq. (5) that simultaneous increase of D_H and E is possible when λ increases. This does not contradict the hypothesis of proton migration. The addition to the melt of CaO, in which the distance between oxygen ions in the lattice d = 3.41 A is greater [16] than in SiO_2, does in fact lead to an increase in λ. Estimation of the latter from Eq. (5) and the experimentally determined values of D_H and E gives acceptable values of λ. Thus, for slag No. 2, rich in SiO_2, at 1600° the value of $D_H = 1.1 \cdot 10^{-5}$ cm²/sec, E = 0; the distance λ = 0.03 A corresponding to these values is small. On the other hand, for slag No. 7, rich in CaO, $D_H = 2.05 \cdot 10^{-5}$ cm²/sec, E = 20,800 cal/mole, whence λ = 0.71 A. The feasibility of this value is confirmed by its closeness to the difference between the distance d in the CaO lattice and the diameter of the O^{2-} ion: $3.41 - 2 \cdot 1.32 = 0.77$ A.

In conclusion, we would comment that the hypothesis of proton migration needs additional experimental verification.

LITERATURE CITED

1. V. I. Yavoiskii, Gases in the Baths of Steel-Melting Furnaces [in Russian] (Moscow, 1952) pp. 150, 175.
2. R. Barrer, Diffusion in Solids [Russian translation] (IL, 1948), pp. 30, 31, 52, 56, 490.
3. Lin Tsa-Tsao, The Theory of Hydraulic Stability [Russian translation] (IL, 1958) p. 134.
4. J. O'M. Bockris, J. W. Tomlinson, and J. L. White, Trans. Faraday Soc. 52, 299 (1956).
5. Mak-Keferi, Sovetskaya Metallurgiya No. 3, 152 (1932).
6. Thermophysical Properties of Substances, Textbook edited by N. B. Vargaftik [in Russian] (Moscow-Leningrad, 1956) pp. 323, 324.
7. H. Towers, M. Paris, and J. Chipman, J. Metals 5, No. 11, 1455 (1953).
8. H. Towers and J. Chipman, J. Metals 9, No. 6, 769 (1957).
9. E. S. Vorontsov and O. A. Esin, Izv. Akad. Nauk SSSR, Otdel. Tekh. Nauk No. 2, 152 (1958).
10. O. A. Esin, The Electrochemical Nature of Liquid Slags [in Russian] (1946).
11. J. S. Machin and Tin Boo Jee, J. Am. Ceram. Soc. 31, No. 7, 200 (1948).
12. S. Glasstone, K. Laidler, and T. Eyring, The Theory of Absolute Reaction Rates [Russian translation] (IL, Moscow, 1948) p. 533.
13. N. E. Khomutov, Zhur. Fiz. Khim. 34, No. 2, 380 (1960).
14. B. E. Conway, Canad. J. Chem. 37, No. 1, 178 (1959).
15. M. Huggins, J. Phys. Chem. 40, 723 (1936).
16. B. F. Ormont, The Structure of Inorganic Substances [in Russian] (Moscow, 1950) pp. 451, 509.

INVESTIGATION OF THE PARAMAGNETIC RESONANCE OF SOLUTIONS OF SOME COPPER HYDROXYAZO COMPOUNDS

A. K. Piskunov, D. N. Shigorin, B. I. Stepanov, and É. R. Klinshpont

L. Ya. Karpov Institute of Physical Chemistry and
D. I. Mendeleev Institute of Chemical Technology, Moscow
(Presented by Academician V. A. Kargin, June 20, 1960)
Translated from Doklady Akademii Nauk SSSR,
Vol. 136, No. 4, pp. 871-874, February, 1961
Original article submitted June 1, 1960

The electron paramagnetic resonance (epr) spectra of chloroform solutions of the copper complexes of 2-chlorobenzene-(1-azo-1')-naphthol-2' (I), 2-methoxybenzene-(1-azo-1')-naphthol-2' (II), 2-nitrobenzene-(1-azo-1')-naphthol-2' (III), 2-butoxybenzene-(1-azo-1')-naphthol-2' (IV), 2,6-dichlorobenzene-(1-azo-1')-naphthol-2' (V), 2-hydroxy-1,1'-azonaphthalene (VI), 2-chloro-2'-hydroxy-1,1'-azonaphthalene (VII), and 8-chloro-2'-hydroxy-1,1'-azonaphthalene (VIII) were investigated at a frequency of 9375 Mc.

Apart from four lines of hyperfine structure (hfs) due to the interaction of an unpaired electron with the copper nucleus ($I = {}^3/_2$), a secondary hyperfine breakdown was discovered. The form of the spectrum from the four main hfs lines is similar to that observed by McGarvey [1] in solutions of copper acetylacetonate and its derivatives, and can readily be integrated using the relaxation theory developed by McConnell [2], which explains the asymmetry of the spectrum in terms of the relationship between the contribution of anisotropic hyperfine interaction to paramagnetic relaxation and the nuclear spin quantum number I_z. This relationship leads to the fact that the hfs lines differ in width for different values of I_z. The spacings between the four hfs components vary between the limits of 60-70 gauss for different compounds.

With the exception of the solution of compound VIII, the secondary five-line hfs is clearly resolved in the most intense line of the basic hfs spectrum ($I_z = -{}^3/_2$), whereas it is almost imperceptible even in the second line ($I_z = -{}^1/_2$). This is in complete accordance with McConnell's relaxation mechanism, since the widening of the hfs components of the basic spectrum accompanying an increase in I_z should cause reduced resolution of the supplementary hfs. The secondary hyperfine spacing implies that the unpaired electron is not localized in the copper atom but is also in the field of two of the nitrogen nuclei of the two azo groups. Interaction of the electron with only two of the nitrogen atoms (one from each azo group), can evidently be explained by the fact that the π-electrons of the azo-groups do not take part in the formation of chemical bonds with the copper atom, since additional energy is required to excite them for this. It is known that the energy of the π-bonds in an azo group is almost twice as great as the energy of the σ-bonds [3]. The copper atom, using two valence electrons (s and p), forms two chemical bonds with the oxygen atoms. Copper forms two other bonds with the aid of its two unfilled orbits (p and d), and the unshared pairs of electrons of the nitrogen atoms of the azo groups. Thus, if our supposition is correct, the free electron density must be distributed over only two nitrogen atoms, which participate in the formation of bonds with the copper atom. More remote atoms affect the width of the hfs lines and the g factors, and also the resolution of the secondary hfs spectrum. The position and resolution of the spectra are considerably dependent on the solvents. The biggest variations in spectra were observed in the study of compounds dissolved in dioxane.

Values of g Factors and Widths of Hyperfine Structure Lines for M/100 Chloroform Solutions of Copper Complexes

No.	Compounds	g_1	g_2	g_3	ΔH_1 (gauss)	ΔH_2, gauss	ΔH_3, gauss
I	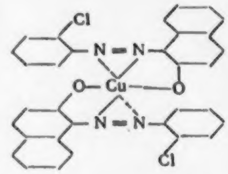	2.042	2.079	2.117	5 secondary hfs lines with spacing of 11 gauss	29	33
II	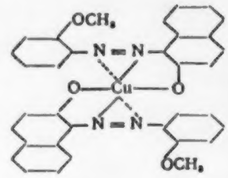	2.041	2.086	2.124	The same	35	38
III	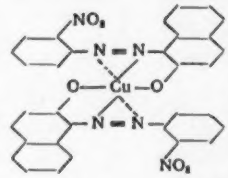	2,030	2,072	2.116	• •	38	42
IV	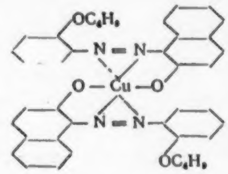	2,043	2.082	2.117	• •	34	39
V	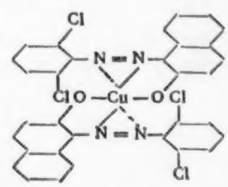	2,021	2.067	2.110	• •	32	36
VI	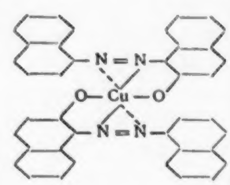	2.036	2.072	2.111	• •	32	35

(continued)

No.	Compounds	g_1	g_2	g_3	ΔH_1,gauss	ΔH_2,gauss	ΔH_3,gauss
VII	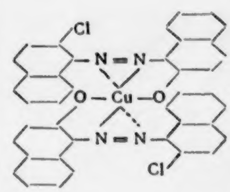	2.024	2.068	2.113	The same	36	38
VIII	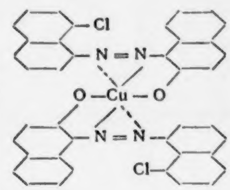	2.050	2.090	2.126	27	30	35

The traces of epr spectra of M/100 solutions of I, V, and VIII are given in the figure (the spectra of II and III differ little from the spectrum of I, and the spectrum of VII from that of V; the resolution is better in the spectra of IV and VI than in I). The measured g factors and widths of the fully resolved lines of the basic hfs spectrum (between points of maximum slope) are given in the table. The resolution of the secondary hfs depends on the nature of the substituents, their number, and position in the aromatic rings. A similar type of substituent effect on the resolution of hfs spectra has been observed in chromocenes [4].

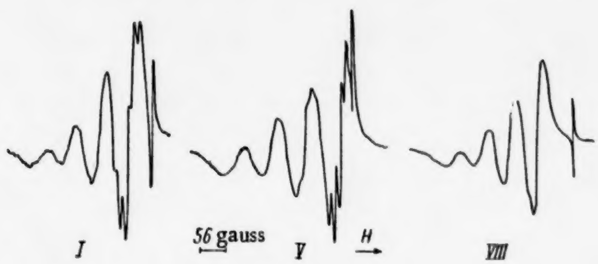

It can be seen from the spectra given in the figure that the resolution of the spectrum of compound V, which contains two chlorine atoms in the ortho position with respect to the azo group, is increased with respect to compound I. It is impossible to explain the observed changes in the spectra only in terms of the mechanisms of line widening considered by McGarvey [5]. It is known from the study of luminescence spectra that complex molecules with a large number of π-electrons, particularly those having unpaired electrons, can associate with one another even in very dilute solutions. The formation of such associated systems in the solutions we have studied would promote a magnetic dipole-dipole and an exchange interaction between molecules; on the other hand, the reorientation times for the associated systems would be greater than for separate molecules. The power to form associated systems is evidently so great for the copper complex of benzeneazonaphthol-2, which contains no substituents in the aromatic rings, that it is impossible to dissolve it in chloroform or other solvents (benzene, dioxane, tetrahydrofuran, pyridine, and toluene).

Introduction of the substituents Cl and OR, which possess large van der Waals' radii, would reduce the possibility of forming associated systems. The better resolution of the secondary hfs in solution V compared with solution I is probably due to the greater power of I to associate. Thus, in the analysis of variations observed in epr spectra it is essential to take into consideration the effect of the tendency of the compounds to associate in solution on the form of the spectrum,as well as other mechanisms.

Attention is drawn to the relationship between the resolution of the secondary hfs and the g factors of the hfs line of maximum intensity, due to the interaction of an electron with the copper nucleus.

For all the compounds investigated, except IV, the smaller the g factor, the better the resolution.

The fact that no secondary hfs is observed in spectrum VIII can probably be explained by steric hindrance effects, which interfere with the interaction of the unpaired electron with nitrogen nuclei. The proximity of the nitrogen and chlorine atoms in VIII may lead to the loss of the planarity of the molecule. This would considerably weaken interaction between an electron and nitrogen nuclei.

In solidified solutions, the hfs completely disappears and wide asymmetrical lines of the order of 200-250 gauss are observed. The polycrystalline samples of these compounds, which were investigated previously [6], had a line width of 30-50 gauss. Consequently, exchange interactions have a substantial effect on the line widths for polycrystalline samples.

All the compounds studied are readily soluble in acetylacetone and give the same spectrum, consisting of four lines with $g_1 = 2.052$, $g_2 = 2.097$, $g_3 = 2.141$, $g_4 = 2.175$, and $\Delta H_1 = 26$, $\Delta H_2 = 24$, $\Delta H_3 = 28$, and $\Delta H_4 = 37$ gauss.

Displacement of molecules of the azo compounds from the complexes by acetylacetone molecules evidently takes place on solution.

When investigating epr in magnetically dilute polycrystals of copper bis-salicylaldehydeimine, Maki and McGarvey [7] observed a secondary 11-line hfs resulting from the interaction of an unpaired electron with nitrogen nuclei and protons from the hydrogen in the CH groups. Solutions of this compound and a series of its derivatives in pyridine, dioxane, and tetrahydrofuran which we studied gave no secondary hfs.

LITERATURE CITED

1. B. R. McGarvey, J. Phys. Chem. 60, 71 (1956).
2. H. M. McConnell, J. Chem. Phys. 25, 709 (1956).
3. Ya. K. Syrkin and M. E. Dyatkina, The Chemical Bond and the Structure of Molecules [in Russian] (Moscow, 1946).
4. V. V. Voevodskii, Yu. N. Molin, and V. M. Chibrikin, Optika i Spektroskopiya 5, 90 (1958).
5. B. R. McGarvey, J. Phys. Chem. 61, 1232 (1957).
6. A. K. Piskunov, D. N. Shigorin, V. I. Smirnova, and B. I. Stepanov, Doklady Akad. Nauk SSSR 130, No. 6, 1284 (1960).
7. A. H. Maki and B. R. McGarvey, J. Chem. Phys. 29, 35 (1958).

All abbreviations of periodicals in the above bibliography are letter-by-letter transliterations of the abbreviations as given in the original Russian journal. *Some or all of this periodical literature may well be available in English translation.* A complete list of the cover-to-cover English translations appears at the back of this issue.

THE THERMODYNAMIC AND DIFFUSION CHARACTERISTICS OF THE SILICATE CONSTITUENTS OF CEMENT ON SOLUTION IN WATER

V. B. Ratinov, G. D. Kucheryaeva, and G. G. Melent'eva

Scientific Research Institute for Reinforced Concrete Products, Structural, and Nonmetallic Materials

(Presented by Academician P. A. Rebinder, September 22, 1960)
Translated from Doklady Akademii Nauk SSSR,
Vol. 136, No. 4, pp. 875-878, February, 1961
Original article submitted September 14, 1960

Results are set out below for the measurement of the thermodynamic (metastable solubility) and diffusion characteristics of tricalcium silicate (C_3S) and β-dicalcium silicate (C_2S), a knowledge of which is of importance for the construction of a theory of the hardening of concrete. The solubility of the aluminate constituents of cements was first determined by E. E. Segalova, E. S. Solov'eva, and P. A. Rebinder [1,2]. By the solubility of the binder C_S we mean the maximum possible concentration of it corresponding to saturation of the solution with respect to the binder; therefore, the value of C_S is related to the free-energy change on solution ΔF by the well-known relationship :

$$C_s = \exp\left\{\frac{\Delta F - \varphi}{RT}\right\}, \tag{1}$$

where $\varphi = RT \ln f$; f is the activity coefficient.

The difficulties in arriving at a value of C_S for clinker minerals and many other salts which are capable of forming solutions which are supersaturated with respect to products formed in the solution are due to the fact that when they react with water a new phase* may begin to crystallize out at a high rate even before concentrations corresponding to the solubility of the initial substance are attained in the solution; consequently, more material will be expended from unit volume of solution per unit time on the crystallization of products (generally hydrates) than will be taken up by the dissolution of the initial material, and the directly measured concentration of the latter will not attain the value C_S.

For this reason we determined the solubility of alite and belite by several independent methods, including one which made it possible to exclude the stage of product crystallization. By means of this method we were also able to measure the diffusion characteristics of the binders.

The theory of the method was evolved by V. G. Levich [3]. For the case where a disk of the material under investigation is rotated in water in conditions of controlled convection, the theory states:

$$C_s = \frac{I\nu^{1/6}}{0{,}62\omega^{1/2}D^{2/3}}, \tag{2}$$

where I is diffusional flow;

$$I = \frac{m}{s\tau}; \tag{3}$$

m is the quantity of substance dissolved; s is the disk surface area; and τ is time of solution.

* The chemical composition of the new phase may be different from the composition of the initial material.

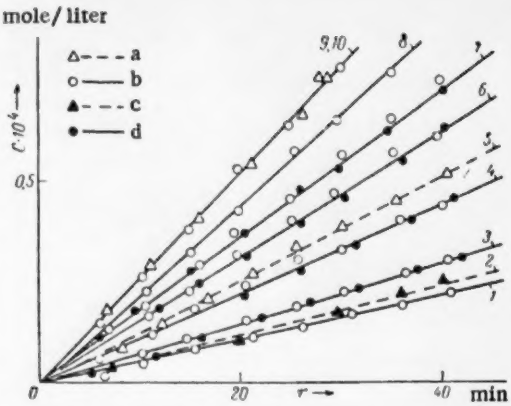

Kinetics of solution in water of disks of C_3S (a), C_2S (b), C_3SH_2 (c), $C_2SH(A)$ (d): 1) 12°; 2, 3, and 5) 20°; 4) 30°; 6) 40°; 7) 50°; 8 and 10) 60°; 9) 70°.

Thermodynamic and Diffusion Characteristics of C_2S

Temp. of expt., °C	Solubility C_s, g/liter	Diffusion coefficient $D \cdot 10^6$, cm^2/sec	Diffusional flow, $I \cdot 10^7$, $g/cm^2 \cdot sec$
2	0.155	–	–
12	0.172	2.4	3.2
20	0.190	3.7	4.3
30	0.203	5.2	6.6
40	0.212	6.3	8.3
50	0.236	7.4	10.5
60	0.258	8.1	12.4
70	–	–	14.3

Knowing the kinematic viscosity of the solution ν, and given a constant angular velocity for the disks ω, it is possible to find the values of C_s for alite and belite if their diffusion coefficients D are known. We determined the value of D by carrying out experiments with disks of calcium hydrosilicates having the same basicity as the corresponding anhydrites C_3SH_2 and $C_2SH(A)$.

Both hydrates were synthesized in a bomb, the first from C_3S and the second from sand and limestone*; their solubilities were determined in the normal way – the analysis of the solution obtained when the solid and liquid phases had reached equilibrium. Silicate ion concentration was determined colorimetrically by the formation of a colored complex with ammonium molybdate in sulfate solution [4], and calcium ion concentration by trilonometric titration [5]. The experiments were carried out under nitrogen to avoid carbonization. The disks of C_3S, C_2S, and the hydrates were prepared by the technique of pressing the dry powders up to a pressure of 20,000 kg/cm^2 in special molding presses [6]. The technique adopted ensured good reproducibility of the results in repeat experiments.

The diffusion coefficients for these hydrates, which we took to be equal to the values of D for the corresponding anhydrites, were calculated from the data obtained for C_3SH_2 and $C_2SH(A)$ (see figure) by formula (2); the rest of the data needed to calculate C_s were obtained from the experimental curves given in the figure.

In addition, disks were also used for an alternative method for determining the solubility of C_3S and C_2S, which made it possible to eliminate the diffusion coefficient from the calculation and to avoid the use of the calcium hydrosilicates. This method requires the running of at least two experiments: the first at an initial concentration of the substance under investigation equal to C_1, and the second at C_2. Equation (2) may then be written in the form:

$$I_1 = K\,(C_s - C_1), \tag{4a}$$

$$I_2 = K\,(C_s - C_2). \tag{4b}$$

Constancy of the coefficient K is ensured in dilute solutions by using small differences between the values of C_1 and C_2; practically speaking, the values of D and ν do not then vary.

Solving Eqs. (4a) and (4b) for C_s, we get

$$C_s = \frac{C_2 I_1 - C_1 I_2}{I_1 - I_2}. \tag{5}$$

At $C_1 = 0$, Eq. (5) is simplified

*C_3SH_2 was synthesized by L. N. Rashkovich, and $C_2SH(A)$ by O. I. Gracheva, to whom the authors express their gratitude. The purity and phase composition of C_3S and C_2S and the hydrates were determined by chemical and x-ray analysis; the latter was carried out by L. N. Rashkovich and O. I. Gracheva on a URS-50I diffractometer.

A formula of similar type,

$$C_s = \frac{C_m v_n - C_n v_m}{v_n - v_m}, \tag{5a}$$

was used to obtain the rising portion of the experimental kinetic curve for the rate of solution of C_3S and C_2S suspensions.

Here, v_n and v_m are the mean rates of solution over arbitrarily chosen time intervals $\Delta\tau_n$ and $\Delta\tau_m$ (or the true rates at times τ_n and τ_m); C_n and C_m are the corresponding concentrations of the substance in solution.

We also determined the solubility of C_3S and C_2S by direct measurement, working with dilute suspensions containing surface-active additives which retarded the crystallization of products more strongly than the dissolution of the initial compounds. The absence of any appreciable crystallization of hydrates was checked in these and all the other experiments by whether a constant molar ratio of calcium and silicate ions (C_{Ca}:C_{SiO_2}) was maintained.

As the products formed from dilute suspensions of C_3S and C_2S are less basic than the initial compounds, a rise in the value of C_{Ca}:C_{SiO_2} in the solution indicated that crystallization had started; in the absence of crystallization the ratio was constant and equal to 3 and 2, respectively.

The values of C_s, for C_3S and C_2S at 20° obtained by the methods stated did not differ from one another by more than 10%; this indicated that the values for the diffusion coefficients for molecules and ions in the solution of C_3S, C_2S, C_3SH_2, and $C_2SH(A)$ were close and that the first method could also be used for the determination of C_s and D at higher temperatures. The results of these measurements are presented in the table.

At 2°, the solubility of C_3S was 0.256 g/liter, at 10°, 0.338 g/liter, at 20°, 0.387 g/liter; the diffusion coefficients were $2.6 \cdot 10^{-6}$, $3.0 \cdot 10^{-6}$, and $3.4 \cdot 10^{-6}$ cm²/sec, respectively; the diffusional flows were $0.5 \cdot 10^{-6}$, $0.67 \cdot 10^{-6}$, and $1.0 \cdot 10^{-6}$ g/cm² · sec, respectively. (In all cases, the rate of rotation of the disks was equal to 10 rev /sec.)

The heat of solution Q, for C_2S equal to 1.5 kcal/mole, was calculated from the data obtained by the equation

$$\frac{d \ln C_s}{dT} = -\frac{Q}{RT^2} \tag{6}$$

and, by a formula of similar type, the activation energy of diffusion on dissolution in water, equal to 6.3 kcal/mole.

Knowing the solubility and heat of solution of C_2S, its other thermodynamic properties can also be calculated from well-known formulas.

The values which we determined for $I' = (I/\omega^{\frac{1}{2}})10^7$ g/cm² · sec on solution in water for gypsum, lime, tricalcium aluminate, C_3S, and C_2S at 20° were 8.1, 3.2, 1.9, 1.2, and 0.5, respectively;they fall into the same order as their hardening rates in concentrated suspensions; this serves as yet another proof that the mechanism of binder hardening elaborated in [5-7] is correct.

LITERATURE CITED

1. E. E. Segalova, E. S. Solov'eva, and P. A. Rebinder, Doklady Akad. Nauk SSSR 117, No. 5 (1957).
2. E. S. Solov'eva and E. E. Segalova, Koll. Zhur. 20, No. 5 (1958).
3. V. G. Levich, Physicochemical Hydrodynamics [in Russian] (AN SSSR Press, 1959).
4. V. M. Bereznyak, V. A. Begma, and V. I. Zhuravskaya, Zavod. Lab. 21, No. 3, 298 (1955).
5. V. B. Ratinov, Ya. I. Zabezhinskii, and T. I. Rosenberg, Doklady Akad. Nauk SSSR 109, No. 5 (1956); Collected Work of the All-Union Scientific Research Institute of Reinforced Concrete, No. 1 [in Russian] (1957).
6. V. B. Ratinov and V. A. Grigoryan, Structural Materials, No. 3 [in Russian] (1960).
7. V. B. Ratinov and T. I. Rosenberg, Collected Work of the All-Union Scientific Research Institute for Reinforced Concrete, No. 2 [in Russian] (1959).

ELECTRON DENSITY DISTRIBUTION IN GALLIUM ARSENIDE

Academician of the Acad. Sci. Belorus.SSR N. N. Sirota

and N. M. Olekhnovich

Solid State and Semiconductor Physics Section, Academy of Sciences Belorus.SSR
Translated from Doklady Akademii Nauk SSSR,
Vol. 136, No. 4, pp. 879-881, February, 1961
Original article submitted September 19, 1960

In the present work, the most important results of a study of electron-density distribution in gallium arsenide are reported. The method of investigation was basically the same as that described previously [1,2]. Semi-crystalline gallium arsenide, purified by zone melting, was ground to a fine powder in an agate mortar and elutriated in toluene to a particle size of 5-8μ. The x-ray pattern was obtained at room temperature with CuK_α radiation, using a URS-50 recording x-ray apparatus, and with a Geiger–Müller counter. The line intensities were determined from peak areas recorded on an ÉPP-09 automatic potentiometer.

Using experimentally determined absolute reflex intensities I_{hkl}, the squares of the structural amplitudes F^2 were calculated for three types of lines – lines with even indices, the sum of which is divisible by four (F_1^2), odd indices (F_2^2); and even indices, the sum of which is not divisible by four (F_3^2) (see Fig. 1a). From the data on the squares of the structure factors, the values of the atomic scattering factors for gallium and arsenic ions were calculated (Fig. 1b). Values of the logarithms of the atomic scattering factors for various values of Σh_i^2 are shown in Fig. 2. As may be seen from Fig. 2, at $\Sigma h_i^2 > 12$ for arsenic ions, and at $\Sigma h_i^2 > 10$ for gallium ions, the logarithms of the atomic scattering factors fall on straight lines. This fact indicates the possibility of using a method described previously [3] for the summation of three-term Fourier series, and the calculation of the electron-density distribution over the whole unit cell of gallium arsenide, using the values obtained for the atomic scattering factors.

The electron-density distribution map for plane (110) of the unit cell of gallium arsenide is given in Fig. 3. The electron-density distribution between Ga–As–Ga ions in the [111] direction (Fig. 4a) and between Ga–As ions in the [113] direction (Fig. 4b) in plane (110) are given in Figs. 4a, b. In the (110) plane, a "bridge" of increased electron density of a minimum value of 0.49 electrons/ A^3 is observed between the gallium and arsenic ions in the [111] direction between points 000 and $\frac{1}{4}\,\frac{1}{4}\,\frac{1}{4}$. Similar "bridges" are observed in crystals of silicon, germanium, and indium arsenide. In indium arsenide the minimum electron density in the "bridge" is 0.45 electrons/ A^3, and the width of the bridge is somewhat less.

The "bridge" of increased electron density observed between the gallium and arsenic ions in the [113] direction is not so clearly defined as that which occurs in indium arsenide. At the same time, an area of minimum electron density ("valley") typical of germanium and silicon crystals is not observed. Unlike indium arsenide, somewhat higher electron densities occur in gallium arsenide between the metal ions Ga–Ga in the [001] and [110] directions.

In gallium arsenide, as in indium arsenide, the electron density in the [111] direction near the point $\frac{3}{4}\,\frac{3}{4}\,\frac{3}{4}$ is nearly zero. The nonsphericity of the arsenic ion is most strikingly noticeable in gallium arsenide. In indium arsenide, nonsphericity of the arsenic ion is also noticeable but is not so clearly defined. It should also be noted that the maximum electron density at the location of the center of the arsenic ion is considerably higher in gallium arsenide than in indium arsenide. It is possible that this fact is connected with the difference in the characteristic temperature of these compounds.

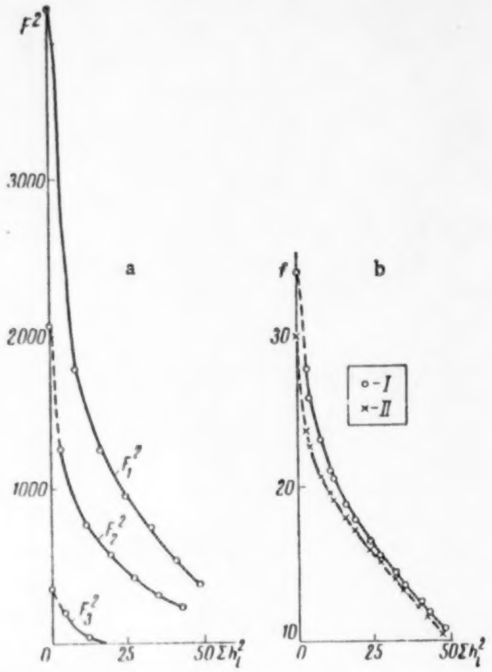

Fig. 1. Variation of the square of the structure function F^2 for gallium arsenide (a) and the atomic scattering factors (b) for arsenic ions (I) and gallium ions (II) in gallium arsenide as a function of Σh_i^2.

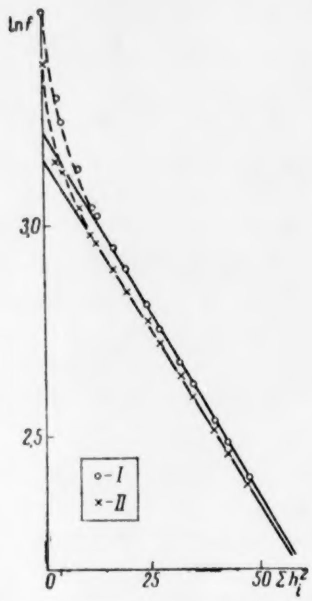

Fig. 2. Variation of the logarithms of the atomic scattering factors for arsenic ions (I) and gallium ions (II) as a function of Σh_i^2.

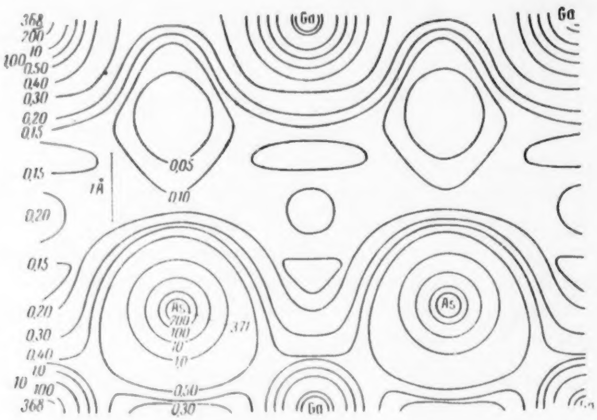

Fig. 3. Electron density distribution map in the (110) plane of a unit cell of gallium arsenide.

The data obtained on electron density distribution enable some estimate of the ionic radii of gallium and arsenic to be made.

On the basis of an electron density level of 0.5 electrons/A^3, the ionic radius of gallium is equal to 0.8 A, and the ionic radius of arsenic is 1.65 A. At the same time, the ionic radius of arsenic in the [113] direction is somewhat less — of the order of 1.3 A. If the ionic radius is determined taking a somewhat higher electron-density level, the ionic radius of gallium changes relatively little, whereas the ionic radius of arsenic is greatly reduced.

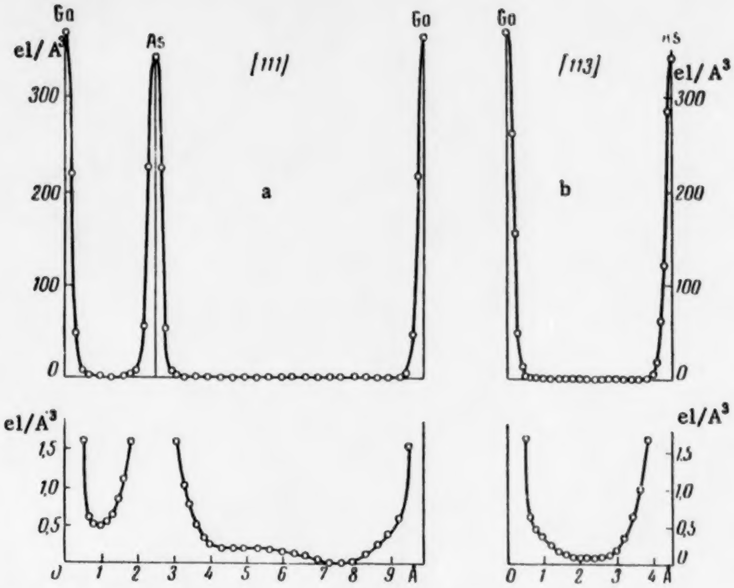

Fig. 4. Electron density distribution in the [111] (a) and [113] (b) directions in the (110) plane of a unit cell of gallium arsenide.

At an electron density level of 0.25 electrons/ A³, the ionic radius of gallium is 1.3 A, and the ionic radius of arsenic is 1.45 A. In indium arsenide, at an electron density level of 0.5 electrons/ A³, the ionic radius of indium is equal to 0.9 A, while the ionic radius of arsenic is 1.2-1.10 A. At an electron density level of 0.25 electrons/ A³, the ionic radius of indium is approximately equal to 1.5 A, while the ionic radius of arsenic is equal to about 1.35 A.

The ionic radius values given, although they are of an approximate and preliminary nature, are of considerable interest and in particular indicate that sphalerite structures, being the structures with the densest packings, may only to a first approximation be studied by a consideration of the nature of their electron-density distribution.

LITERATURE CITED

1. N. N. Sirota and N. M. Olekhnovich, Doklady Akad. Nauk SSSR 136, No. 3 (1961).
2. N. N. Sirota and A. U. Sheleg, Doklady Akad. Nauk SSSR 135, No. 5 (1960).
3. N. N. Sirota, N. M. Olekhnovich, and A. U. Sheleg, Doklady Akad. Nauk SSSR 132, No. 1, 160 (1960).

All abbreviations of periodicals in the above bibliography are letter-by-letter transliterations of the abbreviations as given in the original Russian journal. *Some or all of this periodical literature may well be available in English translation.* A complete list of the cover-to-cover English translations appears at the back of this issue.

INITIATION OF POLYMERIZATION BY SOLID POTASSIUM AMIDE AND ALCOHOLATE IN DIMETHOXYETHANE

A. I. Shatenshtein, E. A. Yakovleva, and É. S. Petrov

L. Ya. Karpov Physicochemical Institute

(Presented by Academician V. A. Kargin, August 28, 1960)
Translated from Doklady Akademii Nauk SSSR,
Vol. 136, No. 4, pp. 882-885, February, 1961
Original article submitted July 22, 1960

It is well known that by changing the reaction medium it is possible to affect the reactivity of substances and even the direction in which chemical processes proceed. The study of hydrogen isotope exchange provides striking examples of this [1]. Reactions due to electron donors or bases involving hydrogen exchange, formation of organometallic compounds, isomerization with a displacement of a multiple bond, alkylation, and anionic polymerization, in the course of which,in the final case,carbanions are formed, come under the general field of organic anion chemistry [2]. Reactions which give rise to anionic radicals have a certain similarity to such reactions. It is often possible, by analyzing the results obtained in the investigation of certain reactions, to predict the effect of some factor or condition on other reactions whose direction is determined by similar laws. In the present study we have attempted to approach anionic polymerization from this point of view. The methods of initiating polymerization by means of solid potassium amide and alcoholate in dimethoxyethane, which are described below, were suggested by studies devoted to the investigation of deuterium exchange between hydrocarbons and bases, and the study of the conditions of formation of anionic radicals.

It has been shown previously [3] that hydrogen exchange and isomerization which take place in an ammoniacal solution of potassium amide can be carried out on the surface of solid potassium amide in the absence of a solvent. We decided to apply heterogeneous catalysis by means of potassium amide to polymerization, as we considered that in the absence of ammonia, which tends to rupture the polymer chain, it would be possible to obtain polymers of considerably higher molecular weight than in ammoniacal solution. This prediction turned out to be correct – in our work, styrene polymers with molecular weights of several millions were obtained over solid potassium amide, whereas according to literature data [4,5], confirmed in our laboratory, only low molecular weight polymers (molecular weight 2000-4000) are formed in styrene polymerization catalyzed by potassium or sodium amides in liquid ammonia.

The idea of initiating a polymerization reaction by means of an alcoholate in dimethoxyethane arose from a comparison of the observed effects of solvents on the catalytic activity of alcoholates in deuterium exchange and on the stability of anionic radicals. A sharp rise in the catalytic activity of C_2H_5OK (or $NH_2CH_2CH_2OK$) with respect to hydrogen isotope exchange in triphenylmethane was noted [6] if ethylenediamine was used as the solvent instead of ethanol (or ethanolamine). This effect may be considered a result of the enhanced capacity of the alcoholate to act as an electron donor, due to stronger solvation of the cation in ethylenediamine than in alcohol. The formation of a stable solvate between the cation and the solvent eliminates ionic interaction in which non-Coulombian forces of a donor–acceptor nature participate [1], and the anion becomes a stronger base. One indication of high solvation power of a solvent with respect to alkali-metal cations is solubility of the latter, accompanied by the formation of blue,electrically conductive solutions [7,8]. Ethylenediamine is such a solvent [6]. The role of solvation of metallic cations in the formation of anionic benzene and toluene radicals is considered in [9]. Solvents can be arranged in a series by relative concentration of anionic radicals, as determined by measuring the electron paramagnetic resonance spectra. At the head of the series is 1,2-dimethoxyethane, in which, as is well known [7,8], potassium is soluble.

Taking into account the recorded facts and opinions, we expected alcoholates to possess considerable electron-donor activity on solution in dimethoxyethane. We confirmed this supposition by the fact that when $CH_3OCH_2CH_2OK$ in the stated solvent acted on fluorene the latter ionized, forming carbanions, which could be seen from the spectrum of the solution. In Fig. 1, light absorption curves of solutions at several concentrations are given. The positions of the maxima in the curves (λ 365, 465, 480 mμ) correspond to those found in the reaction of fluorene with caustic potash in liquid ammonia [10]. A less acidic hydrocarbon – triphenylmethane – does not ionize in these conditions. An alcoholate in dimethoxyethane is also capable of initiating the polymerization of vinyl monomers. For example, $CH_3OCH_2CH_2OK$ brings about the rapid polymerization of methylmethacrylate. Polymerization is also observed on the mixing of styrene with a solution and suspension of $CH_3OCH_2CH_2OK$ or CH_3OK.

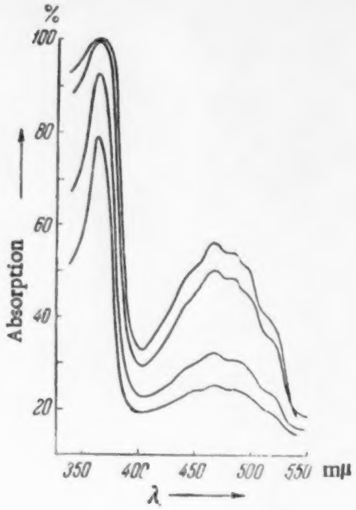

Fig. 1.

According to literature data [11-13], alcoholates initiate the anionic polymerization of more reactive monomers (acrylonitrile, β-nitrostyrene). The polymerization of methylmethacrylate was recently reported [14], using sodium methoxide in liquid ammonia solvent, which strongly solvates cations and readily dissolves alkali metals.

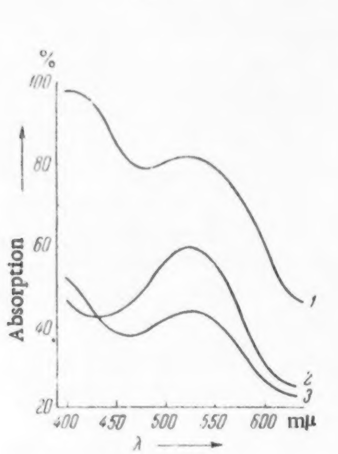

Fig. 2.

Let us pass to the description of the experiments. The monomers, purified in the usual way, were given additional purification prior to the experiment. Styrene was partially polymerized over metallic potassium and recondensed under high vacuum, while methylmethacrylate was distilled under high vacuum, taking the middle fraction. The potassium amide was prepared by reaction with liquid ammonia, using the apparatus described in [15], and was applied to the surface of glass packing, as used for the packing of distillation columns. After stripping off the ammonia, the system was kept under vacuum for 1-2 hours while heating in a water bath, and the monomer was added under vacuum. On contact with the solid potassium amide, the styrene acquired a red coloration. Determination of the absorption spectra indicated the existence of wide bands with maximum absorption at λ = 520 mμ (Fig. 2,1). The intensity of the coloration gradually increases, and then falls. In two or three days at room temperature the styrene polymerizes completely, and a solid polymer is obtained which dissolves slowly in benzene. It was precipitated from benzene solution with methanol, dried under vacuum at 80°, and the viscosity of a toluene solution at 25° was determined. The following values of the characteristic viscosity [η] (neglecting pressure drop) were obtained for the samples of polymer produced: 6.0, 6.8, 5.4, 8.8, 7.3, 5.1, and 7.5. These polymers are therefore characterized by a very high molecular weight. If the surface area of the potassium amide is reduced, the over-all picture remains the same, but the polymer is formed more slowly. In a control experiment carried out without potassium amide, the styrene still had the appearance of a viscous liquid even after three weeks. On the addition of methanol, a few percent of polymer was precipitated. In one experiment, a portion of the colored styrene was separated under vacuum from the styrene on the potassium amide, and the vessel was sealed off. The styrene remaining on the potassium amide almost completely lost its color after 2 days and then turned into a solid polymer, whereas the separated portion of the monomer retained its reddish-violet coloration and remained completely fluid for the month during which it was observed. It is therefore probable that the intense coloration which occurs when styrene is acted on by bases, and which determines the maximum in the light absorption spectrum in the region of a wavelength of λ > 500 mμ (Fig. 2),is not due to carbanions playing a leading part in the polymerization process. The reactions of styrene with alcoholates in dimethoxyethane, described below, and also the facts presented in [16], which is devoted to a discussion of the mechanism of the initiation of styrene polymerization

by potassium amide in liquid ammonia agree with this supposition. It is suggested that this problem should be studied further.*

Methylmethacrylate is a more reactive monomer than styrene with respect to anionic polymerization, and was converted in the course of a few minutes over potassium amide with the liberation of a large amount of heat. The polymer was dissolved in chloroform and precipitated with methanol. The characteristic viscosity of the chloroform solution at 25° [η] was 3.2 and 2.2.

The experiments with alcoholates were carried out using a high-vacuum technique, but some stages were performed under an atmosphere of purified nitrogen. Particular attention was paid to careful purification of the dimethoxyethane and to the complete removal of alcohol from the alcoholate. To this end, the solvent was distilled several times onto the surface of a mirror of metallic potassium, thereby achieving a solution of potassium in dimethoxyethane having a stable blue coloration. About 2 ml of dimethoxyethane containing 0.02 or more ml of alcohol, from 0.01 to 0.1 g metallic potassium for the formation of the alcoholate, and 0.5-3 ml of monomer were taken for the experiments. When the combined solution and suspension of alcoholate in dimethoxyethane were mixed with styrene a blue coloration rapidly appeared, and the solid alcoholate dissolved. In the reactions of styrene with $CH_3OCH_2CH_2OK$ and CH_3OK the colorations are different in shade, but the maximum in the light absorption spectrum is in the same wavelength region of λ = 520-530 mμ (Fig. 2.2 and 2.3). It is noted that the coloration is retained and only weakens when the solution comes into contact with air, or even when alcohol is added. The yield of styrene polymer was 3-30%, depending on the reaction conditions. The characteristic viscosity of toluene solutions of the polymers formed in the presence of $CH_3OCH_2CH_2OK$ was equal to [η]: 1.3, 0.3, 0.3, 0.3, 0.9, 0.6, 0.5, 1.2, 1.3, 0.6, and 0.2 using CH_3OK. Polymer was absent in the control experiments carried out without alcoholate.

When methylmethacrylate was mixed with a combined solution and suspension of $CH_3OCH_2CH_2OK$ in dimethoxyethane, rapid polymerization accompanied by a rise in the temperature of the solution was observed. The polymer yield was higher than in the case of styrene. The characteristic viscosities of chloroform solutions of the polymers [η]: 0.13, 0.20, 0.25, and 0.53.

We plan to continue this work with a view to a more detailed study of anionic polymerization over solid metal amides and other solid bases, and a study of the polymers obtained, and we also intend to compare the effect of solvents on the chemical activity of the alcoholates of various alcohols and metals.

We extend our gratitude to E. A. Rabinovich and Yu. P. Vyrskii for their help in the determination of the spectra and the viscosities of polymer solutions.

LITERATURE CITED

1. A. I. Shatenshtein, Isotope Exchange and the Displacement of Hydrogen in Organic Compounds [in Russian] (AN SSSR Press, 1960).
2. W. Wittig, Eighth Mendeleev Congress, Reports of Foreign Scientists [in Russian] (AN SSSR Press, 1959) p. 19.
3. A. I. Shatenshtein, Yu. G. Dubinskii, E. A. Yakovleva, I. V. Gostunskaya, and B. A. Kazanskii, Izvest. Akad. Nauk, Otdel. Khim. Nauk 1958, 104.
4. J. J. Sanderson and C. K. Hauser, J. Am. Chem. Soc. 71, 1595 (1949).
5. W. C. E. Higginson and N. S. Wooding, J. Chem. Soc. 1952, 760.
6. A. I. Shatenshtein and E. A. Yakovleva, Zhur. Ob. Khim. 28, 1713 (1958).
7. J. L. Down, J. Lewis, B. Moore, and G. Wilkinson, J. Chem. Soc. 1959, 3767.
8. F. Cafasso and B. R. Sundheim, J. Chem. Phys. 31, 809 (1959).
9. E. A. Yakovleva, É. S. Petrov, S. P. Solodovnikov, V. V. Voevodskii, and A. I. Shatenshtein, Doklady Akad. Nauk SSSR 133, 645 (1960).
10. I. V. Astaf'ev and A. I. Shatenshtein, Optika i Spektroskopiya 6, 631 (1959).
11. P. Bruylants, Bull. soc. chim. Belg. 23, 317 (1927) (cited by [12]).
12. A. Zilka, Ben-Ami Feit, and M. Frankel, J. Chem. Soc. 1959, 928.

*Note Added in Proof: If the colored styrene is distilled under high vacuum onto a quantity of fresh KNH_2 the styrene remains colorless and polymerization may proceed, accompanied by rise in temperature.

13. A. V. Topchiev, V. P. Alaniya, and I. S. Mazel', Doklady Akad. Nauk SSSR 125, 1048 (1959).
14. W. E. Goode, W. H. Snider, and R. C. Fettes, J. Polymer Sci. No. 140, 366 (1960).
15. A. I. Shatenshtein, Zhur. Fiz. Khim. 15, 246 (1941).
16. I. V. Astaf'ev, E. A. Rabinovich, and A. I. Shatenshtein, Vysokomolek. Soed. 3, No. 3 (1961).

ADSORPTION CAPACITY AND CATALYTIC ACTIVITY OF PLATINIZED CARBON IN RELATION TO ADDITION OF SOME SILANES TO UNSATURATED COMPOUNDS

V. A. Afanas'ev, V. A. Ponomarenko, and N. A. Zadorozhnyi

N. D. Zelinskii Institute of Organic Chemistry, Academy of Sciences of the USSR
(Presented by Academician A. A. Balandin, September 17, 1960)
Translated from Doklady Akademii Nauk SSSR,
Vol. 136, No. 5, pp. 1123-1126, February, 1961
Original article submitted September 14, 1960

As has previously been noted [1-3], in addition reactions of alkyl chloroalkylsilanes to 1,1,2-trifluoro-2-chloroethylallyl ether ($CH_2 = CHCH_2OCF_2CHFCl$) and 1,1,2,2-tetrafluoroallyl ether ($CH_2 = CHCH_2OCF_2CHF_2$), the strength of the adsorption interaction between the reacting molecules and the catalyst surface can play an essential role. In order to verify this, we studied the adsorption capacity of a Pt/C (1% Pt) catalyst in relation to the following alkyl- and chloroalkylsilanes: $(C_2H_5)_3SiH$ (I), $CH_3(C_2H_5)_2SiH$ (II), $C_2H_5(C_3H_7)_2SiH$ (III), Cl_3SiH (IV), $C_2H_5SiHCl_2$ (V), and $CH_3(C_2H_5)SiHCl$ (VI).

The adsorption of these materials was studied in a flow arrangement [4] at 20° and atmospheric pressure, in the relative pressure range of the vapors from 0 to 0.5. The carrier gas used was nitrogen from a cylinder, which had been dried and purified by silica gel and activated charcoal. Prior to adsorption measurements, the catalyst was heated at 300° in vacuo (about 10^{-4} mm) to remove adsorbed moisture and vapors of organic compounds. The saturated vapor pressures (P_s) of adsorbates (I)-(VI), which are needed to construct the adsorption isotherms, were determined in the same apparatus by the gas saturation method [5].

At sufficiently small streaming rates of passage of the carrier gas through the adsorbate, the adsorption rate is limited by the delivery of the vapor of the adsorbate to the weighed quantity of catalyst. The amount of vapor adsorbed will be proportional to the time of passage of the vapor-gas mixture across the catalyst layer. Thus, there is a possibility of finding P_s from the amount of adsorbed vapor and the volume of carrier gas passing through the system. The vapor pressure (P_s) is found from the relation $P_s/P = v/V$, where P is the total pressure in the system (atmospheric), v is the volume of material discharged in unit time, calculated by the Gas Laws from the weight of adsorbed material, and V is the total volume of mixture, calculated from the stream rate, which was measured by a flowmeter.

As can be seen from Fig. 1, the amount of adsorption of all the alkyl silanes is linearly dependent on the time of passage of the stream. Kinetic curves were measured at a stream rate through the adsorbate of $v_1 = 1$ ml/min, and a rate of the diluted stream of $v_2 = 20$ ml/min. The values of P_s calculated from these results are given in Table 1, together with other P_s values, calculated by the method of Gauss and Newton, and by Antuan's* [5] equation, for comparison. The agreement of all the values is quite satisfactory, taking into account the relatively low accuracy in determining P_s from temperatures of boiling points, and from experiments where the error in determining v_1 and v_2 by flowmeters is about 0.1 ml/min.

Figure 2 contains the adsorption isotherms of the materials studied in the P/P_s range from 0 to 0.5. The values of P/P_s were calculated from the formula [4]: $P/P_s = v_1/(v_1 + v_2 - v_2 \cdot P_s/P_a)$, where P_a is atmospheric pressure. The adsorption capacity (a.c.) for the materials was not uniform – the chloroalkylsilanes were adsorbed much more strongly by the catalyst than the alkylsilanes. The materials can be placed in the following sequence, according to increasing a.c.: VI > IV > (V) > II > I > III.

*Name not verified.

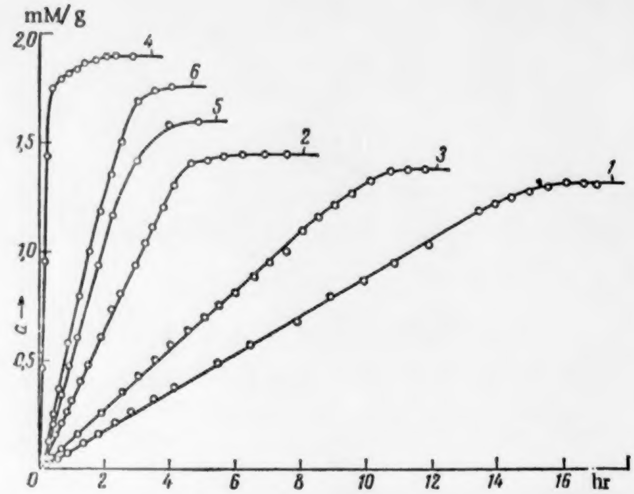

Fig. 1. Kinetic adsorption curves for silane vapors on 1% Pt/C at 20°. The numbers on the curves here and in Fig. 2 correspond to the numbers of the compounds in Table 1.

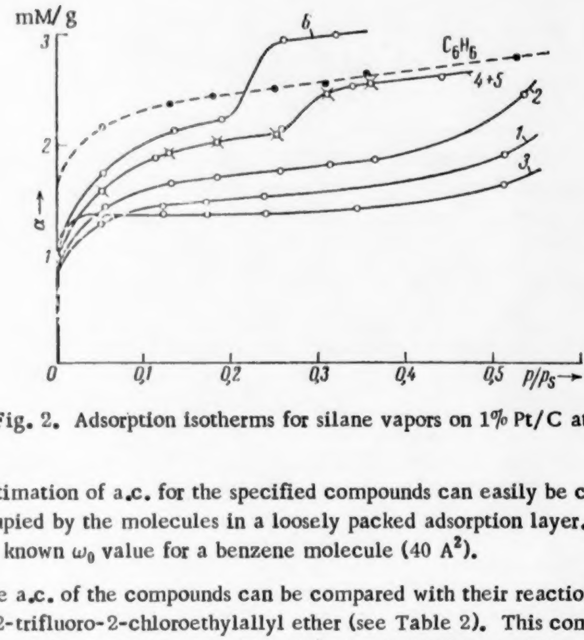

Fig. 2. Adsorption isotherms for silane vapors on 1% Pt/C at 20°.

A quantitative estimation of a.c. for the specified compounds can easily be carried out by comparing the effective areas ω_0 occupied by the molecules in a loosely packed adsorption layer. ω_0 was calculated from the BET equation, from the known ω_0 value for a benzene molecule (40 A^2).

The results for the a.c. of the compounds can be compared with their reaction capacity in competitive addition reactions to 1,1,2-trifluoro-2-chloroethylallyl ether (see Table 2). This comparison shows that with one component of the mixture being kept the same (IV or V) the yield of the addition product of the second component increases with increasing ω_0 (i.e., with decreasing a.c.). This is the case for the mixtures IV + II, IV + I, IV + III, and V + VI, V + III. In addition, for materials with practically the same a.c. (IV and V) the yield of the addition products is also the same.

The effect of the strength of adsorption interaction in competitive addition reactions, taking account of conclusions made earlier [3], can be interpreted in the following way. The increased a.c. of chlorosilanes leads to formation on the surface of very active chlorosilane radicals ($Cl_3\dot{S}i$ and $Cl_2\dot{S}iC_2H_5$), which by trapping the hydrogen of the trialkylsilane form the less active trialkylsilane radical. The latter have already been added to the multiple bond of an unsaturated compound. Direct addition of chlorosilane radicals to unsaturated compounds

TABLE 1

No.	Silane	Molecular weight	Temp., °C	p, mm	P_s (at 20°) expt.	P_s (at 20°) calculated, Gauss and Newton	P_s (at 20°) calculated, Antuan's equation
I	$(C_2H_5)_3SiH$	116,28	107,0	745	27,0	28,1	29,1
II	$CH_3(C_2H_5)_2SiH$	102,25	78,0	748,5	83,4	80,3	84,0
III	$C_2H_5(C_3H_7)_2SiH$	126,19	152,5	754	33,0	33,4	36,4
IV	Cl_3SiH	135,47	31,8	766	467,8	498,5	495,0
V	$C_2H_5SiHCl_2$	129,07	76,0	770	86,9	91,8	91,1
VI	$CH_3(C_2H_5)SiHCl$	108,65	69,0	769	114,0	121,2	120

TABLE 2

No.	Components	No. of compound (per Table 1)	Yield %	Relative activity	ω_0 (A^2)
1	Cl_3SiH	IV	42		50
	$C_2H_5SiHCl_2$	V	42	1	50
2	Cl_3SiH	IV	20		50
	$(CH_3)(C_2H_5)_2SiH$	II	33	1,7	58
3	Cl_3SiH	IV	31		50
	$(C_2H_5)_3SiH$	I	51	1,7	64
4	Cl_3SiH *	IV	29		50
	$(C_2H_5)(C_3H_7)_2SiH$ *	III	63	2,2	70
5	Cl_3SiH	IV	32		50
	$(CH_3)(C_2H_5)SiHCl$	VI	35	1,1	40
6	$C_2H_5SiHCl_2$	V	27		50
	$(CH_3)(C_2H_5)SiHCl$	VI	33	1,2	40
7	$C_2H_5SiHCl_2$	V	25		50
	$(CH_3)(C_2H_5)_2SiH$	II	47	1,9	58

* Analysis of the reaction products in the gas phase (~200 cm^3) here showed that they consisted of up to 96% hydrogen. The formation of hydrogen is evidently due to recombination of H atoms formed during homolytic splitting of the bond $H-Si \equiv Si-H \rightarrow \equiv \dot{S}i + H$.

also takes place. During the addition of $(CH_3)(C_2H_5)(Cl)SiH$ to Cl_3SiH and $C_2H_5SiHCl_2$, the picture changes a little. The increased a.c. and smaller energy of the Si − H bond for $(CH_3)(C_2H_5)(Cl)SiH$ (compared to Cl_3SiH and $C_2H_5SiHCl_2$), favor the preferential formation of $(CH_3)(C_2H_5)(Cl)\dot{S}i$ radicals on the surface. However, this radical cannot trap hydrogen atoms so easily from Cl_3SiH and $C_2H_5SiHCl_2$, where the hydrogen forms a stable bond with the silicon. Therefore, the preferential reaction route of the $(CH_3)(C_2H_5)(Cl)\dot{S}i$ radical is addition to the multiple bond of an unsaturated compound. Thus, in this case, in spite of its increased a.c., $(CH_3)(C_2H_5)(Cl)SiH$ will be more likely to undergo addition than Cl_3SiH or $C_2H_5SiHCl_2$.

The above considerations about the ease of trapping the hydrogen atoms of Si − H bonds by chlorosilane radicals, and the unusual chain transfer, are evidently also applicable to the intermediate radicals $X_3Si\dot{C}H_2\dot{C}H-R$ (X = Cl, the alkyl group R = CH_2OCF_2CFClH).

LITERATURE CITED

1. A. D. Petrov, V. A. Ponomarenko, and G. V. Odabashyan, Doklady Akad. Nauk SSSR 121, No. 2, 307 (1958).
2. A. D. Petrov, V. A. Ponomarenko, G. V. Odabashyan, and S. I. Krokhmalev, Doklady Akad. Nauk SSSR 124, No. 4, 838 (1959).
3. V. A. Ponomarenko, G. V. Odabashyan, and A. D. Petrov, Doklady Akad. Nauk SSSR 131, No. 2, 321 (1960).
4. A. M. Rubinshtein and V. A. Afanas'ev, Peredovoi Nauchno-tekhnich. i Proizvodstv. Opyt. 39 (Moscow, 1957); V. A. Afanas'ev and A. M. Rubinshtein, Zavod. Lab. No. 7, 830 (1958).
5. Physical Methods of Organic Chemistry [Russian translation] (IL, 1952) Vol. 2, p. 349.

SOME ELECTROPHYSICAL PROPERTIES OF POLYMERIC COMPLEXES OF TETRACYANOETHYLENE WITH METALS

A. A. Berlin, L. I. Boguslavskii, R. Kh. Burshtein, N. G. Matveeva, A. I. Sherle, and N. A. Shurmovskaya

Institute of Chemical Physics, Academy of Sciences of the USSR
and Institute of Electrochemistry, Academy of Sciences of the USSR
(Presented by Academician A. N. Frumkin, August 13, 1960)
Translated from Doklady Akademii Nauk SSSR,
Vol. 136, No. 5, pp. 1127-1129, February, 1961
Original article submitted August 13, 1960

It was shown earlier that tetracyanoethylene reacts with metallic powders and metal salts to form polymeric chelate compounds of azoporphyrin structure [1]. The polymeric chelate compounds of tetracyanoethylene and metals are not soluble in the usual organic solvents, alkalis, or weak acids. These materials do not melt, withstand many hours of heating at t = 500°, possess interesting magnetic properties, and their EPR spectra contain wide (600-800 oersted) and narrow peaks. The infusibility and insolubility of these polymeric compounds, as in the case of other polychelate compounds [2], make their investigation and treatment difficult. Recently, theoretical and practical interest has developed in methods of obtaining coatings and plastics based on the polymeric chelates of tetracyanoethylene and its mixtures with di- and tetranitriles [3].

Fig. 1. Infrared spectrum of the polychelate complex of copper.

The present work contains results of an investigation on the electrophysical properties of layers of polymeric chelate compounds of tetracyanoethylene, chemically bonded to metals, which are obtained by treating the surface of metal laminas (copper, iron, nickel, and a series of different metals) with tetracyanoethylene vapor.

The metal laminas, which have been degreased and in some cases electropolished and scoured as well, are placed in a vessel with tetracyanoethylene, and the vessel is then evacuated to 10^{-5} mm Hg. Reaction is carried out between 150-400° for 5-20 hours and results in the formation of a film of polymeric complex stably bound to the metal surface.

The samples so obtained were subjected to further investigations without additional treatment. The thickness of the film was determined from the specific weight of polymer and the weight of the film. In experiments with iron, the thickness of the film of polymeric complex was $5 \cdot 10^{-6}$ to $3 \cdot 10^{-5}$ cm, depending on the conditions of treatment. The films obtained are extremely difficult to ignite, and consequently the microanalytical data give rather low carbon contents. Thus, for the polychelate complex of copper,

Found %: C 43.66, Cu 20.62
Calculated %: C 45.66, Cu 19.88.

The infrared spectrum of the film* obtained on copper (Fig. 1) showed complete absence of any absorption maxima in the region 800-2300 cm^{-1}, which indicates a "parquet-formation" structure of the polymer obtained, and which can probably be represented by the following:

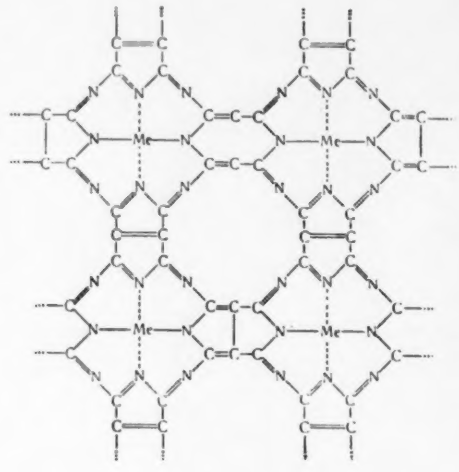

The electrophysical properties of the films were studied by means of a bridge of variable current with a capacity in parallel and a resistance,in the range 200 to 200,000 cps.

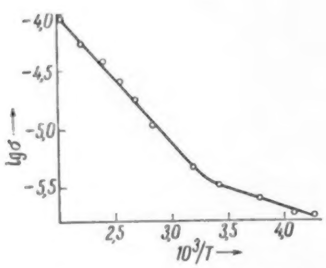

Fig. 2. Dependence of the specific conductivity on the reciprocal of the temperature for a film of polymeric complex on scoured iron; 300°, 10 hr.

Mercury was poured into a test tube,which had a thin section at the end with two wires sealed in. One wire was attached to the lamina which was covered by the polymeric complex and immersed in mercury, and the other connected the mercury contact with the measuring device. Thus, the film of the polymeric complex acted as the dielectric of a condenser whose coatings were the metallic lamina and the mercury.

Measurements were made at 10^{-5} mm Hg. The presence of air usually changed the results; this will be investigated separately.

Specific conductivity and capacity of the polymeric complex films were measured with respect to temperature, duration of heating, and method of treatment of the surface of the metal. With heating of the iron plates in tetracyanoethylene vapor at 250° over 3 hr, the film of the polymeric complex became comparatively thin ($3 \cdot 10^{-6}$ cm), with a specific conductivity of about $3 \cdot 10^{-9}$ $ohm^{-1} \cdot cm^{-1}$; the value of the effective dielectric constant at 3000 cps, calculated from the formula for a flat condenser, was 7. During heating of the plates under the same conditions over 3 hr, their specific conductivity increased to $3 \cdot 10^{-8}$ $ohm^{-1} \cdot cm^{-1}$, and the value of the effective dielectric constant increased to 36. Change of the temperature of treatment of the films from 250 to 450°, but with the same duration (10 hr)** resulted in increase of specific conductivity from $5 \cdot 10^{-8}$ to $5 \cdot 10^{-6}$ $ohm^{-1} \cdot cm^{-1}$; values of the effective dielectric constant reached 70. From the sign of the thermo-emf it follows that the films have a p-type conductivity.

Figure 2 shows the dependence of the specific conductivity on the reciprocal of the temperature for a film of polymeric complex on iron. The measurements were made in the range −40 to +220°. Two linear sections can clearly be seen on the curve. The first section, in the temperature range −40 to +30°, corresponds to an activation energy of 0.07 to 0.12 ev and the second, from 30 to 250°, to an activation energy of 0.21 to 0.28 ev. The ob-

---

* The authors would like to thank Yu. Sh. Moshkovskii and N. D. Kostrova for recording the infrared spectra.

** As in original — Publisher.

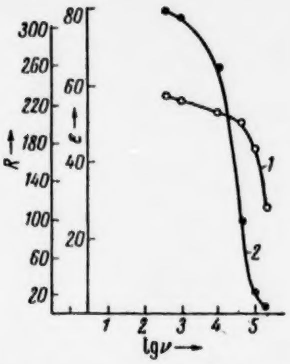

Fig. 3. Dependence of the effective dielectric permeability (1) and resistance (2) on the logarithm of the frequency for a film of polymeric complex on scoured iron; 250°, 10 hr.

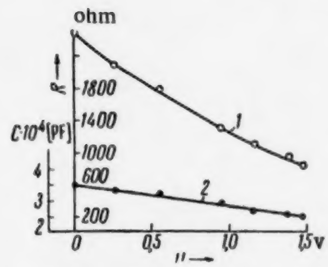

Fig. 4. Dependence of the capacity (2) and resistance (1) of a polymeric complex film on the superimposed constant voltage (on air-oxidized iron); 250°, 20 hr.

served dependence of the logarithm of the specific conductivity on the reciprocal of the temperature is analogous to the case of semiconductors with intermediate conductivity.

We also measured the dependence of the effective dielectric permeability and resistance of the samples on the logarithm of the frequency of the alternating current in the region 400 to 200,000 cps (see Fig. 3). It should be noted that the capacity and resistance of the samples decrease on superposition of a constant voltage, as can be seen from Fig. 4.

An interesting result which was obtained with plastics covered by a film of polymeric complex should also be pointed out. On passing a constant current through an alcoholic solution of copper sulfate, copper is deposited on a polymeric film (obtained on an iron lamina), and is held firmly to the surface of the complex. The comparatively high values of the effective dielectric constants suggest that we have possibly been dealing with polarized "conducting" macromolecules.

For a final explanation of the nature of the electrophysical properties of these films, particularly the possible role of heterogeneous structures, measurements of the effective dielectric constant of the complex should be carried out at higher frequencies, and preparations are being made at present to do this.

We would like to thank Academician A. N. Frumkin for his interest in the work and for his help during it.

LITERATURE CITED

1. A. A. Berlin, N. G. Matveeva, and A. I. Sherle, Izv. Akad. Nauk SSSR, Otdel. Khim. Nauk No. 12, 2261 (1959).
2. A. A. Berlin and N. G. Matveeva, Usp. Khim. 19, Part 3, 277 (1960); see also A. A. Berlin, Usp. Khim. Polimerov Part 3 (1960).
3. A. A. Berlin, N. G. Matveeva, and A. I. Sherle, Author's Certificate No. 126,612, April 7, 1959.

All abbreviations of periodicals in the above bibliography are letter-by-letter transliterations of the abbreviations as given in the original Russian journal. *Some or all of this periodical literature may well be available in English translation.* A complete list of the cover-to-cover English translations appears at the back of this issue.

CRITICAL PHENOMENA IN THE LIQUID PHASE OXIDATION OF BUTANE IN BENZENE

É. A. Blyumberg, A. D. Malievskii, and
Corr. Member AN SSSR N. M. Émanuél'

Institute of Chemical Physics, Academy of Sciences of the USSR
Translated from Doklady Akademii Nauk SSSR,
Vol. 136, No. 5, pp. 1130-1132, February, 1961
Original article submitted October 26, 1960

The efficiency of oxidation of low molecular weight hydrocarbon gases in the liquid phase [1,2] attracted interest to the use of inert solvents, which would allow the liquid-phase system to be maintained at increased temperatures, and at the same time give a high reaction rate. For the oxidation process of liquefied butane, acetic acid, which is the main reaction product, can be used as a solvent [3,4].

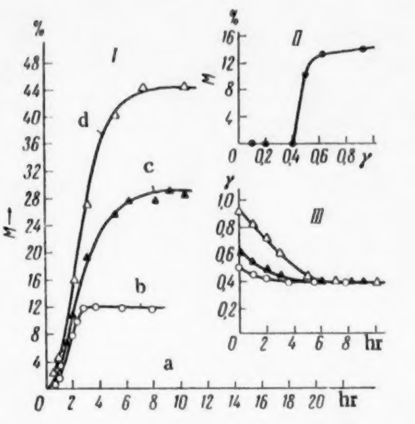

Fig. 1. I) Kinetic curves for formation of acetic acid during oxidation of liquefied butane in benzene at 170° and a pressure of 50 atm: a) $\gamma_{in} \leq 0.4$; b) $\gamma_{in} = 0.49$; c) $\gamma_{in} = 0.61$; d) $\gamma_{in} = 0.92$. II) Relation between the amount of acetic acid formed after 2 hr reaction and γ_{in} under the same conditions. III) Variation of γ with the reaction time at 170° and 50 atm pressure.

The present work deals with an investigation of the oxidation of butane in benzene, during which the unusual kinetic behavior of this solvent was established. It appeared that the reaction rate and maximum formation of products of the liquid-phase oxidation of butane in benzene depended on the ratio of the concentrations of butane and benzene, $\gamma = [RH]/[C_6H_6]$. This relation was clearly of a critical nature, i.e., there was a value of the ratio $[RH]/[C_6H_6] = \gamma_{cr}$ below which the oxidation of butane did not occur at all, and above which the usual autocatalytic reaction developed. The experiments were carried out in a special autoclave, adapted for oxidation of liquified hydrocarbon gases [2]. In order to accelerate the process (to decrease the induction period), some cobalt stearate (0.04 mole% of initial butane) was used. The course of the oxidation was controlled in accordance with the kinetic curve for the formation of the main reaction products, acetic acid and methyl ethyl ketone, and similarly for the intermediate product, the hydroperoxide of n-butane.

Fig. 1,I contains the kinetic curves for the formation of acetic acid during oxidation of liquid butane in benzene at 170° and 50 atm pressure and illustrates the critical nature of the benzene concentration.

It can be seen that the formation of acetic acid decreases with increasing amount of benzene in the initial mixture down to a value of $\gamma = 0.40$, when the reaction stops completely. This effect is shown graphically in Fig. 1, II, which shows the dependence of the amount of acetic acid formed after 2 hr reaction on γ. An insignificant change in the value of γ near to $\gamma_{cr} = 0.40$ results in a sudden transition from complete absence of

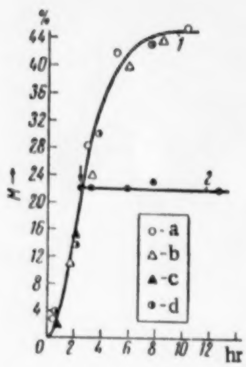

Fig. 2. Introduction of butane and benzene during the course of the reaction at 170° and 50 atm pressure. 1) Kinetic curve for the formation of acetic acid at $\gamma_{in} = 0.92$, transferred from Fig. 1,I. The points represent the kinetics of formation of acetic acid, starting at the moment of addition of butane up to $\gamma = 0.92$ to a mixture with $\gamma_{in} = 0.40$, which had been kept in the vessel: a) 0.5 hr; b) 1.5 hr; c) 2.5 hr; d) 4 hr. 2) Curve for formation of acetic acid during addition to mixtures with $\gamma_{in} = 0.92$ of fresh benzene up to $\gamma = 0.40$. The point at which the benzene was added is marked with an arrow.

reaction to oxidation of butane at a considerable rate. It can easily be seen that under these conditions if a mixture with $\gamma > 0.40$ is taken for the experiment the reaction will go so long as γ does not reach $\gamma_{cr} = 0.40$ during the course of the process. With the help of gas chromatography, we followed the reaction until the butane had been used up, and actually observed cessation of the process as soon as the value of γ had decreased to 0.4 (Fig. 1,III). By beginning with $\gamma_{in} = 0.92$, and artificially decreasing γ to γ_{cr} in the course of the reaction by adding fresh benzene, we also observed complete cessation of the process (Fig. 2, Curve 2). One other series of experiments was also carried out. Into the reaction vessel, in which a mixture of butane and benzene with $\gamma \leq \gamma_{cr}$ had been kept under the reaction conditions for a long time, fresh butane was added until $\gamma > \gamma_{cr}$. The oxidation reaction of butane started immediately. The time the mixture had been kept under the conditions of "no reaction" had absolutely no effect on the nature of the kinetic curves after the mixture had been diluted with butane (different points on Curve 1, Fig. 2). These experiments show that the observed kinetic effects are closely linked with the presence of benzene in a specific concentration, but without formation of any of its conversion products (for example, phenol). The benzene molecules evidently react with peroxide radicals $RO_2^{\bullet}$, forming a new complex radical $[C_6H_6RO_2]^{\bullet}$, which is considerably less active than $RO_2^{\bullet}$, and hence incapable of extending the chain further. Thus, the interaction of benzene with $RO_2^{\bullet}$ is essentially a chain-breaking reaction, and the concurrence of this reaction with that of hydroperoxide formation has a bearing on the principal phenomena which we observed during the oxidation of butane in benzene.

For a theoretical consideration of the mechanism of the process, we will introduce the formation of the complex radical $[C_6H_6RO_2]^{\bullet}$ into the universally adopted scheme of liquid-phase oxidation, as the sole chain termination reaction (we are neglecting quadratic branching $RO_2^{\bullet} + RO_2^{\bullet}$).

$$RO_2^{\bullet} + RH \xrightarrow{k_2} RO_2H + R^{\bullet} \text{ — continuation of chain,}$$

$$RO_2H \xrightarrow{k_3} RO_2^{\bullet} \text{ — chain branching,}$$

$$RO_2^{\bullet} + C_6H_6 \xrightarrow{k_4} [C_6H_6RO_2] \text{ — chain termination.}$$

Here RH represents butane. If the concentration of butane is assumed to remain constant (in the early stages of the process), this scheme yields the two linear differential equations:

$$\frac{d\,[RO_2H]}{dt} = k_2\,[RO_2^{\bullet}]\,[RH] - k_3\,[RO_2H], \tag{1}$$

$$\frac{d\,[RO_2^{\bullet}]}{dt} = w_0 - k_4\,[RO_2^{\bullet}]\,[C_6H_6] + k_3\,[RO_2H], \tag{2}$$

where w_0 is the rate of formation of the radicals. Assuming the concentration of radicals $[RO_2^{\bullet}]$ to be stationary, and solving the two equations, we ootain

$$[RO_2H] = \frac{w_0}{1 - \frac{k_4}{k_2}\frac{[C_6H_6]}{[RH]}}\left\{\exp\left\{\left(\frac{k_2}{k_4}\frac{[RH]}{[C_6H_6]} - 1\right)k_3 t\right\} - 1\right\}. \tag{3}$$

It follows from Eq. (3) that when $t \to \infty$, the value of $[RO_2H]$ tends to a constant value when $\frac{k_4}{k_2}\frac{[C_6H_6]}{[RH]} > 1$, and increases when $\frac{k_4}{k_2}\frac{[C_6H_6]}{[RH]} < 1$.

Thus, the relation $\frac{k_4}{k_2} = \frac{[RH]}{[C_6H_6]}$ is the condition for the transition from a slowly developing process to a rapid autoaccelerated one. The formation of complex radicals of the type $[C_6H_6RO_2]^{\bullet}$ has also been assumed by other workers, for example, in the investigation of the photochlorination reaction of 2,3-dimethylbutane in organic solvents [5], the reaction of triphenylmethyl radicals with a series of benzene derivatives [6], the polymerization reaction of styrene in bromobenzene [7], the decomposition reaction of di-tertiary-butyl peroxide in cyclohexane in the presence of benzene and chlorobenzene [8], the decomposition reaction of benzoyl peroxide in benzene [9], in the EPR investigation of radicals formed during the radiolysis of benzene and its derivatives [10], and others. However, the kinetic characteristics of the elementary reaction of formation of the complex radical could not be obtained from the materials used in these investigations. The results of this present work make it possible to evaluate, to the first approximation, the activation energy for the reaction of the radicals with benzene. We determined experimentally the values of $k_2/k_4 = 1/\gamma_{cr}$ at different temperatures:

T, °C	170	145	140
γ_{cr}	0.40	0.69	0.78

From the dependence of $\lg(k_2/k_4)$ on $1/T$, the difference in activation energy between the chain continuation reaction and the complex radical formation reaction was found: $E_2 - E_4 = 9.0$ kcal/mole. Taking the value $E_2 = 11.5$ kcal/mole (by analogy with the oxidation reaction of n-decane [11]), we obtain a value for E_4 approximately equal to 2.5 kcal/mole, i.e., a very probable value for a direct addition reaction of radicals to molecules. The experimental determination of the value of E_2 for the liquid-phase oxidation of butane will enable us in the future to determine the value of E_4 more accurately.

LITERATURE CITED

1. N. M. Émanuél', Doklady Akad. Nauk SSSR 110, 245 (1950).
2. É. A. Blyumberg, Z. K. Maizus, and N. M. Emanuél', Oxidation of Hydrocarbons in the Liquid Phase [in Russian] (1959) p. 125.
3. H. M. Hutchinson and K. Stevens, U. S. Patent 2,797,209, June 25, 1957; U. S. Patent 2,801,992, August 6, 1957.
4. M. S. Furman, A. D. Shestakova et al., Doklady Akad. Nauk SSSR 124, 1083 (1959).
5. G. A. Russell, J. Am. Chem. Soc. 80, 4987 (1958).
6. R. A. Benkeser and W. Schroeder, J. Am. Chem. Soc. 80, 3314 (1958).
7. F. K. Mayo, J. Am. Chem. Soc. 75, 6133 (1953).
8. G. A. Russell, J. Org. Chem. 24, 300 (1959).
9. G. A. Razuvaev, B. G. Zateev, and G. G. Petukhov, Doklady Akad. Nauk SSSR 130, 336 (1960).
10. Yu. N. Molin, I. I. Chkheidze et al., Doklady Akad. Nauk SSSR 131, 125 (1960).
11. D. G. Knorre, Z. K. Maizus, and N. M. Émanuél', Doklady Akad. Nauk SSSR 112, 457 (1957).

THERMAL DEHYDRATION OF SILICA AND SOME PROPERTIES OF ITS SURFACE

A. V. Bondarenko, V. F. Kiselev, and K. G. Krasil'nikov

M. V. Lomonosov Moscow State University
(Presented by Academician M. M. Dubinin, September 14, 1960)
Translated from Doklady Akademii Nauk SSSR,
Vol. 136, No. 5, pp. 1133-1136, February, 1961
Original article submitted September 8, 1960

In connection with the hypothetical scheme proposed [1] for the mechanism of the dehydration of a silica surface, attempts were made [2,3] to determine more accurately the composition of the products liberated during its thermal treatment. In one study [3] it was found that during the heating of crystalline quartz powders there is liberated in some cases, in addition to water and CO_2, a combustible gas, not frozen by liquid air, which because of this feature was identified as hydrogen. The quantity of hydrogen, determined in this way, varied for different samples of quartz from 10-40% of the quantity of water liberated. One author [4], on repetition of these experiments, also observed the liberation of hydrogen, both from the original quartz powder and after its rehydration. On the assumption that in naturally occurring quartz crystals there may exist free occluded hydrogen, the author [4] attributed the hydrogen liberated from the rehydrated sample as due to dissociation of surface $-OH$ groups.

It was shown earlier [5] that a silica surface, through thermal dehydration, possesses oxidizing properties, i.e., it contains some excess oxygen atoms over and above the stoichiometric ratio. In order to establish the nature and mechanism of formation of these centers, it was necessary to undertake a detailed investigation of the composition of the gaseous phase which is formed during thermal dehydration of silica, as well as of the properties resulting at this dehydrated surface. For solution of the first problem, a very convenient method proved to be mass-spectral analysis [6,7]. As a consequence of the detailed investigation of the dehydration products of a number of samples of amorphous and crystalline silica, we established that liberation of H_2 does not occur in appreciable quantities. The suggestion was made [7] that the authors of the works [2,3] had observed the liberation not of H_2, but mainly of CO, which originated from organic impurities.

During the dehydration of several varieties of a crystalline quartz powder and silica gel, instead of H_2 we unexpectedly detected the liberation of molecular oxygen [6]. This process had two maxima depending on temperature: in the medium temperature range (500-550°) and in the high temperature range (900-950°). The origin of the oxygen liberated at medium temperatures was easily established. It appeared as a consequence of the treatment of the silicas with HNO_3 fumes, which was usually carried out with complete purification of the surface from organic impurities. Obviously, some quantity of nitric oxide becomes attached during this, forming comparatively stable bonds with the silica surface [8]. As for the liberation of O_2 at high temperatures (2nd maximum), when the main part of the "structural" water has already been removed, it was assumed that the oxygen was organically bound to the surface of the silica, and that the process of its liberation could be considered as reflecting some transformations of the surface in question. For this reason, the term "structural" oxygen was introduced [6]. However, it was emphasized that a straight-line relation apparently did not occur between the quantity of structural water contained in the silica and the quantity of O_2 liberated at high temperatures.

Regarding the liberation of O_2, one sample of silica gel (K2) behaved in an unusual way; it had been prepared under laboratory conditions by hydrolysis of $SiCl_4$ with maximum observance of purity and carefulness of operation, and, apart from protracted washing out with redistilled water, it was not subjected to any additional

purification. Mass-spectral investigation of the dehydration products of this sample revealed the absence of appreciable amounts of O_2 and H_2.

Thus, the data obtained up to now proved to be contradictory: For different preparations of silica, depending on the methods of their preparation, purification, and investigation, in certain cases [2,3] the liberation of O_2 was observed; in others, the absence of H_2 and the presence of O_2 [6,7]; and finally, practically complete absence of either (silica gel K2). Liberation of O_2 during thermal treatment of silicas fails to agree with the silica surface acquiring oxidizing properties during this treatment [5]. It is necessary to point out that in [2-4] liberation of hydrogen from silica gels was not observed, and it is only from crystalline silica that H_2 not originating from the surface can be detected.

Clarification of all these points was obtained as a result of additional experiments involving mass-analysis of the dehydration products of silica, while varying the conditions of their preparation and treatment. In particular, it seemed necessary to establish that liberation of H_2, if it occurs, is not prevented by treatment of the silica with HNO_3. New mass-analysis experiments were conducted using an external heating system [7], but without freezing out the H_2O vapors during passage into the mass spectrometer, in order to determine the relative content of other components in the gas separation with respect to H_2O.

A freshly prepared sample of silica gel, type K2, in the purest state possible, was studied both without further treatment and with HNO_3 treatment. In both cases, in the mass-spectrum, a small amount of H_2 was noted, 1-2% with respect to the liberated H_2O, which was independent of temperature. In the first case, O_2 was completely absent over the whole temperature range,and in the second case, as earlier in similar cases [7], the liberation of some quantity of O_2 and NO was observed in the medium temperature range. It may be noted that in previous experiments [7] with other varieties of silica gel, and with quartz powders liberating O_2, hydrogen appeared in the mass-spectrum when the water vapors were not frozen out. The value of the ratio of the ion currents of H_2 and H_2O always remained approximately the same, varying within the limits 1-3%. This obviously signifies that in the experiments mentioned the so-called "fragmentary hydrogen" was observed, which arises through breakdown of the molecules by electron collision in the ion source of the mass-spectrometer. By special experiments with pure water vapor introduced from the heating system into the mass spectrometer, with an invariable working procedure of the latter, it was established that the ratio H_2^+/H_2O^+ also had, in this case, a value practically coincident with that indicated above. Thus, the absence of H_2 in the dehydration products of silica gels was definitely confirmed.

One crystalline silica investigated was the powder of rock crystal with specific surface area 1.5 m^2/g, obtained by pulverizing large crystals under water in a porcelain mortar. In this instance, mass-analysis of the gases from dehydration of the powder showed the liberation of significant amounts of H_2, rapidly increasing with the elevation of the temperature of heating (at 1000° the ratio H_2^+/H_2O^+ was around 200%). Liberation of O_2 was not observed. This powder liberated H_2 also after treatment with nitric acid, although to a lesser degree.

More detailed investigation of the liberation of H_2 from the powder of rock crystal (without HNO_3 treatment) was conducted with exactly the same sample of material, which was subjected to heating up to 1000-1100° four times at one- or two-day intervals. During this time, the sample was either rehydrated or left under vacuum. It appeared that hydrogen was liberated during each period of heating the powder, independently of hydration of its surface. The amount of H_2 liberated in each subsequent experiment (both in absolute quantity and in ratio with H_2O) invariably decreased in proportion to the increase of total duration of heating (see figure). The phenomenon proceeded in a way which indicated that the hydrogen liberated during heating of the quartz powder did not originate from the surface, but had been dissolved in the lattice of the naturally occurring crystals of the mineral. This assumption was confirmed very simply. The same quantity of sample was taken from the same batch of rock crystal in the form of large lumps, with a total surface area approximately 10^4 times less than the surface area of the fine powder. During heating of these lumps, mass-analysis showed the presence of H_2 in an amount close to that observed for the fine powder. During a second heating (without rehydration) there was again recorded a marked liberation of H_2, although in smaller amounts (see figure).

Thus, it may be considered certain that in all cases of liberation of H_2 from crystalline silica [2-4] the observations related to a volume of evolved hydrogen, liberation of which was not connected with the surface hydroxyl layer. At the same time, some part of the nonfrozen combustible gas apparently was CO, since mass-analysis invariably showed its presence among the dehydration components of all silica.

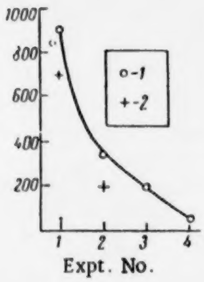

Intensity of liberation of H_2 from the powder (1) and from large lumps (2) of rock crystal (in conventional units) related to the duration of heating (number of consecutive experiments) at 1000°. Expt. No. 1) Original condition; 2) powder after a second hydration (large crystals without rehydration); 3) powder without previous rehydration; 4) powder after a third hydration.

The origin of the oxygen liberated during heating of some silica samples in the high-temperature range [6,7] remained unexplained. Since the liberation of O_2 did not occur from the purest silica gel K2, nor from rock crystal powder prepared in the laboratory and not subject to additional purification, the assumption was made that this phenomenon was caused by breakdown during heating of some impurities, the removal of which was not successful even by means of very careful purification. Such impurities might be iron oxide, Fe_2O_3, and others which get into the crystalline quartz powder and into the technical silica gel during the process of their preparation.

In order to verify this assumption, the sample of pure silica gel (K2) from which the liberation of O_2 was not observed was rendered impure by immersion in a $FeCl_3$ solution and subsequently washed until there was no further reaction for chloride. Subsequent mass-spectral investigation of the dehydration of this sample showed the liberation of O_2 in appreciable amounts, starting at 800° and above, i.e., in the region of the second maximum. NO and H_2 were not detected. Thus, the liberation of O_2 on heating silica at high temperatures was shown to result from the breakdown of the iron oxide impurity.

The investigations carried out show that during thermal decomposition of the surface of hydrated silica only water is liberated, i.e., on the surface, centers are formed in equivalent amount. Such a surface, irrespective of whether the centers join up to form radicals according to

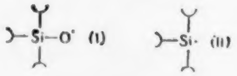

the scheme or not, cannot possess the oxidizing properties discovered earlier [5] for samples of silica gel heated in air. From this point of view, the cause of the appearance of oxidizing properties of the silica surface was naturally sought in the interaction of atmospheric oxygen with the dehydrated section. In this connection, we attempted

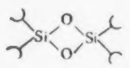

to detect the formation of active forms of oxygen during contact of atmospheric air with the silica surface at high temperatures. The experiment was carried out in the following way: A stream of purified air was passed across the sample in a quartz tube set in a furnace, and then across a solution of KI. For silica gel treated with HNO_3 vapors at furnace temperatures of 400-500°, liberation of I_2 was observed, which could be inferred as due to oxides of nitrogen, in agreement with the data of the mass-spectral analysis. For all rehydrated samples of pure silica gel and quartz up to temperatures of 900°, liberation of I_2 from the KI solution was not detected.

The formation of a surface possessing oxidizing properties must arise through interaction of atmospheric oxygen with the centers (II) and formation of the centers (I). In order to exclude the possible chemisorption of atmospheric oxygen, experiments were carried out on dehydrated silica gel under high vacuum. The silica gel was heated in a quartz ampoule connected with a glass collar, to which was fused an ampoule containing a KI solution previously deaerated in vacuum. The silica gel, heated at 700° and then cooled, was drenched with the solution of KI by breaking the glass diaphragm separating the solution from the silica gel. The silica gel immersed in the KI solution was withdrawn from the ampoule, and the liberated I_2 was back-titrated with a hyposulfite solution. These experiments showed that the silica gel surface dehydrated under vacuum, as well as in air, possessed oxidizing properties. The oxidizing properties of the investigated sample were on an average $1 \cdot 10^{-2}$ μequiv/m^2. Thus, the oxidizing properties of the silica surface are not related to chemisorption of oxygen.

Corresponding to the best screening of Si^{4+}, as indicated in [9], oxygen atoms must be present on the silica surface. From this viewpoint, the centers (II) appear to be unstable forms. As noted earlier [5], the majority of the centers (I) and (II) self-unite, forming strained regions of the siloxane surface. However, isolated, incomplete SiO_3^+ tetrahedra (II) apparently change orientation, so that oxygen atoms appear on the surface. This leads to a manifestation of oxidizing properties of the dehydrated silica surface, and also to the formation of space defects.

LITERATURE CITED

1. W. A. Weyl, Research 3, 230 (1950).
2. L. Müller, Koll. Z. 142, No. 2/3, 117 (1955).
3. W. Stöber, Koll. Z. 145, No. 1, 17 (1956).
4. S. P. Zhdanov, Izvest. Akad. Nauk SSSR, Otdel. Khim. Nauk No. 2, 352 (1959).
5. V. F. Kiselev, K. G. Krasil'nikov, and E. A. Sysoev, Doklady Akad. Nauk SSSR 116, 990 (1957).
6. A. V. Bondarenko, Doklady Akad. Nauk SSSR 125, No. 3, 573 (1959).
7. A. V. Bondarenko, Vestn. Moskovsk. Univ., Ser. III, No. 1, 11 (1960).
8. L. M. Roev and A. N. Terenin, Doklady Akad. Nauk SSSR 125, No. 3, 588 (1959).
9. W. A. Weyl, A New Approach to the Chemistry of the Solid State and Its Application to Problems in the Field of Silicate Industries (Pennsylvania, 1958).

All abbreviations of periodicals in the above bibliography are letter-by-letter transliterations of the abbreviations as given in the original Russian journal. *Some or all of this periodical literature may well be available in English translation.* A complete list of the cover-to-cover English translations appears at the back of this issue.

SOME PROPERTIES OF POLYMERIC SEMICONDUCTING MATERIALS

R. M. Voitenko and É. M. Raskina

Institute of Petrochemical Synthesis, Academy of Sciences of the USSR
(Presented by Academician V. A. Kargin, September 12, 1960)
Translated from Doklady Akademii Nauk SSSR,
Vol. 136, No. 5, pp. 1137-1138, February, 1961
Original article submitted August 4, 1960

The electroconductivity-temperature relationship of the recently obtained semiconducting polymers based on polyacrylonitrile and polyvinylchloride has an exponential character

$$\sigma \sim e^{-\Delta E/2RT}. \tag{1}$$

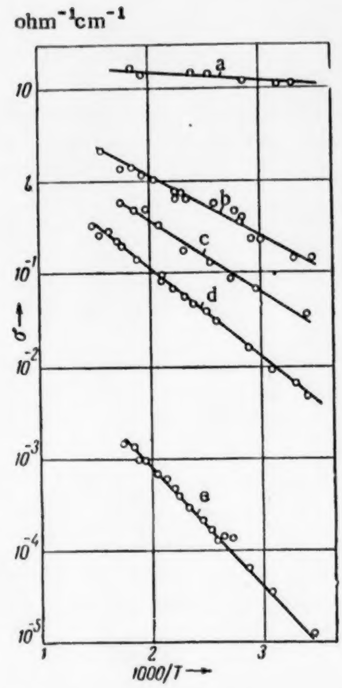

Fig. 1. Electroconductivity-temperature relationship for some samples of polyacrylonitrile: a) sample No. 1, ΔE = = 0.18 ev; b) No. 2, ΔE = 0.26 ev; c) No. 3, ΔE = 0.32 ev; d) No. 4, ΔE = = 0.39 ev; e) No. 5, ΔE = 0.51 ev.

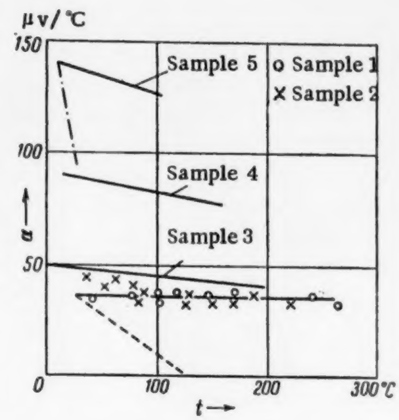

Fig. 2. Differential thermoelectromotive force-temperature relationship for the same samples of polyacrylonitrile as in Fig. 1.

The activation energies ΔE of these materials lie in the range 1.7 to 0.18 ev, depending on the nature of the treatment of the original polymer [1,2].

If the usual assumption is made that σ = enu, where e is the electronic charge, n is the concentration of current carriers, and u is the mobility of the current carriers, then such an electroconductivity-temperature relationship can be produced either by an exponential increase of the number of current carriers n, when ΔE is the width of the forbidden band (if the band model is used for consideration

of the semiconducting polymers), or by an exponential increase of the mobility of the current carriers u ~ ~ $e^{-\Delta E/RT}$.

Investigation of the temperature-differential thermoelectromotive force relationship can give the answer to the question proposed above. If increase of electroconductivity is dependent on the increase of concentration of carriers, then it ought to be accompanied by a decrease of the differential thermoelectromotive force.

In this case, following the band theory,

$$\alpha = \frac{k}{e}\left(A - \frac{\Delta E}{2RT}\right), \tag{2}$$

where A is a coefficient nearly independent of temperature. If the concentration of carriers is not dependent on temperature, the thermoelectromotive force ought to increase logarithmically with increase of temperature [3]. In Fig. 1 are shown the temperature-conductivity relationships of some samples of polyacrylonitrile. In Fig. 2 are shown the temperature-thermoelectromotive force relationships of these same samples.* In Fig. 2 are shown, for comparison, the lines of the theoretical temperature-thermoelectromotive force relationships which were plotted on the basis of formula (2) for ΔE = 0.18 ev (dotted line) and ΔE = 0.51 ev (dot-dash line).

From the figures it is clear that the thermoelectromotive force in general changes little, or not at all, with temperature.

From this, it appears that the conclusion can be made that the temperature-conductivity relationship of the materials investigated is determined in the main by an exponential increase of the mobility of the current carriers with temperature.

LITERATURE CITED

1. A. V. Topchiev, M. A. Geiderikh, B. É. Davydov, V. A. Kargin, B. A. Krentsel', I. M. Kustanovich, and L. S. Polak, Doklady Akad. Nauk SSSR 128, No. 2, 312 (1959).
2. M A. Geiderikh, B. É. Davydov, B. A. Krentsel', I. M. Kustanovich, L. S. Polak, A. V. Topchiev, and R. M. Voitenko, International Symposium on Macromolecular Chemistry [in Russian] (1960) Section III, p. 85.
3. A. F. Ioffe, Physics of Semiconductors [in Russian](Izd. AN SSSR, 1957).

All abbreviations of periodicals in the above bibliography are letter-by-letter transliterations of the abbreviations as given in the original Russian journal. *Some or all of this periodical literature may well be available in English translation.* A complete list of the cover-to-cover English translations appears at the back of this issue.

*For samples 3, 4, and 5, the integral thermoelectromotive force was measured as a function of the temperature gradient by the method of charged condensers. In the figure is shown the differential thermoelectromotive force obtained by differentiation of the experimental relationship.

DESOLUBILIZATION OF HYDROCARBONS FROM SOLUTIONS OF NAPHTHENIC ACID SOAPS AND POTASSIUM LAURATE

P. A. Demchenko and Corr. Member AN SSSR A. V. Dumanskii

Institute of General and Inorganic Chemistry, Academy of Sciences of the USSR
Translated from Doklady Akademii Nauk SSSR,
Vol. 136, No. 5, pp. 1139-1141, February, 1961
Original article submitted November 5, 1960

Solubilized systems are formed during manufacture of synthetic detergents, alkaline purification of petroleum fractions, emulsion polymerization of monomers, and in other branches of industry. Insufficient study of the different factors affecting the processes of solubilization and desolubilization prevents development of the theoretical basis of the breaking-down of solubilized systems into the separate components and industrial preparation of pure surface-active agents. Solubilization and desolubilization appear to be the least-studied problem of colloid chemistry. Investigation of solubilization has been the subject of a small amount of work [1-5], but apparently desolubilization has not yet been studied.

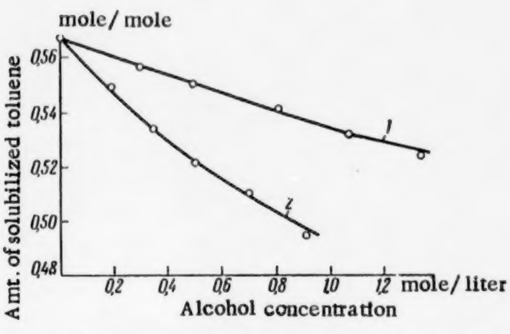

Fig. 1. Effect of ethylene glycol (1) and glycerine (2) on the solubilization of toluene in 0.3 M solutions of potassium laurate (at 60°).

In the process of solubilization, the hydrocarbons become disposed in the oleophilic region of the micelle [1,2]. Desolubilization of them is possible through breakdown of the micellar structures, and reduction of the oleophilic properties of the detergent solutions. This assumption was confirmed by investigation of the desolubilization of hydrocarbons from aqueous solutions of naphthenic acid soaps and potassium laurate. Low molecular organic compounds containing oxygen were used as desolubilizers: aliphatic alcohols, glycols, glycerine, formalin, dioxane, and others. In a solution containing soap at the most critical concentration for micelle formation [6], the maximum quantity of hydrocarbon was solubilized by the method described earlier [7]. A measured amount of this solution was then transferred to the apparatus, the calculated amount of desolubilizer was added, and the separation of the solubilized hydrocarbon as a separate phase in the graduated tube of the apparatus was observed. Experimental data are presented in Figs. 1-4.

Addition of increasing amounts of glycol and glycerine to a 0.3 M solution of sodium laurate reduces its solubilizing capacity with respect to toluene, the desolubilizing action of glycerine being greater than that of glycol (Fig. 1). Aliphatic alcohols show a complex effect on solubilization of hydrocarbons in detergent solutions, depending on the length of their hydrocarbon chain: If of low molecular weight, they reduce; if of high molecular weight, they increase the solubilization. Thus, for example, from Fig. 2 it is seen that amyl and butyl alcohols sharply increase, but ethyl and methyl alcohols decrease the solubilization of n-heptane in 0.3* M solutions of sodium naphthenate (mol. wt. 297). Propyl alcohol possesses intermediate properties. Small additions of propanol considerably decrease the solubilization, but with a concentration of more than 15 moles per mole of soap,

*Cf. note on page 164.

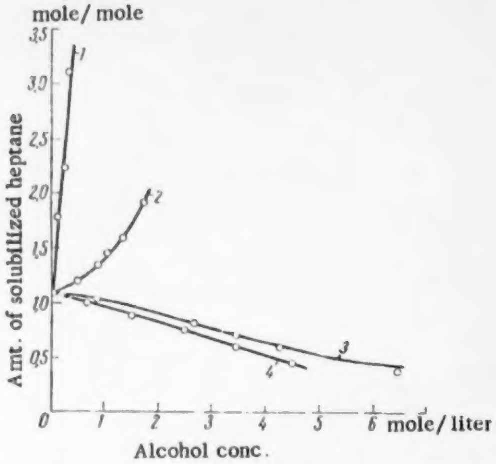

Fig. 2. Effect of aliphatic alcohols on the solubilization of n-heptane in 0.1*M sodium naphthenate solution: 1) n-amyl alcohol; 2) n-butyl alcohol; 3) ethyl alcohol; 4) methyl alcohol.

the solubilization noticeably increases. Acetone and dioxane proved to be more effective desolubilizers than low molecular weight alcohols. By addition of approximately 3 mole/liter of dioxane to an 0.3 M sodium naphthenate solution, its solubilizing capacity is decreased nearly 2.3 times (Fig. 3).

In view of the importance of desolubilization in the purification of naphthenic acids from the unsaponified impurities, the system sodium naphthenate—heptane—acetone—water was systematically investigated. From the experimental data given in Fig. 4 it is seen that with increasing additions of acetone the solubilization of heptane in 0.3 M sodium naphthenate (mol. wt. 334) solution sharply decreases, and at an acetone concentration of approximately 3.0-3.5 mole/liter the curve passes through a minimum. Further increase in the acetone concentration of the system increases the absorption of heptane into the volume of the solution. An analogous regularity was observed for mixtures of sodium soaps of naphthenic acids. A particularly sharp decrease of

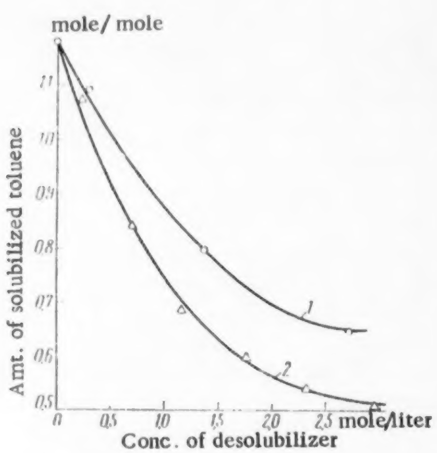

Fig. 3. Effect of addition of acetone (1) and dioxane (2) on the solubilization of toluene in 0.3 M sodium naphthenate solution (mol. wt. 297) at 40°.

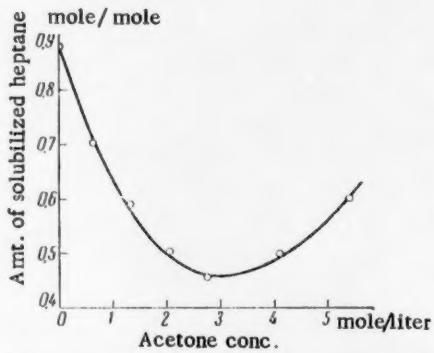

Fig. 4. Effect of addition of acetone on the solubilization of heptane in 0.3 M sodium naphthenate solution (mol. wt. 334).

solubilization of hydrocarbons was observed by introduction into the soap solution of 1.5-2.0 mole/liter of acetone and dioxane. It was found that high molecular weight hydrocarbon impurities were completely desolubilized in the presence of low-boiling hydrocarbons.

Based on the experimental data obtained, there was developed a technique for the separation of hydrocarbon impurities from solutions of naphthenic acid soaps by a desolubilization method, as follows: Technical naphthenic acids containing hydrocarbon impurities were dissolved in petroleum ether, to which was added acetone and the equivalent amount of aqueous alkali necessary for obtaining the naphthenic acid soaps. After saponification of the naphthenic acids, the system separated into two phases with a clear interface: The upper phase comprised petroleum ether containing the unsaponified impurities, and the lower a water-acetone solution of the naphthenic acid soaps. The addition of acetone was calculated so that after saponification the aqueous phase content of it would be approximately 3 mole/liter. This amount of desolubilizer is sufficient to prevent the formation of micellar structures with high oleophilic properties, and sharply decreases the solubilization of the hydrocarbons.

* As in original — Publisher

It is interesting to note that the desolubilizers also prove to be effective deemulsifiers; this guarantees simultaneous separation from detergent solutions of separate phases, with a clear interface, of the solubilized and the emulsified portions of the hydrocarbons. The hydrocarbon phase was separated by distillation. The recovered petroleum ether can be used repeatedly for dilution of the crude naphthenic acids before saponification, and the high-boiling hydrocarbons extracted from the naphthenic acids can be utilized to give consistent greases, emulsols, and other requirements. The sodium soaps of the naphthenic acids were salted out from the water-acetone solution by means of a concentrated solution of caustic soda. Through this, a soap was obtained with a 60-62% content of naphthenic acids. The "undersoap lye," consisting of the water-acetone solution of caustic soda, was reused for saponification of fresh batches of naphthenic acids. Since clear soaps of naphthenic acids with faint specific odor are formed, they can be used as independent detergents, emulsifiers, flotation agents, thickeners, and for introduction into the formulation of washing agents. The naphthenic acids liberated from the soap by mineral acid have a clear yellow color, faint odor, and contain hydrocarbon impurities amounting to 0.6-0.9%. The naphthenic acids are high-grade products which in a number of cases can be substituted for fats and fatty acids. All operations for purification of naphthenic acids of hydrocarbon impurities were carried out at ordinary temperature and with little heating. The possibility of utilization of the acetone, petroleum ether, and alkali arising from the salting-out was shown. This permits consideration that the proposed method of purification of naphthenic acids by means of desolubilization of hydrocarbon impurities may prove to be effective and economic for introduction into practice. The possibility of desolubilization of hydrocarbons from the detergent solutions by means of low molecular weight compounds containing oxygen was shown, for example, with potassium laurate and sodium naphthenate.

LITERATURE CITED

1. Z. N. Markina, K. A. Pospelova, and P. A. Rebinder, Transactions of the Third All-Union Conference on Colloid Chemistry [in Russian] (Izd. AN SSSR, 1956) p. 410.
2. M. E. L. McBain and E. Hutchinson, Solubilization and Related Phenomena (New York, 1955).
3. P. A. Rebinder, Khim. nauka i prom. No. 4, 554 (1960).
4. A. B. Taubman, Khim. nauka i prom. No. 4, 566 (1960).
5. P. A. Demchenko and A. V. Dumanskii, Koll. Zhur. 22, 272 (1960).
6. P. A. Demchenko, Masloboino-zhirovaya Prom. No. 9, 26 (1960).
7. P. A. Demchenko, Masloboino-zhirovaya Prom. No. 10, 22 (1959).

THE STABILITY OF DETONATION WAVES IN GASEOUS MIXTURES

R. M. Zaidel'

(Presented by Academician Ya. B. Zel'dovich, August 18, 1960)
Translated from Doklady Akademii Nauk SSSR,
Vol. 136, No. 5, pp. 1142-1145, February, 1961
Original article submitted April 28, 1960

Investigation of the stability of a detonation wave (d.w.) is of interest for the explanation of spin detonation. As shown in [1],at a discontinuity in the d.w. there is a hypercompression in the region of which the combustion of the mixture is accelerated. On the basis of these ideas, qualitative criteria were obtained in [2] for a d.w. instability occurring far from detonation limits. At the same time, as experiments showed [3], multiple spin develops. In the present work, the stability of a d.w. is examined with respect to small perturbations.

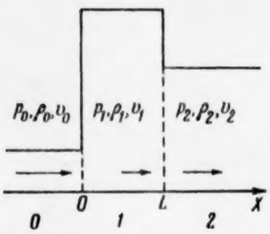

Fig. 1.

Let the d.w. be propagated from the right side to the left, and the reference system chosen so that the wave front is at rest in, and coincides with the plane YOZ,Cartesian system of coordinates. The axis OX coincides with the direction of motion of the gas (see Fig. 1). We assume, as in [2], that in the zone of the chemical reaction peak (region 1) all the values remain constant, and at a distance $L = v_1\tau$ from the front of the d.w. the reaction proceeds instantaneously, so that the final condition 2 is reached by a rapid change. In region 2 also we assume the values of p_2, ρ_2, v_2 are constant, since eventually the gradients of all quantities become as small as desired. For simplicity, we will assume that the gas is ideal and has a constant specific heat. The isentropic indexes γ before the reaction (in regions 0 and 1) and after the reaction (region 2) are equal to γ_1 and γ_2, respectively. It is considered, with no loss of generality, that the perturbations depend only on $\underline{x}$, $\underline{y}$, $\underline{t}$, and that the component of the velocity along the axis OZ equals zero.

By solution of the linearized hydrodynamic equations, in region 1 there will occur a sum of terms of the form: $A_s \exp[i(k_s x + k_0 y - \omega t]$ $(s = 1, 2, 3)$, where k_0 is the assigned wave number, ω is the unknown natural frequency, A_s are constants, $k_1 = \omega / v_1$, k_2 and k_3 are found from the equation

$$(v_1 k - \omega)^2 - c_1^2 (k_0^2 + k^2) = 0.$$

Analogously, in region 2, in the solution the terms become: $B_s = \exp[i(q_s x + k_0 y - \omega t]$ $(s = 1, 2, 3)$, where B_s are constants, $q_1 = \omega / v_2$, q_2 and q_3 are found from the equation

$$(v_2 q - \omega)^2 - c_2^2 (k_0^2 + q^2) = 0.$$

In the hypercompressed d.w. $(v_2 < c_2)$ in region 2 the disturbances must be propagated both with the gas flow $(q = q_2)$, and against the flow $(q = q_3)$. The problem consists in finding the values of ω, for which a nontrivial solution exists with the condition that the amplitude of a wave coming from infinity to the front equals zero. By analysis of the stability of a d.w. by the Chapman-Jouguet method, the calculations are not essentially changed. Such a statement corresponds to the problem of the passage of a sound wave incident to the d.w., with the condition that the amplitude of the incident sound wave reverts to zero.

Let $\epsilon_1(y,t) = \Delta_1 \exp[i(k_0 y - \omega t]$ be the displacement of the front of the shock wave ($x = 0$); $\epsilon_2(y,t) = = \Delta_2 \exp[i(k_0 y - \omega t]$ be the displacement of the reaction front ($x = L$); Δ_1 and Δ_2 are constants. The boundary conditions for the disturbances at $x = 0$ and $x = L$ are obtained (similarly to the procedure in [4]) by variation of the conditions of continuity of the flow of mass, momentum, energy, and the tangential component of the velocity. We shall characterize the kinetic reaction by the lag time τ, which depends on the effective values of the pressure and temperature in the chemical reaction peak. Let the reaction process in a given molecule of gas be described by the equation

$$d\psi/dt = f(p; T), \tag{1}$$

where ψ is the concentration of one component of the mixture. If in a certain molecule of the gas the reaction begins at the moment t and ends at a moment $t + \tau$, then, integrating (1), we obtain

$$\psi_2 - \psi_1 = \int_t^{t+\tau} f(p_1; T)\, dt', \tag{2}$$

where ψ_1 and ψ_2 are concentrations of the given component in the original mixture and in the reaction products, respectively. We assume that during the presence of the disturbance the reaction proceeds to completion, so that variation of ψ_1 and ψ_2 yields zero. Our approximation is in the fact that in the unperturbed motion the actual temperature and pressure profile are replaced by the constant values $p = p_1$, $T = T_1$. Instead of (2) there will now be $\psi_2 - \psi_1 = f(p; T_1)\tau$. For the presence of a disturbance, the expression (2) becomes

$$\psi_2 - \psi_1 = \int_t^{t+\tau+\tau'} f(p_1 + p_1'; T_1 + T_1')\, dt'. \tag{3}$$

Here τ' equals a small change of the lag time due to pressure and temperature perturbations (p_1' and T_1') in region 1. We introduce the expression $M = \partial \ln f / \partial \ln p$; $N = \partial \ln f / \partial \ln T$ (the derivatives are chosen for $p = p_1$, $T = T_1$). Restricting to first-order terms, we find from (2) and (3):

$$\tau' = -\int_t^{t+\tau} \left(M \frac{p_1'}{p_1} + N \frac{T_1'}{T_1} \right) dt'. \tag{4}$$

Integration over dt' is made along the path of the given molecule. In the unperturbed motion, the path was the line $x = v_1(t' - t)$, where t equals the instant at which the molecule passes the front of the shock wave. The presence of the disturbances bends the path of the molecule by an amount of first order of magnitude. In the calculation of τ' this correction can be neglected. During the time from t to $t + \tau + \tau'$ along the axis OX, the molecule traverses the path

$$l = \int_t^{t+\tau+\tau'} (v_1 + v_{1x}')\, dt' \approx L + v_1\tau' + \int_t^{t+\tau} v_{1x}' dt', \tag{5}$$

where v_{1x}' is the disturbance of the xth component of the velocity. If the reaction starts in the molecule at the instant t at the point $\epsilon_1(t)$ and ends at the moment $t + \tau + \tau'$ at the point $x = L + \epsilon_2(t + \tau + \tau') \approx L + + \epsilon_2(t + \tau)$, it is known that for this time from the same starting position $\epsilon_1(t)$ the molecule traverses the path l, i.e., $\epsilon_1(t) + l = L + \epsilon_2(t + \tau)$. Substituting here (4) and (5), we record the expression as:

$$v \int_t^{t+\tau} \left(M \frac{p_1'}{p_1} + N \frac{T_1'}{T_1} - \frac{v_{1x}'}{v_1} \right) dt' - \varepsilon_1(t) + \varepsilon_2(t + \tau) = 0.$$

The integral is taken along the line $x = v_1(t' - t)$. Displacement of the molecules along the axis OY can be neglected in the linear approximation. Substitution of the derivatives in the boundary expressions leads to a system of 9 linear homogeneous equations. The condition that the determinant of this system equal zero can be written

$$G_2 D_3 - G_3 D_2 = 0, \tag{6}$$

where the symbols introduced are

$$
\begin{aligned}
G_s &= \frac{\omega}{a_s}\left[1+\left(\frac{\omega}{k_0 v_1}\right)^2\right]+\frac{1-\delta}{2}\left[\frac{v_0}{v_1}+\left(\frac{\omega}{k_0 v_1}\right)^2\right],\\
D_s &= \frac{E}{a_s}-\frac{v_0-v_1}{1+(\omega/k_0 v_1)^2}\left[1+\frac{v_1}{v_0}\left(\frac{\omega}{k_0 v_1}\right)^2\right]E_s R_s,\\
E_s &= \left(\mu\frac{v_1^2}{c_1^2}+1+\frac{\omega}{a_s}\right)\frac{F_1}{v_1 a_s}-\frac{F_s}{c_2^2},\\
F_s &= \frac{1-\alpha}{2\alpha}\left(h_2-\frac{v_0}{v_2}\right)\left\{\frac{k_0}{a_s}\left[1+\left(\frac{\omega}{k_0 v_1}\right)^2\right]-\right.\\
&\quad \left.-\frac{\omega}{k_0 v_1}\left(\frac{1}{v_1}-\frac{1}{v_2}\right)\left(\frac{2\omega}{a_s}\frac{v_2}{v_1}+1-\frac{v_1^2}{c_1^2}\right)\right\}-\\
&\quad -\frac{k_0}{2(v_2 q_2-\omega)}\left[1+\left(\frac{\omega}{k_0 v_2}\right)^2\right]\left\{\frac{c_2^2}{\gamma_2 v_1^2}\left(h_2+\frac{p_1}{p_2}\right)\left[\left(1-\frac{v_1}{v_2}\right)\frac{2\omega}{a_s}+\right.\right.\\
&\quad \left.\left.+\left(2-\frac{v_1}{v_2}\right)\left(1-\frac{v_1^2}{c_1^2}\right)\right]+\left(\frac{v_2}{v_1}-1\right)\left(1-\frac{v_1^2}{c_1^2}\right)\right\},\\
&\quad R_s = e^{ia_s\tau}-1,\quad a_s = v_1 k_s-\omega,\quad s=2,3;
\end{aligned}
\tag{7}
$$

$$
\begin{aligned}
E &= i\omega\tau\left(\frac{1}{v_1}-\frac{1}{v_0}\right)\left[\frac{v_0-v_1}{1+(\omega/k_0 v_1)^2}+\frac{2v_1 N}{1-\delta}\left(\frac{v_1^2}{c_1^2}-\delta\right)\right]F_1+F_0,\\
F_0 &= \frac{k_0}{\gamma_2}\left(\frac{1}{v_2}-\frac{1}{v_0}\right)\left(h_2+\frac{p_0}{p_2}\right)\left\{\frac{\omega}{v_2 q_2-\omega}\left[1+\left(\frac{\omega}{k_0 v_2}\right)^2\right]+\frac{1-\alpha}{2}\left[\frac{v_0}{v_2}+\left(\frac{\omega}{k_0 v_2}\right)^2\right]\right\},\\
F_1 &= \frac{k_0}{\gamma_2}\left(\frac{1}{v_1}-\frac{1}{v_2}\right)\left\{\frac{\omega}{v_2 q_2-\omega}\left[1+\left(\frac{\omega}{k_0 v_2}\right)^2\right]\left(h_2+\frac{p_1}{p_2}\right)+\right.\\
&\quad \left.+\frac{h_2+1}{2}\left(1-\frac{v_2^2}{c_2^2}\right)\left[\frac{v_1}{v_2}+\left(\frac{\omega}{k_0 v_2}\right)^2\right]\right\},\\
&\quad h_1=\frac{\gamma_1+1}{\gamma_1-1},\quad h_2=\frac{\gamma_2+1}{\gamma_2-1},\quad \mu=\gamma_1 M+(\gamma_1-1)N,\\
&\quad \delta=-j^2\left(\frac{\partial V_1}{\partial p_1}\right)_H=\frac{c_0^2}{v_0^2},\quad \alpha=-j^2\left(\frac{\partial V_2}{\partial p_2}\right)_H=j^2\frac{h_2 V_2-V_0}{h_2 p_2+p_0},\\
&\quad V_0=1/\rho_0,\quad V_1=1/\rho_1,\quad V_2=1/\rho_2,\quad j=\rho_0 v_0.
\end{aligned}
\tag{8}
$$

In the case when the reaction zone is small in comparison with the wavelength of the disturbance ($k_0L \ll 1$), assuming $\tau = 0$, for (6) we obtain:

$$
\frac{\omega}{v_2 q_2-\omega}\left[1+\left(\frac{\omega}{k_0 v_2}\right)^2\right]+\frac{1-\alpha}{2}\left[\frac{v_0}{v_2}+\left(\frac{\omega}{k_0 v_2}\right)^2\right]=0. \tag{9}
$$

Considering the case of a very broad reaction zone ($k_0L \gg 1$), we note that in seeking the condition leading to instability we assume that $\mathrm{Im}\,\omega > 0$. Then, the functions $\exp[i(k_2x + k_0y - \omega t)]$ and $\exp[i(k_3x + k_0y - \omega t)]$, respectively, diminish and increase exponentially with the magnitude of coordinate $\underline{x}$. Therefore, for $k_0L \gg 1$, we have $|R_3| \gg |R_2|$ and $|D_3| \gg |D_2|$. For (6) we obtain $G_2 = 0$, i.e.,

$$
\frac{\omega}{v_1 k_2-\omega}\left[1+\left(\frac{\omega}{k_0 v_1}\right)^2\right]+\frac{1-\delta}{2}\left[\frac{v_0}{v_1}+\left(\frac{\omega}{k_0 v_1}\right)^2\right]=0. \tag{10}
$$

Equations (9) and (10) are of the same form as the characteristic equation which S. P. D'yakov [4] obtained. By using his result, we found that in the two limiting cases considered the d.w. was stable. Instability can only appear for $k_0L \sim 1$, which, however, is obvious.

Let $\omega = 0$ for $k_0 = \kappa$. It can be shown that κ will be real under the condition

$$\mu\left(\frac{v_2}{v_1}-1\right)\frac{v_1^2}{c_1^2} > 2 - \frac{v_2}{v_1} + \left[2\frac{v_2}{v_1} - 1 + (\gamma_2 - 1)\left(\frac{v_2}{v_1} - 1\right)\frac{v_2^2}{c_2^2}\right]\sqrt{\frac{1 - v_1^2/c_1^2}{1 - v_2^2/c_2^2}}. \tag{11}$$

If now in Eq. (6) a power expansion of ω and $k_0 - \kappa$ is made, then in the vicinity of the point $k_0 = \kappa$, the value $\Omega = -i\omega$ will be positive. Thus, the expression (11) appears sufficient, provided that the hypercompressed d.w. was unstable.

We consider a d.w. by the Chapman-Jouguet method: $v_2 = c_2$. For simplicity, we will assume that $p_0 = 0$; $\gamma_1 = \gamma_2 = (h+1)/h-1)$. Then Eq. (6) takes the form:

$$^1/_2 w(u_2 - u_3)B + \Phi_2\Psi_2R_2 - \Phi_3\Psi_3R_3 = 0 \tag{12}$$

where

$$B = h - \frac{(h-1)(h+2)}{h+1}\left(\frac{h^2-1}{1-w^2} + 2N\right)w\xi,$$

$$\Phi_s = w(u_s - w) - \frac{h+1}{2h}(h - w^2),$$

$$\Psi_s = (h-1)(h+2)\left(\frac{\mu}{h+1} + 2 + \frac{w}{u_s - w}\right)\frac{w}{u_s - w} + h(h+1) \tag{13}$$

$$R_s = e^{-\xi(u_s - w)} - 1, \quad s = 2, 3, \quad w = \Omega/k_0v_1, \quad \xi = k_0v_1\tau,$$

$$u_{2,3} = [-w \pm \sqrt{(h+1)(h+w^2)}]/h.$$

We designate the left-hand side of Eq. (12) by F(w); then $F(0) > 0$, F(1) is bounded. For $w \to +\infty$, $R_3 \gg$ $\gg R_2 \gg 1$; therefore, if

$$\mu > (h+3)(h+1+\sqrt{h+1})/(h-1)(h+2), \tag{14}$$

then $F(+\infty) < 0$, i.e., Eq. (12) will have a root $w > 0$. Thus, the expression (14) appears sufficient for instability of the d.w. by the Chapman-Jouguet method. We note that in the example quoted in [2] expression (14) results in the inequality $4.80 > 2.17$. Thus, in the specified case, the d.w. was unstable, which confirms the conclusion of K. I. Shchelkin.

For a more detailed investigation of the characteristic of Eq. (6), a numerical method is necessary. This task is lightened by the fact that Eq. (6) can be solved for the parameter N (or M). Then, by employing the complex number ω along a certain contour, the value may be sought for which $N(\omega)$ becomes real (positive).

In conclusion, I offer my thanks to Academician Ya. B. Zel'dovich for suggesting the topic, and for his constant interest in the work.

LITERATURE CITED

1. Ya.B. Zel'dovich and A. S. Kompaneets, Detonation Theory [in Russian] (Moscow, 1955).
2. K. I. Shchelkin, Zhur. Éksp. i Teor. Fiz. 36, 2 (1959).
3. Yu. N. Denisov, Ya. K. Troshin, and K. I. Shchelkin, Izvest. Akad. Nauk SSSR, Énergetika i Automatika 6 (1959).
4. S. P. D'yakov, Zhur. Éksp. i Teor. Fiz. 27, No. 3 (19) (1954).

All abbreviations of periodicals in the above bibliography are letter-by-letter transliterations of the abbreviations as given in the original Russian journal. *Some or all of this periodical literature may well be available in English translation.* A complete list of the cover-to-cover English translations appears at the back of this issue.

THE STEADY-STATE POTENTIALS OF ZINC AND ZINC AMALGAM IN SULFATE SOLUTIONS CONTAINING VARYING QUANTITIES OF ZINC AND HYDROGEN IONS

V. I. Kravtsov and A. F. Ermolova

A. A. Zhdanov Leningrad State University
(Presented by Academician A. N. Frumkin, July 20, 1960)
Translated from Doklady Akademii Nauk SSSR,
Vol. 136, No. 5, pp. 1146-1149, February, 1961
Original article submitted July 9, 1960

The electrode potential established at a metal — solution interface in the absence of an external polarizing current is determined by the electrode processes taking place at the electrode under consideration [1,2]. It was shown by A. N. Frumkin [1] that when metals dissolve (with the evolution of hydrogen) in acidic electrolytes the potentials obtained can be either practically equilibrium values or differ substantially from the equilibrium values, depending on the relative rates of the electrode processes occurring on the surface of the metal while dissolving. Typical examples of metals which dissolve at nonequilibrium potentials in acidic solutions are iron [3] and nickel [4]. Their steady-state potentials vary linearly as the logarithm of hydrogen ion concentration in the solution, and are independent of the concentration of their own ions. Unlike iron and nickel, such metals as lead [5] and cadmium [6] dissolve at practically equilibrium potentials in acidic electrolytes. The difference in the behavior of the metals mentioned is due to the fact that in the case of the solution of metals of the first group in solutions of their own ions the cathode process occurs primarily due to the discharge of hydrogen ions, but in the case of the second group of metals, mainly through the discharge of ions of the metal itself [1,2,7].

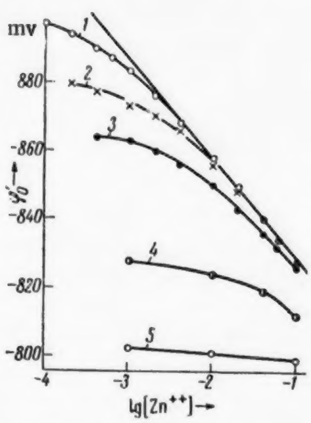

Fig. 1. Steady-state potential of zinc at different H_2SO_4 concentrations: 1) 10^{-4}N; 2) $5 \cdot 10^{-4}$N; 3) 10^{-3}N; 4) 10^{-2}N; 5) 10^{-1}N.

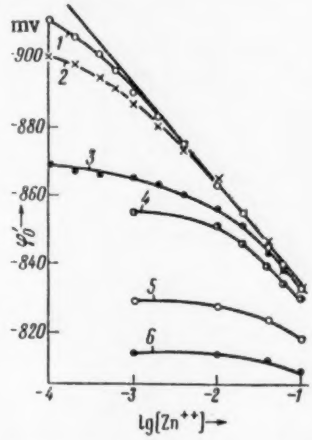

Fig. 2. Steady-state potential of zinc amalgam at different H_2SO_4 concentrations: 1) 10^{-3}N; 2) 10^{-2}N; 3) 10^{-1} N; 4) $2 \cdot 10^{-2}$N; 5) $5 \cdot 10^{-1}$N; 6) 1N.

TABLE 1

Steady-State Potentials of Zinc and Zinc Amalgam in Solutions Not Containing Added $ZnSO_4$

$[H_2SO_4]$, N / pH		10^{-4} / 4,85	10^{-3} / 3,84	10^{-2} / 2,81	10^{-1} / 1,74	$2\cdot10^{-1}$ / 1,44	$5\cdot10^{-1}$ / 0,67	1,0 / 0,36
φ_0', v	Zn	0,897	−0,864	−0,832	−0,805	—	—	−0,774
	Zn(Hg)	—	−0,915	−0,903	−0,870	−0,858	−0,829	−0,814

In the present study, the case where the quantities of hydrogen and metal ions participating in the cathode process are commensurable is investigated, taking zinc and zinc-amalgam electrodes as samples. According to data available in the literature [8,9], the solution of zinc in H_2SO_4 and HCl solutions takes place at a potential which is substantially different from the equilibrium value. It was possible to suppose that reduction in the acid concentration and increase in the zinc-ion concentration would make it possible to bring about a shift from non-equilibrium to practically equilibrium values of the zinc potential. In this connection, sodium sulfate containing varying quantities of H_2SO_4 and $ZnSO_4$ was used as the electrolyte. The total concentration of H_2SO_4 + Na_2SO_4 was maintained constant (1N). Polycrystalline zinc containing $1 \cdot 10^{-4}$% impurities* was employed as the material for the electrodes. The salts were recrystallized twice and calcined, and the acid and the water were distilled twice. The measurements were carried out in an atmosphere of purified hydrogen at 25°. The electrode potentials presented in this paper are referred to zero on the hydrogen scale.

Curves of $\varphi_0^\bullet - \lg[Zn^{++}]$, which indicated the relationship between the steady-state potential of the zinc electrode and zinc-ion concentration at different H_2SO_4 concentrations, are given in Fig. 1. Zinc concentration $[Zn^{++}]$ is expressed in terms of normality. The curves in Fig. 1 are constructed on the basis of the mean values of the potentials observed in the solutions, which were agitated by means of hydrogen. The errors in determining the potential of the zinc were 0.5-1 mv when $[H_2SO_4] \lesssim 10^{-3}$ N, and 3-5 mv when $[H_2SO_4] \simeq 10^{-2}$ to 10^{-1} N. It may be seen from Fig. 1 that a linear relationship between $\varphi_0^\bullet$ and $\lg[Zn^{++}]$, corresponding to the Nernst equation (Curve 1) is observed at $[H_2SO_4] = 10^{-4}$ N in a range of $[Zn^{++}]$ concentrations from $3 \cdot 10^{-3}$ to $1 \cdot 10^{-1}$ N. The slope of the linear portion of Curve 1 in Fig. 1 is equal to 29 mv, i.e., it agrees, within the limits of experimental error, with the theoretical value. With increasing acidity of the solution, the $\varphi_0^\bullet - \lg[Zn^{++}]$ curves deviate progressively further from the linear relationship. In a solution of 0.1N H_2SO_4 + 0.9N Na_2SO_4, the zinc potential was practically independent of the concentration of zinc ions in solution.

It can be seen from Fig. 2 that the linear relationship between $\varphi_0^\bullet$ and $\lg[Zn^{++}]$,corresponding to the Nernst equation,is maintained at much higher H_2SO_4 concentrations in the case of zinc amalgam than in the case of zinc.

The mean values of the steady-state potentials for zinc and zinc amalgam $\varphi_0^\bullet$, observed in solutions of different pH in the absence of added zinc sulfate, are given in Table 1 (the electrolytes were agitated by means of hydrogen).

The $\varphi_0^\bullet$ − pH curve, calculated for the zinc electrode on the basis of the data in Table 1, has a linear portion with slope 28 mv, which agrees with the data of A. L. Rotinyan, N. P. Fedot'ev, and Li Un Sok [9], who obtained $\partial \varphi_0^\bullet / \partial \text{pH}$ = 25-30 mv for zinc in 0.01-5N H_2SO_4 solutions. In the case of zinc amalgam, the linear portion of the $\varphi_0^\bullet$ − pH curve was less well defined.

The increased divergence of the $\varphi_0^\bullet - \lg[Zn^{++}]$ curves from the Nernst equation, which is observed with increasing acidity of the solution (Figs. 1 and 2), is evidently connected with an increase in the relative importance of the role of hydrogen ions in the cathode process. At a steady-state potential $\varphi_0^\bullet$ the rate of the cathode process, the discharge of hydrogen ions, will be balanced by the difference between the rates of the anode and cathode processes, in which zinc atoms and ions participate**:

* The surfaces of the electrodes were treated with HNO_3 and then washed with water before the experiments.

** The normalization $\alpha_1 + \beta_1 = 2$ is made in Eq. (1) in line with [10]. Constancy of the activity coefficients of the ions and of the ψ_1-potential is assumed.

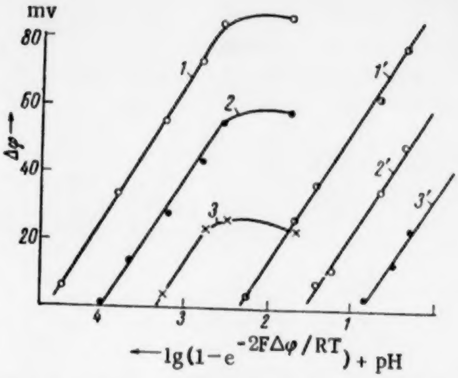

Fig. 3. Curves 1-3: zinc; Curves 1'-3': zinc amalgam at different $ZnSO_4$ concentrations: 1), 1') 10^{-3}N; 2), 2') 10^{-2}N; 3), 3') 10^{-1}N.

TABLE 2

Drop in Zinc Electrode Potential $\Delta\varphi_a$(mv) Observed as an Effect of Agitation*

$[ZnSO_4]$, N	$[H_2SO_4]$, N					
	10^{-4}	10^{-3}	$4\cdot10^{-3}$	10^{-2}	$2\cdot10^{-2}$	10^{-1}
10^{-3}	2,0	4,5	8,0	9,5	9,0	0,5
10^{-2}	1,0	4,0	6,5	10,0	8,5	0,5
10^{-1}	0	1,5	8,0	9,5	5,0	0,5

*Further increase in the intensity of agitation of the solution did not change the value of $\Delta\varphi_a$.

$$k_1 [H^+]_s e^{-\alpha F\varphi_0'/RT} = k_2' e^{\beta_1 F\varphi_0'/RT} - k_2 [Zn^{++}]_s e^{-\alpha_1 F\varphi_0'/RT}. \quad (1)$$

In Eq. (1), $[H^+]_s$ and $[Zn^{++}]_s$ are the concentrations of zinc and hydrogen ions at the electrode surface, which, when a metal dissolves in a solution of its own ions, will, generally speaking, be different from the values $[H^+]_0$ and $[Zn^{++}]_0$ in the bulk of the solution. Let us assume, for the sake of simplification, that $[H^+]_s = [H^+]_0$ and $[Zn^{++}]_s = [Zn^{++}]_0$. The smaller the rate of solution of the electrode, and the higher the intensity of mixing of the electrolyte, the better this condition is met.

The steady-state potential φ_0^* will lie to the positive side of the equilibrium potential φ_0 by an amount $\Delta\varphi = \varphi_0^* - \varphi_0$. If the rate of the cathode process, the discharge of hydrogen ions at an equilibrium potential φ_0 and concentration $[H^+]_0 = 1$ is denoted by I_0', then, after substituting $\varphi_0^* = \varphi_0 + \Delta\varphi$ in Eq. (1), we obtain:

$$I_0' [H^+]_0 e^{-\alpha F\Delta\varphi/RT} = i_0 (e^{\beta_1 F\Delta\varphi/RT} - e^{-\alpha_1 F\Delta\varphi/RT}), \quad (2)$$

where i_0 is the transference current, corresponding to the given zinc-ion concentration $[Zn^{++}]_0$. Solving Eq. (2) with respect to $\Delta\varphi$, we obtain

$$\Delta\varphi = a + k\,[\lg(1 - e^{-2F\Delta\varphi/RT}) + \mathrm{pH}], \quad (3)$$

where

$$a = -\frac{2{,}3RT}{E(\alpha+\beta_1)} \lg \frac{i_0 f_{H^+}}{I_0'}, \quad k = \frac{2{,}3RT}{F(\alpha+\beta_1)}. \quad (4)$$

It follows from Eq. (4) that a will be constant when $[Zn^{++}]$ = const and f_{H^+} = const.

The extent of the validity of the assumption made in the derivation of Eq. (3), that there are no concentration changes in the layer of solution at the electrode surface, may be assessed in the light of the effect of agitation in the solution on electrode potential. Experiments performed with zinc amalgam indicated that the electrode potentials remain practically unchanged in going from agitation of the solution by hydrogen to agitation by means of a magnetic stirrer,* which supports the stated assumption. Similar determinations with the zinc electrode indicated that going to a more intense agitation displaces the potential of the zinc electrode in the positive direction to values which reached 10 mv (see Table 2). A similar effect of electrolyte agitation in the $Zn/ZnSO_4$ system was observed by other authors, who interpreted it as concentration polarization with respect to hydrogen ions [11]. In connection with the foregoing statements, the experimental test of Eq. (3) was carried out taking into account the potential drops $\Delta\varphi_a$.

It may be seen from Fig. 3 that basically the experimental data are in good agreement with Eq. (3), the derivation of which is based on the theory of retarded discharge. Substantial divergences from the linear relationship are only observed in the case of the solution of a zinc electrode in the most acidic electrolyte investigated ($0.1N\ H_2SO_4 + 0.9N\ Na_2SO_4$). Activation of the surface of the solid zinc electrode at the appreciable rate of solution into a solution of its own ions appeared to be a possible reason for these deviations. The absence of a similar effect in the case of the zinc amalgam is a point in favor of this explanation.

*The small displacements of the potential of zinc amalgam in the negative direction, which do not exceed 1 to 2 mv, are evidently caused by a slight increase in zinc ion concentration in the layer at the electrode surface.

The linear portions of Curves 1-3 in Fig. 3, in agreement with Eq. (3), have practically the same slopes, $k = 40$ mv.* On the basis of Eq. (4), we obtain $\alpha + \beta = 1.47$ for the zinc electrode. Using the value $\alpha = 0.5$, obtained for a zinc cathode in [9], we obtain $\beta_1 = 0.97$, which agrees with the value $\beta_1 = 0.92$, obtained in [12] from anode oscillograms ($b_A = 64$ mv). Plots 1'-3' in Fig. 3 have slope $k = 37$ mv.

LITERATURE CITED

1. A. N. Frumkin, Transactions of the Second Symposium on Metal Corrosion [in Russian] (Moscow, 1940) Vol. 1.
2. A. N. Frumkin, V. S. Bagotskii, Z. A. Iofa, and B. N. Kabanov, The Kinetics of Electrode Processes [in Russian] (Moscow, 1952).
3. S. Bodforss, Z. Phys. Chem. A160, 141 (1932); I. L. Rozenfel'd, Zhur. Fiz. Khim. 25, 732 (1951).
4. Ya. M. Kolotyrkin and A. N. Frumkin, Doklady Akad. Nauk SSSR 33, 446, 451 (1941).
5. Z. A. Iofa, Zhur. Fiz. Khim. 19, 117 (1945).
6. Ya. V. Durdin and S. A. Nikolaeva, Vestnik Leningradskogo Gosudarstvennogo Universiteta No. 5, 163 (1955); V. I. Kravtsov and I. S. Loginova, Zhur. Fiz. Khim. 31, 2438 (1957).
7. Ya. M. Kolotyrkin, Zhur. Fiz. Khim. 25, 1248 (1951).
8. K. A. Dvorkin and Ya. V. Durdin, Vestnik Leningradskogo Gosudarstvennogo Universiteta No. 4, 69 (1958).
9. A. L. Rotinyan, N. P. Fedot'ev, and Li Un Sok, Zhur. Fiz. Khim. 31, 1294 (1957).
10. V. V. Losev and A. M. Khopin, Transactions of the Fourth Symposium on Electrochemistry [in Russian] (Moscow, 1959) p. 116; G. M. Budov and V. V. Losev, Doklady Akad. Nauk SSSR 122, 90 (1958).
11. S. Procopiu, Z. Phys. Chem. 154, 322 (1931); C. G. Fink and H. B. Linford, Electrochem. Soc. 72, No. 9, 147 (1937).
12. V. A. Roiter, E. S. Poluyan, and V. A. Yuza, Zhur. Fiz. Khim. 13, 805 (1939).

All abbreviations of periodicals in the above bibliography are letter-by-letter transliterations of the abbreviations as given in the original Russian journal. *Some or all of this periodical literature may well be available in English translation.* A complete list of the cover-to-cover English translations appears at the back of this issue.

* The value $\partial\varphi_0/\partial pH = 41$ mv was obtained for metallic zinc in solutions not containing zinc ions when agitated by a magnetic stirrer.

A MORE PRECISE SOLUTION OF THE EQUATION FOR HEAT CONDUCTION IN A FLAME

A. I. Rozlovskii

The State Scientific Research and Design Institute for the Nitrogen Industry and for Organic Synthesis Products

(Presented by Academician Ya. B. Zel'dovich, August 19, 1960)
Translated from Doklady Akademii Nauk SSSR,
Vol. 136, No. 5, pp. 1150-1153, February, 1961
Original article submitted August 1, 1960

The theory of normal gas combustion proposed by Ya. B. Zel'dovich and D. A. Frank-Kamenetskii [1,2] describes the single process of flame propagation along x coordinates, characterized by the diffusion of one limiting initial component and by similarity of the temperature and concentration regimes, in terms of the equation

$$y\,dy/dz + my - \varphi(z) = 0 \tag{1}$$

at the boundary conditions $y(0, 1) = 0$; $\varphi(0, 1) = 0$. Here, m is a dimensionless parameter proportional to combustion rate; $z = (T_b - T)/(T_b - T_0)$; T is the temperature in plane x; the dimensionless variable y is approximately proportional to dT/dx; the subscript b is applied to quantities referring to the combustion products, and 0 to the initial state; $\varphi = \Phi(a, T)/\Phi(a_0, T_b)$; Φ is the reaction rate, a is the dimensionless concentration of the limiting component of the mixture in grams per gram of mixture; the heat capacity and thermal conductivity of the mixture are assumed to be constant.

In the solution of Eq. (1), two approximations are made which sometimes cause some doubt as to the applicability of the theory for small activation energies. It is possible to avoid these approximations by numerical solution of (1), but this method is not only very laborious but also complicates the analysis of the kinetic laws of the reaction occurring in the flame, for which is required a simple analytical relationship between combustion rate and the kinetic parameters.

The exponential character of the temperature dependence of reaction rate leads to the occurrence of a sharp maximum in the value of φ at T in the region of T_b. At some value of z equal to $\beta < 1$, it is possible to calculate with the required accuracy that $\varphi \approx 0$. This makes it possible to calculate the boundary conditions

$$m_{\max} = \left[2\int_0^{\beta}\varphi\,d\nu(1+\beta)\right]^{1/2} \text{ and } m_{\min} = \left[2\int_0^{\beta}\varphi\,d\nu\right]^{1/2},$$

between which lies the value of the parameter m; ν is the variable with respect to which the function is integrated. The smaller the value of β, the smaller the difference $m_{\max} - m_{\min}$. In the limit, both values coincide, and the integration may be extended over the full range of variation of z, where

$$m = \left[2\int_0^{1}\varphi\,dz\right]^{1/2}. \tag{2}$$

This approximate expression, to the use of which the first source of error which the theory introduces is due, will be more accurate the higher the activation energy A. In order to carry out the integration of (2), the exponential term which enters the expression for Φ is then resolved into a series by the D. A. Frank-Kamenetskii method [3]. This represents the second approximation.

It is assumed that the function Φ has the form

$$\Phi = \mathrm{const} \cdot a^s e^{-A/RT}, \tag{3}$$

where s is the order of reaction with respect to the limiting component [2]. However, it is not the dimensionless concentration (partial pressure) which should be inserted in the kinetic equation but the absolute concentration ρa (ρ is the density) in order to take into account thermal expansion. This refinement gives

$$\varphi(z) = \left(z \frac{T_b}{T}\right)^s e^{\varkappa} e^{-\frac{\varkappa}{1-\omega z}} = \frac{e^{\varkappa}}{\omega^s}\left(\frac{1}{1-\omega z} - 1\right)^s e^{-\frac{\varkappa}{1-\omega z}}, \tag{4}$$

where $\kappa = A/RT_b$, $\omega = (T_b - T_0)/T_b$.

Denote $1/(1 - z\omega) - 1 = p$; then

$$\varphi(p) = \frac{1}{\omega^s} p^s e^{-\varkappa p}, \tag{5}$$

$$\int_0^1 \varphi(z)\,dz = \frac{1}{\omega^{s+1}} \int_0^{\omega/(1-\omega)} \frac{p^s e^{-\varkappa p}\,dp}{(1+p)^2} \approx \frac{1}{\omega^{s+1}} \int_0^{\infty} \frac{p^s e^{-\varkappa p}\,dp}{(1+p)^2}, \tag{6}$$

since $\omega/(1-\omega) = (T_b - T_0)/T_0 \gg 1$; $\kappa \gg 1$.

Considering that $\varphi \neq 0$ only when $z \ll 1$, and therefore $p \ll 1$, assume that $1/(1+p)^2 \approx 1 - 2p$, whence

$$\int_0^1 \varphi\,dz \approx \frac{1}{\omega^{s+1}} \int_0^{\infty} p^s (1-2p) e^{-\varkappa p}\,dp = \frac{1}{\omega^{s+1}}\left[\Gamma(s+1) - \frac{2}{\varkappa}\Gamma(s+2)\right]. \tag{7}$$

For integral values of s

$$\int_0^1 \varphi\,dz = \frac{s!}{(\varkappa\omega)^{s+1}}\left[1 - \frac{2(s+1)}{\varkappa}\right], \tag{8}$$

which in all materially important cases will not differ in principle from the simplified solution $\int_0^1 \varphi\,dz = s!/(\varkappa\omega)^{s+1}$. Making Eq. (3) more precise makes it possible to integrate without resolving the exponential term, which basically eliminates one of the approximations.

We will assess the error introduced by Eq. (2). Introducing the function $y_0(z) > y(z)$, determined by the condition

$$y_0 \frac{dy_0}{dz} = \varphi(z), \quad y_0(z) = \left[2\int_0^z \varphi\,dz\right]^{1/2}. \tag{9}$$

Substituting in (1) for y (but not for dy/dz) the larger value y_0, we find

$$dy/dz > \varphi/y_0 - m = dy_0/dz - m = dy_1/dz, \tag{10}$$

$$y_1 = y_0 - mz + C_1, \tag{10'}$$

where C_1 is the constant of integration. At $z = 0$, $y_0 = 0$, i.e., $C_1 = 0$.

The function y(z) determines the required lower limit of y. In order to determine its upper limit y_2, we substitute y_1 for y in (1) in a similar manner:

$$dy/dz < \varphi/y_1 - m = dy_2/dz = \varphi/(y_0 - mz) - m. \tag{11}$$

Since $mz \ll y_0$ in the zone of significant reaction rates, but when this condition is not fulfilled the term $\varphi/(y_0 - mz) \approx 0$, the condition $1/(y_0 - mz) \approx 1/y_0 + mz/y_0^2$ is valid. This makes it possible to calculate the upper value of m, m_{max}:

$$\frac{dy_2}{dz} = \frac{dy_0}{dz} + \frac{m}{y_0}\frac{dy_0}{dz} z - m. \tag{12}$$

Integration of (12), taking into consideration the condition $y_2(1) = 0$* gives

$$m_{\max} = \frac{y_0}{1 - \int_0^1 \frac{1}{y_0}\frac{dy_0}{dz} z\,dz} = \frac{y_0}{1 - \int_0^1 \frac{1}{y_0^2}\varphi(z) z\,dz} = \left[2\int_0^1 \varphi(\nu)\,d\nu\right]^{1/2} \Bigg/ \left[1 - \int_0^1 \frac{\varphi(z) z\,dz}{2\int_0^z \varphi(\nu)\,d\nu}\right]. \tag{13}$$

The lower value m_{min} is obtained from (10*):

$$m_{\min} = y_0(1) = \left[2\int_0^1 \varphi(z)\,dz\right]^{1/2}. \tag{14}$$

In order to estimate the error of formula (14), the integral $I = \int_0^1 \frac{\varphi(z) z\,dz}{2\int_0^z \varphi(\nu)\,d\nu}$ is determined numerically for reasonable values of the kinetic parameters for the reaction occurring in the flame.** Using Eqs. (4) and (5), we write

$$\int_0^z \varphi(\nu)\,d\nu = \frac{1}{\omega^{s+1}} \int_0^{z\omega/(1-z\omega)} \frac{p^s e^{-\varkappa p}\,dp}{(1+p)^2} \approx \frac{1}{\omega^{s+1}} \int_0^{z\omega} p^s e^{-\varkappa p} dp. \tag{15}$$

It will be noted that the error is not introduced into the index of the exponent.

At $s = 1$,

$$I = \frac{\varkappa\omega^2 e^{\varkappa}}{2} \int_0^1 \frac{z^2 e^{-\varkappa/(1-z\omega)}\,dz}{[1-(1+z\omega)e^{-\varkappa\omega z}](1-z\omega)} \approx \frac{\varkappa\omega^2}{2}\int_0^1 \frac{z^2 dz}{e^{\varkappa\omega z} - 1 - \omega z}; \tag{16}$$

at $s = 2$,

$$I = \frac{\varkappa\omega^3 e^{\varkappa}}{2} \int_0^1 \frac{z^3 e^{-\varkappa/(1-\omega z)}\,dz}{(1-z\omega)^2\,[2/\varkappa^2 - e^{-\varkappa\omega z}(2/\varkappa^2 + 2\omega z/\varkappa + \omega^2 z^2)]} \approx \frac{\varkappa\omega^3}{2}\int_0^1 \frac{z^3 dz}{\frac{2}{\varkappa^2}(e^{\varkappa\omega z} - 1) - \frac{2\omega z}{\varkappa} - \omega^2 z^2}. \tag{17}$$

---

* The approximate solutions for y_1 and y_2 must satisfy the boundary conditions of the function y, which is achieved if the appropriate values of m are selected.

** The magnitude of the integral I characterizes the value of z at which the function φ can be determined so as to give no appreciable error in the determination of the parameter m.

TABLE 1

κ	ω=1		ω=0,85	
	s=1	s=2	s=1	s=2
5	0,425	0,763	0,478	0,845
10	0,226	0,423	0,264	0,494
20	0,111	0,214	—	—

The results of calculations of the value of I, given in Table 1, show that in cases where the reaction order with respect to the limiting component is not higher than one the use of the approximate theory does not lead to significant errors, right up to $\kappa = 10$ to 7. At the same time, the difference between m_{max} and m_{min} does not exceed 25%. Thus, not only can the relationship between flame speed and combustion temperature, pressure, and composition be described in terms of the equations derived from the approximate theory, but the absolute value of u_n can as a rule be calculated. Only at s = 2 does it lead to appreciable error at $\kappa = 10$, and in this case it is necessary to use numerical integration in order to calculate the absolute values of $u_n \cdot s = 2$; however, this apparently arises extremely rarely, for example in the flame formed by the decomposition of hydrazine [4].

As the refinement (8) reduces m_{min}, while the true value $m > m_{min}$, by assuming $m = s!/(\kappa\,\omega)^{s+1}$ two errors of opposite sign, which partially cancel each other, are introduced. To illustrate the role of this fact, values of m for a series of actual combustion systems (T_0 = 293°K, s = 1) which have been obtained by a rigorous solution of Eq. (1) by numerical integration are compared in Table 2 with the approximate values $m_0 = s!/(\kappa\,\omega)^{s+1}$.

TABLE 2

Combustion system	T_b, °K	A, kcal/mole	κ	ω	m_0	m
16% CO + 84% air	1670	40	12,1	0,825	0,1415	0,1396
33,8% CO + 20,9% O_2 + + 45,3% N_2	2535	40	7,94	0,884	0,2013	0,1715
70% Cl_2 + 30% H_2	1596	34,6	11,2	0,816	0,05663	0,05561
N_2O (dec.)	1860	52,5	14,2	0,842	0,1179	0,1150

For chlorine/hydrogen mixtures $a/a_0 = z/\vartheta$ (see [2]), where ϑ is the ratio of the diffusion coefficient to thermal diffusivity, which was calculated by the methods of the theory given in [5]. From Table 2 it follows that the actual error in the approximate theory does not exceed 17% in the cases considered. Allowance for the temperature dependence of the thermal conductivity of the mixture also reduces the error of the approximate equation somewhat. If similarity of the temperature and concentration regimes is established

$$\frac{d}{dx}\frac{\lambda}{c}\frac{dH}{dx} - u\rho\frac{dH}{dx} + h\Phi = 0, \tag{18}$$

where λ is the thermal conductivity, c is the heat capacity of the mixture, h is the heat effect of reaction, $H = \int_0^T c\,dT$. The substitution $n = \frac{\lambda}{c}\frac{dH}{dx}$ gives

$$n\frac{dn}{dz} + u\rho(H_b - H_0)\,n - h(H_b - H_0)\frac{\lambda}{c}\Phi = 0. \tag{19}$$

This equation differs from Eq. (1) [in which φ is determined by expression (4)] by a stronger temperature dependence of the free term, which is equivalent to an increase in the effective value of the parameter κ.

I wish to express my indebtedness to Academician Ya. B. Zel'dovich for his invaluable advice.

LITERATURE CITED

1. Ya. B. Zel'dovich and D. A. Frank-Kamenetskii, Zhur. Fiz. Khim. 12, 100 (1938); Doklady Akad. Nauk SSSR 19, 693 (1938).
2. Ya. B. Zel'dovich, Zhur. Fiz. Khim. 22, 27 (1948).
3. D. A. Frank-Kamenetskii, Doklady Akad. Nauk SSSR 18, 511 (1938).
4. R. C. Murray, A. R. Hall, Trans. Faraday Soc. 47, 743 (1951); G. K. Adams and G. W. Stocks, Fourth Symposium on Combustion (1953) p. 239; P. Gray, J. C. Lee, H. A. Leach, and D. C. Taylor, Sixth Symposium on Combustion (1958) p. 255.
5. J. O. Hirschfelder, C. F. Curtiss, and R. B. Bird, Molecular Theory of Gases and Liquids (New York, 1954); C. F. Curtiss and J. O. Hirschfelder, J. Chem. Phys. 17, 550 (1949).

THE EFFECT OF ALKALI NATURE AND CONCENTRATION ON OXYGEN OVERPOTENTIAL AT A NICKEL ANODE

Ya. I. Tur'yan and A. I. Tsinman

The Lisichansk Branch of the State Scientific Research and Design Institute for the Nitrogen Industry and for Organic Synthesis Products

(Presented by Academician A. N. Frumkin, September 19, 1960)
Translated from Doklady Akademii Nauk SSSR,
Vol. 136, No. 5, pp. 1154-1157, February, 1961
Original article submitted September 16, 1960

The data given in [1,2] on the effect of alkali concentration $[OH^-]$ on oxygen overpotential η at a smooth nickel anode are contradictory and cover only low current densities i. The observation made in the discussion of [3] regarding the variation of η with variation in the nature of the alkali $K^+ < Na^+ < Li^+$ does not give further details.

The conditions of our experiment* were similar to those in [4], except that in our work the electrode was not rotated ($i \leq 1$ amp/cm²), and in order to obtain a more accurate correction for ohmic voltage drop several salt bridges [5], whose apertures were situated at different distances from the electrode (galvanic Ni on Pt wire), were used. It was established that at i = const the potential varied linearly with this distance. This facilitated extrapolation to zero distance. A relationship of this kind was somewhat different than that considered in [6].

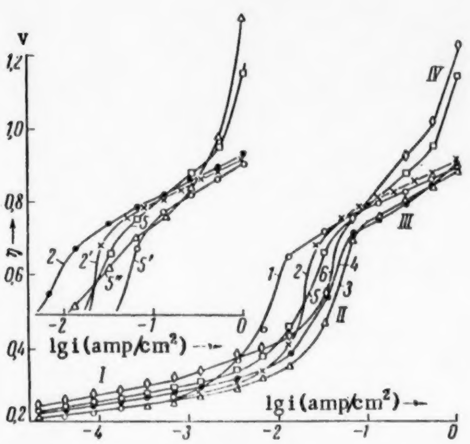

Fig. 1. $\eta - \lg i$ curves in KOH: 1) 7.5 M; 2) 5.0 M; 2') 5.0 M, 48 hr; 3) 3.7 M; 4) 2.2 M; 5) 1.3 M; 5') 1.3 M, 12 hr; 5") 1.3 M, 48 hr; 6) 0.6 M.

The investigation was carried out at 25° using carefully purified KOH, NaOH, and LiOH. The $\eta - \lg i$ curves, corresponding to the potentials which were established over a period of time, were plotted, going from the higher values of i to the lower ones, after anode polarization for a period of 24 hr with a current density i = 1 amp/cm². In concentrated alkali (2.5-7.5 M) this period of time was sufficient to reach η = const, but in dilute solution ($[OH^-] \leq 1$M), particularly with KOH, further rise of η with time was observed at high values of i (about 1 amp/cm²) (see Fig. 1).

In the $\eta - \lg i$ curves for KOH and NaOH (Figs. 1 and 2) at $[OH^-]$ = 2.0-9.5 M, there are three sections: I) linear slope at $i \cong 10^{-5}$ to 10^{-3} amp/cm²; II) increasing slope at $i \cong 10^{-3}$ to 10^{-1} amp/cm²; III) linear slope again at $i > 10^{-1}$ amp/cm².

*L. F. Gushchina took part in the experimental part of the work.

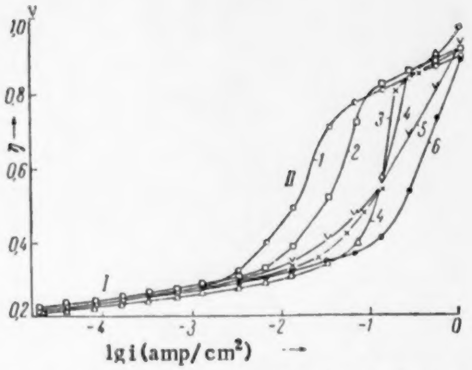

Fig. 2. η – lgi curves for NaOH: 1) 9.5 M; 2) 7.5 M; 3) 5.0 M; 4) 2.5 M; 5) 1.0 M; 6) 0.4 M.

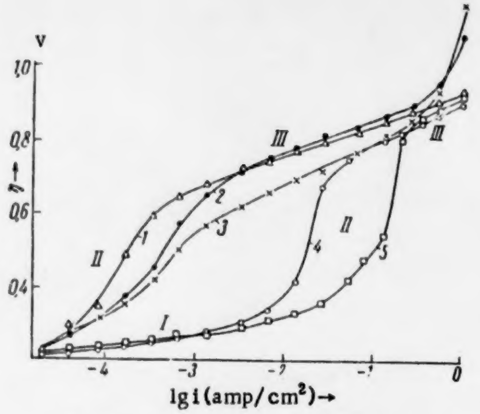

Fig. 3. η – lgi curves for LiOH, KOH, and NaOH: 1) 5 M LiOH; 2) 2.5 M LiOH; 3) 0.5 M LiOH; 4) 5 M KOH; 5) 5 M NaOH.

Thus, the occurrence of a wave-shaped polarization curve for a nickel anode [4,7-11,15] is also confirmed by an investigation carried out in alkalies of different nature and concentration, and the fact that only two sections of the curve, I and II, were reported in [2] is explained by the use of lower values of i in [2].

According to [7-9], the rate-controlling stage for KOH solutions over section I is

$$Ni_2O_3 + 2OH_{ads} \rightarrow 2NiO_2(Ni_2O_4) + H_2O \tag{1}$$

or

$$2OH_{ads} \rightarrow H_2O + O_{ads}$$

having a rate equation

$$\eta = \text{const} + \frac{RT}{2F} \ln i, \tag{2}$$

while for section III

$$OH^- - e \rightarrow OH_{ads} \tag{3}$$

having a rate equation [12]

$$\eta = \text{const} + \frac{RT}{\alpha F} \ln i - \frac{1-\alpha}{\alpha} \frac{RT}{F} \ln [OH^-] - \psi_1 \frac{1-\alpha}{\alpha}. \tag{4}$$

The effect of the nature of the alkali on η in the ranges of i encountered in sections I and III can be seen from Figs. 1-3; at high $[OH^-]$ (2-7.5 M), η increases in the order $K^+ < Na^+ < Li^+$, which is in agreement with [3], but at lower $[OH^-]$ the pattern changes: $Na^+ < K^+ < Li^+$. The fact that the pattern of the effect of the nature of the alkali cation is the same in sections I and III, and is the opposite of that observed with a Pt anode [13], confirms the view that it is impossible to explain the effect in question merely by the effect of the cation on the structure of the electrical double layer. Most probably, variation of the catalytic properties of the anode surface due to penetration into the oxide lattice of alkali metal ions is of dominant importance for an Ni anode [3].

With change in the nature and concentration of the alkali cation, which produces different effects when cations penetrate the oxide lattice, the length of section III (complete surface coverage by NiO_2 [14]), increases in the order $Na^+ < K^+ < Li^+$, so that it is impossible to observe section I in the case of LiOH right down to $i = 10^{-5}$ amp/cm² (Fig. 3). Section III is shortened with decrease in $[OH^-]$ and increase in the preliminary polarization period (NaOH, Fig. 2) until it vanishes completely, and a new section, IV, appears (KOH, LiOH, Figs. 1 and 3), which is also observed with 7.5 M KOH, but at higher values of i [4].

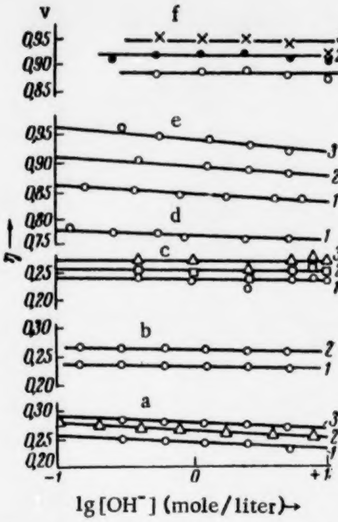

Fig. 4. $\eta - \lg[OH^-]$ curves. a) KOH: 1) $i = 10^{-4}$ amp/cm^2; 2) $4 \cdot 10^{-4}$ amp/cm^2; 3) 10^{-3}; b) NaOH: 1) $i = 7 \cdot 10^{-5}$ amp/cm^2; 2) $7 \cdot 10^{-4}$; c) NaOH from $\eta - \lg i$ curves: 1) $i = 10^{-4}$ amp/cm^2; 2) $4 \cdot 10^{-4}$; 3) 10^{-3}; d) LiOH: 1) $i = 7 \cdot 10^{-3}$ amp per cm^2; e) KOH: 1) $i = 0.16$ amp per cm^2; 2) 0.33; 3) 0.55; f) NaOH: 1) $i = 1$-0.35 amp/cm^2; 2) 0.70; 3) 1.05.

The relationship between the length of section III and the composition of the electrolyte used for the deposition of the nickel [15] is also explained, in our view, by a difference in the catalytic properties of the anode surface. The authors of [15] explained this effect by a change in the true surface area, but as may be seen from the data given in [15] a 10- to 100-fold change in the true surface area would be required for this, which is hardly possible.

A point in favor of the hypothesis of alkali cation penetration into the oxide lattice is the retarded rise in η at i = const, which we also observed when a small quantity of LiOH was added to the KOH.

It may be seen from Fig. 3 that the increase in η with LiOH in comparison with NaOH and KOH is significant only when $10^{-3} < i < 10^{-2}$ to 10^{-1} amp/cm^2. It appears to us to follow from this that when an alkali storage battery is charged with a current density $i > 10^{-1}$ amp/cm^2 (square centimeter of effective surface), the effect on the capacity of the storage battery of adding LiOH should be insignificant.

The dependence of η on $[OH^-]$ is presented in Fig. 4. Assuming that the catalytic properties of the anode surface change slowly with cation concentration due to the slowness of the secondary processes, change of oxide concentration and structure, in order to eliminate this effect as far as possible in the study of the $\eta - [OH^-]$ relationship we adopted the procedure of diluting the alkali rapidly with water at i = const without switching off the current. Before these determinations were commenced, constant η had been reached in the concentrated alkali.

The complete independence of η of $[OH^-]$ in the case of NaOH over sections I and III follows from Fig. 4. The catalytic effect of the Na^+ ion at low values of i is apparently so slight that the same conclusion can also be drawn from the $\eta - \lg i$ curves (see Figs. 2 and 4).*

In the case of KOH (Fig. 4), the $\eta - \lg[OH^-]$ relationship over sections I and III is linear with slope 0.012 to 0.015 (Fig. 4), while for LiOH the slope over section III is 0.010 (Fig. 4).

We suggest that the negligible effect of $[OH^-]$ on η in the case of KOH and LiOH is entirely due to change in the catalytic activity of the anode surface with change in $[K^+]$ and $[Li^+]$, and that η is independent of $[OH^-]$ over sections I and III for both KOH and LiOH. These data for KOH over section I agree with [2], but do not agree with [1].

The slope of $\eta - \lg i$ for section I, 0.032-0.047 (7.5-0.6 M KOH), and 0.030-0.031 (9.5-0.4 M NaOH), and the indepencence of η of $[OH^-]$ confirm that stage (1), as suggested in [7-9], is the rate-controlling stage.

The slope for section III of the $\eta - \lg i$ curve, 0.090-0.130, corresponds to stage (3) being rate controlling, and it must be assumed in order to explain the independence of η of $[OH^-]$ that

$$\psi_1 \simeq \text{const} - \frac{RT}{F} \ln [OH^-], \qquad (5)$$

although theoretically [12] this relationship is obtained in the case of more dilute solutions. It is possible that in this case specific adsorption of OH^- ions takes place, which should also displace the ψ_1 potential in the negative direction.

* It is impossible to draw any definite conclusion for other solutions from $\eta - \lg i$ curves (Figs. 1 and 3) regarding the relationship between η and $[OH^-]$, as is done in [10]. The reason for this apparently lies in the fact that when the $\eta - \lg i$ relationship is obtained over a long period of time, a change in the state of the anode surface occurs as the concentration of the alkali cation changes.

The validity of Eq. (4) was also confirmed for a completely charged oxide—nickel electrode, but for the case of $\psi = 0$, i.e., there is an appreciable difference between the behavior of this electrode and the smooth nickel anode studied by us.

LITERATURE CITED

1. L. M. Volchkova and A. I. Krasil'shchikov, Zhur. Fiz. Khim. 23, 441 (1949).
2. L. M. Elina, T. I. Borisova, and T. I. Zalkind, Zhur. Fiz. Khim. 28, 785 (1954).
3. P. D. Lukovtsev, Transactions of Symposium on Electrochemistry [in Russian] (AN SSSR, 1959) p. 302.
4. Ya. I. Tur'yan and I. S. Gol'denshtein, Zhur. Priklad. Khim. 28, 379 (1956).
5. J. O'M. Bockris and A. M. Azzam, Trans. Faraday Soc. 48, 145 (1952).
6. B. N. Kabanov, Zhur. Fiz. Khim. 10, 486 (1936).
7. Ya. I. Tur'yan, Thesis [in Russian] (Central Asian Industrial Institute, 1948).
8. V. N. Fiseiskii and Ya. I. Tur'yan, Zhur. Fiz. Khim. 24, 567 (1950).
9. V. N. Fiseiskii and Ya. I. Tur'yan, Trudy Sredneaziatsk. Politekh. Inst. 2, 42, 46 (1950).
10. T. Mine, T. Seiymaa, and W. Sakai, J. Chem. Soc. Japan Indust. Chem. Soc. 58, 725 (1955).
11. Ya. I. Tur'yan, Zhur. Fiz. Khim. 33, 948 (1959).
12. A. N. Frumkin, V. S. Bagotskii, Z. A. Iofa, and B. N. Kabanov, Kinetics of Electrode Processes [in Russian] (1952).
13. T. Érdei-Gruz and I. Shafarik, Transactions of Symposium on Electrochemistry [in Russian](AN SSSR, 1959) p. 263.
14. I. Ya. Tur'yan and I. S. Gorodetskii, Doklady Akad. Nauk SSSR 117, No. 4, 655 (1957).
15. G. A. Tsyganov and A. M. Mirzakarimov, Uzbek. Khim. Zhur. 3, 65 (1958).
16. S. A. Gantman and P. D. Lukovtsev, Transactions of Symposium on Electrochemistry [in Russian] (AN SSSR, 1953) p. 504.

CURRENT-TIME CURVES FOR THE REDUCTION OF ANIONS AT A DROPPING ELECTRODE

Academician A. N. Frumkin, O. A. Petrii, and N. V. Nikolaeva-Fedorovich

Electrochemistry Faculty, M. V. Lomonosov Moscow State University

Translated from Doklady Akademii Nauk SSSR, Vol. 136, No. 5, pp. 1158-1161, February, 1961
Original article submitted November 22, 1960

The determination of the relationship between the current I through a growing drop and time t is a convenient method for studying the effect of adsorption on the kinetics of electrode processes. Hitherto, the I – t curves for reduction processes, whose rate decreases with the adsorption of neutral organic substances and organic cations, have been investigated [1-3].* It is known, however, that the rate of some reactions rises sharply on adsorption of cations. Thus, tetrabutylammonium (TBA), tetraamylammonium (TAA), tetrahexylammonium (THA), and La^{3+} cations increase the rate of reduction of the anions $S_2O_8^{2-}$ and $Fe(CN)_6^{3-}$ [5,6]. The cations mentioned are effective at such low concentrations C that at these concentrations the quantity of cations on the surface of the growing drop is determined by diffusion [8]. At the same time, the rate of reduction of anions at a surface which is completely covered with organic cations in many cases remains so high that the rate of the process is limited by diffusion of the particles undergoing reduction to the electrode surface.

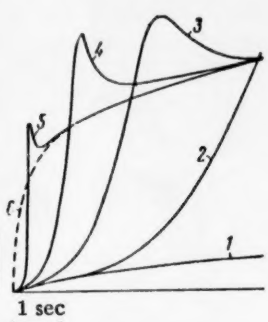

Fig. 1. I – t curves for the reduction of $S_2O_8^{2-}$ in a solution of 10^{-3} N $K_2S_2O_8 + 5 \cdot 10^{-3}$ N Na_2SO_4 at $\varphi = -1.1$ in the presence of $[(C_4H_9)_4N]I$ at the following concentrations: 1) 0; 2) $2 \cdot 10^{-5}$ N; 3) $3 \cdot 10^{-5}$ N; 4) $5 \cdot 10^{-5}$ N; 5) 10^{-4} N; 6) 10^{-3} N.

We have studied the I – t curves for the reduction of $S_2O_8^{2-}$ and $Fe(CN)_6^{3-}$ anions at a dropping mercury electrode in the presence of TBA, TAA, THA, and La^{3+} cations, and for the reduction of the anion $PtCl_4^{2-}$ in the presence of the TAA cation. Measurements of the I – t curves were carried out with the aid of a model 01 TsLA oscillographic polarograph [9]. The potentials φ are given in volts, referred to the normal calomel electrode.

In a solution of 10^{-3} N $K_2S_2O_8 + 5 \cdot 10^{-3}$ N Na_2SO_4 at $\varphi = -0.55$, at which value a limiting diffusion current I_d is observed on the I – φ curve, the current is proportional to $t^{1/6}$. In the presence of $[(C_4H_9)_4N]I$ at different concentrations, the I – t curve does not change at this potential. At the potential corresponding to the minimum on the I – φ curve, $\varphi = -1.1$, the current is proportional to $t^{2/3}$, i.e., it has a purely kinetic character (Fig. 1, 1). I – t curves, measured at $\varphi = -1.1$ in the presence of TBA at various concentrations, are given in Fig. 1. It may be seen from this figure that the initial portions of the

*Volchkova [4] has studied I – t curves in the case where accelerated reduction of an adsorbed substance occurs. However, the effect of the acceleration of the reactions studied by here is relatively ill defined.

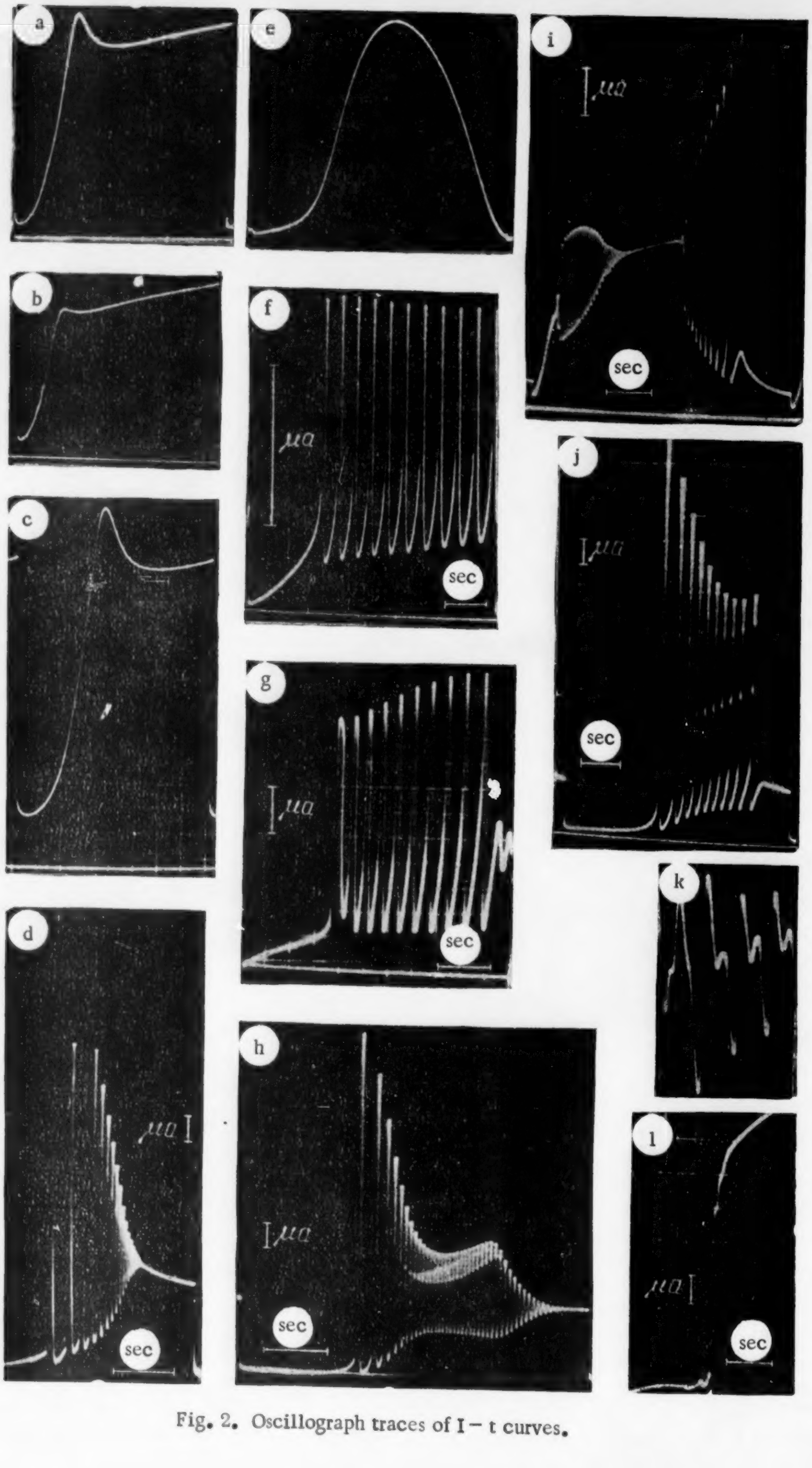

Fig. 2. Oscillograph traces of I − t curves.

I – t curve in the presence of TBA practically coincide with the curve obtained without adding TBA. Furthermore, a steep rise in the current is observed for a relatively small increment of time. The current reaches values in excess of the limiting diffusion current, then, having passed through a maximum, begins to drop, approaching I_d. Similar I – t curves are also observed in the reduction of $S_2O_8^{2-}$ in the presence of TAA, THA, and La_3^+. The I – t curve determined in a solution of 10^{-3} N $K_2S_2O_8$ + 5 • 10^{-3} N Na_2SO_4 + 5 • 10^{-5} N $[(C_6H_{13})_4N]Br$ at $\varphi = -1.1$ is given in Fig. 2a, and the I – t curve for a solution of 10^{-3} N $K_2S_2O_8$ + 2 • 10^{-3} N Na_2SO_4 + 5 • 10^{-5} N $La_2(SO_4)_3$ at $\varphi = -1.45$ volts * is given in Fig. 2b.

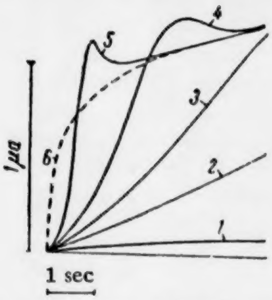

Fig. 3. I – t curves for the reduction of $Fe(CN)_6^{3-}$ in a solution of 10^{-3} N $K_3Fe(CN)_6$ at $\varphi = -1.6$ in the presence of $La_2(SO_4)_3$, at the following concentrations: 1) 0; 2) 10^{-5} N; 3) 2 • 10^{-5} N; 4) 3 • • 10^{-5} N; 5) 5 • 10^{-5} N; 6) 10^{-3} N.

Measurements of the I – t curves for a solution of 10^{-3} N $K_3Fe(CN)_6$ show that at $\varphi = -0.5$ the current is proportional to $t^{1/6}$, while at potentials corresponding to the minimum of the I – φ curve a kinetic current, proportional to $t^{2/3}$, occurs. On the basis of the I – t curves measured in this solution at different values of φ and corrected for charging current, the relationship between the instantaneous current I_{inst} and φ for t = 3.3 sec was constructed. There is a flat minimum on the I – φ curve obtained in this manner. Thus, the deduction regarding the shape of the reduction curve for the $Fe(CN)_6^{3-}$ anion which is made in [10] is borne out by direct measurement. The same current-time relationship is observed in the presence of TBA, TAA, and THA at potentials corresponding to the minimum in the I – φ curve, as in the reduction of $S_2O_8^{2-}$. The I – t curve determined in a solution of 10^{-3} N $K_3Fe(CN)_6$ + 5 • 10^{-5} N $[(C_4H_9)_4N]I$ at $\varphi = -1.4$ is given in Fig. 2c. The effect of La^{3+} cations on the I – t relationship in the reduction of the $Fe(CN)_6^{3-}$ anion is similar to the effect of the organic cations and La^{3+} on the reduction of $S_2O_8^{2-}$ (Fig. 3).

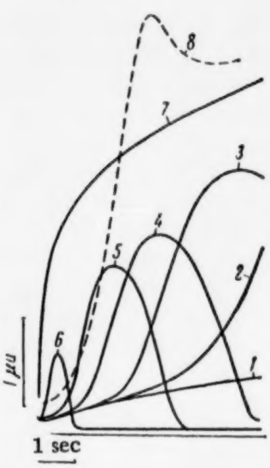

Fig. 4. I – t curves for the reduction of $PtCl_4^{2-}$ in a solution of 10^{-3} N K_2PtCl_4 + 4 • 10^{-3} N Na_2SO_4 at $\varphi = -0.87$ volt in the presence of $[(C_5H_{11})_4N]Br$ at the following concentrations: 1) 0; 2) 2 • 10^{-5} N; 3) 3 • 10^{-5} N; 4) 4 • 10^{-5} N (oscillograph trace Fig. 2g); 5) 5 • 10^{-5} N; 6) 10^{-4} N; 7) time dependence of I_d for the reduction of $PtCl_4^{2-}$; 8) I – t curve for a solution of 10^{-3} N $K_2S_2O_8$ + 5 • 10^{-3} N Na_2SO_4 + + 3 • 10^{-5} N $[(C_5H_{11})_4N]Br$ at φ = = –1.1.

A complete quantitative theory for I – t curves obtained with a dropping electrode has not yet been constructed. The case of an electrochemical reduction process, the rate of which depends linearly on the extent of coverage of a surface by a substance which may either retard or accelerate reaction, has been analyzed [2]. In explaining the shape of the I – t curves which is observed in the case of a retarded electroreduction of cations, a deduction is made in [3] regarding the necessity of taking into account not only surface coverage, but also the effect of change in ψ_1 potential, which, in accordance with the Frumkin-Florianovich equation [7], leads to an exponential relationship between I and the amount of substance adsorbed. In this case, however, only retardation of the process was considered, and a quantitative theory is only given for the initial part of the I – t curve.

The qualitative observations of the time dependence of current in the reduction of anions, particularly the existence of maxima in the values of I_{inst}, which exceed the usual Ilkovič limiting diffusion current, may be explained in the following way. In the absence of a catalyst (organic cations or La^{3+}), the reduction of $S_2O_8^{2-}$ and

* The drop in current observed in the very initial period of drop growth in many of the oscillograph traces in Fig. 2 is due to a non-Faradaian (capacitance) current which is proportional to $t^{-\frac{1}{2}}$, and which falls to zero with increasing time. Corrections for capacitance current were introduced into the I – t curves in Figs. 1 and 3.

$Fe(CN)_6^{3-}$ proceeds very slowly, so that the anion concentration in the layer nearest the electrode remains practically constant and equal to the concentration of these particles in the bulk of the solution during the initial period of drop growth. Therefore, by the time that a sufficient amount of cations has accumulated at the electrode surface to accelerate the reaction, the anion concentration in the neighborhood of the electrode still remains high. This leads to reduction currents which exceed I_d. The substance in the neighborhood of the electrode is then, however, consumed; the current falls and, when the anion concentration at the surface drops to zero, approaches the value I_d. A significant increase of I_{inst} above I_d can evidently only be observed where there is an exponential relationship between the rate of anion reduction and the degree of cation coverage of the electrode.

In [7] it was discovered that the effect of La^{3+} cations on the reduction of $S_2O_8^{2-}$ and $Fe(CN)_6^{3-}$ is decreased and completely disappears at sufficiently low La^{3+} concentrations, e.g.$1.2 \cdot 10^{-5}$ N, at strongly negative values of φ, and the hypothesis was advanced that the reason for this is a reduction in the time of drop formation of the mercury electrode, as a result of which La^{3+} does not have time to be adsorbed. From the I – t curves obtained for the reduction of $S_2O_8^{2-}$ and $Fe(CN)_6^{3-}$ in the presence of La^{3+} at different values of φ, we constructed the $I_{inst} - \varphi$ relationship for constant t. It appeared that La^{3+} cations at $C = 1.2 \cdot 10^{-5}$ N accelerate reduction of the anions both at less and at more negative values of φ, but their action is more effective in the former case. This phenomenon is evidently due to the fact that in the stated conditions of the determinations the La^{3+} concentration at the electrode surface is the same at different values of φ, and their action should be more effective when the surface is weakly charged,when the K^+ concentration in the double layer is less.

It has already been established by the determination of I – t curves [5] that TAA at low concentrations accelerates the reduction of $PtCl_4^{2-}$ at the potentials encountered in the falling portion of the polarization curve but retards the process at higher concentrations. The results of I – t measurements for the reduction of $PtCl_4^{2-}$ in the presence of TAA are presented in Fig. 4. At low TAA concentrations at the surface acceleration of the reduction of $PtCl_4^{2-}$ is observed, and the initial portions of the I – t curves obtained in this case are reminiscent of the initial portions of the I – t curves described above. However, when sufficient quantity of TAA accumulates at the electrode surface, reduction of $PtCl_4^{2-}$ is retarded. Comparison of Curves 3 and 8 of Fig. 4 shows that TAA accelerates the reduction of $PtCl_4^{2-}$ much less than the reduction of $S_2O_8^{2-}$. The reasons for this are analyzed in [5]. In order to explain the data obtained in the present study, it is evidently not sufficient merely to use the concepts previously evolved of the effect of organic cations on the reduction of anions [5], but it is probably also necessary to take into account surface coverage by adsorbed cations, which causes retardation of the reaction. When acceleration of the process by cations is comparatively slight, retardation of the reaction occurs at high surface coverages.

In certain circumstances, the I – t curves determined in dilute solutions at the potentials encountered in the falling region of the I – φ curve are distorted by current oscillations. Spontaneous oscillations were first encountered in the reduction of $S_2O_8^{2-}$ on mercury [11]. The I – t curve which we obtained in a solution of 10^{-3} N $K_2S_2O_8 + 3 \cdot 10^{-5}$ N $[(C_4H_9)_4N]I$ at a cell voltage of U = –1.29 volts (Hg anode in the same solution) is given in Fig. 2d. Spontaneous oscillations are also observed in a 10^{-3} N $K_3Fe(CN)_6$ solution when a 47 kohm resistance is placed in series with the cell (Fig. 3f, U = –0.8 volt). Spontaneous oscillations for a solution of 10^{-3} N $K_2PtCl_4 +$ $+ 3 \cdot 10^{-5}$ N $[(C_4H_9)_4N]I$ are shown for U = –1.09 volts in Fig. 2h and for U = –1.10 volts in Fig. 2j. In a solution of 10^{-3} N $K_2PtCl_4 + 5 \cdot 10^{-5}$ N $[(C_4H_9)_4N]I + 10^{-1}$ N Na_2SO_4 at U = –1.2 volts, it is possible to observe the current oscillations at different instants of drop life (Fig. 2i, R = 30 kohm). The observation of oscillations in this case is also of interest because there is a falling region on the I – φ curve for this solution, but no polarographic maximum of the first type. Oscillations are observed in the reduction of the CrO_4^{2-} anion, whose I – φ curve has a falling region [12] in a solution of 10^{-3} N $K_2CrO_4 + 3 \cdot 10^{-5}$ N $(C_4H_9)_4NI$ at U = –0.97 volts (Fig. 2g). The relationship between the frequency and amplitude of the spontaneous oscillations and voltage in the cases studied is in agreement with the results in [11] and is apparently connected with variation in the state of the layer at the electrode at the instant at which the oscillations begin. The form of the oscillations agrees with that described in [11], although more complex oscillations were observed in some cases (some of the oscillations in Fig. 2h are given in Fig. 2k with the t scale magnified by a factor of 16). In 10^{-3} N $K_2S_2O_8$, 10^{-3} N K_2PtCl_4, and 10^{-3} N $HgCl_2$, in the absence of additives, oscillations are not observed in the conditions in which these

studies were carried out, but "jumps" in the current occur until the value of I encountered at the polarographic maximum is reached. The characteristic zigzag-shaped lags described in [11] (indicated by arrows in Fig. 2*l*, 10^{-3} N $K_2S_2O_8$, U = −1.1 volts)* were observed, however, in the first two cases as the curve was rising to the maximum. It follows from the experiments carried out that oscillations disappear when the resistance of the circuit is reduced, and therefore in the main part of the work the determinations were carried out with solutions which contained low Na_2SO_4 concentrations.

LITERATURE CITED

1. P. Delahay and I. Trachtenberg, J. Am. Chem. Soc. 78, 2355 (1957); 80, 2094 (1958); R. Schmid and C. Reilley, J. Am. Chem. Soc. 80, 2087 (1958).
2. J. Weber, J. Koutecký, and J. Koryta, Z. Elektrochem. 63, 583 (1959).
3. J. Kůta, J. Weber, and J. Koutecký, Coll. Czech. Chem. Commun. 25, 2376 (1960).
4. V. Volková, Nature 185, 743 (1960).
5. A. Frumkin, Trans. Faraday Soc. 55, 156 (1959); N. Nikolaeva-Fedorovich, B. B. Damaskin, and O. A. Petrii, Coll. Czech. Chem. Commun. 25, 2982 (1960).
6. T. A. Kryukova, Doklady Akad. Nauk SSSR 65, 517 (1949).
7. A. N. Frumkin and G. M. Florianovich, Doklady Akad. Nauk SSSR 80, 907 (1951); Zhur. Fiz. Khim. 29, 1827 (1955).
8. A. N. Frumkin and B. B. Damaskin, Doklady Akad. Nauk SSSR 129, 862 (1959).
9. C. B. Tsfasman, Electronic Polarographs [in Russian] (Moscow, 1960).
10. A. N. Frumkin, O. A. Petrii, and N. V. Nikolaeva-Fedorovich, Doklady Akad. Nauk SSSR 128, 1006 (1959).
11. A. Ya. Gokhstein and A. N. Frumkin, Doklady Akad. Nauk SSSR 132, 388 (1960).
12. L. Gierst, Cinétique d'approche et réactions d'électrodes irréversibles (Bruxelles, 1958).

All abbreviations of periodicals in the above bibliography are letter-by-letter transliterations of the abbreviations as given in the original Russian journal. *Some or all of this periodical literature may well be available in English translation.* A complete list of the cover-to-cover English translations appears at the back of this issue.

*The fact that oscillations are best observed in the presence of small additions of TBA is probably due to the effect of cations on the $I-\varphi$ curve, particularly the existence on the curve of a small region of limiting current between the polarographic maximum and the falling region of the $I-\varphi$ curve. At the same time, the oscillations which are observed in the presence of La^{3+} or small (of the order of 10^{-4} N) additions of Na_2SO_4 differ with respect to frequency and amplitude from the oscillations obtained when TBA is added.

RAYLEIGH LIGHT SCATTERING AND THE ORIENTATED ORDERING OF MOLECULES

M. I. Shakhparonov

M. V. Lomonosov Moscow State University
(Presented by Academician V. V. Shuleikin, October 26, 1960)
Translated from Doklady Akademii Nauk SSSR,
Vol. 136, No. 6, pp. 1162-1164, February, 1961
Original article submitted October 24, 1960

Let a uniform isotropic system consist of $N = \sum_i N_i$ ($i = 1, \ldots, M$) molecules and occupy volume V. The subscript i denotes the kind of molecule. Then the intensity of monochromatic light I_a scattered by fluctuating anisotropy at an angle θ to the direction of incident unpolarized radiation whose intensity is equal to I_0 may be expressed by the function

$$I_a = \frac{I_0}{2r^2}\left(1 + \cos^2\theta\right)\left(\frac{2\pi}{\lambda}\right)^4\left[\sum_j (\Delta\varepsilon_{jlk}^{aH})\,\frac{v_j}{4\pi}\right]^2, \tag{1}$$

where the summation is carried out over the independent volume elements $v_j \ll \lambda^3$, $\sum_j v_j = V$; $\Delta\varepsilon_{jlk}^{aH}$ is the fluctuation in the optical dielectric constant in the volume element v_j, due to fluctuations in orientation; λ is the wavelength of the light; r is the distance from the center of the volume causing the scattering to the point of observation. Using the Lorentz-Lorentz equation we obtain, after carrying out a series of well-known rearrangements [1],

$$I_a = Q\left\{\sum_{k=y,z}\sum_{i=1}^{M}\sum_{j=1}^{N_i}\overline{(\Delta a_{zkij})^2} + \sum_{k=y,z}\sum_{i=1}^{M}\sum_{j=1}^{N_i}\sum_{i'=1}^{M}\sum_{j'=1}^{N_{i'}}{}' \overline{\Delta a_{zkij}\Delta a_{zki'j'}}\right\}, \tag{2}$$

$$Q = \frac{I_0}{2r^2}(1 + \cos^2\theta)\left(\frac{2\pi}{\lambda}\right)^4\left(\frac{n^2+2}{3}\right)^4.$$

Here, x and y are the Cartesian axes of coordinates defining the direction of the electrical vector of the radiation; Δa_{zkij} and $\Delta a_{zki'j'}$ are the components of the fluctuation of the anisotropic polarizability of molecule j of kind i, or molecule j' of kind i', respectively; n is the refractive index.

The first part of Eq. (2) expresses the contribution of the independent orientations of all the molecules; the second part takes into account the relationship between the orientations of different molecules ij and i'j'.

As we have already shown [2], the method of differentiating the Lorentz–Lorentz equation proposed by Rocard [3] does not withstand criticism. The method of differentiation already employed by Einstein [4] is correct. The factor $(n^2 + 2)/3$ in Eq. (2) is therefore raised to the fourth power, and not to the second.

Let molecule ij have a random but fixed orientation. Let us arrange within the molecule a system of coordinates such that the axes $\xi_{ij}\ \eta_{ij}\ \zeta_{ij}$ coincide with the principal semiaxes of the polarizability ellipsoid of molecule ij. Molecule i'j' has no fixed orientation. Let us introduce axes of coordinates $\xi_{i'j'}$, $\eta_{i'j'}$, $\zeta_{i'j'}$,

Liquid	t, °C	n_D	$\left(\frac{n_D^2+2}{3}\right)^2$	$\left(\frac{n_D^2+2}{3}\right)^4$	λ, A	$a_\xi \cdot 10^{23}$	$a_\eta \cdot 10^{23}$	$a_\zeta \cdot 10^{23}$	I	$\Delta \cdot 100$	I_a expt1.	I_a from Eq.(5)	I_a from [3,11]	$\overline{(\sigma, \varkappa)^2}$
C_6H_6	25	1,5011	2,01	4,02	5460	1,114	1,114	0,733	1,00	42,0	0,64	0,58	0,39	1/3
C_6H_5Cl	20	1,525	2,08	4,30	4360	1,470	1,240	0,818	1,47	60,0	1,19	1,16	0,82	1/3
C_6H_5Br	25	1,557	2,20	4,86	5460	1,684	1,213	0,956	1,78 (14)	62,0	1,48	1,72	1,14	1/3
$C_6H_5NO_2$	25	1,554	2,16	4,70	5460	1,600	1,360	0,690	3,14 (13)	71,5	2,90	2,89	1,77	1/3
$C_6H_5CH_3$	25	1,494	2,00	4,00	5460	1,377	1,253	0,904	1,12	48,0	0,79	0,74	0,49	1/3
$o\text{-}C_6H_4(CH_3)_2$	25	1,503	2,02	4,07	5460	1,639	1,352	1,075	1,31	55,0	1,00	0,82	0,55	1/3
$(CH_3)_2CO$	20	1,359	1,64	2,70	4360	0,70 (*)	0,684	0,482	0,26	25,0	0,110	0,110	0,098	1/3
CS_2	25	1,625	2,40	5,78	5460	—	—	—	4,12	62,0	3,42	4,15*	2,30	~1/3
$CHCl_3$	20	1,446	1,86	3,46	5460	0,90	0,67	0,67	0,40	24,2	0,17	0,18	0,13	1/3
$(C_2H_5)_2O$	25	1,3500	1,62	2,63	5460	0,807	1,120	0,673	0,35 (11)	7,0	0,049	0,038	0,031	1/3
CH_3OH	20	1,330	1,60	2,55	4360	0,400	0,256	0,314	0,14 (2)	7,3	0,021	0,085	0,079	<1/3

*Calculated from data on δ^2 and α given in [9].

coincident with the principal semiaxes of the polarizability ellipsoid of molecule i'j', and changing their position in space with molecule i'j'. Using the method of calculation developed by M. Born, R. Gans, et al. (see, for example, [1], pp. 238-241), the following general expression for I_a may be obtained:

$$I_a = \frac{13}{45} QN \left\{ \sum_{i=1}^{M} x_i \gamma_i^2 + \frac{1}{2} \sum_{\varkappa} \sum_{\sigma} \sum_{i} \sum_{i'} x_i x_{i'} a_{\varkappa i} a_{\sigma i'} \left[3\, \overline{(\varkappa\sigma)^2} - 1\right] \right\},$$
$$\gamma^2 = {}^1\!/_2 \left[(a_{\xi i} - a_{\eta i})^2 + (a_{\xi i} - a_{\zeta i})^2 + (a_{\eta i} - a_{\zeta i})^2\right],$$
$$\varkappa = \xi_{ij}, \eta_{ij}, \zeta_{ij}; \quad \sigma = \xi_{i'j'}, \eta_{i'j'}, \zeta_{i'j'}. \tag{3}$$

Here, $a_{\kappa i}$ and $a_{\sigma i'}$ are the principal values of the polarizability tensor of molecules of kind $\underline{i}$, and $\overline{i'(\kappa\sigma)^2}$ is the statistical mean square of the cosine of the angle between axes κ and σ. If the orientations of the molecules are randomly distributed, all values of $\overline{(\kappa\sigma)^2} = 1/3$. Then,

$$I_a = \frac{13}{45} QN \sum_{i=1}^{M} x_i \gamma_i^2. \tag{4}$$

For a single component system in the general case,

$$I_a = \frac{13}{45} QN \left\{ \gamma^2 + \frac{1}{2} \sum_{\varkappa} \sum_{\sigma} a_\varkappa a_\sigma \left[3\, \overline{(\varkappa\sigma)^2} - 1\right] \right\}. \tag{5}$$

Equation (5) may readily be rearranged to obtain the expression derived by Ansel'm [5].

By comparing the values of I_a calculated from Eq. (4) with the experimental values and using Eqs. (3) and (5), information on the orientated order of the molecules may be obtained. The results of such calculations for a series of specific liquids are given in the table. The total intensity of Rayleigh light scattering for the same wavelength in benzene at 25° was taken as the unit of measurement of I_a at a wavelength λ. In these units, $I_a = \frac{R_a}{R_{C_6H_5}}$, where $R = \frac{I}{I_0} \frac{r^2}{V}$. We took the "high" values obtained by Carr and Zimm [6] and a number of other authors, after correction for refractive index and scattering volume, as the scattering coefficient of benzene $R_{C_6H_6}$. At 25° these values are equal to $48.5 \cdot 10^{-6}$ (λ = 4358 A) and $16.3 \cdot 10^{-6}$ (λ = 5460 A); at 20° the values of $R_{C_6H_6}$ are $46.8 \cdot 10^{-6}$ and $15.7 \cdot 10^{-6}$, respectively. In the table the wavelength of the radiation for which the calculation is carried out is indicated. The values of a_κ are taken from the work of LeFévre and co-workers [7-9]. The values of a_κ given in the papers by Stuart and Volkmann (see, for example, [10]), are evidently incorrect [5]. Attempts to use these values [8] to calculate I_a lead in many cases to obviously erroneous results. Results of the calculation of I_a using the "low" values [11] for $R_{C_6H_6}$, and substituting the factor $[(n^2 + 2)/3]^4$ for $[(n^2 + 2)/3]^2$, are given in the table. As the squares of the differences in the values for a_κ are contained in Eq. (4), possible errors in the values of a_κ have a large effect on the results of the calculations, and this must be borne in mind in comparing experiment with theory. The table shows that for all the liquids except methyl alcohol the values of I_a calculated from Eq. (4) using $[(n^2 + 2)/3]^4$ and the high values for $R_{C_6H_6}$ agree, within

the limits of possible errors, with the values of I_a calculated from experimental data on the total intensity and degree of depolarization Δ of the scattered light.

It should be noted that data which were known to be inaccurate [10] were used, for lack of better, in the calculation of I_a for methyl alcohol. However, it is conceivable that the discrepancy between Eq. (4) and the experimental result in this case is due not only to inaccuracy of the values taken for a_κ, but also to an orientated arrangement of CH_3OH molecules. Acetone, nitrobenzene, chlorobenzene, bromobenzene, chloroform, and ether conform approximately to the theory of polar dielectrics developed by Onsager, which gave some basis for assuming the absence, or at least the insignificance, of an orientated order in these liquids [12]. The data in the table are new and independent evidence for this assertion.

Summing up, we may say that uniform isotropic molecular systems (gases, liquids, etc.) can be divided into two groups: a) systems without an orientated arrangement of molecules and b) systems having an orientated arrangement of molecules. The investigation undertaken by us opens up the possibility of establishing physical criteria for a division of this kind and in many cases of elucidating the nature of the orientated arrangement of the molecules by the calculation of $\overline{(\kappa\,\sigma)^2}$ from the I_a and a_κ data.

LITERATURE CITED

1. M. V. Vol'kenshtein, Molecular Optics [in Russian] (Moscow-Leningrad, 1951).
2. L. P. Zatsepina and M. I. Shakhparonov, Vestnik Mosk. Univ. No. 4 (1960).
3. I. Rocard, Ann. Phys. 10, 154 (1928).
4. A. Einstein, Ann. Phys. 33, 1275 (1910).
5. A. I. Ansel'm, Zhur. Éksp. i Teor. Fiz. 17, 489 (1947).
6. C. I. Carr and B. H. Zimm, J. Chem. Phys. 18, 1616 (1950).
7. C. LeFévre and R. LeFévre, Problems in Modern Physics [Russian translation] (IL, 1955) No. 5, p. 21.
8. C. LeFévre and R. LeFévre, J. Chem. Soc. 1953, 4041.
9. R. LeFévre and B. Rao, J. Chem. Soc. 1957, 3644.
10. Londolt-Börnstein, Zahlenwerte und Funktionen, 6 Aufl., 1, 3 Teil (Berlin, 1951) p. 511.
11. G. Vauculeurs, Ann. Phys. 6, 213 (1951).
12. M. I. Shakhparonov, Zhur. Fiz. Khim. 34, 1478 (1960).
13. D. K. Beridze and M. I. Shakhparonov, Ucheniye Zapiski Mosk. Oblast. Pedogogicheskogo Inst. imeni N. K. Krupskoi 92, 49 (1960).
14. M. F. Vuks and I. I. Bilenko, Zhur. Éksp. i Teor. Fiz. 23, 105 (1952).

All abbreviations of periodicals in the above bibliography are letter-by-letter transliterations of the abbreviations as given in the original Russian journal. *Some or all of this periodical literature may well be available in English translation.* A complete list of the cover-to-cover English translations appears at the back of this issue.

APPLICATION OF IONIZING RADIATIONS TO THE INVESTIGATION OF THE DECOMPOSITION PROCESSES OF COPPER AND NICKEL OXALATES

V. A. Gordeeva, E. V. Egorov, G. M. Zhabrova, B. M. Kadenatsi, M. Ya. Kushnerev, and Corr. Member AN SSSR S. Z. Roginskii

Institute of Physical Chemistry, Academy of Sciences of the USSR
Translated from Doklady Akademii Nauk SSSR,
Vol. 136, No. 6, pp. 1364-1367, February, 1961
Original article submitted October 17, 1960

The purpose of this work was to determine whether the topochemical processes of decomposition of solid inorganic compounds resulting from electron radiation are the same as ordinary thermal decomposition processes. Irradiation of solids with fast electrons leads to excess current carriers – secondary electrons and holes – and also to radiation defects, i.e., deformation of the periodic crystal structure.

Therefore, ionizing radiations may affect the rate of topochemical processes, and also the structural and chemical characteristics of the products formed. Although the radiation defects and the primary active forms occurring in solids as the result of ionizing radiations are unstable [1], they may develop into secondary, more stable forms which affect the rate of topochemical processes. It must be noted that the participation of the additional current carriers in certain stages of the topochemical processes is possible. This is of interest, due to the repeatedly voiced assumption in recent years that the electron mechanism plays an important role in topochemical processes of the decomposition of compounds of the azide and oxalate types [2-5].

Our samples of copper and nickel oxalates were prepared by precipitation from 0.2 N copper and nickel nitrates with 0.4 N oxalic acid at 50°C. According to the results of structural x-ray analysis, the phase composition of copper oxalate corresponded to the formula $CuC_2O_4 \cdot \frac{1}{2} H_2O$, and that of nickel oxalate to $NiC_2O_4 \cdot 2H_2O$.

The oxalates were irradiated in air with fast electrons with energies of 0.6-2 Mev. The density of the beam was checked for homogeneity photometrically by the darkening of photographic plates or films. For higher radiation doses (about 10^6 rad/sec), the samples were placed in an open metallic container having a massive extension (heat sink) immersed in liquid nitrogen or solid carbon dioxide. For lower radiation doses (10^4 rad/sec), the samples were irradiated in open containers or cuvettes made of molybdenum glass, which were cooled with solid carbon dioxide or a stream of cold air.

The temperature within the samples was measured with a thermocouple. When the heat loss to liquid nitrogen was large, the temperature was 40-50°, and it was found that there is a correspondence between the amount of energy received by the solid and that spent on evaporation of nitrogen. When heat losses were lower, the temperature within the sample was 100-150°. The thickness of the layer of samples corresponded approximately to the free path of electrons of a given energy. The radiation dose was calculated by the intensity of current, and measured with a chemical dosimeter (recommended by the L. Ya. Karpov Physicochemical Institute), whose reagent was composed of 0.02 mole/liter $CuSO_4$, 0.002 mole/liter $FeSO_4$, 0.02 N H_2SO_4. The emission of Fe^{3+} was determined with an SF-4 spectrophotometer, G = 0.65.

The irradiated samples were subjected to kinetic and x-ray analysis to determine the phase composition of the products formed and the depth of transformation. The kinetics of the composition of irradiated and unirradiated samples was studied in a vacuum apparatus with a spiral quartz balance.

Phase Composition of Radiation and Thermal Decomposition Products of Copper and Nickel Oxalates in Air and in Vacuum

Radiation decomposition			Thermal decomposition	
Temp., °C	Dose, rad.	Comp., %	Temp., °C	Comp., %
		Copper oxalate		
100 (in air)	$3.6 \cdot 10^9$	Cu, 30 Cu_2O, 30 No decomp., 40	300 (in air)	Cu_2O, 50 CuO, 50
100 (in air)	$1 \cdot 10^{10}$	Cu, 90 No decomp., 10	280 (in vacuum)	Cu, 85 Cu_2O, 15
		Nickel oxalate		
100-150 (in air)	$8 \cdot 10^9$	Ni, 5 No decomp., 95	310 (in air)	NiO, 10
100-150 (in air)	$3 \cdot 10^{10}$	Ni, 80 No decomp., 20	280 (in vacuum)	Ni, 95 NiO, 2 No decomp.
40-50 (in air)	$3.3 \cdot 10^{10}$	Ni, 80 No decomp., 2?		

The topochemical decomposition process of copper and nickel oxalates may proceed with formation of a mixture of metals and oxides:

$$MeC_2O_4 \longrightarrow Me + 2CO_2; \tag{1}$$

$$MeC_2O_4 \longrightarrow MeO + CO + CO_2. \tag{2}$$

We determined that a third reaction occurs during the decomposition of copper oxalate, with formation of a cuprous oxide:

$$2MeC_2O_4 \longrightarrow Me_2O + CO + 3CO_2. \tag{3}$$

The rate of the processes and their direction depend to a great extent on the conditions of the experiment: temperature, gaseous media, and the effect of ionizing radiation. Thus, thermal decomposition of unirradiated copper oxalate in vacuum proceeds essentially according to reactions (1) and (3), beginning at 225°, while nickel oxalate decomposes essentially with formation of metallic nickel (1), beginning at 240°. The decomposition of both oxalates in air becomes measurable at higher temperatures (250° for copper oxalate and 300° for nickel oxalate). CuO and Cu_2O are formed in the first case, and NiO in the second.

The decomposition of oxalates in air as the result of irradiation begins at a temperature 200-250° lower than thermal decomposition, and the decomposition products have a different phase composition. The depth of decomposition increases with increasing radiation dose. The decomposition yield under the effect of radiation is a few tenths of a molecule per 100 ev.

A summary of the results characterizing the phase composition of the products of thermal and radiation decomposition of copper and nickel oxalates is given in the table. These data were obtained by structural x-ray analysis.

The table shows that the radiation decomposition of oxalates in air proceeds according to reaction (1) for nickel oxalate, and according to reactions (1) and (3) for copper oxalate. No formation of NiO and CuO was observed. Since the topochemical process due to radiation proceeds at low temperature, there is little oxidation of the decomposition products – metals – and the oxides formed are not revealed by x-ray analysis. It has been shown in special experiments that the oxidation of copper and nickel resulting from decomposition of oxalates (in vacuum) begins at 175° and becomes intense at 200°.

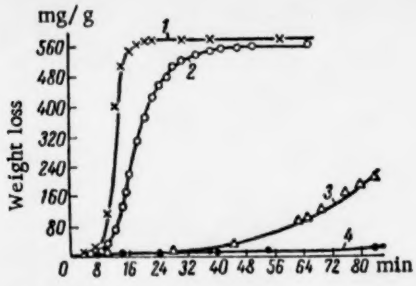

Fig. 1. Kinetic decomposition curves of copper oxalate in vacuum: 1) at 280°; 2) 263°; 3) 240°; 4) 225°.

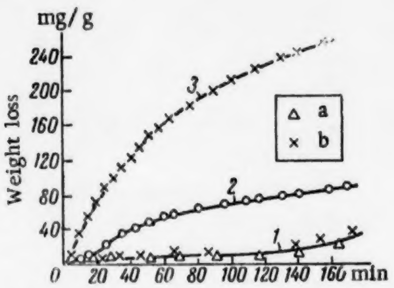

Fig. 2. Effect of radiation on the kinetics of decomposition of copper oxalate in vacuum at 225°: 1a) unirradiated sample; 1b) irradiated sample (dose $2.2 \cdot 10^8$ rad); 2) irradiated sample (dose $6 \cdot 10^8$ rad); 3) irradiated sample (dose $1.1 \cdot 10^9$ rad). The power of the dose was from 10^4 to 10 rad/sec.

Let us note that the thermal decomposition of oxalates in vacuum, which occurs at a higher temperature than radiation decomposition, also led essentially to the formation of metals in the case of nickel oxalate, and to a mixture of metal and metal oxide in the case of copper oxalate.

To clarify the effect of radiation on the kinetics of the topochemical processes investigated, we have drawn the kinetic curve of decomposition of unirradiated and irradiated copper oxalate in vacuum in the temperature range of 220-280°. Before the measurements, the samples were treated for a long time up to a constant weight at 150° to eliminate the water of crystallization.

Figure 1 shows that the kinetic decomposition curve of unirradiated copper oxalate at low temperatures has a shape characteristic of autocatalytic reactions with a long induction period (about 100 min at 200°). With increasing temperature, the induction period decreases. The activation energy of decomposition of copper oxalate calculated from the reciprocal of the time necessary to reach the maximum rate is equal to 29 kcal/mole. Figure 2 represents the decomposition curves of irradiated (in air) and unirradiated samples of copper oxalate. They were decomposed in vacuum at low temperature (220°).

From the data of Fig. 2 it follows that irradiation of copper oxalate with a dose of $2.2 \cdot 10^8$ rad does not affect the character of the kinetic curve for practical purposes. However, irradiation with a dose of $6 \cdot 10^8$ rad leads to a sharp decrease of the induction period (down to 10 min) and to a considerable increase of the rate. Even larger effects and a complete disappearance of self-acceleration were observed during the decomposition of the sample irradiated with a dose of $1 \cdot 10^9$ rad. It should be noted that according to the kinetic data such a radiation dose does not produce any noticeable decomposition products.

It can be assumed that excitation and ionization under the effect of a beam of electrons are accompanied by the creation of additional current carriers in the crystals. The doubly charged oxalate ions interact with electron holes and are transformed into singly charged or neutral oxalate radicals. The latter, moving within the crystal (e.g., by the relay mechanism [5]), gradually approach the outer surface, where, decomposing, they evolve into gaseous carbon dioxide. Simultaneously within the oxalate crystal and on its surface the cations having a double positive charge are reduced by the secondary electrons resulting from irradiation. The doubly charged cations may also pass through the intermediate stage of singly charged cations (formation of Cu_2O) to become metal atoms, with subsequent aggregation into groupings of atoms or crystallites.

Due to the mobility of the electrons of the conducting zone, these processes may occur at any place in the crystal where favorable conditions are created by the electron traps (e.g., by anion vacancies or neutral atoms of the metal in the intersites). The radiation defects can also serve as traps. The total process can be conceived as shown on the following page, where $\vec{e}$ represents the flow of electrons, $\underline{p}$ and $\underline{n}$ are additional current carriers (electron hole and electron) formed during irradiation. The rate of both processes depends on the concentration of additional current carriers. Determination of the character of this dependence requires further experiments concerning the effect of the energy of the radiation dose on the rate of the processes. It must be noted that the temperature coefficient of topochemical radiation processes is apparently not very large (see table).

$$C_2O_{4\,\mathrm{vol}}^{2-} + \vec{e} \longrightarrow C_2O_{4\,\mathrm{vol...p}}^{-} + n \qquad Me^{++} + n \longrightarrow Me^{+}$$

$$C_2O_{4\,\mathrm{vol...p}}^{-} \longrightarrow C_2O_{4\,\mathrm{surf...p}}^{-} \qquad Me^{+} + n \longrightarrow Me$$

$$C_2O_{4\,\mathrm{surf...p}}^{-} + p \longrightarrow \underset{\substack{|\\ 2CO_2}}{C_2O_{4}}{}_{\mathrm{surf}} \qquad kMe \longrightarrow (Me)_h$$

The thermal topochemical decomposition process of oxalates in vacuum may proceed according to the same mechanism, and the concentration of current carriers is then determined by thermal motion and is a function of temperature. The topochemical decomposition processes of copper and nickel oxalates resulting from irradiation occur at lower temperatures than the thermal decomposition processes (in vacuum), since the increase of the concentration of current carriers in the crystal is much greater as a result of ionizing radiation than as a result of temperature.

We determined that oxygen slows down the decomposition rate of copper and nickel oxalates, apparently as the result of oxidation of the metal atoms formed during decomposition. Therefore, thermal decomposition of oxalates in air occurs at higher temperatures than in vacuum and leads to the formation of oxides. Let us note that according to the assumed electron mechanism irradiation may create a certain number of metal atoms and other crystallization centers in the crystal. Subsequently, this leads to an increase of the decomposition rate and to a decrease of the induction period, which is apparently related to the process of formation of crystallites (or nuclei) of a new phase [6].

Thus, the application of ionizing radiation to the investigation of topochemical decomposition processes of nickel and copper oxalates, together with kinetic experiments and data from structural x-ray analysis, give results in favor of the electronic mechanism for these processes.

LITERATURE CITED

1. R. Smoluchowski, Radiation Res., Supplement 1, 36 (1959).
2. J. A. Allen and D. E. Scaife, J. Phys. Chem. No. 8, 667 (1954).
3. J. J. Macdonald, F. C. Waddington, and P. Gray, Disc. Faraday Soc. 23, 230 (1957).
4. V. V. Boldyrev, Zhur. Fiz. Khim. 33, 2539 (1959); Kinetika i Kataliz 1, 203 (1960).
5. S. Z. Roginskii, Khim. Nauka i Prom. 5, No. 5, 482 (1960).
6. P. W. M. Jacobs and F. C. Tompkins, Chemistry of the Solid State (London, 1955).

All abbreviations of periodicals in the above bibliography are letter-by-letter transliterations of the abbreviations as given in the original Russian journal. *Some or all of this periodical literature may well be available in English translation.* A complete list of the cover-to-cover English translations appears at the back of this issue.

THE THEORY OF THE BROWNIAN MOVEMENT IN THE CRITICAL RANGE

I. R. Krichevski and L. A. Rott

State Scientific Research and Design Institute for the Nitrogen Industry
and Synthetic Organic Products
(Presented by Academician A. N. Frumkin, September 19, 1960)
Translated from Doklady Akademii Nauk SSSR,
Vol. 136, No. 6, pp. 1368-1371, February, 1961
Original article submitted September 16, 1960

Since it has been experimentally established that diffusion stops in the critical region of separation into layers [1,2], it can clearly be seen that the diffusion equation is nonlinear. It means that the diffusion coefficient is dependent on concentration, and this coefficient practically falls to zero at the critical point [1,3].

Since the diffusion coefficient is not a constant quantity, attention must also be directed to the behavior of a Brownian particle in the critical range. It is known that the mean-square displacement of a particle is proportional to the time, i.e.,

$$\overline{S}^2 = 2Dt. \tag{1}$$

Since the coefficient D has the significance of the diffusion coefficient, a Brownian particle at the critical point should remain in the same place, i.e., in practice we should observe that the Brownian movement ceases. Experimental confirmation of this suggestion is to be found in essence in the results given in [4]. There it is shown that molecules of iodine forming an infinitely dilute solution with CO_2 in its critical phase (it may be assumed that the addition of an infinitely small quantity of a second component does not change the state of the critical phase of a pure solvent) show no noticeable displacement under the microscope, in contrast to the situation outside the critical range.

The study of thermodynamic effects makes it possible to examine the microscopic features of the critical state of a substance. The possibility of this approach has been pointed out, for example, in [5], in which the relaxation time of concentration fluctuations was determined.

The peculiar features of the fluctuation mechanism in the critical range should have an influence on the nature of the movement of a Brownian particle. The suggested possibility that the particle "stops" at the critical state of the pure substance has important foundations.

The defining equation in the theory of the Brownian movement is Smolukhovskii's integral equation [6]:

$$\omega(t_0, \overline{R}_0; t+\tau, \overline{R}) = \int \omega(t_0, \overline{R}_0; t, \overline{r})\, \omega(t, \overline{r}; t+\tau, \overline{R})\, d\overline{r}, \tag{2}$$

where ω is the probability density for the transfer of a particle from a state $\overline{R}_0$ to a state $\overline{r}$ in the time $t - t_0$. The integration is carried out over the whole range of change in $\overline{r}$.

Since the rate of change of the concentration fluctuations outside the critical region is large, it may be assumed that the particle is displaced in a homogeneous medium (this implies a certain degree of averaging). In the critical range, however, the rate of the fluctuations practically falls to zero. The stable (with a strong correlational connection) fluctuations in the density also determine the behavior of the Brownian particle. It must be assumed that in this case the movement now takes place in a nonhomogeneous medium.

If this were in fact the situation it would make necessary a certain generalization of Eq. (2) for the range of the critical point. This can be shown by considering the following theoretical model for random motion.

Let us consider the one-dimensional case. We are interested in the possibility of transferring the particle along a straight line in a series of steps of two kinds. Each displacement can be made to the right and to the left. The probability of displacement taking place is the same for both directions and is equal to one-half if neighboring steps are of the same type. If, however, for example, the step from the right is of a second type, then the probability of displacement from a step of the first type to the right will be $p_2 > \frac{1}{2}$ (the probability of displacement to the left in the direction of a step of the same type is $p_1 = 1 - p_2$).

The probability that the particle will be displaced continuously to the right by N steps, if among them there are n steps of the second type (not extremes, and separated by not less than 2 steps of the first type), is

$$P = (^1/_2)^{N-2n} p_1^n p_2^n. \tag{3}$$

This quantity will be a maximum when $p_1 = \frac{1}{2}$, which corresponds to the case where the steps are of the same type.

Let us extend this example. Let us assume that in length L there are N steps of the second type. Let us calculate the probability of displacement by a length $l < L$ in continuous fashion to the right for an arbitrary arrangement, on the selected region, of m and n steps of the first and second type, respectively. The density of steps of the second type will be distributed according to Poisson's law $f_\lambda(n)$, where $\lambda = (N/L)\,l$, $m > n$, and $n \gg 1$. The probability which we are seeking is then

$$\mathrm{P_I} = \sum_n f_\lambda(n) \sum_{\beta=0}^{n} \sum_{\gamma=0}^{[n/2]} \varphi(n)\,(^1/_2)^{m+n-4\gamma-2\beta}\,(p_1p_2)^{\beta+2\gamma} \qquad (\beta \leqslant n-2\gamma), \tag{4}$$

where $\varphi(n)$ is the probability of a given arrangement of n steps of the second type on length l. We shall subsequently assume that all arrangements are equally probable. γ is the number of groups in which there are not less than two steps of the second type; β is the number of steps of the same type to the left and right, of which there are not less than two steps of opposite (first) type. If to the left and right of a step of the second type there is one step of the first type, there is essentially no difference between them. We can therefore exclude this case: this restriction of the number of possible arrangements of steps does not narrow the content of the problem. In this case

$$\varphi(n) = \left\{1 + \sum_{\gamma=1}^{n/2} (n - 2\gamma + 1)\right\}^{-1}. \tag{5}$$

Carrying out the summation in Expression (4), we obtain

$$P_{\mathrm{I}} = \sum_n f_\lambda(n)\,\varphi(n)\,\frac{1 - (4p_1p_2)^n\,[2 + {}^1/_2 n - 16\,({}^1/_2 n + 1)\,p_1^2p_2^2]}{2^{m+n}\,(1 - 4p_1p_2)^2\,(1 + 4p_1p_2)}. \tag{6}$$

In addition to the general case (4), let us examine the particular arrangement for which $\gamma = 0$. The probability which we are seeking is then

$$P_{\mathrm{II}} = \sum_n f_\lambda(n)\,(^1/_2)^{m-n}\,p_1^n p_2^n. \tag{7}$$

There will exist an analogy between the actual movement of a Brownian particle and the above model examples if a step of the first type is taken to correspond to the denser regions of the volume, and a step of the second type to the less dense regions. The expression (4) corresponds to the case where the relaxation time of the density is small, and the Brownian particle is displaced in a homogeneous medium. The expression (7), however, corresponds to the case of the critical state: The more dense and less dense regions follow one another in strictly stable order. p_2 denotes the probability of the transfer of a particle from an element of volume of higher density to a volume element of lower density, so that we assume $p_2 > \frac{1}{2}$. Comparison of the values of the probabilities (6) and (7) shows that $P_I \gg P_{II}$.

The above model problems can also be formulated by Markov's method [7], which makes it possible to put them in their most general form.

The sharp difference in the probabilities of displacement in homogeneous and nonhomogeneous media gives grounds for assuming that the original equation describing the movement of a Brownian particle in the critical range should take account of the value of the local density. It is natural to assume that the latter should be taken into account in Eq. (2), which we can rewrite in the form

$$\omega(t_0, \overline{R}_0, \rho_0;\ t+\tau, \overline{R}, \rho_R) = \\ = \int \omega(t_0, \overline{R}_0, \rho_0;\ t, \bar{r}, \rho_r)\,\omega(t, \bar{r}, \rho_r;\ t+\tau, \overline{R}, \rho_R)\,d\bar{r}\,d\rho_r, \tag{8}$$

where $\rho_r = \rho(\bar{r})$ is the value of the density.

Expanding the function ω into a series in the neighborhood of the critical density of the medium

$$\omega(t_0, \overline{R}_0, \rho_0;\ t, \bar{r}, \rho_r) = \omega(t_0, \overline{R}_0, \rho_{cr};\ t, \bar{r}, \rho_r) + \left.\frac{\partial\omega}{\partial\rho_0}\right|_{\rho_{cr}} (\rho_0 - \rho_{cr}) + \ldots \tag{9}$$

Restricting ourselves to the first two terms of the expansion (9) and then multiplying Eq. (8) by the distribution function $f(\rho_0, \rho_R)$, and integrating over the whole volume (the last integration does not relate to the Brownian particle), we obtain

$$\int \omega(t_0, \overline{R}_0, \rho_0;\ t+\tau, \overline{R}, \rho_R)\,f(\rho_0, \rho_R)\,dV\,d\rho_0\,d\rho_R = \\ = \int \omega_{0r}(\rho_{cr}, \rho_r)\,\omega_{rR}(\rho_{cr}, \rho_R)\,f(\rho_0, \rho_R)\,d\bar{r}\,dV\,d\rho_0\,d\rho_r\,d\rho_R + \ldots \\ \ldots + \int \left.\frac{\partial\omega_{0r}}{\partial\rho_0}\right|_{\rho_{cr}} \left.\frac{\partial\omega_{rR}}{\partial\rho_R}\right|_{\rho_{cr}} (\rho_0 - \rho_{cr})(\rho_R - \rho_{cr})\,f(\rho_0, \rho_R)\,d\bar{r}\,dV\,d\rho_0\,d\rho_r\,d\rho_R. \tag{10}$$

Equation (10) can be written in the general form

$$A = B + C\int_V \overline{(\rho_0 - \rho_{cr})(\rho_R - \rho_{cr})}\,dV. \tag{11}$$

The quantities A and B cannot become infinity, but the integral in the right-hand side of Eq. (11) becomes infinity at the critical point of a pure substance [8]. The equation may be observed if C, i.e., the first derivative of ω with respect to the density, becomes zero.

Taking account of the subsequent terms in the expansion (9), it can be shown that higher derivatives should also become zero. Here we make use of the fact that at the critical point the integral with respect to volume of the static moment $\overline{(\rho - \bar{\rho})^{\alpha}}$ $(\bar{\rho} = \rho_{cr})$ is equal to infinity for all even powers α, and equal to zero for all odd powers ($\Delta\rho$ follows the normal distribution law).

Consequently, in the neighborhood of the critical point the probability density for the displacement of a Brownian particle becomes zero. This also means that relationship (1) does not apply in this case. In fact, the relationship (1) was obtained from the condition for independence of the events. It is assumed that

$$\overline{S^2} = \overline{(S_1 + S_2)^2} = \overline{S_1^2} + \overline{S_2^2}.$$

All this is applicable for a homogeneous medium. In a nonhomogeneous medium, on the contrary, $\overline{S_1 S_2} \neq 0$, so that we cannot obtain the functional equation

$$f(t) = f(t_1) + f(t - t_1),$$

from which (1) was obtained.

Experimental study of the behavior of a Brownian particle, like the study of diffusion in the critical region, is of considerable interest, and reveals valuable further possibilities for the study of microscopic relaxation processes.

LITERATURE CITED

1. I. R. Krichevskii, N. E. Khazanova, and L. P. Linshits, Doklady Akad. Nauk SSSR 99, 113 (1954).
2. I. R. Krichevskii and Yu. V. Tsekhanskaya, Zhur. Fiz. Khim. 30, 2315 (1956).
3. L. A. Rott, Doklady Akad. Nauk SSSR 121, 678 (1958).
4. I. R. Krichevskii, N. E. Khazanova, and L. R. Linshits, Inst. Fiz. Zhur. 3, 117 (1960).
5. L. A. Rott, Doklady Akad. Nauk SSSR 134, No. 2, 394 (1960).
6. M. A. Leontovich, Statistical Physics [in Russian] (1944).
7. S. Chandrasekar, Stochastic Problems in Physics and Astronomy [Russian translation] (IL, 1947).
8. L. Landau and E. Lifshits, Statistical Physics [in Russian] (1951).

THERMODYNAMIC CHARACTERISTICS OF NIOBIUM OXIDES

(EQUILIBRIUM WITH HYDROGEN AND ELECTROCHEMICAL MEASUREMENTS)

V. I. Lavrent'ev, Corr. Member AN SSSR Ya. I. Gerasimov,

and T. N. Rezukhina

Translated from Doklady Akademii Nauk SSSR,
Vol. 136, No. 6, pp. 1372-1375, February, 1961
Original article submitted November 30, 1960

In the niobium–oxygen system there exist at least three oxides: Nb_2O_5, with a range of homogeneity from $NbO_{2.5}$ to $NbO_{2.4}$,* NbO_2, and NbO, with extremely narrow ranges of homogeneity [1-7]. The conditions for equilibrium in the reduction of Nb_2O_5 to NbO_2 by hydrogen and carbon monoxide have already been studied [3-7]. The results of some work [3,4] are not, however, free from errors associated with the effect of thermal diffusion; [5] gives only tentative values for the equilibrium constants. Other work [6] is known to us only from a short description in the monograph [22], which gives no values for the equilibrium constants. In more recent work [7], the equilibrium between niobium pentoxide and hydrogen was measured for only one temperature. The equilibrium between lower oxides of niobium and hydrogen has apparently not been studied. In the present work a study was made of the equilibrium reduction of niobium pentoxide to NbO, and measurements were made of the emf of the galvanic cell formed by the lower oxide of niobium NbO and metallic niobium. The work was carried out with niobium pentoxide (99.9% Nb_2O_5) and metallic niobium (98.6% Nb, 0.08% Fe, 0.06% Ti, 0.10% Pb, 0.04% Si, and 0.12% C).

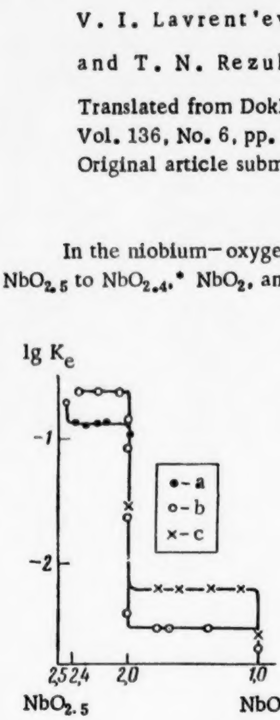

Fig. 1. Isotherms for the reduction of Nb_2O_5 for temperatures: a) 1207°, b) 1400°, c) 1550°.

The equilibrium between niobium oxides and hydrogen in the temperature range 1200-1550°C was studied by the circulation method in the apparatus described in [8]. The test specimen, in the form of tablets, was placed on a platinum support in a molybdenum short-circuited furnace in such a way that the tablet touched the platinum in few places. The gross composition of the reduction products was determined from the gain in weight of the specimen when ignited in air to Nb_2O_5, and the phase composition was determined by x-ray diffraction methods. Studies were made of the two stages of the reduction of Nb_2O_5:

$$2.5\,NbO_{2.4} + H_2 \rightarrow 2.5\,NbO_2 + H_2O, \qquad (I)$$

$$NbO_2 + H_2 \rightarrow NbO + H_2O. \qquad (II)$$

* Nb_2O_5 remains homogeneous in the range $NbO_{2.5}$ to $NbO_{2.39}$ according to [1], and in the range $NbO_{2.5}$ to $NbO_{2.42}$ according to [6].

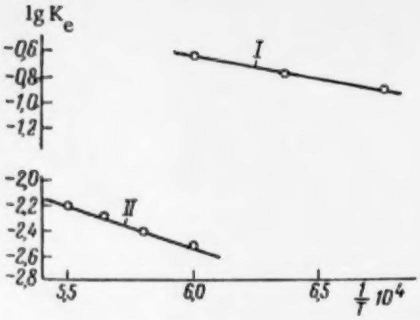

Fig. 2.

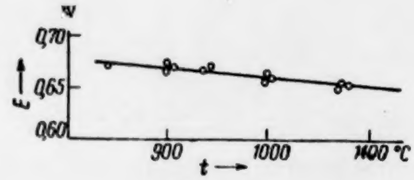

Fig. 3.

The values of the equilibrium constants $K_e = P_{H_2O}/P_{H_2}$ are given in Table 1 and Fig. 1. In the composition range from $NbO_{2.4}$ to $NbO_{2.5}$, the values of K_e increase rapidly, and they could not be measured sufficiently accurately on our apparatus. The logarithmic polythermals of the equilibrium constants for the two stages of the reduction of Nb_2O_5 (Fig. 2) are given (with an error of ± 0.2% for the first, and ± 0.3% for the second) by the following equations:

$$\lg K_{p_I} = -15050/4{,}575T + 1{,}3306 \qquad (1480 - 1673°K),$$
$$\lg K_{p_{II}} = -29490/4{,}575T + 1{,}3334 \qquad (1673 - 1823°K),$$

from which

$$\Delta G_I^0 \text{ (cal)} = 15\,050 - 6{,}087\,T, \quad \Delta G_{II}^0 \text{ (cal)} = 29\,490 - 6{,}10\,T.$$

Combining reactions I and II with the reaction for the formation of water vapor

$$H_2 + {}^1/_2\,O_2 \rightarrow H_2O\,(g) \qquad \text{(III)}$$

whose free energy, according to Chipman [9], is given by the equation ΔG_{III}^0 (cal) = $-59{,}251 + 2{,}006 \lg T - 7{,}5 \cdot 10^{-5}T^2 + 4{,}08 \cdot 10^5 T^{-1} + 6{,}8085T$, and using the literature data for the heat capacities of NbO_2 and NbO from [10], and of O_2 from [11], we can calculate ΔG_{IV}^0 and ΔG_V^0 (and also ΔH_{IV}^0, ΔH_V^0, ΔS_{IV}^0, and ΔS_V^0) for the formation of $NbO_{2.4}$ and NbO_2 at 298.2°K. For the reactions

$$NbO_2 + {}^1/_5\,O_2 \rightarrow NbO_{2,4}, \qquad \text{(IV)}$$

$$NbO + {}^1/_2\,O_2 \rightarrow NbO_2, \qquad \text{(V)}$$

$\Delta G_{IV}^0 = -26.2$ kcal; $\Delta H_{IV}^0 = -28.1$ kcal; $\Delta S_{IV}^0 = -6.36$ eu; $\Delta G_V^0 = -87.33$ kcal; $\Delta H_V^0 = -94.95$ kcal; and $\Delta S_V^0 = -25.57$ eu.

For the formation of Nb_2O_5 from NbO_2:

$$2NbO_2 + {}^1/_2 O_2 \rightarrow Nb_2O_5 \qquad \text{(VI)}$$

by linear extrapolation from the composition $NbO_{2.4}$ to $NbO_{2.5}$, we obtain for 298.2°K: $\Delta H_{VI}^0 = -70.25$ kcal; $\Delta G_{VI}^0 = -65.5$ kcal; and $\Delta S_{VI}^0 = -15.91$ eu.*

We were unable to achieve equilibrium reduction of niobium oxides to the metal by hydrogen. In order to determine the thermodynamic functions for the lower oxide of niobium NbO, therefore, we used the emf method. Measurements of E for the cell

$$Pt \mid Fe,\ Fe_{0.95}O \mid \underset{\text{electrolyte}}{\text{solid}} \mid NbO,\ Nb \mid Pt \qquad \text{(A)}$$

*Calculation of ΔG_{VI}^0 (and ΔH_{VI}^0 and ΔS_{VI}^0) with the assumption that the reduction of Nb_2O_5 takes place according to the equation $Nb_2O_5 + H_2 \rightarrow 2NbO_2 + H_2O$ gives, for 298.2°K: $\Delta H_{VI}^0 = -70.5$ kcal; $\Delta G_{VI}^0 = -65.9$ kcal; and $\Delta S_{VI}^0 = -15.6$ kcal.

TABLE 1

Temp. °C	Comp. of equilibrium spec.		K_e	Temp. °C	Comp. of equilibrium spec.		K_e
	gross	phase			gross	phase	
1207	$NbO_{2.44}$	Nb_2O_5	0.191	1400	$NbO_{2.00}$	NbO_2	0.0225
1207	$NbO_{2.37}$	Nb_2O_5, NbO_2	0.131	1400	$NbO_{2.00}$	"	0.00508
1207	$NbO_{2.30}$	"	0.127	1400	$NbO_{1.79}$	NbO_2, NbO	0.00306
1207	$NbO_{2.21}$	"	0.129	1400	$NbO_{1.73}$	"	0.00303
1207	$NbO_{2.19}$	"	0.126	1400	$NbO_{1.40}$	"	0.00301
1207	$NbO_{2.00}$	NbO_2	0.115	1400	$NbO_{1.01}$	NbO	0.00207
1300	$NbO_{2.42}$	Nb_2O_5	0.261	1450	$NbO_{1.63}$	NbO_2, NbO	0.00389
1300	$NbO_{2.33}$	Nb_2O_5, NbO_2	0.176	1500	$NbO_{1.55}$	"	0.00496
1300	$NbO_{2.21}$	"	0.170	1500	$NbO_{1.70}$	"	0.00500
1300	$NbO_{2.07}$	"	0.175	1550	$NbO_{2.00}$	NbO_2	0.0352
1400	$NbO_{2.20}$	"	0.229	1550	$NbO_{1.77}$	NbO_2, NbO	0.00628
1400	$NbO_{2.09}$	"	0.236	1550	$NbO_{1.64}$	"	0.00618
1400	$NbO_{2.34}$	"	0.228	1550	$NbO_{1.35}$	"	0.00638
1400	$NbO_{2.02}$	NbO_2	0.144	1550	$NbO_{1.12}$	"	0.00617
1400	$NbO_{2.01}$	"	0.0812	1550	$NbO_{1.00}$	NbO	0.00234

TABLE 2

Reaction	ΔH^0_{298} kcal	ΔS^0_{298}	Source	Reaction	ΔH^0_{298} kcal	ΔS^0_{298}	Source
$2NbO_2 + \frac{1}{2}O_2 \rightarrow Nb_2O_5$	−73.3	−17.77	(17)	$Nb + O_2 \rightarrow NbO_2$	−190.4		(17)
	−74.0		(18)		−199.3	−44.68	(18)
	−75.2		(19)		−190.4		(20)
	−70.3	−15.9	our data		−191.7	−45.8	(19)
					−193.3		our data
$NbO + \frac{1}{2}O_2 \rightarrow NbO_2$	−90.5	−22.98	(18)	$2Nb + \frac{5}{2}O_2 \rightarrow Nb_2O_5$	−455.2	−107.21	(20)
	−94.0		(19)		−472.6		(19)
	−95.0	−25.6	our data		−454.8		(22)
					−458.6		(19)
$Nb + \frac{1}{2}O_2 \rightarrow NbO$	−108.8	−21.57	(18)		−455.1		(21)
	−99.9		(22)		−456.9	−107.4	our data
	−97.7	−20.2	(19)				
	−98.4		our data				

were carried out on the apparatus described in [12], in the temperature range 841-1073°C. The solid electrolyte used in the experiments consisted of mixed crystals from the $ThO_2 - La_2O_3$ system. In individual cases, after the experiment with cell A had been carried out, the electrolyte tablet was used to measure E for the cell

$$Pt|Fe_3O_4,\ Fe_{0.95}O\ |\ \substack{\text{solid}\\ \text{electrolyte}}\ Fe_{0.95}O,\ Fe\ |\ Pt \qquad (B)$$

As an example, we give the values of E for cell B, obtained in one experiment:

Temperature, °C	900	1000	1100
E, v (our data)	0.102	0.131; 0.131	0.166
E, v (from [13])	0.101-0.103	0.132-0.136	0.165-0.166

The agreement between these data and the literature data [13] confirms the correctness of the choice of electrolyte.* The reference electrode ($Fe_{0.95}O$, Fe) and the electrolyte were prepared as previously described [12].

*Preliminary experiments showed that mixed crystals from the $ZrO_2 - CaO$ system cannot be used as electrolyte, due to penetration of the electrode material (apparently Nb and NbO) into the electrolyte; this electrolyte has, however, been found suitable for other cells [12,13].

The test electrode was prepared by compressing tablets from a mixture of the calculated quantities of Nb and Nb_2O_5, with subsequent annealing at 1700°C for 3 hr in vacuo.

The following values were obtained for the equilibrium emf of cell A, corresponding to the free energy change ($\Delta G^0_{VII} = -2FE$) for the reaction

$$Fe_{0.95}O + Nb \rightarrow 0.95Fe + NbO. \quad \text{(VII)}$$

Temp., °C	841	900	1000	905	935	940	1000	1000	1000	1071	1071	1073
E, v	0,671	0,675	0,664	0,666	0,666	0,670	0,657	0,669	0,654	0,653	0,658	0,660

These data and Fig. 3 show that the greatest deviation from linearity for the curve showing the relationship between E and T does not exceed ± 0.008 v, i.e., approximately 1.2% of the quantity being measured. The experimental data in the temperature range studied are given (to within ± 0.7%) by the equation ΔG^0_{VII} (cal) = $= -34{,}500 + 3.15T$. Using the values of ΔG^0_T for the reactions $Fe_{0.95}O + CO \rightarrow 0.95Fe + CO_2$ [14] and $CO + \frac{1}{2}O_2 \rightarrow CO_2$ [15], and the relationship between the heat capacities and temperature for NbO from [10], Nb and O_2 from [11], we obtain for the formation of NbO:

$$Nb + {}^1/_2\, O_2 \rightarrow NbO, \quad \text{(VIII)}$$

$$\Delta G^0_{VIII}(\text{cal}) = -98\,450 - 0{,}564\,T \lg T - 0{,}63 \cdot 10^{-3}T^2 - 0{,}08 \cdot 10^5 T^{-1} + + 22{,}10\,T\ (298 - 1346°\,K).$$

ΔG^0_{VIII} (cal) = $-98{,}450 - 0.564T \lg T - 0.63 \cdot 10^{-3}T^2 - 0.08 \cdot 10^5 T^{-1} + 22.10T$ (298 − 1346°K), from which, for 298.2°K: $\Delta G^0_{VIII} = -92.36$ kcal; $\Delta H^0_{VIII} = -98.39$ kcal; and $\Delta S^0_{VIII} = -20.19$ eu. Combining reactions (V), (VI), and (VIII), we obtain for the formation of Nb_2O_5 from the elements:

$$2\,Nb + {}^5/_2\, O_2 \rightarrow Nb_2O_5 \quad \text{(IX)}$$

at 298.2°K: $\Delta H^0_{IX} = -456.9$ kcal; $\Delta G^0_{IX} = -424.9$ kcal; and $\Delta S^0_{IX} = -107.43$ eu, and for the formation of NbO_2 from the elements

$$Nb + O_2 \rightarrow NbO_2 \quad \text{(X)}$$

at 298.2°K: $\Delta H^0_X = -193.3$ kcal; $\Delta G^0_X = -179.7$ kcal; and $\Delta S^0_X = -45.76$ eu.

Table 2 gives for comparison the values of ΔH^0_{298} and ΔS^0_{298} for reactions V, VI, VIII, IX, and X given by different authors: The ΔH^0_{298} values were obtained calorimetrically [18-21] and the ΔS^0_{298} values were calculated by making use of the entropies at 298.2°K: $S^0_{Nb} = 8.73$ [11]; $S^0_{NbO} = 11.5$ [11], $S^0_{NbO_2} = 13.07$ [16], $S^0_{Nb_2O_5} = 32.8$ [11], and $S^0_{O_2} = 49.02$ [11].

LITERATURE CITED

1. G. Brauer, Z. anorg. u. allgem. Chem. 248, 1 (1941).
2. S. I. Alyamovskii, G. P. Shveikin, and P. V. Gel'd, Zhur. Neorg. Khim. 3, 2437 (1958).
3. P. Sûe, Compt. rend. 208, 1088 (1939).
4. P. Sûe, J. Chim. Phys. 36, 280 (1939).
5. G. Grube, O. Kubaschewski, and K. Zwiauer, Z. Elektrochem. 45, 885 (1939).
6. G. Grube and M. Flad, KWJ Metallforschung, Stuttgart, 1945.
7. H. Schäfer and I. Breil, Z. anorg. Chem. 267, 165 (1952).
8. L. A. Zharkova, V. I. Lavrent'ev, et al., Doklady Akad. Nauk SSSR 134, 872 (1960).
9. J. Chipman, Trans. Am. Soc. Metals 22, 385 (1934).
10. P. V. Gel'd and R. G. Kusenko, Izvest. Akad. Nauk SSSR, Otd. Khim. Nauk No. 2, 79 (1960).
11. O. Kubaschewski and E. Evans, Metallurgical Thermochemistry (1958).
12. T. N. Rezukhina, V. I. Lavrent'ev, et al., Zhur. Fiz. Khim. (in press).
13. K. Kiukkola and C. Wagner, J. Electrochem. Soc. 104, 379 (1957).
14. L. S. Darken and R. W. Gurry, J. Am. Chem. Soc. 67, 1938 (1945).
15. H. Peters and H. H. Möbius, Z. Phys. Chem. 209, 298 (1958).
16. E. G. King, J. Am. Chem. Soc. 76, 3289 (1954).
17. A. Mah, J. Am. Chem. Soc. 80, 3872 (1958).

18. M. P. Morozova and L. L. Getskina, Zhur. Obshch. Khim. 29, 1049 (1959).
19. F. G. Kusenko and P. V. Gel'd, Sibirsk. Otd. Akad. Nauk SSSR No. 2 (1960).
20. G. L. Humphrey, J. Am. Chem. Soc. 76, 978 (1954).
21. F. G. Kusenko and P. V. Gel'd, Zhur. Obshch. Khim. 30, No. 11 (1960).
22. O. Kubaschewskii and A. A. Catteral, Thermochemical Data of Alloys (1956).
23. M. P. Morozova and T. A. Stolyarova, Zhur. Obshch. Khim. 30, 3848 (1960).

All abbreviations of periodicals in the above bibliography are letter-by-letter transliterations of the abbreviations as given in the original Russian journal. *Some or all of this periodical literature may well be available in English translation.* A complete list of the cover-to-cover English translations appears at the back of this issue.

INTERMOLECULAR TRANSFER OF ENERGY IN COLLISIONS OF CHEMICALLY ACTIVE MOLECULES

E. E. Nikitin

Chemical Physics Institute, Academy of Sciences of the USSR
(Presented by Academician V. N. Kondrat'ev, September 29, 1960)
Translated from Doklady Akademii Nauk SSSR,
Vol. 136, No. 6, pp. 1376-1379, February, 1961
Original article submitted September 27, 1960

In recent years, in connection with the intensive study of nonequilibrium processes in gases, a number of calculations have been made of the cross sections of the vibrational excitation of molecules on collision (see [1], for example). The model theories of collision on which these calculations are based reduce, for the most part, to the introduction of some spherically symmetrical potential of intermolecular interaction. In those cases where the actual angular dependence of the interaction is small the corrections introduced when allowance is made for it may lead to a certain change in the cross section, but the dependence of the cross section on the energy transferred, and on the temperature, remains unchanged [2]. It is significant that these models give an unsatisfactory description of the process of energy transfer on the collision of molecules which can take part in chemical reactions. In order to explain the high cross sections of vibrational excitation of chemically active molecules, a mechanism involving nonadiabatic collisions has been suggested [3]. In the present work, it is shown that the marked dependence of the energy of interaction on the configuration of the colliding molecular pair, which appears in the case where chemical reaction between these molecules is possible, also leads to a high cross section of vibrational excitation. This conclusion is of very great significance for explaining, in particular, the mechanism of vibrational relaxation in exchange reactions.

Let us examine as a model the collision of a diatomic molecule AB with an atom C, and let us assume that for a sufficiently high relative energy $\epsilon = \epsilon^*$ the exchange reaction

$$AB + C \longrightarrow A + BC \tag{1}$$

is possible. The interaction of AB and C can be described by a potential energy surface [4]. The valley point of this surface corresponds to the activated complex A – B – C, stable with respect to symmetrical stretching of the bonds AB and BC, and unstable with respect to unsymmetrical stretching. The transition through this point corresponds to a redistribution of the atoms, which we shall not consider. In addition to this point, there exists a large number of points in which the system is stable with respect to deformational vibrations of ABC, but unstable with respect to increase in the distance between the molecules. Movement of the representational point in this region describes the vibrational relaxation of the AB molecules on collisions of AB and C. Subsequently, we shall assume that the energy minimum corresponds to the linear configuration of the activated complex (qualitative deductions, however, are independent of this assumption), and that the relative energy ϵ is less than the activation energy ϵ^*.

The Hamiltonian of the colliding molecules on relative coordinates $\mathbf{r}$ and $\mathbf{R}$, diagonalizing the kinetic-energy operator, has the form

$$-\frac{\hbar^2}{2m}\Delta_r - \frac{\hbar^2}{2M}\Delta_R + U(r, R) + W(R, r, \theta), \tag{2}$$

where r is the vector of the internuclear distance of the AB molecules, R is the radius-vector of the C atom relative to the center of gravity of the AB molecule; m and M are the reduced masses of the AB molecule and the colliding pair; U(r,R) is the vibrational potential of the AB molecule; and W(R,r,θ) is the energy of interaction of AB and C. Since the exchange of energies takes place close to the turning point of the trajectory of the relative movement of AB and C, we shall seek an approximate solution of the wave equation in this region. In order to simplify the Hamiltonian, we shall make use of the condition that the interaction is markedly dependent on the angle ABC. If the frequency of the deformational vibration ω' close to the turning point is much greater than the average frequency of rotation of the complex ABC as a whole, the rotation of the whole system can be approximately separated. The errors thus introduced are associated with the neglect of centrifugal and Coriolis forces. After separation of the rotation, four coordinates remain – the angles θ and φ, corresponding to the doubly degenerate deformational vibration, and the linear coordinates r and R. Denoting the displacement from the equilibrium position of the atom B by x, we can write the Hamiltonian in the form

$$H = T(x) + T(R) + T(R, \theta) + U(x, R) + W(R) + \frac{k(R)}{2}\theta^2 + \\ + \alpha x W(R) + \alpha x \frac{k(R)}{2}\theta^2. \tag{3}$$

Formally, this Hamiltonian is identical with the vibrational Hamiltonian of a linear triatomic molecule. In this case, U(x,R) and $\frac{k(R)}{2}\theta^2$ are in fact vibration potentials, but W(R) corresponds to repulsion of the atoms B and C (with the condition, of course, that $\epsilon < \epsilon^*$) as a result of the exchange interaction. The last two terms in (3) describe the interaction of the vibrations of AB with relative translational movement of the colliding molecules and the deformational vibrations of the complex. Here and subsequently we assume that U is independent of θ, in accordance with the valence forces potential. Terms proportional to αx are obtained by expansion of the potential of interaction of the molecules to powers of the ratio of the displacement of the B atom to the radius of action of the exchange forces $1/\alpha$, since it may be assumed that the exchange interaction decreases approximately exponentially with increase in R.

If we put k = 0 in (3), we obtain a Hamiltonian corresponding to the model of Schwartz and Herzfeld [5]. The effect of rotation of the whole system is then, in general, insignificant, since the moment of the molecule AB and the relative moment of AB + C are preserved independently. In accordance with the accepted model, we assume, on the contrary, that $\alpha x\frac{k\theta^2}{2} \gg \alpha x W(R)$, so that only the last term in (3) appears as a perturbation responsible for the transfer of energy.

Let us seek nonperturbated wave functions of the form

$$\Phi_{vnm} = \varphi_v(x, R)\,\psi_n(\theta, \varphi, R)\,\chi_{vnm}(R). \tag{4}$$

For this purpose, it is necessary to use adiabatic separation of the vibrations and translational movement of the molecules; estimation shows that this is possible for typical values of the frequency of vibrations ω_0 of the AB molecule, the deformational frequency ω', and the relative velocity of the molecules V, characterizing the colliding pair (see below).

The probability of the transition $vnm \to v'n'm'$, calculated by the method of distorted waves, will be relatively large if at a certain point $R = R_0$ the frequency of the oscillations Ω of the product $\chi_{vnm}\chi_{v'n'm'}$ becomes zero (see [6], p. 352). With these conditions, the matrix element of the perturbation can be calculated by the stationary-phase method, and the expression for the probability of the transition acquires the form

$$P = \frac{\pi}{2}\,|(\alpha x)_{vv'}|^2\,\frac{\hbar\,[\omega'(R_0)]^2}{V_0\,|F_{v,n} - F_{v',n-2}|}\,n(n-1), \qquad n' = n-2, \tag{5}$$

where $F_{v,n}$ and $F_{v',n-2}$ are forces determining the relative movement of AB and C in the vibrational states v, n and v', n – 2 close to the resonance point R_0; V_0 is the relative velocity at this point. We note that if the molecule AB can be approximated to a harmonic oscillator, the transfer can take place only between two potential curves corresponding to the vibrational states v, n, and $v \pm 1$, $n \mp 2$.

For the frequency Ω to become zero, it is necessary that on mutual approach of the molecules AB and C, the frequency of the vibrations of the molecule AB for some intermolecular distance R_0 should be equal to twice the frequency of the deformational vibrations of the complex ABC. Unfortunately, the calculation of potential energy surfaces is not very accurate, so that it is difficult to make any definite statements regarding the fulfilling of the resonance condition. The most accurate calculation of H_3, for example, gives $\omega = 1945\ cm^{-1}$, and $\omega' = 952\ cm^{-1}$ for the valley point [7]. However, one has to consider that the participation of the p-electrons in the formation of the chemical bonds considerably increases ω'. It should, however, be taken into account that the frequency of the deformational vibrations of the complex ABC is close to the frequency of the deformational vibrations of linear triatomic molecules, i.e., for $M \approx 10$ we pute $\omega' \approx 500\ cm^{-1}$. On the other hand, close to the valley point the frequency ω decreases compared with the frequency of the free vibrations of AB (for the collision of $H_2 + H$, for example, the decrease in the frequency amounts to approximately $2000\ cm^{-1}$ [7]), so that for the same reduced mass we may put $\omega(R_0) \approx 1000\ cm^{-1}$. Thus, it is quite probable that the difference $\omega - 2\omega'$ becomes zero, i.e., that resonance takes place at some point.

Averaging of the probability (5) with respect to the thermal distribution of the colliding molecules can be carried out within the framework of the transition-state method, since it has been assumed that the colliding molecules are described by the equilibrium distribution function for relative motion (and in this case for deformational vibration also). Averaging with respect to $\underline{n}$ is not difficult. As far as averaging with respect to velocities is concerned, this leads to a decrease in the contribution of the slow collisions to the averaged probability P. This is due to the fact that at low velocities the colliding molecules may not reach the resonance point at all, so that the corresponding probability of energy transfer will be exponentially small. In practice, therefore, the averaging must begin from zero velocity at the resonance point, which corresponds, however, to a definite energy ϵ_0 at infinity. When $V \to 0$, the stationary phase approximation adopted is not applicable, and in order to calculate the probability it is necessary to use the function χ_{vnm} close to the turning point. Following the method of calculation given in [3], we obtain without difficulty

$$P \simeq \frac{\pi}{2} \left| (\alpha x)_{v,\, v-1} \right|^2 \frac{\omega'}{\overline{V}\alpha}\, \overline{n(n-1)} \exp\left(\frac{-\varepsilon_0}{kT}\right), \qquad \varepsilon_0 \ll \gamma kT;$$
$$P \simeq \frac{\pi}{2} \left| (\alpha x)_{v,\, v-1} \right|^2 \gamma^2 \overline{n(n-1)} \exp\left(\frac{-\varepsilon_0}{kT}\right), \qquad \varepsilon_0 \gg \gamma kT, \tag{6}$$

where $\overline{V}$ denotes the average velocity of the colliding molecules, and an approximation is made by putting $|F_{v-1,\, n} - F_{v,\, n-2}| = \alpha\hbar\omega'$, $\gamma = (2M\omega'^2 / \varepsilon_0\alpha^2)^{1/2}$

The expression (6) differs significantly from the formula of Schwartz and Herzfeld [5]: The probability of the resonance transfer of energy is much greater than the probability of the direct conversion of the kinetic energy of the colliding molecules to vibrational energy, and the temperature dependence of the probability is given by the Arrhenius formula with activation energy ϵ_0, and not by the Landau – Teller formula.

For the final averaging of the probability, it is necessary to take account of all configurations of the colliding pair. In accordance with the transition-state method, this can be done if we introduce into (6) a further factor f_{vib}/f_{rot}, where f_{vib} is the statistical sum of the doubly degenerate deformational vibration, and f_{rot} is the statistical sum of the rotation of the molecule AB. Thus, if we express the radius of action of the exchange forces in terms of the number of vibrational quanta N of the Morse oscillator, we can easily obtain, for the probability of the single-quantum vibrational deactivation of AB with the condition $\epsilon_0 \leq kT$ and $\hbar\omega' \geq kT$, the expression

$$P_{v,\, v-1} = \frac{\pi}{2} \frac{v}{N} \left(\frac{m_A}{m_A + m_B}\right)^2 \frac{\omega'}{\alpha\overline{V}} \frac{f_{vib}}{f_{rot}}. \tag{7}$$

In analogous fashion, we can obtain a formula for the case of $\hbar\omega' \ll kT$. Here, it is important that the condition $\hbar\omega' \ll kT$, taken in conjunction with the fact that $\epsilon_0 \leq kT$, does not contradict, over a wide range of change in ω', the condition of adiabatic separation of the translational and vibrational motions.

For a qualitative estimation of the probability from (7), we put $T = 300°K$, $M \approx 10$, $m_A \approx m_B$, $\omega' \approx 500\ cm^{-1}$, $f_{vib} \approx 1$, $f_{rot} \approx 10^2$, and $N \approx 10^2$. In this case, the probability of deactivation of the first vibrational quantum proves to be of the order of 10^{-3}. The theory of Schwartz and Herzfeld leads to values which are smaller by 2-4 orders of magnitude. In this connection it is of interest to cite the experimental values of the probability of deactivation of the first vibrational quantum of Cl_2, which were discussed by Pritchard [8] in an article on the

exchange of energy in substitution reactions. For the transition v = 1 → v = 0 of chlorine, an average of 43,000 collisions $Cl_2 + N_2$ are necessary, and only 230 Cl_2 + CO collisions. The marked increase in the probability of deactivation in the second case is due to the chemical affinity of Cl_2 and CO.

In conclusion, we would point out that the suggested mechanism of exchange of energies may be significant in connection with a number of other kinetic problems, particularly the nonequilibrium theory of chemical exchange reactions, which takes account of the breakdown of the Boltzmann distribution of the reacting molecules throughout the vibrational states.

I wish to thank Professor N. D. Sokolov for discussing this work.

LITERATURE CITED

1. V. N. Kondrat'ev, The Kinetics of Gaseous Chemical Reactions [in Russian] (AN SSSR Press, 1958).
2. K. F. Herzfeld, Z. Phys. 156, 265 (1959).
3. E. E. Nikitin, Optika i Spektroskopiya 9, 16 (1960).
4. S. Glasstone, K. Laidler, and H. Eyring, The Theory of Absolute Reaction Rates [Russian translation] (IL, 1948).
5. R. N. Schwartz and K. F. Herzfeld, J. Chem. Phys. 22, 767 (1954).
6. L. Landau and E. Lifshits, Quantum Mechanics [in Russian] (1948).
7. R. F. Weston, J. Chem. Phys. 31, 891 (1959).
8. H. O. Pritchard, Rec. Trav Chim. 74, 779 (1955).

All abbreviations of periodicals in the above bibliography are letter-by-letter transliterations of the abbreviations as given in the original Russian journal. *Some or all of this periodical literature may well be available in English translation.* A complete list of the cover-to-cover English translations appears at the back of this issue.

THE DEVELOPMENT AND CLOSURE OF CRACKS IN AN ISOTROPIC SOLID

M. S. Ostrikov

Rostov-on-Don State University
(Presented by Academician P. A. Rebinder, September 24, 1960)
Translated from Doklady Akademii Nauk SSSR,
Vol. 136, No. 6, pp. 1380-1383, February, 1961
Original article submitted August 10, 1960

The actual strength of solids is much lower than the theoretical strength, and is determined often not only by the physicochemical character of the solid but also by the nature of the defects in its structure [1].

The chief process in the development of an individual crack takes place at its blind end under the combined influence of external forces and internal stresses opposing the intermolecular cohesive forces of the solid phase. It is here, according to P. A. Rebinder [1], that the adsorptive influence of the medium (decrease in the free surface energy), as a result of the development of the adsorption layer, reaches a maximum value, and this is the most significant cause of the sharp decrease in strength.

It has already been pointed out [2] that in the dynamics of dispersion, particularly when the applied external forces are intermittent, variable, and of changing sign, the efficiency of these forces depends on the conditions of operation of the dispersion mechanism. In this, the most important parts are played by the following factors: a) the rate of development of the cracks with displacement of the points at which the stresses are concentrated; b) the rate of closure of the cracks after the removal of the load; c) the kinetics of "accretion" in the closed part of the crack; d) the rate of penetration of liquid inside the developing cracks; and e) the influence of different media on the rate of development of the cracks, and on the process of closure and self-healing.

With an unfavorable combination of these factors, periodic work applied to the creation of cracks in their reversible (closing) part may be to a considerable extent ineffective, for example in the case where the rate of development and closure of the cracks is much greater than the rate of movement of the molecular layers of the liquid phase along the newly formed surfaces. It is therefore important to study each of the above factors, and to establish the regular relationships between them, which influence the process of breakdown and deformation of solids.

The development of cracks in thin glass has already been studied, and the influence of various liquids on this process has been established [3], and a study has been made of the development and closure of cracks in a crystalline solid along the cleavage planes [4]. We have examined the same processes on specimens of silicate glass of different thicknesses. These experiments are of interest since they provide macromodels which permit a visual study of the elementary processes taking place in the individual intricately branching microcracks in the "prebreakdown zone" [2]. These experiments are also of interest in that the development of a crack in a specimen may take place in any direction, independent of the structure, isotropically. In macromolecular glasses, this should take place with the formation of free surface radicals, which can also be studied by the above method. The direction of the process of development of cracks is determined at first only by the direction of the previously applied initial crack, but displacement of the point of application of the load and of the bearing points can arbitrarily change the initial direction of the crack during its subsequent growth.

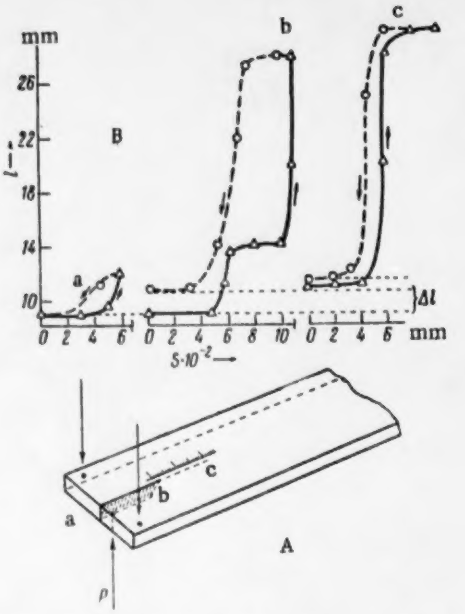

Fig. 1. A) Diagrammatic representation of an experimental plate with a developing crack; B) relationship between the length l of the crack and the deflection S of the plate during development and closure of the crack; a) reproducible cycle; b), c) nonreproducible curves.

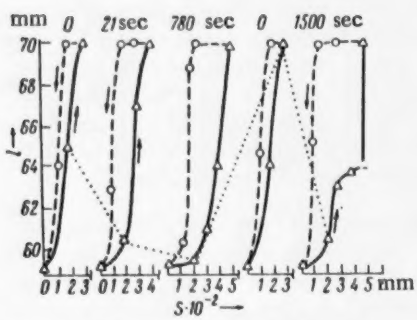

Fig. 2. A series of repeated cycles carried out after the cracks have been in the closed state for different periods of time. The dotted line joins points for which S = 0.02 mm. The strength of the regenerated bonds in the prebreakdown zone increases with increase in the duration of the process of "self-healing" of the crack.

The closure of a crack when the load is removed takes place at a considerable distance (sometimes up to 6-7 cm) and in the majority of cases cannot be detected optically (it can, however, be detected mechanically!).

Figure 1A gives a diagrammatic representation of an experimental plate with a crack developing under a load P, applied from below to the central point a. The bearing points are indicated by arrows. The dotted section b-c denotes the closed part of the crack after removal of the load.

The development of the crack with increase in the deflection S (which is proportional to the load) and the closure accompanying gradual removal of the load are shown in Fig. 1B. The cycle a is readily reproducible when repeated many times, in spite of the considerable hysteresis. If, however, the load P exceeds a certain limiting value, the steeply rising branch, as shown in Curve b, changes to a horizontal section and then to a new vertical section. Afterward the descending branch does not return to the starting point on the ordinate. The irreversible part of the crack Δl is greater the greater the amount by which the load exceeds the limiting value. The development of the crack takes place in stepwise fashion with continuous increase in the load.

The strength of the binding in the closed part of the crack increases markedly with time in the closed state. Figure 2 shows that the length of the crack for a given value of S = 0.02 mm decreases with increase in the time of "regeneration" of the molecular bonds in the prebreakdown zone (the corresponding points on the curve are joined by a dotted line).

The influence of a liquid medium and capillary forces is revealed extremely clearly in the kinetics of the development of the cracks under suitably selected constant loads (P). The results obtained with two specimens are shown in Curves a and b in Fig. 3. The lower initial sections of the curves reflect the development of the cracks with time, which takes place either at a decreasing rate or linearly, depending on the mechanical conditions. The rate increases sharply when a drop of water is applied to the point at which the stresses are concentrated. When the drop is applied to the crack at some distance from this point, the increase in the rate takes place only after the layer of liquid penetrating along the crack has reached its blind end. The rate of development of the crack decreases again suddenly if the applied drop is removed from the specimen (points marked rem), and increases again when the drop is subsequently reapplied. In this way it is possible to obtain a curve with several steps, as shown in Fig. 3b.

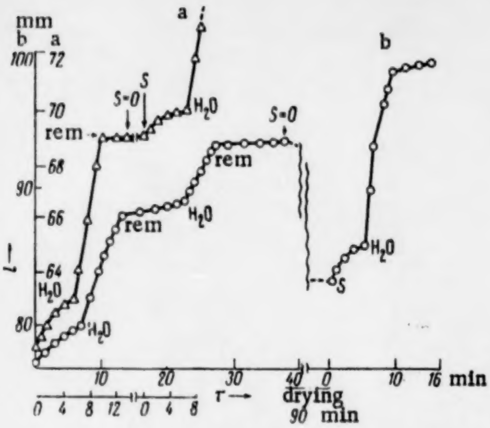

Fig. 3.

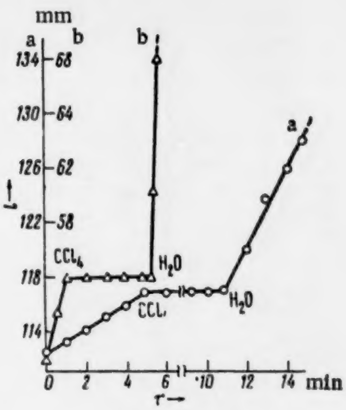

Fig. 4.

The experiment is particularly interesting because it shows very convincingly the mechanical compressive action of the capillary forces on the surface of the menisci in the mouths of the cracks. This effect exceeds the adsorptive and wedge-splitting pressure of the molecular layers of water remaining in the crack. If the load is removed after the drop has been removed (S = 0), the liquid remaining in the crack comes out along the whole line and collects in the form of very fine droplets which evaporate very rapidly.

In this state, specimen b was dried for 90 min. After this time, the crack had closed over a considerable region under the mechanical action of the elastic forces of the plate and, to an appreciable extent, the action of capillary contraction forces [5]. The strength of the regenerated bonds in the closed part of the crack increased, since when the previous load (S) was restored the development of the crack took place more slowly. The influence of water on this closed section is, however, particularly intense.

Figure 3a shows the results of experiments with the same specimen of glass, but with a higher load P. When the latter was removed (S = 0) and again restored (S), the development of the crack took place at a very much reduced rate. Here, also, the compressive action of the capillary forces is shown.

Nonpolar liquids (hexane, benzene, carbon tetrachloride, and liquid paraffin) under the conditions of the experiments described above have an effect which is the exact opposite of that produced by water. This can be seen clearly from Fig. 4, which gives results obtained for two different loads on the specimen. The development of the cracks stops when a drop of carbon tetrachloride is applied to them. This retarding action continues for a fairly long time, and stops when the nonpolar liquid in question has evaporated from the crack. If, however, a drop of water is applied to a crack in the presence of a nonpolar liquid which has stopped the development of the crack, the water instantly penetrates along the surface into the breakdown zone and produces its usual effect.

This is in good agreement with the general theories put forward earlier by Academician P. A. Rebinder and Aslanova, according to which clean surfaces of polar solids are wetted completely by both polar and nonpolar individual liquids with different values of the energy of wetting. The difference is revealed sharply in the surface activity and in the capillary antagonism of liquids of different polarity when these are present without having been mixed on a given surface; this is shown by the last experiment.

The above data indicate that there exist considerable opportunities for controlling the rate of the breakdown processes during dispersion, the mechanical cold-working of solid metals, and the treatment of various materials under operating conditions (friction, variable loads). It is necessary in these cases to take account of the physicochemical nature of the interaction of the solid phase with the medium, and the predominant importance of water for polar solids.

In subsequent studies it is intended to look for reagents capable of producing an effect in any of these directions.

The author wishes to thank Academician P. A. Rebinder for discussion of the present work.

LITERATURE CITED

1. P.A.Rebinder, Jubilee Collection Dedicated to the Thirtieth Anniversary of the Great Socialist October Revolution [in Russian] (AN SSSR Press, 1947) Part I, p. 533.
2. P. A. Rebinder, L. A. Shreiner, and K. F. Zhigach, Hardness and Boring Figures [in Russian] (AN SSSR Press, 1944).
3. V. P. Berdennikov, Zhur. Fiz. Khim. 5, Nos. 2-3, 358 (1934).
4. I. V. Obreimov, Proc. Roy. Soc. A127, 290 (1926).
5. M. S. Ostrikov, G. D. Dibrov, and E. P. Danilova, Doklady Akad. Nauk SSSR 118, No. 4 (1958).

All abbreviations of periodicals in the above bibliography are letter-by-letter transliterations of the abbreviations as given in the original Russian journal. *Some or all of this periodical literature may well be available in English translation.* A complete list of the cover-to-cover English translations appears at the back of this issue.

A GENERALIZED LEVER RULE

L. S. Palatnik

A. M. Gor'kii Khar'kov State University

(Presented by Academician P. A. Rebinder, September 27, 1960)
Translated from Doklady Akademii Nauk SSSR,
Vol. 136, No. 6, pp. 1384-1387, February, 1961
Original article submitted September 26, 1960

The lever rule is used to determine the ratio of the masses of the phases in an equilibrium two-phase system. Its generalization for the case of equilibrium in a three-phase system is the center-of-gravity rule; we have proposed a generalized center-of-gravity rule for the case of a multicomponent many-phase equilibrium system containing an arbitrary number of components [1]. This rule is used for the quantitative study of equilibrium states in complex multicomponent heterogeneous systems, and has been used to derive certain general regular features and rules relating to the structure of the equilibrium diagrams of such systems [2,3].

In this article we put forward a generalized lever rule, which is a new generalization of the above rules. Its essential feature is that in the study of different processes in equilibrium multicomponent systems, instead of considering the figurative points of each of the phases separately, we examine the figurative points of several (two) conglomerates of phases (see below) in equilibrium. This generalization makes possible the easy study (in stages or continuously) of the most complex processes in many-phase systems, which are extremely complicated when dealt with by the usual methods.

Let M – a figurative point (or the corresponding composition vector) inside a concentration simplex [3] – represent as a whole an equilibrium multicomponent heterogeneous system with unit mass. Then,

$$M = \sum_i X_i A_i = \sum_j m_j B_j = \sum_k \nu_k C_k, \qquad (1)$$

where A_i is the apex corresponding to the ith component of the concentration simplex (or vector of the ith component); X_i is the concentration of the ith component in the system; B_j is the jth apex in the phase simplex (vector of the jth phase); m_j is the mass of the jth phase; C_k is the vector of the kth conglomerate; ν_k is the mass of the kth conglomerate; i = 1, 2, . . . , is the number of the component; j = 1, 2, . . . , r is the number of the phase; and k = 1, 2, . . . , s is the number of the conglomerate of phases.

Formula (1) describes the above system M in terms of its components A_i, in terms of the coexisting phases B_j in the system, or conglomerates of phases C_k into which the system M is broken down. Equation (1) gives simultaneous conversion from one baricentric system of coordinates (the components of the system) to another (its phases or conglomerates of phases). At the same time, the geometrical dimensions R_A, R_B, and R_C of the concentration, phase, or conglomerate simplexes in the general case may be different. Thus, for example, for a three-component two-phase system, the concentration simplex is a Gibbs triangle ($R_A = 2$), while the phase simplex is a section of a straight line (a conode) ($R_B = 1$); for a four-component, three-phase system, the concentration simplex is a Roozeboom – Fedorov tetrahedron ($R_A = 3$), while the phase simplex is a triangle ($R_B = 2$), and so on. The dimensions of R_A and R_B may also be identical, for example for a three-component, three-phase system ($R_A = R_B = 2$), for a four-component, four-phase system ($R_A = R_B = 3$), etc.

In the case where $s = 2$ ($R_C = 1$), i.e., when the system breaks down into two-phase conglomerates, Eq.(1) becomes the generalized lever-rule equation

$$M = \sum_i X_i A_i = \sum_i m_i B_i = \nu L + (1-\nu) D, \qquad (2)$$

where L and D are the vectors of the two conglomerates of phases with masses ν and $(1-\nu)$, respectively. For example, in the case of the crystallization of a multicomponent alloy, L corresponds to the liquid phase (or conglomerate of liquid phases), and D corresponds to a conglomerate of all solid phases, previously separated before the true equilibrium moment.

From the law of conservation of mass for each of the n components of the system we have

$$\nu x_{iL} + (1-\nu) x_{iD} = X_i \quad (i = 1, 2, 3, \ldots, n), \qquad (3)$$

where x_{iL}, x_{iD}, and X_i are the concentrations of the ith component in the liquid phase, in the conglomerate of solid phases, and the system M as a whole, respectively; and ν and $(1-\nu)$ are the masses of the liquid phase and the conglomerate of solid phases.

The solution of Eq. (3) will be

$$\nu = \frac{X_i - x_{iD}}{x_{iL} - x_{iD}}, \quad 1 - \nu = \frac{x_{iL} - X_i}{x_{iL} - x_{iD}}, \qquad (4)$$

from which we obtain the equation for the generalized lever rule

$$\frac{\nu}{1-\nu} = \frac{X_i - x_{iD}}{x_{iL} - X_i}. \qquad (5)$$

By means of Eq. (5) it is possible to calculate the ratio of the masses ν and $(1-\nu)$ of the coexisting liquid phase and conglomerate of solid phases from the concentrations x_{iL}, x_{iD}, and X_i, or to calculate (analytically) the total composition of the conglomerate x_{iD} from a knowledge of ν, x_{iL}, and X_i in an equilibrium system containing an arbitrary number of components, etc.

Thus, when the multicomponent system M is broken down into two subsystems – the liquid phase and the conglomerate of solid phases – represented by the figurative points L and D, the "conglomerate simplex" degenerates into an ordinary (one-dimensional) conode, to which the ordinary lever rule can be applied.

When a reversible process is taking place in any of its stages, the points M, L, and D lie on the same straight line LMD, situated in the $(n-1)$th-dimensional space of the concentration simplex [and at the same time in the $(r-1)$th-dimensional space of the phase simplex]. During the whole process, the point M evidently remains immobile, but the points L and D may move simultaneously inside the concentration simplex (sliding along the boundary between the regions of the phase states) or may in turn remain immobile (in this case, one of the points will move along the straight line inside the one-phase region). The conode (section of the straight line) LMD and also the sections LM and MD may turn in a multidimensional concentration simplex around the point M, or may expand or contract, retaining their direction (they cannot, however, bend). The vector D at any moment of the reversible process can be broken down into its component vectors representing individual phases or other simpler conglomerates of phases (eutectics, etc.), which makes it possible to fix easily any state of the system throughout the whole of the process under study.

By means of the generalized lever rule, it is possible to describe extremely complex crystallization processes. As an example, let us examine the crystallization of a three-component system A – B – C, in which there is formed a ternary compound S with an incongruent melting point (in the liquid state there is complete mutual solubility and in the solid state complete insolubility of the components). Let us follow the process of crystallization for any composition from start to finish.

The figure shows the projection of the liquidus surface on the concentration triangle ABC. The region EP_2P_1E of primary crystallization of S lies outside the point S corresponding to the composition of the solid ternary compound. The ternary point P_1 corresponds to the nonvariant once-incongruent process of crystallization ($-L-A+B+S$). The plus and minus signs were defined on the basis of the center-of-gravity rule: The plus sign

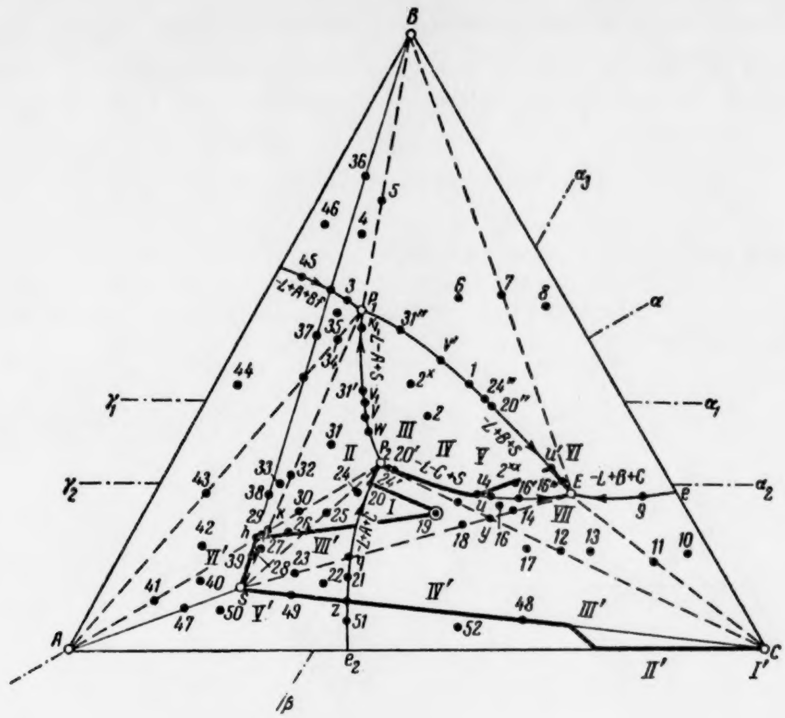

corresponds to the congruent process and the minus sign to the incongruent process (for example, at the point P_1, crystals of S and B separate while A disappears together with the liquid). The point P_2 corresponds to the nonvariant twice-incongruent process (−L−A−C +S); and the point E to the nonvariant congruent process (−L +B+C +S) in which the ternary eutectic (B + C + S) crystallizes.

The line P_1E represents the monovariant congruent (−L+B+S), and the lines P_2P_1 and P_2E represent the monovariant incongruent crystallization processes (−L−A+S) and (−L−C+S), etc. The arrows indicate the direction of the decrease in temperature during crystallization.

In the figure, theheavy lines show the stages in the crystallization from the liquid whose initial composition is given by point 19. The figure shows that on the basis of the generalized lever rule it is easy to establish the trajectory of the figurative points of the liquid phase and conglomerate of solid phases, coexisting at any momoment of the crystallization process. For the point 19, 7 crystallization stages are produced, denoted by Roman numerals: I-VII for the liquid phase and I'-VII' for the conglomerate of solid phases. At different stages of the crystallization the following solid phases coexist in the conglomerate:

$$I'(\mathrm{A});\quad II'(\mathrm{A}+\mathrm{C});\quad III'(\mathrm{A}+\mathrm{C}+\mathrm{S});\quad IV'(\mathrm{C}+\mathrm{S});$$
$$V'(\mathrm{S});\quad VI'(\mathrm{B}+\mathrm{S});\quad VII'(\mathrm{B}+\mathrm{C}+\mathrm{S}).$$

In the course of these seven stages, the variance of the system changes as follows: y = 2, 1, 0, 1, 2, 1, and 0. The mass ratio $\nu/(1-\nu)$ is readily calculated for any moment of the crystallization. By means of the proposed rule, it is easy to establish all stages of the crystallization for any other compositions of the system A − B − C.

We have used the proposed rule to construct various polythermal sections (for example $A\alpha$, $\gamma_1\alpha_1$, $\gamma_2\alpha_2$, $B\alpha_3$, etc.), on the basis of which it is possible to represent the whole of the spatial equilibrium-state diagram for the above complex ternary system.

In the case of multicomponent heterogeneous systems ($n \geq 4$), the generalized lever rule is not so revealing, but it can be used in the analytic form [Eqs. (4) and (5)].

Thus, from Eqs. (5), knowing the experimental values of X_X, x_{ID}, and $\frac{\nu}{1-\nu}$, we can find analytically the equation for the trajectory of the figurative point x_L in a multidimensional concentration simplex. From such data it is possible to obtain valuable information on the structure of the equilibrium diagram of a multicomponent system.

LITERATURE CITED

1. L. S. Palatnik, Doklady Akad. Nauk SSSR 95, 1227 (1954).
2. L. S. Palatnik and V. M. Kontorovich, Zhur. Fiz. Khim. 28, 1599 (1954).
3. L. S. Palatnik and A. I. Landau, Doklady Akad. Nauk SSSR 102, 125 (1955); 109, 954 (1956); 114, 837 (1957); Zhur. Fiz. Khim. 30, 2399 (1956); 31, 304 (1957); 31, 2739 (1957); Zhur. Neorg. Khim. 3, 637 (1958); Zhur. Tekh. Fiz. 28, 2340 (1958).

All abbreviations of periodicals in the above bibliography are letter-by-letter transliterations of the abbreviations as given in the original Russian journal. *Some or all of this periodical literature may well be available in English translation.* A complete list of the cover-to-cover English translations appears at the back of this issue.

OXIDATION–REDUCTION POTENTIAL OF THE Ti^{2+}/Ti^{3+} SYSTEM AND THE EQUILIBRIUM CONSTANT OF THE $2Ti^{3+} + Ti \rightleftharpoons 3Ti^{2+}$ REACTION IN MOLTEN CHLORIDES

M. V. Smirnov, L. A. Tsiovkina, and N. A. Loginov

Institute of Electrochemistry of the Ural Section, Academy of Sciences of the USSR
(Presented by Academician A. N. Frumkin, September 5, 1960)
Translated from Doklady Akademii Nauk SSSR,
Vol. 136, No. 6, pp. 1388-1391, February, 1961
Original article submitted August 31, 1960

The equilibrium reaction

$$Ti^{3+}(\text{molten}) + {}^{1}/_{2}\,Ti_{(s)} \rightleftarrows {}^{3}/_{2}\,Ti^{2+}(\text{molten}) \quad (1)$$

has been studied by a number of investigators [1-3]. However, none of them has given the expression for the temperature dependence of the equilibrium constant. Only one attempt was made [4] to measure the oxidation–reduction potential of the Ti^{2+}/Ti^{3+} system by potentiometric titration of titanium trichloride with hydrogen in a eutectic molten mixture of lithium and potassium chlorides. The formal value of the oxidation–reduction potential $E^0_{Ti^{2+}/Ti^{3+}}$ determined in this way was about 0.6 v more electropositive than the equilibrium potential of titanium, which we measured [5] under almost identical conditions. If the values found were correct, then the ratio of ion fraction concentrations in molten mixtures in equilibrium with metallic titanium should be of the order of 10^{-3}. In reality, however, $[Ti^{3+}]/[Ti^{2+}] \approx 10^{-1}$, according to direct measurements [1-3].

We have investigated cathodic polarization during electrolysis of molten chlorides containing trivalent titanium [6], and we have found that $E^0_{Ti^{3+}/Ti^{2+}}$ is about -1.7 v with respect to the chlorine reference electrode at 700-800°. This value is not only in good agreement with the kinetic data on the cathodic process, but also with the values of the concentrations of Ti^{2+} and Ti^{3+} in equilibrium with metallic titanium.

The validity of the method of potentiometric titration of $TiCl_3$ with hydrogen in molten salts is doubtful, since the rate of the reduction of $TiCl_3$ to $TiCl_2$ at 400-500° is very slow and incomplete [7]. The authors of this work [4] apparently have measured not the value $E^0_{Ti^{2+}/Ti^{3+}}$, but the potential in the system by which the equilibrium reaction was reached: $TiCl_3\,(\text{molten}) + \frac{1}{2}H_{2(g)} \rightleftharpoons TiCl_2\,(\text{molten}) + HCl_{(g)}$.

To be certain that this is actually so, we repeated the potentiometric titration of titanium trichloride with hydrogen in an equimolar mixture of sodium and potassium chlorides at 700°. The potential of the indicating electrode (molybdenum) was measured directly with respect to the chlorine reference electrode.

Figure 1 shows three typical experimental curves which we obtained. As can be seen, the shape of these curves is not the same as that of the potentiometric titration curve relative to the equation $E = E^0_{Ti^{2+}/Ti^{3+}} + \frac{RT}{F}\ln\frac{[Ti^{3+}]}{[Ti^{2+}]}$, which has a bend or a small plateau corresponding to $[Ti^{3+}] = [Ti^{2+}]$ when $E = E^0_{Ti^{2+}/Ti^{3+}}$. The curves tend toward a constant oxidation–reduction potential, which is about 0.5 v more positive than the equilibrium potential of titanium.

In our study we also used the method of potentiometric titration, but we used metallic titanium instead of hydrogen. This reducing agent, contrary to hydrogen, ensures without any doubt that during the process of reduction of Ti^{3+} to Ti^{2+} the reaction passes through a region where their concentrations become equal.

TABLE 1

Expt. No.	Initial $TiCl_3$ conc., wt%	t, °C	$E^0_{Ti^{2+}/Ti^{3+}}$, v	Expt. No.	Initial $TiCl_3$ conc., wt%	t, °C	$E^0_{Ti^{2+}/Ti^{3+}}$, v
1	1,93	711	−1,720	9		733	−1,731
2		725	−1,718	10	4,52	818	−1,722
3		734	−1,731	11		827	−1,720
4		737	−1,729	12		848	−1,717
5		740	−1,734	13		897	−1,723
6	2,26	713	−1,731	14	6,12	717	−1,727
7	3,96	711	−1,721	15		727	−1,728
8		724	−1,729	16		728	−1,731

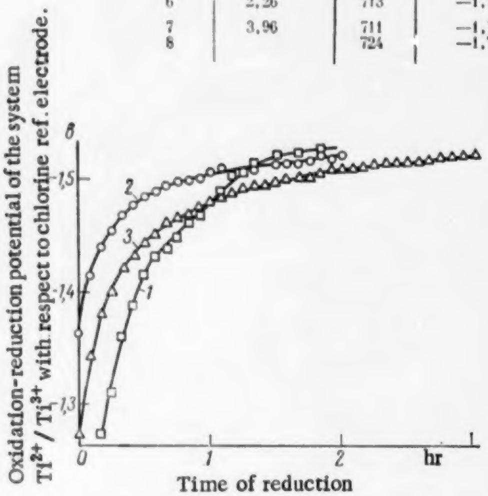

Fig. 1. Curves of potentiometric titration of $TiCl_3$ (4% by weight) in a molten equimolar mixture of NaCl − KCl at 700° from three consecutive experiments.

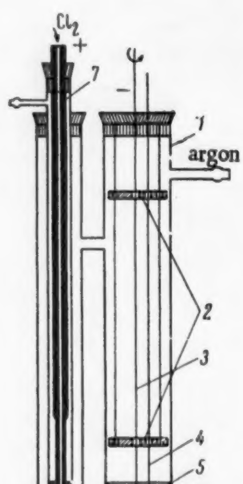

Fig. 2. Cell for measurement of oxidation–reduction potential of the Ti^{2+}/Ti^{3+} system: 1) quartz container; 2) graphite protecting screen; 3) molybdenum electrode; 4) molybdenum leads to titanium; 5) alundum crucible; 6) titanium iodide electrode; 7) chlorine reference electrode.

The salt mixtures were prepared by passing $TiCl_4$ vapor in a stream of pure hydrogen through an equimolar molten mixture of sodium and potassium chlorides. $TiCl_3$ was reduced with metallic titanium in the apparatus shown in Fig. 2. The oxidation–reduction potential of the system was measured with a molybdenum indicating electrode with respect to a chlorine reference electrode. Measurements were made every half a minute. To insure a rapid evening of the concentrations of Ti^{2+} and Ti^{3+} within the whole volume of the molten mixture, the molybdenum indicating electrode was rotated at 60 rpm. The temperature was maintained constant within limits of ± 2°.

The shape of the curve representing the variation of the potential as a function of the time necessary for reduction depends on the conditions (temperature, concentration, agitation of the molten mixture, etc.). The rate of the reduction reaction is particularly sensitive to increases of the surface of metallic titanium. This can be seen in Fig. 3.

However, all the experimental curves have a shape typical of potentiometric titration, namely a bend corresponding to the equality of the concentrations of trivalent and divalent titanium during the reduction process. Apparently the potentials of the molybdenum electrode corresponding to this bend give the formal values of the oxidation–reduction potential $E^0_{Ti^{2+}/Ti^{3+}}$, summarized in Table 1.

The table shows that the formal oxidation–reduction potential of the Ti^{2+}/Ti^{3+} system with respect to the chlorine reference electrode remains constant within the precision of measurement, and equal to

$$E^0_{Ti^{2+}/Ti^{3+}} = -1{,}726 \pm 0{,}005 \text{ v.}$$

We have previously determined [5] the variation of $E^0_{Ti/Ti^{2+}}$ as a function of temperature on the assumption that most of the titanium in the molten mixture is in a divalent state for the equilibrium reaction, and obtained the following:

$$E^0_{Ti/Ti^{2+}} = (-2{,}371 + 6{,}09 \cdot 10^{-4}\, T) \text{ v.}$$

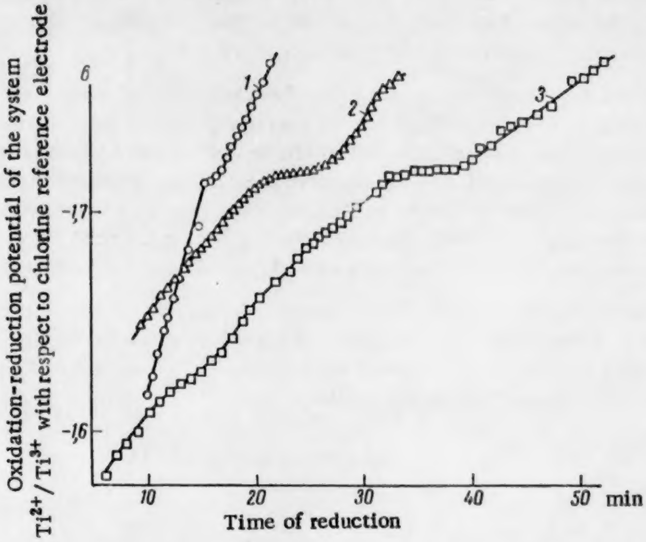

Fig. 3. Curves of potentiometric titration of $TiCl_3$ with metallic titanium in a molten equimolar mixture of NaCl – KCl: 1) 710°, 1.93% (by weight) $TiCl_3$; 2) 897°, 3.96% $TiCl_3$; 3) 824°, 3.96% $TiCl_3$. Curve 1 was obtained with a larger surface of the reducing metal than Curves 2 and 3.

TABLE 2

Temp., °C	Equilibrium constants	
	our data	other authors' data
700	2,82	1,21—0,56 (1) 2,95—1,65 (2)
800	1,35	1,33 (at 780°) (2) $8,6\cdot10^{-4}$—$6,14\cdot10^{-2}$ (at 825°) (3)
900	0,76	—
1000	0,46	—

According to [1,2], the amount of divalent titanium is 90% under this equilibrium condition. Taking this result into account, we obtain a somewhat different equation:

$$E^0_{Ti/Ti^{2+}} = (-2{,}371 + 5{,}73\cdot10^{-4}\,T)\ \mathrm{v}$$

with respect to the chlorine reference electrode.

Knowing $E^0_{Ti/Ti^{2+}}$ and $E_{Ti^{2+}/Ti^{3+}}$, we can easily find the expression for the temperature dependence of $E^0_{Ti/Ti^{3+}}$ in the thermodynamic equation of the equilibrium potential of titanium with respect to its trivalent ions in the molten chloride:

$$E = E^0_{Ti/Ti^{3+}} + \frac{RT}{3F}\ln[Ti^{3+}].$$

From the relationship $E^0_{Ti^{2+}/Ti^{3+}} = 3E^0_{Ti/Ti^{3+}} - 2E^0_{Ti/Ti^{2+}}$, it follows that:

$$E^0_{Ti/Ti^{3+}} = (-2{,}156 + 3{,}82\cdot10^{-4}\,T)\ \mathrm{v}$$

with respect to the chlorine reference electrode.

The equilibrium constant of reaction (1), expressed by the ion fraction concentrations of its component, is related to $E^0_{Ti^{+}/Ti^{2+}}$ and $E^0_{Ti/Ti^{3+}}$ by the expression

$$\ln K = \ln\frac{[Ti^{2+}]^{3/2}}{[Ti^{3+}]} = \frac{3F}{RT}\left(E^0_{Ti/Ti^{3+}} - E^0_{Ti/Ti^{2+}}\right).$$

Passing to ordinary logarithms, and substituting in this expression the temperature dependence of E^0 within the parentheses, we obtain the expression for the equilibrium constant:

$$\lg K = -2{,}888 + 3{,}251/T.$$

It is interesting to compare the value of the equilibrium constant calculated by this equation with the values obtained by other authors (summarized in Table 2). The equilibrium constant decreases with increasing temperature, i.e., the equilibrium reaction (1) displaces to the left.

This phenomenon is to some extent due to the "pulverization" of titanium in molten salts when the metal precipitates on the walls of the container. When the container is heated from the outside, the temperature of the walls is higher than the temperature of the metal within the molten salt. There may be a considerable difference in temperatures when the heat loss of metallic titanium is large. The equilibrium mixture of Ti^{2+} and Ti^{3+} ions formed near the metallic titanium is carried by the convection currents of the molten salt into the hotter region at the walls of the container. As a result, the equilibrium is displaced toward the deposition of metallic titanium, and the nucleation of a new phase favors the contact with the surface of the solid.

The assumption in [4], that the equilibrium constant depends on the concentration of titanium in the molten mixture, even when it is very low, is very doubtful. In our experiments, the original concentration of $TiCl_3$ in the electrolyte changed by more than a factor of three. However, we did not find any definite dependence of the value of the formal oxidation-reduction potential of the Ti^{2+}/Ti^{3+} system on the concentration of titanium.

LITERATURE CITED

1. S. Mellgren and W. Opie, J. Metals 9, 266 (1957).
2. W. C. Kreye and H. H. Kellogg, J. Electrochem. Soc. 104, 504 (1957).
3. Yu. V. Baimakov, M. V. Kamenetskii, and F. Cherny, Izvest. Vyssh. Uchebn. Zaved., Tsvetn. Met. No. 2, 102 (1960).
4. J. A. Menzies, G. J. Hills, L. Young, and J. O'M. Bockris, Trans. Faraday Soc. 55, 1580 (1954).
5. M. V. Smirnov, L. E. Ivanovskii, and N. A. Loginov, Doklady Akad. Nauk SSSR 121, 685 (1958).
6. M. V. Smirnov and L. A. Tsiovkina, Izvest. Sibirsk. Otd. Akad. Nauk SSSR No. 10, 74 (1959).
7. H. Tadenuma and Sh. Kadota, Japanese Patent No. 3067, 1955.

EFFECT OF A DROP OF MERCURY ON THE DEVELOPMENT OF CRACKS IN A ZINC PLATE SUBJECTED TO BENDING

B. D. Summ, Yu. V. Goryunov, N. V. Pertsov, E. D. Shchukin, and Academician P. A. Rebinder

M. V. Lomonosov Moscow State University,
Institute of Physical Chemistry, Academy of Sciences of the USSR

Translated from Doklady Akademii Nauk SSSR,
Vol. 136, No. 6, pp. 1392-1395, February, 1961
Original article submitted November 5, 1960

We have previously investigated the effect of metal coatings with low melting points on the resistance to deformation and mechanical resistance of monocrystalline metals with high melting points. In these experiments we covered the entire surface of the sample with a thin liquid layer, of the order of a few microns. We showed that the presence of a liquid layer of surface-active metal can alter the mechanical properties of the monocrystal: It may lose its resistance and become fragile [1-4]. We explained this phenomenon as the effect of the adsorbed surface material on the mechanical properties of the sample. The loss of resistance is due to the sharp decrease of the free energy of new surfaces developed in the sample in the process of deformation and cracking. As a result of irregular diffusion (two-dimensional migration) the atoms of the surface-active material move along the defects of the crystal structure toward the microcracks developing in the sample.

In the present work we investigate for the first time the development of cracks resulting from a small drop of adsorptionally active material (mercury) on the surface of the sample. The samples were plates of technically pure zinc (98.7% Zn) 0.8-3 mm thick and 50 cm wide. The plates were bent in the apparatus shown in Fig. 1 by a force F, so that the tensile stress p_m on the surface of the plates where the drop was deposited was relatively small – about 7-8 kg/mm^2; (the limit resistance of zinc is $\approx$18 kg/mm^3). Under these conditions, plates without mercury are relatively free of residual deformation during the ordinary period of the experiment (about 10 min). When the stress is further increased, the plates can be bent to a right angle without the appearance of visible cracks.

Mercury was deposited on the upper (elongated) side of the plate at a distance of 15-30 mm from where the sample was fixed in the apparatus. The drop of mercury had a mass $\underline{m}$ from 0.2-40 mg. A small fresh scratch (or a slight etching with alkali) was made at the point where the drop was to be deposited in order to insure contact (wetting) of the zinc with mercury.

When the stress p_m is about 7 kg/mm^2, a crack appears at the point of contact with mercury. This crack absorbs all the mercury almost immediately (a fraction of a second to one or two seconds), and as a result the crack develops rapidly in the direction perpendicular to the direction of application of the stress. The rate of development of the crack then drops, and after 5-10 min becomes very low. At this point, the crack has penetrated almost the entire thickness of the plate. The final length L of the crack is determined by the amount of mercury deposited $\underline{m}$ (see Fig. 2). The development process of the crack can be represented in a first approximation in the following way (proposed by one of the authors, E. D. Shchukin). The crack can grow only as the result of penetration of mercury atoms into the metal immediately beyond the V of the crack. This mercury penetrates by two-dimensional migration along the walls of the crack. As a result of three-dimensional diffusion, mercury is adsorbed simultaneously by the walls along the entire length of the crack. Therefore, the higher the rate of

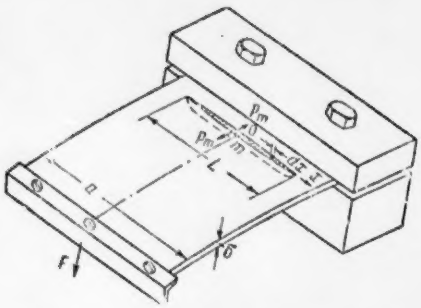

Fig. 1. Sketch of the development of cracks as the result of a drop of mercury on a plate of zinc subjected to bending.

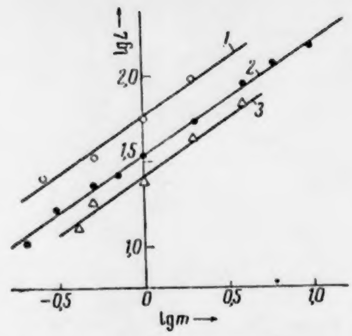

Fig. 2. Variation of the total length of the crack L (mm) as a function of the mass of the drop of mercury m (mg) for different thicknesses δ of the plate: 1) 0.8 mm; 2) 1.85 mm; 3) 3.0 mm. The tangent of the slope of the lines is exactly $^2/_3$.

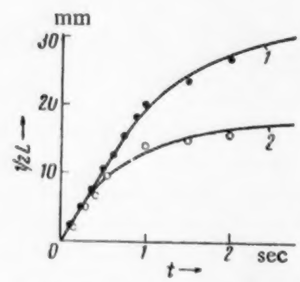

Fig. 3. Rate of growth of the crack as a function of time during the initial stage of its development (in one direction from the point of nucleation) for different masses of mercury m: 1) 40 mg; 2) 10 mg; thickness of the plate δ = 1.85 mm (according to the movie film).

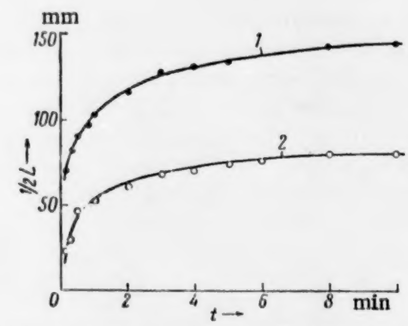

Fig. 4. Rate of growth of the crack during the later stages of its development (in one direction from the point of nucleation) for different masses of mercury m: 1) 40 mg; 2) 10 mg; thickness of plate δ = 1.85 mm.

its migration, the slower the three-dimensional diffusion; and the slower the three-dimensional diffusion, the more "efficient" the utilization of the mercury in terms of extending the V of the crack deeper into the material. Thus, the kinetics of the development of the crack is determined by two competing processes: 1) two-dimensional migration of adsorptionally active atoms along the walls of the crack, and 2) their diffusion into the sample in the direction perpendicular to the walls of the crack.

For simplicity let us assume that the development of the crack (from each side of the drop) proceeds at a constant rate, equal to the migration rate v. Then, an area of the surface dx opens at some time $t_1 = x/v$ after the nucleation of the crack (see Fig. 1). It can be assumed with a certain approximation that the penetration of mercury from the walls of the crack into the sample is described by the ordinary diffusion equation (unidimensional case) with a constant diffusion coefficient D. (In this case, it can be expected that the coefficient will be considerably higher than during normal diffusion into a nondeformed zinc lattice due to weakening of the walls of the crack, which have a great number of defects, pores, and ultramicrocracks; therefore, the process considered should be more correctly called "quasi-three-dimensional.") Under these conditions, at a time t after the opening of a given crack, an amount $C_0(Dt)^{\frac{1}{2}} = kt^{\frac{1}{2}}$ (grams) of the surface-active substance passes into the volume

$(2/\pi)$ of the sample per square centimeter of the surface of the crack (C_0 is the concentration in the surface layer). After a time $\underline{t}$, an amount $k(t-t_1)^{\frac{1}{2}}2\delta dx = 2k\delta(t-x/v)^{\frac{1}{2}}dx$ will pass from an area dx into the volume, and an amount $2k\delta\int_0^{vt}\sqrt{t-x/v}\,dx = \frac{4}{3}k\delta vt^{3/2}$ (grams) of mercury will pass from one half the total wall surface of the crack. If $L = 2vt_f$ (the total finite length of the crack), then after a finite time t_f we have $\frac{m}{2} = \frac{4}{3}k\delta v\left(\frac{L}{2v}\right)^{3/2}$ and therefore

$$L = \frac{1}{2}\left(\frac{3\pi}{2C_0\delta}\right)^{2/3}\left(\frac{v}{D}\right)^{1/3}m^{2/3} = A\delta^{-2/3}m^{2/3},$$

where A is a constant.

Figure 2 indicates that within a wide range of values of $\underline{m}$ the length of the crack is actually proportional to $m^{2/3}$. The indicated variation of L as a function of thickness δ is also in good agreement with the theory.

This simple outline needs to be refined, however. The experiments showed that the length of the crack may depend on the method of applying stress. Namely, if in the experiments with a constant load the stess is increased (due to the decrease of the cross section of the sample and an increase of the concentration of stress at the head of the crack), then L becomes smaller. Apparently this is due to the loosening of the zinc structure in the region of the point of the V of the main crack as a result of the occurrence of a great number of small cracklets which absorb mercury intensely and thus hinder development of the original crack. The main crack branches as a result of this, and this branching can be seen with the naked eye.

A detailed investigation of the kinetics of the growth of the crack would be particularly interesting. The results concerning the initial stage obtained with a movie camera are represented in Fig. 3; Fig. 4 illustrates the next, slower stage of development. These curves clearly illustrate the first, rapid stage of the process, which occurs over a period of time not exceeding one second, when the rate of growth of the crack is constant and independent of $\underline{m}$. During this period, the drop of mercury is drawn into and flows into the crack. The duration of this stage increases with the size of the drop. Later development is apparently as follows: As the crack grows, the amount of mercury is insufficient to fill the whole crack; mercury then covers the walls of the crack in a more or less thick layer. This mercury is used up gradually during the following stage, when mercury is supplied to the zone immediately beyond the point of the V of the crack by surface migration (spreading of the thin adsorptional layers of mercury). The rate of development of the crack then decreases. After a few minutes begins the third, slowest, and longest stage; during this stage there is no more free mercury in the crack, and it can be supplied to the zone immediately below the V only by a redistribution of the mercury remaining in very thin layers on the walls of the crack.

These experiments show that it is possible to analyze in detail the role of two-dimensional migration and three-dimensional diffusion leading to loss of resistance in the metal under the effect of mercury. We think that further development of this investigation will allow us to study in more detail the kinetics and mechanism of migration of adsorptionally active atoms.

LITERATURE CITED

1. P. A. Rebinder, V. I. Likhtman, and L. A. Kochanova, Doklady Akad. Nauk SSSR 111, 1284 (1956).
2. V. N. Rozhanskii, N. V. Pertsov, E. D. Shchukin, and P. A. Rebinder, Doklady Akad. Nauk SSSR 116, 769 (1957).
3. E. D. Shchukin, N. V. Pertsov, and Yu. V. Goryunov, Kristallografiya 4, 887 (1959).
4. L. A. Kochanova, E. D. Shchukin, V. I. Likhtman, and P. A. Rebinder, Doklady Akad. Nauk SSSR 133, 71 (1960).

All abbreviations of periodicals in the above bibliography are letter-by-letter transliterations of the abbreviations as given in the original Russian journal. *Some or all of this periodical literature may well be available in English translation.* A complete list of the cover-to-cover English translations appears at the back of this issue.

SIGNIFICANCE OF ABBREVIATIONS MOST FREQUENTLY ENCOUNTERED IN SOVIET PERIODICALS

FIAN	Phys. Inst. Acad. Sci. USSR.
GDI	Water Power Inst.
GITI	State Sci.-Tech. Press
GITTL	State Tech. and Theor. Lit. Press
GONTI	State United Sci.-Tech. Press
Gosenergoizdat	State Power Press
Goskhimizdat	State Chem. Press
GOST	All-Union State Standard
GTTI	State Tech. and Theor. Lit. Press
IL	Foreign Lit. Press
ISN (Izd. Sov. Nauk)	Soviet Science Press
Izd. AN SSSR	Acad. Sci. USSR Press
Izd. MGU	Moscow State Univ. Press
LEIIZhT	Leningrad Power Inst. of Railroad Engineering
LET	Leningrad Elec. Engr. School
LETI	Leningrad Electrotechnical Inst.
LETIIZhT	Leningrad Electrical Engineering Research Inst. of Railroad Engr.
Mashgiz	State Sci.-Tech. Press for Machine Construction Lit.
MEP	Ministry of Electrical Industry
MES	Ministry of Electrical Power Plants
MESEP	Ministry of Electrical Power Plants and the Electrical Industry
MGU	Moscow State Univ.
MKhTI	Moscow Inst. Chem. Tech.
MOPI	Moscow Regional Pedagogical Inst.
MSP	Ministry of Industrial Construction
NII ZVUKSZAPIOI	Scientific Research Inst. of Sound Recording
NIKFI	Sci. Inst. of Modern Motion Picture Photography
ONTI	United Sci.-Tech. Press
OTI	Division of Technical Information
OTN	Div. Tech. Sci.
Stroiizdat	Construction Press
TOE	Association of Power Engineers
TsKTI	Central Research Inst. for Boilers and Turbines
TsNIEL	Central Scientific Research Elec. Engr. Lab.
TsNIEL-MES	Central Scientific Research Elec. Engr. Lab.—Ministry of Electric Power Plants
TsVTI	Central Office of Economic Information
UF	Ural Branch
VIESKh	All-Union Inst. of Rural Elec. Power Stations
VNIIM	All-Union Scientific Research Inst. of Metrology
VNIIZhDT	All-Union Scientific Research Inst. of Railroad Engineering
VTI	All-Union Thermotech. Inst.
VZEI	All-Union Power Correspondence Inst.

Note: Abbreviations not on this list and not explained in the translation have been transliterated, no further information about their significance being available to us. — Publisher.

Soviet Journals Available in Cover-to-Cover Translation

ABBREVIATION	RUSSIAN TITLE		TITLE OF TRANSLATION	PUBLISHER	TRANSLATION BEGAN Vol.	Issue	Year
AÉ	Atomnaya énergiya		Soviet Journal of Atomic Energy	Consultants Bureau	1	1	1956
Akust. zh.	Akusticheskii zhurnal		Soviet Physics – Acoustics	American Institute of Physics	1	1	1955
	Antibiotiki		Antibiotics	Consultants Bureau	4	1	1959
Astr(on). zh(urn).	Astronomicheskii zhurnal		Soviet Astronomy–AJ	American Institute of Physics	34	1	1957
Avto(mat). svarka	Avtomaticheskaya svarka		Automatic Welding	British Welding Research Association (London)		1	1959
	Avtomatika i Telemekhanika		Automation and Remote Control	Instrument Society of America	27	1	1956
	Biofizika		Biophysics	National Institutes of Health*		1	1957
	Biokhimiya		Biochemistry	Consultants Bureau	21	1	1956
Byull. éksp(erim). biol. i med.	Byulleten' éksperimental'noi biologii i meditsiny		Bulletin of Experimental Biology and Medicine	Consultants Bureau	41	1	1959
DAN (SSSR) Dokl(ady) AN SSSR	Doklady Akademii Nauk SSSR		The translation of this journal is published in sections, as follows:				
		Life Sciences	Doklady Biochemistry Section	American Institute of Biological Sciences	106	1	1956
		Life Sciences	Doklady Biological Sciences Sections (Includes: Anatomy, biophysics, cytology, ecology, embryology, endocrinology, evolutionary morphology, genetics, histology, hydrobiology microbiology, morphology, parasitology, physiology, zoology sections)	American Institute of Biological Sciences	112	1	1957
		Life Sciences	Doklady Botanical Sciences Sections (Includes: Botany, phytopathology, plant anatomy, plant ecology, plant embryology, plant physiology, plant morphology sections)	American Institute of Biological Sciences	112	1	1957
		Chemical Sciences	Proceedings of the Academy of Sciences of the USSR, Section: Chemical Technology	Consultants Bureau	106	1	1956
		Chemical Sciences	Proceedings of the Academy of Sciences of the USSR, Section: Chemistry	Consultants Bureau	106	1	1956
		Chemical Sciences	Proceedings of the Academy of Sciences of the USSR, Section: Physical Chemistry	Consultants Bureau	112	1	1957
		Earth Sciences	Doklady Earth Sciences Sections (Includes: Geochemistry, geology, geophysics, hydrogeology, mineralogy, paleontology, petrography, permafrost sections)	American Geological Institute	124	1	1959
		Earth Sciences	Proceedings of the Academy of Sciences of the USSR, Section: Geochemistry	Consultants Bureau	106-123	1 6	1957-1958
		Earth Sciences	Proceedings of the Academy of Sciences of the USSR, Sections: Geology	Consultants Bureau	106-123	1 6	1957-1958
		Mathematics	Doklady Soviet Mathematics	The American Mathematics Society	131	1	1961
		Physics	Soviet Physics–Doklady (Includes: Aerodynamics, astronomy, crystallography, cybernetics and control theory, electrical engineering, energetics, fluid mechanics, heat engineering, hydraulics, mathematical physics, mechanics, physics, technical physics, theory of elasticity sections)	American Institute of Physics	106	1	1956
		Physics	Proceedings of the Academy of Sciences of the USSR, Applied Physics Sections (does not include mathematical physics or physics sections)	Consultants Bureau	106-117	1	1956-1957
Derevoobrabat. prom-st'.	Derevoobrabatyvayushchaya promyshlennost'		Wood Processing Industry	Timber Development Association (London)		9	1959
	Élecktrosvyaz		Telecommunications	Massachusetts Institute of Technology*		1	1957
Éntom(ol). oboz(renie)	Éntomologicheskoe obozrenie		Entomological Review	American Institute of Biological Sciences	38	1	1959
Farmakol. (i) toksikol(ogiya)	Farmakologiya i toksikologiya		Pharmacology and Toxicology	Consultants Bureau	20	1	1957
FMM	Fizika metallov i metallovedenie		Physics of Metals and Metallography	Acta Metallurgica*	5	1	1957
Fiziol. zhurn. SSSR (im. Sechenova)	Fiziologicheskii zhurnal im. I. M. Sechenova		Sechenov Physiological Journal USSR	National Institutes of Health*		1	1957
Fiziol(ogiya) rast.	Fiziologiya rastenii		Plant Physiology	American Institute of Biological Sciences	4	1	1957
	Geokhimiya		Geochemistry	The Geochemical Society		1	1958
FTT	Fizika tverdogo tela		Soviet Physics–Solid State	American Institute of Physics	1	1	1959
Izmerit. tekh(nika)	Izmeritel'naya tekhnika		Measurement Techniques	Instrument Society of America		1	1959
Izv. AN SSSR, O(td). Kh(im). N(auk)	Izvestiya Akademii Nauk SSSR: Otdelenie khimicheskikh nauk		Bulletin of the Academy of Sciences of the USSR: Division of Chemical Sciences	Consultants Bureau		1	1952

continued

Izv. AN SSSR, O(td). T(ekhn). N(auk): Met(all). i top.	(see Met. i top.)					
Izv. AN SSSR Ser. fiz(ich).	Izvestiya Akademii Nauk SSSR: Seriya fizicheskaya	Bulletin of the Academy of Sciences of the USSR: Physical Series	Columbia Technical Translations		1	1954
Izv. AN SSSR Ser. geofiz.	Izvestiya Akademii Nauk SSSR: Seriya geofizicheskaya	Bulletin (Izvestiya) of the Academy of Sciences USSR: Geophysics Series	American Geophysical Union		1	1954
Izv. AN SSSR Ser. geol.	Izvestiya Akademii Nauk SSSR: Seriya geologicheskaya	Izvestiya of the Academy of Sciences of the USSR: Geologic Series	American Geological Institute		1	1958
Kauch. i rez.	Kauchuk i rezina	Soviet Rubber Technology	Research Association of British Rubber Manufacturers	18	1	1959
	Kinetika i kataliz	Kinetics and Catalysis	Consultants Bureau	1	3	1960
	Koks i khimiya	Coke and Chemistry USSR	Coal Tar Research Association (Leeds, England)		1	1958
Kolloidn. zh(urn).	Kolloidnyi zhurnal	Colloid Journal	Consultants Bureau	14	1	1952
	Kristallografiya	Soviet Physics — Crystallography	American Institute of Physics	2	1	1957
Metalov. i term. obrabot. metal.	Metallovedenie i termicheskaya obrabotka metallov	Metal Science and Heat Treatment of Metals	Acta Metallurgica	6	1	1958
	Metallurg	Metallurgist	Acta Metallurgica		1	1957
Met. i top.	Metallurgiya i topliva	Russian Metallurgy and Fuels	Eagle Technical Publications		1	1960
Mikrobiol.	Mikrobiologiya	Microbiology	American Institute of Biological Sciences	26	1	1957
OS	Optika i spektroskopiya	Optics and Spectroscopy	American Institute of Physics		6	1959
	Pochvovedenie	Soviet Soil Science	American Institute of Biological Sciences		1	1958
	Priborostroenie	Instrument Construction	British Scientific Instrument Research Association		1	1959
Pribory i tekhn. éks(perimenta)	Pribory i tekhnika éksperimenta	Instruments and Experimental Techniques	Instrument Society of America		1	1957
Prikl. matem. i mekh.	Prikladnaya matematika i mekhanika	Applied Mathematics and Mechanics	American Society of Mechanical Engineers		1	1958
PTÉ	(see Pribory i tekhn. éks.)					
	Problemy Severa	Problems of the North	National Research Council of Canada			
Radiotekh.	Radiotekhnika	Radio Engineering	Massachusetts Institute of Technology*	12	1	1957
Radiotekh. i élektronika	Radiotekhnika i élektronika	Radio Engineering and Electronics	Massachusetts Institute of Technology*	2	1	1957
	Stanki i instrument	Machines and Tooling	Production Engineering Research Assoc.		1	1959
	Stal'	Stal (In English)	Iron and Steel Institute		1	1959
Stek. i keram.	Steklo i keramika	Glass and Ceramics	Consultants Bureau	13	1	1956
Svaroch. proiz-vo	Svarochnoe proizvodstvo	Welding Production	British Welding Research Association		4	1959
Teor. veroyat. i prim.	Teoriya veroyatnostei i ee primenenie	Theory of Probability and Its Applications	Society for Industrial and Applied Mathematics		1	1956
Tsvet. Metally	Tsvetnye metally	Nonferrous Metals	Primary Sources		1	1960
UFN	Uspekhi fizicheskikh Nauk	Soviet Physics — Uspekhi (partial translation)	American Institute of Physics	66	1	1958
UKh	Uspekhi khimii	Russian Chemical Reviews	The Chemical Society (London)		1	1960
UMN	Uspekhi matematicheskikh nauk	Russian Mathematical Surveys	London Mathematical Society	15	1	1960
Usp. fiz. nauk	(see UFN)					
Usp. khim(ii)	(see UKh)					
Usp. matem. nauk	(see UMN)					
Usp. sovr. biol.	Uspekhi sovremennoi biologii	Russian Review of Biology	Oliver and Boyd		48	1959
Vest. mashinostroeniya	Vestnik mashinostroeniya	Russian Engineering Journal	Production Engineering Research Assoc.		4	1959
Vop. gem. i per. krovi	Voprosy gematologii i perelivaniya krovi	Problems of Hematology and Blood Transfusion	National Institutes of Health*		1	1957
Vop. onk.	Voprosy onkologii	Problems of Oncology	National Institutes of Health*		1	1957
Vop. virusol.	Voprosy virusologii	Problems of Virology	National Institutes of Health*		1	1957
Zav(odsk). lab(oratoriya)	Zavodskaya laboratoriya	Industrial Laboratory	Instrument Society of America	25	1	1959
ZhAKh Zh. anal(it). khimii	Zhurnal analiticheskoi khimii	Journal of Analytical Chemistry USSR	Consultants Bureau	7	1	1952
ZhETF Zh. éksperim. i teor. fiz.	Zhurnal éksperimental'noi i theoreticheskoi fiziki	Soviet Physics—JETP	American Institute of Physics	28	1	1955
ZhFKh Zh. fiz. khimii	Zhurnal fizicheskoi khimii	Russian Journal of Physical Chemistry	The Chemical Society (London)		7	1959
ZhMÉI Zh(urn). mikrobiol. épidemiol. i immunobiol.	Zhurnal mikrobiologii, épidemiologii i immunobiologii	Journal of Microbiology, Epidemiology and Immunobiology	National Institutes of Health*		1	1957
ZhNKh Zh(urn). neorgan(ich). khim(ii)	Zhurnal neorganicheskoi khimii	The Russian Journal of Inorganic Chemistry	The Chemical Society (London)		1	1959
ZhOKh Zh(urn). obshch(ei) khimii	Zhurnal obshchei khimii	Journal of General Chemistry USSR	Consultants Bureau	19	1	1949
ZhPKh Zh(urn). prikl. khimii	Zhurnal prikladnoi khimii	Journal of Applied Chemistry USSR	Consultants Bureau	23	1	1950
ZhSKh Zh(urn). strukt. khimii	Zhurnal strukturnoi khimii	Journal of Structural Chemistry	Consultants Bureau	1	1	1960
ZhTF Zh(urn). tekhn. fiz.	Zhurnal teknicheskoi fiziki	Soviet Physics—Technical Physics	American Institute of Physics	26	1	1956
Zh(urn). vyssh. nervn. deyat. (im. Pavlova)	Zhurnal vysshei nervnoi deyatel'nosti (im. I. P. Pavlova)	Pavlov Journal of Higher Nervous Activity	National Institutes of Health*		1	1958

*Sponsoring organization. Translation through 1960 issues is a publication of Pergamon Press.